Universiteit
Leiden
The Netherlands

Cellular therapy after spinal cord injury using neural progenitor cells

Vroemen, Maurice

Citation

Vroemen, M. (2006, January 17). *Cellular therapy after spinal cord injury using neural progenitor cells*. Retrieved from https://hdl.handle.net/1887/4319

Version:	Corrected Publisher's Version
License:	Licence agreement concerning inclusion of doctoral thesis in the Institutional Repository of the University of Leiden
Downloaded from:	https://hdl.handle.net/1887/4319

Note: To cite this publication please use the final published version (if applicable).

Cellular Therapy after Spinal Cord Injury using Neural Progenitor Cells

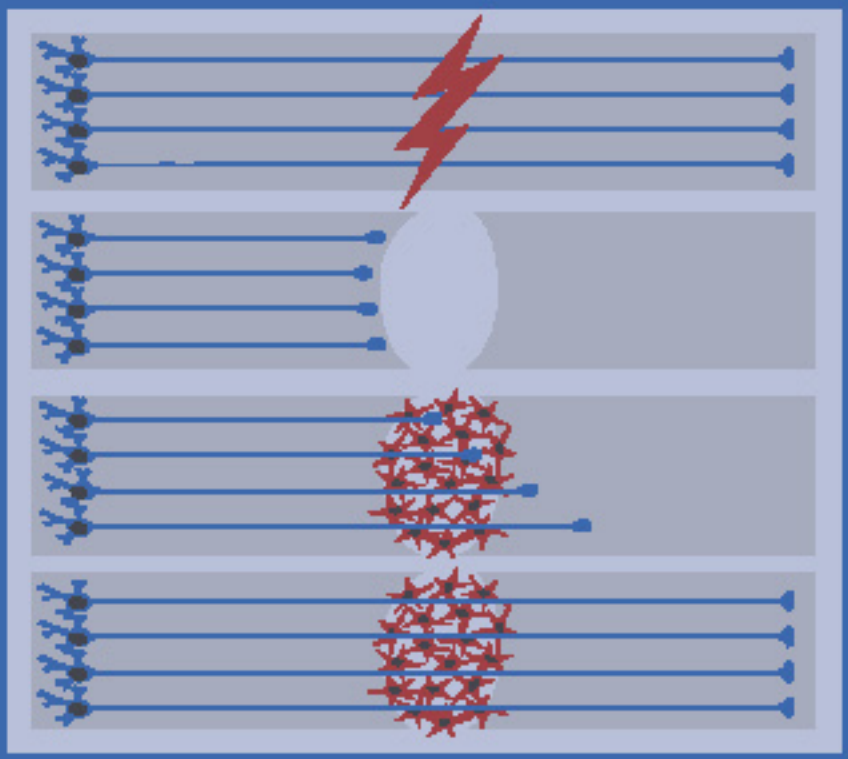

Maurice Vroemen

CELLULAR THERAPY AFTER SPINAL CORD INJURY USING NEURAL PROGENITOR CELLS

Proefschrift

ter verkrijging van
de graad van Doctor aan de Universiteit Leiden,
op gezag van de Rector Magnificus Dr. D.D. Breimer,
hoogleraar in de faculteit der Wiskunde en
Natuurwetenschappen en die der Geneeskunde,
volgens het besluit van het College voor Promoties
te verdedigen op dinsdag 17 januari 2006
klokke 14.15 uur

door

Maurice Vroemen
geboren te Heerlen
in 1973

Promotiecommissie

Promotores:	Prof. Dr. E. Marani
	Prof. Dr. J. Winkler (Universität Regensburg)
Co-promotor:	Dr. N. Weidner (Universität Regensburg)
Referent:	Prof. Dr. M. Tuszynski (University of California, San Diego)
Overigen leden:	Prof. Dr. R. T. W. M. Thomeer
	Prof.Dr. J. G. van Dijk
	Prof. Dr. R. A. C. Roos

The research described in this thesis was performed at the Department of Neurology, University of Regensburg and at the Department of Neurosciences, University of California, SanDiego.

veur Pap en Mam

TABLE OF CONTENTS

Chapter 1

General Introduction

1. BRIEF INTRODUCTION INTO SPINAL CORD INJURY

Injuries to the central nervous system (CNS) cause irreversible loss of function since the CNS of higher vertebrae has a very limited capacity to appropriately regenerate damaged axonal connections. This failing regenerative capacity is one of the main reasons for the catastrophic outcome of most CNS injuries in humans. Traumatic insults to the spinal cord are particularly devastating since the spinal cord contains both the motor and sensory connections between higher brain centers such as the cortex and the brainstem and effectors like muscles and glands within a very small area. Therefore, even limited injuries of the spinal cord parenchyma can lead to complete and life-long loss of voluntary motor and sensory function below the level of injury. Additionally, reflexes of the autonomic nervous system often become dysfunctional after spinal cord injury (SCI), leading to impairment of autonomic functions such as blood pressure dysregulation, loss of bladder and bowel control.

The regenerative failure of CNS axons has been described in detail for the first time in the early 20th century by Santiago Ramon y Cajal. By employing novel methods that enabled reliable staining of axon profiles, Cajal described the dystrophic endbulbs of lesioned CNS axons and concluded that after axonal injury in the adult mammalian CNS, only abortive sprouting of lesioned axons occurs [1]. For several decades, there has been a general assumption that this failure of regeneration represented a fundamental property of CNS axons. A series of experiments by the laboratory of Albert Aguayo, however, proved that CNS axons are able to regenerate over long distances when the tip of a severed CNS axon is exposed to a peripheral nerve environment, suggesting that CNS axons have the intrinsic capacity to regenerate [2, 3]. These findings dramatically accelerated research efforts to further augment SCI regeneration.

During the last decades, biomedical research gained a lot of insight in the pathomorphological mechanisms of SCI and was able to identify many factors that play a role for the failure of the CNS to recuperate following injury. This knowledge has lead to the development of experimental therapy approaches that employed numerous interventions including cellular replacement, neurotrophic factor delivery, axon guidance, neutralization of growth inhibitory molecules, breakdown of scar tissue, manipulation of intracellular signaling, bridging using artificial conduits, and modulation of the immune response [4-13]. Although some of these approaches induced a modest functional recovery in animal models of SCI, a real breakthrough justifying the hope for an effective therapy, which promotes robust functional recovery after SCI in humans, is still missing. Thus far, only 2 therapeutic interventions are routinely employed to ameliorate the pathomorphological changes following SCI, namely surgical stabilization of the fractured vertebral column and the administration of high dose steroids. The surgical removal of bone fragments,

which is intended to reduce the ongoing compression of the spinal cord, is able to limit secondary damage. However, already severed spinal cord parenchyma is irreversibly lost preventing intrinsic structural and functional restoration. The intravenous administration of high doses of steroids within 8 hours of injury has been shown to decrease secondary damage by reducing the injury induced edema and by neutralizing free radicals [14]. The efficacy of these approaches in humans is modest at best and alternative strategies are actively sought [15].

2. EPIDEMIOLOGY OF SPINAL CORD INJURY

The incidence of SCI in developed countries varies between 30 and 50 cases per million inhabitants per year [16-18]. Since many investigators used different definitions and methods in their research, the epidemiological data in the existing literature can be compared only to a limited extent. Nevertheless, it is clear that the combination of decreased mortality of acute SCI victims and a longer life expectancy of the chronic SCI patient raises the prevalence of SCI in developed countries [19]. In the USA, the prevalence of SCI currently is between 721 and 906 per million population [19].

The severity of the neurological outcome after a traumatic insult of the spinal column strongly correlates with the extent of damaged long distance axonal connections. After a functionally complete SCI, there is no detectable voluntary motor or conscious sensory function of the body below the lesion site, in contrast to incomplete injuries, where residual function is observed. Approximately 45% of all SCI cases are neurologically complete [20]. During the last decades, the relative distribution of complete versus incomplete SCI has changed in favor of the incomplete injury [21, 22]. This can be attributed to the improved avoidance of secondary damage during transport and the much more aggressive intervention to avoid hypotension and hypoxia directly after trauma. Nevertheless, even after a complete lesion functionally, spared white matter can be detected most frequently. These cases are referred to as anatomically incomplete lesions [23]. Since function is lost below the lesion site, it is evident that the location of the injury greatly determines the extent of the functional deficits. Injuries to the thoracic or lumbar spinal cord only affect axon projections innervating the lower extremities resulting in a more or less severe paresis of both lower extremities (paraplegia). Injury to the cervical spinal cord disrupts axon pathways to both lower and upper extremities with respective functional deficits in all four extremities (quadriplegia) and potentially respiration. Of all SCI cases, a majority of 55% of the injuries is located at cervical level [20].

The average age of SCI victims is around 31 years and the most frequently occurring age at injury is 19 years [24]. Considering the severe outcome of most SCI and the lack of a therapeutic perspective for the patient, the fact that an over-proportional part of the victims are young adults adds to the devastating nature of the inju-

ry. The main causes for SCI in developed countries are traffic accidents, workplace-related accidents and recreational activity related accidents, which further indicates that a major part of the SCI victims are active young adults [20]. Additionally, more than 75% of the victims are male [20]. For many patients, a SCI leads to severe impairments, loss of economic productivity and a life-long dependency on nursing. A SCI therefore is not only a tragedy for the patient personally but also leads to enormous costs for the society in general.

3. THE PATHOMORPHOLOGY OF SPINAL CORD INJURY

The pathological response to SCI can be divided into three different phases. In the acute injury phase, which starts at the moment of injury and extends over the first few days, the force of the traumatic insult causes direct mechanical damage to the spinal cord tissue. Additionally, the correct ionic segregation in cells at the lesion epicenter is disturbed, causing axolemmal depolarization and localized edema, which results in a state of spinal shock[25]. Spinal shock represents a transient generalized failure of circuitry of the spinal neural network that is characterized by the absence of spinal reflexes, a typical hallmark of the acute injury phase [26]. In the following secondary injury phase ranging from days to months after the initial injury, the pathophysiological disturbances that are initiated by the primary injury in the acute injury phase persist leading to a progressive loss of spinal cord parenchyma. As a result, the size of the final lesion is remarkably larger as compared to the lesion area immediately after injury. Finally, in the chronic injury phase the typical cytoarchitecture of the spinal cord has been irreversibly changed. Necrosis and apoptosis at the lesion epicenter has lead to extensive tissue degeneration and the development of cystic lesion defects [27]. Apoptosis of oligodendrocytes causes demyelination, which leads to conduction defects of spared axons [28]. Moreover, extracellular matrix produced by infiltrated fibroblasts, reactive astrocytes and macrophages/activated microglia promotes fibroglial scar formation delineating the lesion center from the surrounding spinal cord parenchyma [29]. In some instances, even in the later stage chronic SCI, progression of degenerative events can be observed. A blockade of cerebrospinal fluid circulation through the central canal for instance can induce a centrally located cyst formation, so called syringomyelia, which can lead to secondary pressure damage of the spinal cord tissue rostral to the actual injury site [30].

Injury induced plasticity phenomena represent an often-underestimated aspect of SCI in chronic stages. Compensatory collateral sprouting, activation of redundant pathways and alterations in the receptor number/phenotype or excitability of surviving neurons and glia of partially denervated targets can be observed after incomplete lesions. In rodent animal models, injury induced plasticity is shown to be associated with functional recovery after SCI [31]. Also in humans, many SCI patients exhibit a modest degree of func-

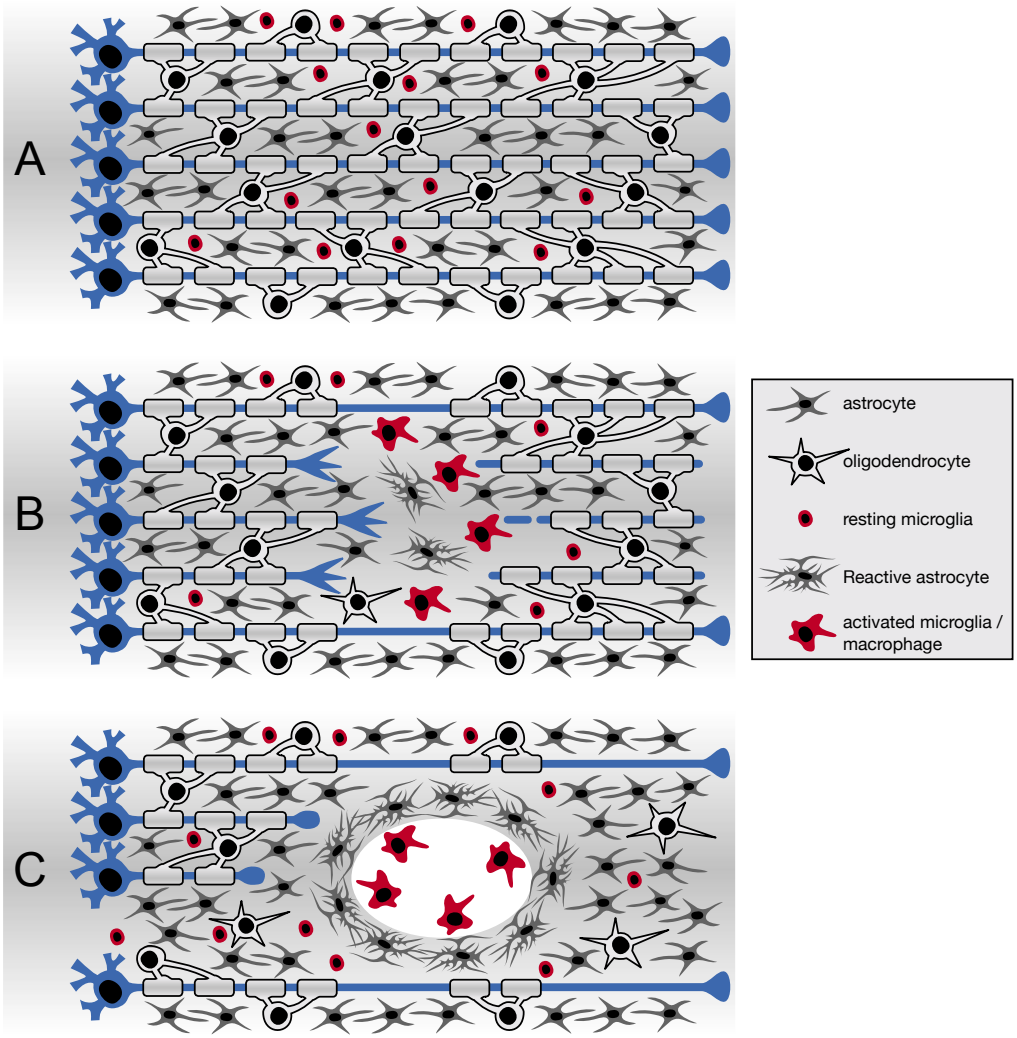

Figure 1: *Schematic representation of spinal cord injury. (A) In the intact spinal cord, neurons innervate distant targets with their axons (blue). In most fiber tracts, the axons are myelinated by oligodendroglia, whereas the astroglia give structural and homeostatic support (grey). The resident microglia are in a resting state (red). (B) After a traumatic insult, the mostly blunt injury leads to disruption of axon fiber tracts. Necrosis at the lesion center and degeneration of the distal portion of the lesioned axons induces microglia activation and the invasion of peripheral macrophages. Furthermore, proliferation and hypertrophy of astrocytes leads to reactive gliosis. (C) In the chronically injured spinal cord, a cystic lesion cavity that is surrounded by reactive astrocytes has developed. Apoptosis of oligodendrocytes has lead to demyelination of otherwise intact axons. Furthermore, lack of trophic support can lead to neuronal loss.*

tional recovery over weeks to months after the initial injury [32].

The steady progression of tissue damage in the proximity of the injury site exceeding by far the size of the initial damage is typical for SCI in particular and CNS injuries in general. It therefore is generally accepted that there are two separate mechanisms of damage after acute spinal cord injury: the primary injury and secondary injury mechanisms [33, 34]. Although both mechanisms cannot be strictly temporarily separated, the primary and secondary damage events possess distinct pathophysiological characteristics.

3.1 Primary injury mechanisms

The primary injury includes the tissue damage that can be directly attributed to the force of the traumatic insult. The primary injury induces disruption of the axon pathways, cell membrane damage and mechanical damage to the spinal cord vasculature. Particularly in the lower spinal cord, the initial traumatic insult most frequently causes the deformation of the spinal canal, leading to a contusion injury that is followed by an acute compression of the soft spinal cord tissue. Additionally, the mechanical impact can cause the dislocation of bony fragments and disc material, which leads to penetration and laceration of the spinal cord [35]. Sharp insults or direct transection of the spinal cord tissue on the contrary is a less frequent occurring injury type that often takes place after gun shot or knife wounds [19]. At the cervical region of the spinal cord, hyperextension injuries are occurring more frequently than crush injuries because of the greater flexibility of the cervical spinal column. Hyperextension injuries directly cause disruption of axons and typically occur due to falls on the head for instance after diving in shallow water [20].

3.2 Secondary injury mechanisms

The primary damage to the spinal cord tissue elicits the autocatalytic processes that are involved in the secondary damage phase. The secondary damage phase consists of a wide repertoire of vascular events, biochemical disturbances and cellular responses that evolve over minutes to hours after the primary injury, leading to massive additional loss of spinal cord tissue, scar tissue formation and demyelination. Since it predominantly is the loss of white matter that is decisive for the loss of function after SCI, it is hypothesized that therapeutical interventions that prevent secondary damage could be able to improve functional outcome after SCI [14]. It therefore is of obvious interest to better understand the pathophysiology of the secondary injury processes.

3.2.1 Vascular events

Within minutes after the primary injury, vasospasms and the loss of vascular autoregulation cause a reduced perfusion at the injury site [36]. Particularly in the spinal cord grey matter, this leads to a remarkably impaired microcirculation [37]. In combination with the systemic hypotension and the reduced cardiac output typically occurring after SCI [38], the vascular changes cause post traumatic ischemia of the

spinal cord parenchyma in the segments surrounding the injury site [34]. Especially in hemorrhagic regions of the injured spinal cord, the posttraumatic ischemia leads to infarction and necrosis of the spinal cord tissue [39]. Furthermore, damage to the vasculature endothelial lining causes disruption of the blood-brain barrier (BBB), which leads to a progressive edema that spreads to adjacent segments of the injured spinal cord [40].

3.2.2 Biochemical alterations

Directly following the primary injury, synaptic overactivity leads to the uncontrolled release of the amino acid glutamate, the major excitatory neurotransmitter in the adult mammalian CNS [41, 42]. Elevated levels of glutamate cause the activation of the NMDA subclass of glutamate receptors, which have been shown to induce Ca^{2+} influx resulting in a cellular Ca^{2+} overload [43]. A further disturbance of the ionic homeostasis is caused by a reduction of the Na^{+}/K^{+}-ATPase activity in cells at the lesion epicenter [44]. In physiological normal CNS tissue, the intracellular concentration of Na^{+} and Ca^{2+} is kept at a low level, while cell organelles such as the endoplasmatic reticulum and mitochondria function as intracellular Ca^{2+} storage. The increase of intracellular Na^{+} and Ca^{2+}, however, is thought to reverse the normal action of the intracellular Na^{+}/Ca^{2+} exchanger by pumping out Ca^{2+} that is accumulated in the intracellular Ca^{2+} stores in reverse of Na^{+} [44]. It is the increase of cytoplasmic Ca^{2+} levels, which starts a detrimental cascade of events inducing both axon degeneration and cell death [45]. First, increased levels of cytosolic Ca^{2+} concentrations are shown to destabilize the cytoskeleton and the cell membrane, causing impaired axoplasmic transport [46, 47]. Furthermore, high concentrations of cytosolic Ca^{2+} activate a series of cell death inducing catabolic enzymes such as proteinases, cysteine proteases, and phospholipases [48-50]. The state of impaired Ca^{2+} homeostasis is autocatalytic and self-propagating since it can lead to the opening of the mitochondrial permeability transition pore. This is not only detrimental for the cell's ATP production, which further reduces the Na^{+}/K^{+}-ATPase activity, but also leads to release of cytochrome c, which induces apoptotic cell death by caspase 3 activation [51].

After collapse of the oxidative metabolism, incomplete electron transport in the respiratory chain causes the overproduction of free radicals such as super oxide (O^{2-}) [52]. Free radicals are highly reactive oxygen metabolites that possess an extra electron in the outer orbit. The enzyme superoxide dismutase converts the superoxide in the free radical species H_2O_2, which in its turn is degraded into H_2O and O_2 by catalase and gluthatione peroxidase activity. In the presence of free iron that originates from hemoglobin, transferrin or ferretin, H_2O_2 forms the highly reactive hydroxyl radicals (•OH) [53]. The uncontrolled and excessive release of these free radicals causes lipid peroxidation in the cell membranes, which leads to impairment of the phospholipid dependent enzymes, disruption of ionic membrane gradients and eventually dis-

Table 1 *Pathophysiological Events of the Secondary Injury that Occur After Acute Spinal Cord Injury*

Vascular events	
	Post traumatic ischemia
	Edema
	Disruption of blood brain barrier
Biochemical alterations	
	Uncontrolled excitatory amino acid release
	Ca2+ influx into cells
	Na+ influx into mitochondria
	Collapse of oxidative metabolism and ATP production
	Cytochrome c release
	Free radical overproduction
	Lipid peroxidation
Cellular Events	
	Invasion of blood bound immune cells
	Microglia activation
	Reactive Astrogliosis
	Wallerian degeneration
	Rupture of terminal clubs resulting in hydrolytic enzyme release
	Apoptosis of glial cells
	Invasion of fibroblast and Schwann cells

ruption of the cell membrane [54]. When a cell membrane is destroyed, the fatty acids that make up the cell membrane are released and form, when peroxidated, highly toxic compounds such as acrolein and 4-hydroxynonenal. These on their turn destroy cell membranes, releasing more fatty acids that undergo peroxidation, resulting in an autocatalytic cell lysis process, which is typical for the secondary damage phase of SCI [55, 56].

3.2.3 Cellular events

The response of the immune system represents the first cellular event that takes place in the secondary damage phase of SCI. Within 6 hrs after the primary injury, neutrophils enter the lesion site and start to remove tissue debris by phagocytosis [57]. Besides the restoration of tissue homeostasis, neutrophils contribute to the progress of the secondary damage phase by releasing proteases and reactive oxygen species. Microglia, the resident immune cells in the CNS, respond quickly to the changes in the microenvironment and become activated [58]. Activated microglia remove degenerated fibers by phagocytes and function as antigen presenting cells to mediate the T-cell response. [59]. Several days after the initial injury, blood born macrophages and lymphocytes infiltrate the injured spinal cord tissue [57]. The infiltration and prolonged activation of immune cells has been shown to have both beneficial and deleterious effects on

the functional outcome after SCI. The release of pro-inflammatory cytokines such as tumor necrosis factor-alpha and inducible nitric oxide synthase, are thought to induce cellular degeneration in the secondary damage phase [60, 61]. In a more chronic phase of the injury, activated immune cells produce growth factors that contribute to neuronal survival and tissue repair [62, 63]. Furthermore, the clearance of myelin and axonal debris by immune cells may promote axonal regeneration considering that adult myelin contains potent axonal growth inhibitors [64].

CNS injury induces astroglial hypertrophy, process extension and moderate cell division. These so called reactive astroglial cells can be detected by the increased production of intermediate filament protein such as glial fibrillary acidic protein (GFAP) and vimentin [65]. Reactive astrocytes seal the injury site by producing a wide variety of extracellular matrix (ECM) proteins. Reactive astrogliosis is often regarded as detrimental to functional outcome since they partly form the scar tissue surrounding the injury site, which is thought to act as a major obstacle for axon regeneration [66, 67]. Nevertheless, reactive atrocytes are essential for wound healing and blood–brain barrier repair. In addition, reactive astrocytes are able to restrict inflammation, protect neurons and oligodendrocytes, and preserve motor functions after mild or moderate SCI [68, 69]. Thus, reactive astroglia have an ambivalent role in the injured spinal cord, secreting factors, which inhibit axonal regeneration, on one hand, and stabilizing the injured tissue during the secondary damage phase on the other hand.

Axonal breakdown takes place in the ascending fiber tracts above the lesion and descending fiber tracts below the lesion and is spatially associated with phagocytosis of tissue debris by activated microglia, a process which as also known as Wallerian degeneration [70]. Abortive sprouting can be observed along the proximal part of lesioned CNS axons, which has already been described by Ramon y Cajal [1]. As a result of continuing proximodistal axonal transport, terminal club structures are formed at the distal tip of lesioned axons. After rupture of the terminal club, the hydrolytic enzymes that are enriched in the terminal clubs are released, causing autolysis of the spinal cord tissue [71].

The described vascular events, biochemical alterations and responses of the immune system as part of the secondary damage phase also affect spinal cord cells that initially survived the injury. The programmed cell death machinery becomes activated through death receptors, mitochondrial malfunction or caspases, ultimately leading to loss of glial and neuronal cells [72]. The number of apoptotic cells is the highest close to the lesion epicenter. Apoptosis of oligodendroglia in the proximity of spared axons causes chronic demyelination, which often represents the morphological correlate for the delayed sensory and motor dysfunction occuring after SCI [73].

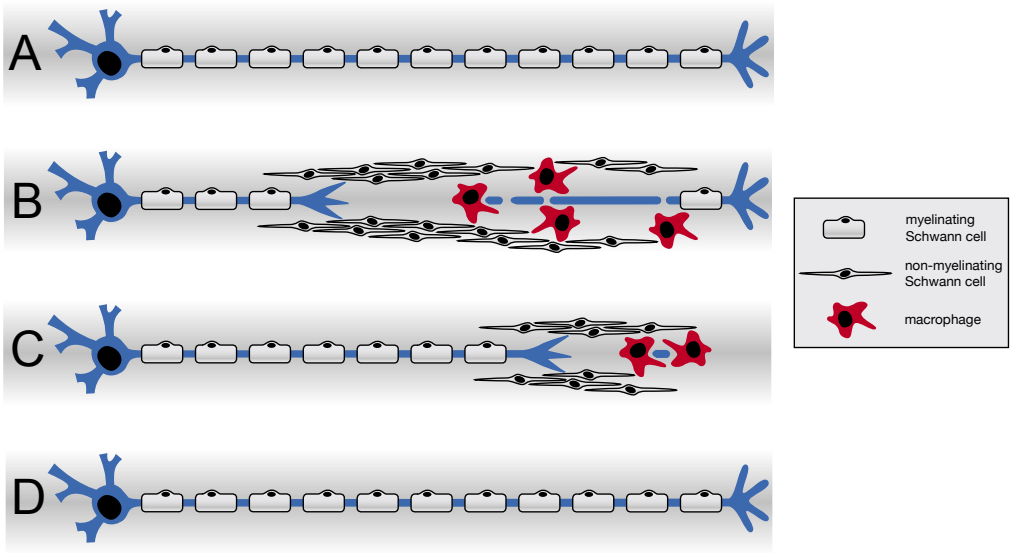

Figure 2: *Axonal regeneration in the peripheral nervous system. (A) Peripheral axons (blue) are either ensheathed or myelinated by Schwann cells (grey). (B) As long as the perineurium is intact, lesioned peripheral axons are able to spontaneously regenerate over considerable distances. Therefore, resident Schwann cells that lose axonal contact start to proliferate and form axon-guiding structures, the so-called bands of Büngner. Schwann cells furthermore, produce neurotrophic factors and guidance molecules that enhance axonal regeneration. Infiltrated macrophages (red) remove the debris that originates from the degenerating distal part of the lesioned axons. (C) Regenerating axons become remyelinated by the resident Schwann cells. (D) Ultimately, the regenerating peripheral axons are capable of reinnervating their target organ.*

4. CAUSES FOR THE POOR REGENERATIVE CAPACITY OF THE CENTRAL NERVOUS SYSTEM

In contrast to the CNS, the peripheral nervous system (PNS) is capable of spontaneous recovery after axonal damage. Schwann cells, which are the resident PNS glial cells, play a crucial role in this regeneration process. When the distal part of a lesioned PNS axon degenerates, the Schwann cells that lose axonal contact start to proliferate and form a cell strand within the basal lamina tube, the so-called bands of Büngner [74]. Furthermore, the Schwann cells in the denervated nerve stump express adhesion molecules and neurotrophic factors essential for axon regeneration. Severed axons sprout into the Schwann cell columns of the distal nerve segment, which ultimately can lead to reinnervation of the denervated target, in most cases the skeletal muscle [75].

Although CNS axons are capable of long distance axonal sprouting into a peripheral nerve graft, injured CNS neurons react differently compared to PNS neurons. However, in particular the inhospitable environment surrounding severed CNS axons determines their inability to regrow [2, 3]. Substantial progress has been made revealing the biological bases of the

regeneration inhibiting properties of the CNS in comparison to the PNS. A number of factors have been identified: the presence of extrinsic axonal growth inhibiting factors, decreased intrinsic regenerative potential of CNS axons, the absence of remyelination and the development of a cystic tissue defect, which all are thought to play a significant role for the poor regenerative capacity after SCI.

4.1 Extrinsic axonal growth inhibiting factors

4.1.1 Glial scar

Glial scar formation represents a major obstacle for axonal regeneration after SCI. The glial scar consists of reactive astrocytes and their ECM proteins. As soon as the surrounding dura mater gets disrupted in more severe lesions, invading fibroblasts will contribute to the glial scar. Subsequently, astrocytes start to up-regulate the expression of proteoglycans, a class of ECM molecules [76]. Proteoglycans have been identified as potent inhibitors of CNS axon extension both *in vitro* and *in vivo* [6, 77-79]. Ultrastucturally, growth cones of sprouting axons are not able to regenerate through the glial scar and form dystrophic endbulbs [66, 67]. Remarkably, cellular sources of proteoglycans in the lesion site also produce axon growth permissive ECM components such as L1 and laminin. [80]. Both *in vitro* and *in vivo*, the balance between inhibitory and permissive ECM components substantially influences the ability of axons to regenerate [80, 81]. Therefore, the obstruction of neurite extension by inhibitory ECM components such as proteoglycans and the growth promoting capacity of permissive ECM components of the glial scar cannot be described as an "all or nothing" mechanism [80]. Moreover, it is now clear that at least certain subpopulations of dystrophic axons are able to return to an active growth state when they are given a proper stimulus, for instance additional neurotrophic factor support[82, 83].

In addition to proteoglycans, several other inhibitors for axonal regeneration are upregulated in the glial scar. The secreted protein semaphorin 3 is upregulated in invading fibroblasts and acts as a chemorepellent for neuropilin expressing neurons. [84]. Furthermore, *Slit* proteins along with their glypican 1 receptors, which are important inhibitors for axonal elongation during development, are upregulated in reactive astrocytes [85]

The formation of the glial scar starts after disruption of the BBB and is most likely triggered by the influx of molecules, normally absent in the CNS, and the invasion of activated microglia in the injured CNS parenchyma [86]. The search for potential candidate molecules, which may promote reactive gliosis, is ongoing. However, there is clear evidence that both interleukin-1 and transforming growth factor-*beta* (TGF-*beta*) produced by macrophages play a major role in the transformation of normal astrocytes into the reactive phenotype [87, 88]. Furthermore, the secretion of the inflammatory cytokine interferon-*gamma* mediates glial scarring after brain injury [89]. Additionally, signaling between B-ephrins and EphB receptors in response to injury

supports the fibroglial scar formation initiated by meningeal fibroblasts, which invade the injured spinal cord in the adult CNS [90].

4.1.2 Myelin associated inhibitors

Distinct from the already described growth cone dystrophy is the collapse of growth cones where mature regenerating CNS axons encounter mature oligdendrocytes or myelin. Growth cone collapse results in a shrunken growth cone in combination with a stalled forward progress that can restart over time, and has been described best *in vitro* [91]. It is unclear whether growth cone collapse precedes growth cone dystrophy.

Three different classes of myelin-associated molecules have been described causing growth cone collapse and inhibition of neurite outgrowth: Nogo, Myelin-Associated Glycoprotein (MAG) and Oligodendrocyte Myelin Glycoprotein (OMGP). Nogo exists in three isoforms, Nogo-A, Nogo-B and Nogo-C and is mostly associated with the endoplasmatic reticulum of oligodendrocytes, however, a proportion can be detected on the cell surface. The three isoforms share the inhibitory Nogo-66 domain, Nogo-A has an additional inhibitory domain, amino-Nogo, at the N-terminus [92-94]. MAG, a member of the immunoglobulin superfamily, is a sialic acid-binding protein and can be found in both CNS and PNS myelin [95, 96]. OMGP is a glycosyl phosphatidylinositol-linked protein not only expressed by oligodendrocytes, but also in by Schwann cells, their counterparts in the PNS [97]. Interestingly, all three classes of myelin inhibitors seem to act through the neuronal expressed Nogo-receptor (*Ngr*) [98-100]. *Ngr* uses p75 low affinity NGF receptor (p75-LNGR) as a co-receptor to activate the small GTPase *Rho* and its signal transduction pathway to inhibit neurite outgrowth [101, 102].

The role of myelin inhibitors in growth cone collapse and inhibition of neurite outgrowth has been impressively demonstrated *in vitro*, the exact role of myelin inhibition *in vivo* remains unclear. Inhibition of Nogo using specific neutralizing antibodies elicit an axonal response and improved functional outcome after SCI [103, 104], presumably through the activation of collateral sprouting of uninjured axons [105]. The inhibition of *Ngr* signaling after SCI through specific antibodies promotes local sprouting, however, long range axon regeneration is minimal [7, 103]. Animals lacking either specific or all three Nogo variants allow only limited axonal regeneration at best [106-108]. Furthermore, adult sensory neurons regrow in both intact and degenerating white matter tracts of adult mice [79, 109]. There is strong evidence suggesting that the geometrical organization of myelin is biologically relevant *in vivo*, which is based on the finding that white matter supports parallel axonal sprouting but inhibits nonparallel sprouting against the orientation of the white matter tracts [110]. Therefore, it is likely that myelin associated inhibitory molecules could be essential for oriented and fascicled long distance axon growth [111]. Myelin-associated inhibition is considered to be crucial to maintain the topography of highly specific nervous

system projections, which is supported by studies inducing aberrant sprouting of local circuitry in the adult intact cerebellum after neutralizing Nogo [112]. In other words, neutralizing myelin based inhibitors as a repair strategy for SCI could induce aberrant and dysfunctional sprouting of non-injured systems.

4.1.3 Other inhibitors

Besides myelin-associated inhibitors, there are indications that at least some of the chemoattractant and repulsive effectors that play a role during development also are present in the adult spinal cord. The highly conserved laminin-related molecule netrin system with its receptors DCC and Unc5 can function both as an attractant and repellent for growing axons, depending on the cAMP or cGMP level within the growth cone [113]. In the injured rat spinal cord, Netrin-1 is expressed throughout grey and white matter by oligodendrocyte precursors still undergoing division [114]. Furthermore, grafts of netrin-1 over-expressing fibroblasts reduce axonal growth after adult spinal cord injury, which suggest a role for endogenous netrin-1 as an inhibitor of intra-spinal neuron derived axon regeneration [115].

4.2 Intrinsic regeneration limiting factors

4.2.1 Regeneration-associated genes

Besides the above described extrinsic factors that limit the regenerative capacity of CNS axons, differences in the intrinsic state of the lesioned neurons contributes significantly to the poor regenerative capacity of the diseased CNS. Neurons react upon axotomy by up-regulating the expression of regeneration-associated genes (RAG), including growth-associated proteins such as GAP-43 and CAP-23 and adhesion molecules like L1, N-CAM. Most changes in RAG expression occur in response to axotomy of CNS neurons and are qualitatively and quantitatively different from those that occur in the PNS. In general, up-regulation of RAG is weaker and more transient or even absent in CNS neurons compared to PNS neurons [116, 117]. The expression level of RAG appears to correlate with the regenerative capacity of an axotomized neuron [118]. Under certain conditions, the over-expression of multiple RAG is sufficient to induce axonal regeneration, even in a CNS environment [119].

4.2.2 Trophic support

The differential expression of growth factors and their receptors after axotomy represents another significant difference between PNS and CNS neurons. In contrast to PNS neurons, CNS neurons fail to induce sufficient expression of trophic factors such as BDNF and NT-4/5 after axotomy, which results in significant atrophy of fiber tracts such as the rubrospinal and the corticospinal tract [120]. After administration of BDNF and NT-3 in rodent models of SCI, structural and functional recovery has been reported [5, 121]. Functional improvements are most likely attributable to the reduced atrophy of axons and stimulation of injury-induced plasticity of surviving axons, since long-distance

tract regeneration was not observed [5, 8, 121, 122]. These findings support the notion that the administration of neurotrophic factors is a promising strategy to induce axonal and functional recovery after SCI.

4.3 Demyelination

Loss of oligodendrocytes through programmed cell death contributes significantly to functional deficits observed after SCI. The resulting demyelination slows down or even blocks completely appropriate nerve conduction in uninjured axons. In contrast to the PNS, the CNS exhibits only a limited capacity to remyelinate affected fiber tracts [123]. Replacement of oligodendroglia and remyelination has been achieved by transplanting Schwann cells, olfactory ensheathing cells or oligodendrocyte precursor cells [124-126]. Either protection of intrinsic oligodendrocytes or their appropriate replacement to maintain myelination will result in significant improvement in functional outcome after spinal cord injury.

4.4 Cyst formation

Necrosis and apoptosis of spinal cord parenchyma results in a fluid filled lesion cavity forming at the lesion epicenter. Subsequently, a disturbed cerebrospinal fluid circulation along the central canal often supports the development of a fluid filled cavity – so called syringomyelia. It is evident that cystic lesion cavities represent a major obstacle for the regeneration of severed axons. In the PNS, the resident Schwann cells react upon the injury by proliferation and cells migrate into the lesion site, providing a substrate for regenerating axons [75]. Although some proliferation of astrocytes can be observed after SCI, the extent of cell renewal, even after the application of growth factors, does not allow to replace the cystic lesion cavity [4]. Therefore, strategies need to be developed, which provide regrowth conducive substrates either through cell transplantation approaches or through implantation of appropriate acellular matrices.

5. INDUCING RECOVERY AFTER SPINAL CORD INJURY

Recovery after spinal cord injury can be described on both structural and functional levels. Structural recovery can be observed in terms of tissue repair, axonal growth and elongation, remyelination and synapse formation and is measured using descriptive tests that determine the integrity of the injured system. Functional recovery describes improved function of the injured subject after therapeutical intervention. Functional recovery can be determined using electrophysiology and specific behavioral tests that describe the ability of the injured system to perform a certain task. Although the induction of structural recovery is the most compelling approach to induce functional recovery, it is not the only means that has the potential to improve the outcome after SCI.

5.1 Prevention of secondary damage

The disruption of ascending and descending axon pathways in the white matter represents the main structural

correlate for functional impairment caused by spinal cord trauma. Of note, a small percentage of spared axon projections is sufficient to maintain a large degree of function [127]. Pathophysiological changes during the secondary injury phase are responsible to a significant extent for the ultimate white matter damage occuring over time after the initial injury. Therefore, therapeutic interventions need to be introduced before the cascade of secondary damage events starts, in order to promote white matter sparing and improved functional outcome. The inhibition of earlier described effectors of secondary damage (for instance free radical cellular damage, cytochrome C release and Na^+ and Ca^{2+} influx-related cell death) has been shown to induce tissue sparing and improvement of functional outcome after SCI in animal models [9, 128, 129]. Most interventions to reduce secondary damage require either pre- or immediate post-injury application in order to be effective, which of course is problematic to realize in a clinical setting [130]. Moreover, the benefits of the standard administration of a high dose methylprednisolone immediately after the spinal trauma in order to reduce secondary damage are still under dispute [15]. No doubt, the investigation of approaches to attenuate sequelae of secondary injury events will be an important research topic in the future. However, the translation into clinically relevant strategies continues to be a challenging task.

5.2 Induction of injury-induced plasticity

The success of a therapeutic intervention aiming for functional recovery depends on the ability to reestablish a critical number of connections between supraspinal and spinal neurons. The fact that 55% of the SCI patients have neurological incomplete lesions and that even a majority of the complete SCI patients exhibit spared rims of white matter at the lesion epicenter suggests that enhancing the injury-induced plasticity of spared axons represents a promising mechanism to induce functional recovery after SCI [23]. Indeed, there have been several animal studies in which the enhancement of compensatory collateral sprouting after incomplete SCI can be induced by the administration of neurotrophic factors, GAP-43 up-regulation or the neutralization of myelin-associated inhibitors [13, 131, 132]. The efficacy of strategies enhancing the intrinsic plasticity remains to be determined. However, this approach can only be applied for structural incomplete SCI. After denervation in complete SCI, only therapies that induce regeneration of severed axons and subsequently target reinnervation will be able to promote functional regeneration.

5.3 Induction of axonal regeneration

Axonal growth can represent either plasticity or regeneration. Therefore, it is important to strictly define the possible axonal growth phenomena. First, the most restricted form is reactive synaptogenesis, which depicts local ingrowth of otherwise non-injured afferents that terminate in the

close proximity of the denervated sites. Furthermore, new connections can be established by ectopic ingrowth of sprouts from non-injured axons that originally project at remote locations, which is defined axonal sprouting. Alternatively when the axonal growth originates from the amputated axon itself, it is referred to as regenerative sprouting. Axonal regeneration finally describes regenerative sprouting that leads to reconnection of lesioned axon with their original targets [133]. The ultimate goal of SCI research is to induce axonal regeneration of disrupted fiber tracts, leading to regain of function, which further is referred to as functional axonal regeneration.

It is of utmost importance to keep in mind that if functional recovery is observed, this not necessarily has to be the direct correlate of the elicited structural recovery. Since the majority of experimental SCI models employed represent incomplete injuries, a limited degree of regain of function after SCI most frequently can be explained by compensation of spared connections. It therefore is very challenging to determine whether the observed functional recovery can be attributed to true axonal regeneration or by plasticity phenomena within spared axon projections. Before functional axonal regeneration can be claimed, each individual aspect of structural recovery, including cell survival, axon growth, synapse formation and remyelination must be described for the injured connection. Furthermore, it must be proven that the observed functional recovery can be attributed to the observed morphological changes, for instance by specifically targeting regenerates with pharmaceutical (e.g. by neurotransmitter antagonists) or surgical interventions (e.g. by retransection) to reverse functional improvement. Numerous studies report regenerative sprouting in combination with behavioral recovery [4-13]. Although these studies provide valuable insights into the regenerative mechanisms that play a role after SCI, most studies only provide data on a limited series of tests. The true significance of the described regeneration therefore remains subject of further investigations.

The development of a therapeutic intervention that enables regeneration of lesioned axons over long distances is often considered to be an essential aspect to induce functional axonal regeneration. Nevertheless, it remains to be determined in which degree long distance axonal regeneration is required in order to induce substantial functional recovery. It is possible that only bridging the lesion site is sufficient to form a connective relay with spared axonal fibers below the lesion. The functional recovery that can be observed after injury-induced plasticity indicates that the wiring of the adult spinal cord could be more plastic then expected [134]. In this respect, it is an interesting observation that the axonal reconnection in cold-blooded species that are capable of axonal regeneration after SCI predominantly occurs by regeneration of cells that are closely rostral to the injury site [135]. Significant axonal regeneration of lesioned CNS axons over long distances within the CNS has never been shown.

5.4 Cellular therapy as a multi-facet tool to enable functional axonal regeneration

In order to achieve the challenging goal of functional axonal regeneration, injured neurons must survive, extend axons through an adversive environment, find appropriate target neurons and ultimately form functionally relevant synapses. It is evident that a multi-facet therapeutic intervention is needed in order to accomplish these complex tasks. Moreover, if the regenerative failure of injured CNS axons is perceived as an imbalance between the present stimulators and inhibitors of axonal regeneration, a combined therapy that both neutralizes inhibition and provides additional growth stimulation is most likely to be effective. Since the CNS is not able to intrinsically replace lost spinal cord parenchyma sufficiently, cellular replacement is considered to be a crucial prerequisite in a putative therapeutical approach. The regenerative properties of the PNS can be be transferred to a limited extent to the CNS by the transplantation of Schwann cells and olfactory ensheathing cells. Schwann cells induce axonal regeneration by providing a growth supportive substrate and by supplying trophic support [136]. Furthermore, Schwann cells are able to remyelinate CNS axons to restore proper nerve conduction. However, Schwann cells do not facilitate axonal regrowth beyond the graft to reenter the caudal host spinal cord [137]. Alternatively, olfactory ensheathing cells (OEC) are shown to be interesting candidates for the use in a cellular therapy approach after SCI. OEC represent a “hybrid” between CNS (astroglia) and PNS glial cells (Schwann cells) that promote reentry of olfactory nerve endings from the PNS into the CNS throughout life. The olfactory system is unique in terms of its constant renewal of adult neuronal cells [138]. OEC can be isolated from adult olfactory nerves. When OEC are grafted into the lesioned spinal cord, tissue repair, axonal regeneration, remyelination and functional recovery can be observed to a limited degree. Whether the observed functional recovery can be attributed to axonal regeneration of lesioned axons has not been shown yet [139, 140].

Neural stem cells (NSC) as a source for cell-based therapies have the important advantage to give rise to all three major cell types of the central nervous system (CNS): neurons, astrocytes and oligodendrocytes. Therefore, they can replace degenerated spinal cord parenchyma in an organotypcially appropriate manner. NSC have been isolated from both the developing and adult CNS and can be expanded in culture using epidermal growth factor and fibroblast growth factor as mitogens [141, 142]. Embryonic derived NSC have been shown to promote partial functional recovery following spinal cord injury [12, 143]. Since ethical and logistic concerns restrict the large-scale use of embryonic derived stem cells, NSC derived from adult neural tissue are preferable. Furthermore, adult NSC could be isolated from the patient’s own

neural tissue, thus avoiding the need of life long immunosuppression in transplanted subjects to avoid graft rejection. The potential of adult derived NSC to induce axonal regeneration remains to be determined.

6. INTRODUCTION TO THE USED SPINAL CORD INJURY MODELS

6.1 Animal models of spinal cord injury

In animal models of SCI, both structural and functional regeneration can be investigated. Unfortunately, the conclusions obtained from animal models of SCI can be transferred to the human situation only to a limited extent. On both the structural and functional level, the human spinal cord differs significantly with the animal situation. Already the sheer difference in size means that axons need to regenerate over tens of centimeters in humans instead of only a few centimeters in animals, particularly in rodents. Furthermore, the cytoarchitecture of the human spinal cord is significantly different when compared to the rat, which is the most frequently used laboratory animal in SCI research. In this respect, the most prominent example is the significance of the rubrospinal and corticospinal tract, which are the major descending axon pathways that project to the spinal cord.

During phylogenetic development, the ability to make precise movements became more and more advantageous, which required increasingly complex motor control systems. Therefore, the red nucleus in the brain stem and its rubrospinal tract that represents the major somatic motor system in phylogenetic more primitive vertebrates was copied to the motor cortex and its corticospinal tract in phylogenetically more advanced mammals. The additional space for projection neurons and supraspinal input in the cortex as compared to the brainstem is paralleled with a much more refined somatopy of the motor cortex when compared to the red nucleus, which has lead to an increased capacity to perform complicated motor tasks. Additionally, the rubrospinal tract consists of considerably less descending fibers in humans than in rats [144]. As a consequence, the rubropsinal tract has only very limited significance for the motor abilities of humans, whereas in rats, the rubrospinal tract is crucial for skilled locomotion [145]. It therefore is not surprising that the comparison of function between humans and animal models of SCI is problematic. This is further explained by the fact that humans are the only obligatory bipedal animals. To a great extent, the unique gait of humans is controlled by supraspinal control [146]. This is in contrast to the locomotion of four-legged animals in which the motor activity of stepping and gait is predominantly controlled by specialized reflex circuits, known as the central pattern generators (CPGs) [147]. Since interneurons only are lost at the injured segment, reflexes remain intact above and below the lesion. Therefore, it is not surprising that even after a severe SCI, locomotion is preserved significantly in four-legged animals as long as the CPG is not affected directly. There are significant differences in the control of locomotion between humans and animals, e.g. the role of

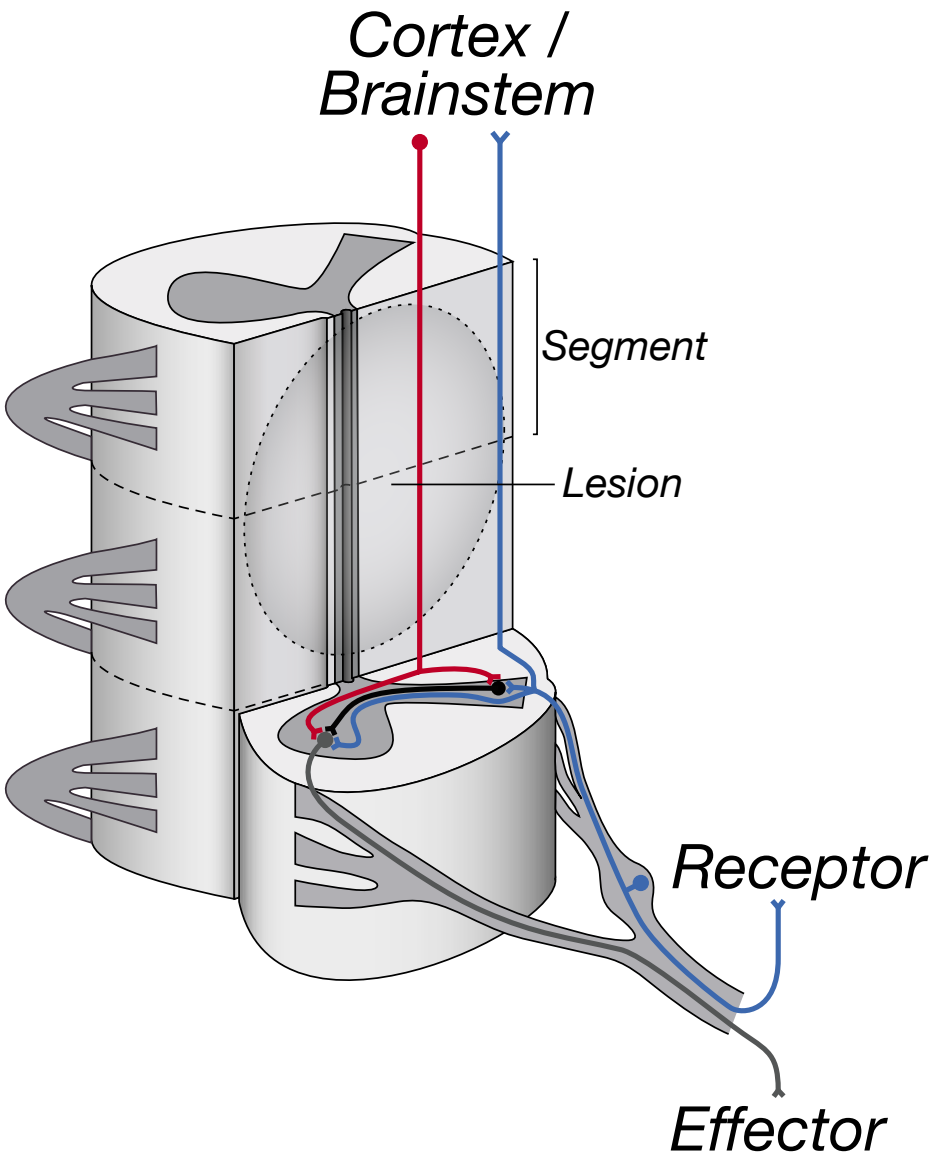

Figure 3: *Schematic graph showing the consequences of SCI on spinal cord projections. Decisive for the functional outcome after SCI is the damage to the long axonal connections in the spinal cord white matter. Mechanical and functional disruption of descending and ascending connections prevents voluntary motor and conscious sensory control, leading to the compartmentalization of the body in a functional and a dysfunctional part. Interneurons only are lost in the injured segments, leaving spinal reflexes intact above and below the injured segments. The blue projection represents the sensory afferent, black the interneuron and grey the lower motor neuron. The corticospinal tract projection is schematized in red.*

the CPG in humans has yet to be clarified [148]. Nevertheless, assessment of locomotor ability is the most frequently employed functional parameter in animal models of SCI [149, 150]. It therefore is important to evaluate whether observed functional recovery of locomotion in SCI animals can be explained by hyperactive reflex responses rather than by reestablishment of functional connections.

The outcome parameters of interest determine the choice for the appropriate SCI animal model. SCI models ideal for the investigation of axonal regeneration may be less suitable for the assessment of function and vice versa. In transection models of SCI for instance, the selective disruption of fiber tracts enables the reliable assessment of the regenerative response of the injured axons. The functional outcome of transection injuries however is less clinically relevant since most SCI represent contusion injuries. Experimental contusion injuries on the other hand are the most relevant in terms of their proximity to pathomechanisms in human SCI [151], but are less reproducible when compared to transection models. Furthermore, the diffuse axonal damage in contusion injuries makes it almost impossible to recognize functional axonal regeneration, since the eventually observed structural and functional recovery cannot be reliably attributed to the regeneration of specific fiber tracts. Alternatively, many alternative models of SCI have been described, including chemical agent induced and aspiration injuries [152-154].

6.2 Cervical dorsal column transection using a tungsten wire knife device

In this thesis, a lesion model for SCI was used in which the cervical dorsal column of rats is specifically transected using a tungsten wire knife device. The stereotactic guidance of the wire knife device allows reproducible transection of the dorsal columns without causing unnecessary damage to the spinal cord grey matter. Unlike suggested by the terminology “wire knife”, the tungsten wire induces a rather blunt transection, causing the formation of a restricted cystic cavity at the lesion site. Because of the minimal disruption of the meninges and surrounding vasculature, a wire knife lesion causes very little vascular disruption (hemorrhage, ischemia) and major invasion of meningeal fibroblasts into the lesion is avoided. The preservation of meningeal sheats allows injecting cell suspension grafts with almost no leaking of cells out of the graft site.

The employed dorsal column transection model is specifically developed to completely lesion the crossed dorsal component of the CST, which represents approximately 95% of all CST axons [155, 156]. The CST plays an important role in the control of fine coordinated movement through its terminations in the ventral horn [157]. However, permanent functional deficits in fine motor tasks such as forelimb reaching are only found when a cervical dorsal column transection injury is combined with a ventral transection of the uncrossed ventral component of the CST [31]. Thus, the isolated transection of the dorsal CST, as used

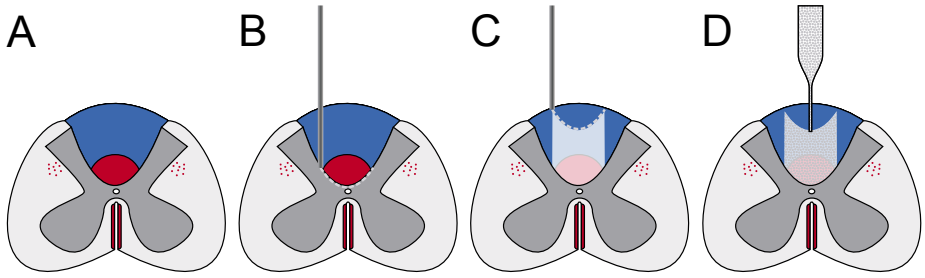

Figure 4: *Schematic representation of the used cervical dorsal column transection model. (A) In rats, the corticospinal tract axons (red) project in the spinal cord through a crossed dorsal component that contains 95% of the axons and an ipsilateral ventral component containing less than 5% of all CST axons. Additionally, there exists a minor dorsolateral component of the CST, containing less than 2% of CST axons. Strikingly, the main part of crossed portion of the CST fibers in humans is located in the dorsolateral component of the CST. The other fibers in the dorsal column (Blue) represent ascending collaterals of the primary sensory afferents and ascending projections of spinal neurons projecting to other segments to the spinal cord. (B) In the used SCI model, a small dural incision is made and the wire knife device is stereotactically lowered into the spinal cord parenchyma. At the correct depth, the tungsten wire is extruded, forming a wire arch below the dorsal CST. (C) Subsequently, the wire knife device with the extruded wire is raised until the tip of the wire is visible, transecting a large part of the dorsal columns, while leaving the dura intact. (D) Directly following the lesion, cellular grafts can be injected into the lesion defect through a pulled glass capillary.*

here, only allows to determine morphological changes, in particular regeneration of corticospinal axons[31]. To a limited extend, ascending proprioceptive axon projections in the dorsal columns will be transected as well. Obvious behavioral alterations have not been observed. The precise functional impact of proprioceptive axon disruption has yet to be determined.

6.3 *Contusive spinal cord injury using the Infinitive Horizon Impactor device*

In addition, a contusion injury model was used in which a blunt spinal cord trauma in adult rats is induced at thoracal level by employing the computer-controlled Infinite Horizon (IH) spinal cord injury device (Precision Systems & Instrumentation, Lexington, USA). The IH impactor allows the execution of a defined force on the exposed surface of the spinal cord that leads to a reproducible and well-defined contusion injury [158]. Unlike the used wire-knife lesion model, a severe contusion injury at thoracal level induces lasting behavioral deficits and thus allows the assessment of behavioral data such as the locomotor ability [150]. Furthermore, the more clinical relevant nature of the contusion injury allows the pathomorphological comparison between the animal model and injured patients. Reproducibility is often problematic with contusion injury models. However, since the IH impactor is equipped with a force-feedback impounder and uses a defined force rather than displacement to define the severity of the contusion injury, highly

reproducible injuries can be induced using this device [158].

7. AIM OF THIS THESIS

The aim of this thesis was to investigate the capacity of grafts of adult derived neural progenitor cells (NPC) to induce structural regeneration and contact-mediated axon guidance in the injured spinal cord. Therefore, the properties of NPC grafts were carefully studied in small animal models of SCI. Furthermore, the isolation of autologous cell material and the ability to genetically modify NPC using viral vectors was investigated. Finally, non-invasive imaging in small animal models of SCI was investigated in order to facilitate future studies in which the potential of NPC grafts to induce functional regeneration in the injured spinal cord is tested.

In *Chapter 2*, we describe the isolation of NPC, survival, differentiation and tissue replacement capacity after transplantation into the acutely lesioned spinal cord. After having determined that NPC grafts require a supporting matrix to replace cystic lesion defects, we developed a co-transplantation protocol using NPC and syngenic skin fibroblasts, which is described in *chapter 3*. Subsequently, Schwann cells, which not only replace cystic lesion defects, but also have intrinsic regeneration promoting capabilities, were studied. In *chapter 4a*, we describe a fast and efficient method to purify adult Schwann cell from peripheral nerve homogenates for autologous cell therapy. Co-transplantation of NPC with Schwann cells is described in *chapter 4b*. The overexpression of ectopic genes using *ex vivo* gene therapy has been shown to represent a promising tool to augment the regenerative potential of grafted cells in a cellular therapy approach, e.g. by overexpressing growth factors. Experiments investigating the applicability of *ex vivo* gene therapy using adult derived NPC are described in *chapter 5*. In order to enable the monitoring of NPC induced regeneration in future studies, non-invasive imaging techniques need to be developed that allow *in vivo* imaging of neuropathological changes in small animal models of SCI. Therefore, high-resolution magnetic resonance imaging of spinal cord injured rats was studied in *chapter 6*. Finally, in *chapter 7*, the presented studies are discussed in respect to their potential to promote functional axonal regeneration after SCI.

8. REFERENCES

1. Cajal, R. y. Degeneration and Regeneration of the Nervous System (Oxford University Press, New York, 1991).
2. Richardson, P. M., McGuinness, U. M. & Aguayo, A. J. Axons from CNS neurons regenerate into PNS grafts. Nature 284, 264-5 (1980).
3. David, S. & Aguayo, A. J. Axonal elongation into peripheral nervous system “bridges” after central nervous system injury in adult rats. Science 214, 931-3 (1981).
4. Kojima, A. & Tator, C. H. Intrathecal administration of epidermal growth factor and fibroblast growth factor 2 promotes ependymal proliferation and functional recovery after spinal cord injury in adult rats. J Neurotrauma 19, 223-38 (2002).

5. Houweling, D. A., Lankhorst, A. J., Gispen, W. H., Bar, P. R. & Joosten, E. A. Collagen containing neurotrophin-3 (NT-3) attracts regrowing injured corticospinal axons in the adult rat spinal cord and promotes partial functional recovery. Exp Neurol 153, 49-59 (1998).
6. Bradbury, E. J. et al. Chondroitinase ABC promotes functional recovery after spinal cord injury. Nature 416, 636-40 (2002).
7. Li, S. & Strittmatter, S. M. Delayed systemic Nogo-66 receptor antagonist promotes recovery from spinal cord injury. J Neurosci 23, 4219-27 (2003).
8. Grill, R., Murai, K., Blesch, A., Gage, F. H. & Tuszynski, M. H. Cellular delivery of neurotrophin-3 promotes corticospinal axonal growth and partial functional recovery after spinal cord injury. J Neurosci 17, 5560-72 (1997).
9. Teng, Y. D. et al. Minocycline inhibits contusion-triggered mitochondrial cytochrome c release and mitigates functional deficits after spinal cord injury. Proc Natl Acad Sci U S A 101, 3071-6 (2004).
10. Roonprapunt, C. et al. Soluble cell adhesion molecule L1-Fc promotes locomotor recovery in rats after spinal cord injury. J Neurotrauma 20, 871-82 (2003).
11. Hauben, E. et al. Vaccination with dendritic cells pulsed with peptides of myelin basic protein promotes functional recovery from spinal cord injury. J Neurosci 23, 8808-19 (2003).
12. Teng, Y. D. et al. Functional recovery following traumatic spinal cord injury mediated by a unique polymer scaffold seeded with neural stem cells. Proc Natl Acad Sci U S A 99, 3024-9 (2002).
13. Z'Graggen, W. J., Metz, G. A., Kartje, G. L., Thallmair, M. & Schwab, M. E. Functional recovery and enhanced corticofugal plasticity after unilateral pyramidal tract lesion and blockade of myelin-associated neurite growth inhibitors in adult rats. J Neurosci 18, 4744-57 (1998).
14. Bracken, M. B. et al. Efficacy of methylprednisolone in acute spinal cord injury. Jama 251, 45-52 (1984).
15. Hurlbert, R. J. The role of steroids in acute spinal cord injury: an evidence-based analysis. Spine 26, S39-46 (2001).
16. Koning, W. & Frowein, R. A. Incidence of spinal cord injury in the Federal Republic of Germany. Neurosurg Rev 12 Suppl 1, 562-6 (1989).
17. Kalsbeek, W. D., McLaurin, R. L., Harris, B. S., 3rd & Miller, J. D. The National Head and Spinal Cord Injury Survey: major findings. J Neurosurg Suppl, S19-31 (1980).
18. Bracken, M. B., Freeman, D. H., Jr. & Hellenbrand, K. Incidence of acute traumatic hospitalized spinal cord injury in the United States, 1970-1977. Am J Epidemiol 113, 615-22 (1981).
19. Sekhon, L. H. & Fehlings, M. G. Epidemiology, demographics, and pathophysiology of acute spinal cord injury. Spine 26, S2-12 (2001).
20. Kraus, J. F., Silberman, T. A. & McArthur, D. L. in Principles of Spine Surgery (eds. Menezes, A. H., Sonntag, V. K. H., Benzel, E. C., Cahill, S. W. & McCormack, P.) 41-58 (McGraw-Hill, New York, 1996).
21. Harris, P., Karmi, M. Z., McClemont, E., Matlhoko, D. & Paul, K. S. The prognosis of patients sustaining severe cervical spine injury (C2-C7 inclusive). Paraplegia 18, 324-30 (1980).
22. Hachen, H. J. Idealized care of the acutely injured spinal cord in Switzerland. J Trauma 17, 931-6 (1977).
23. Dimitrijevic, M. R., Faganel, J., Lehmkuhl, D. & Sherwood, A. Motor control in man after partial or complete spinal cord injury. Adv Neurol 39, 915-26 (1983).
24. Stover, S. L. & Fine, P. R. The epidemiology and economics of spinal cord injury. Paraplegia 25, 225-8 (1987).
25. LoPachin, R. M. & Lehning, E. J. Mechanism of calcium entry during axon injury and degeneration. Toxicol Appl Pharmacol 143, 233-44 (1997).
26. Tator, C. H. in Contemporary management of spinal cord injury (eds. Benzel, E. C. & Tator, C. H.) 15-26 (American Association of Neurological Surgeons, Park Ridge, IL, 1995).

27. Kao, C. C. & Chang, L. W. The mechanism of spinal cord cavitation follwing spinal cord transection. Part 1. A correlated histochemical study. J Neurosurg 46, 197-209 (1977).
28. Shuman, S. L., Bresnahan, J. C. & Beattie, M. S. Apoptosis of microglia and oligodendrocytes after spinal cord contusion in rats. J Neurosci Res 50, 798-808 (1997).
29. Fitch, M. T. & Silver, J., 1999. in CNS Regeneration: Basic Science and Clinical Advances (eds. Tuszynski, M. H. & Kordower, J. H.) 55-88 (Academic Press, San Diego, 1999).
30. Potter, K. & Saifuddin, A. Pictorial review: MRI of chronic spinal cord injury. Br J Radiol 76, 347-52 (2003).
31. Weidner, N., Ner, A., Salimi, N. & Tuszynski, M. H. Spontaneous corticospinal axonal plasticity and functional recovery after adult central nervous system injury. Proc Natl Acad Sci U S A 98, 3513-8 (2001).
32. Frankel, H. K. in Outcomes in Neurological and surgical disorders. (ed. Swash, M.) 181-194 (Cambridge University Press, Cambridge, 1998).
33. Collins, W. F. A review and update of experiment and clinical studies of spinal cord injury. Paraplegia 21, 204-19 (1983).
34. Sandler, A. N. & Tator, C. H. Effect of acute spinal cord compression injury on regional spinal cord blood flow in primates. J Neurosurg 45, 660-76 (1976).
35. Tator, C. H. Update on the pathophysiology and pathology of acute spinal cord injury. Brain Pathol 5, 407-13 (1995).
36. Senter, H. J. & Venes, J. L. Loss of autoregulation and posttraumatic ischemia following experimental spinal cord trauma. J Neurosurg 50, 198-206 (1979).
37. Fairholm, D. & Turnbull, I. Microangiographic study of experimental spinal injuries in dogs and rabbits. Surg Forum 21, 453-5 (1970).
38. Dolan, E. J. & Tator, C. H. The treatment of hypotension due to acute experimental spinal cord compression injury. Surg Neurol 13, 380-4 (1980).
39. Nelson, E., Gertz, S. D., Rennels, M. L., Ducker, T. B. & Blaumanis, O. R. Spinal cord injury. The role of vascular damage in the pathogenesis of central hemorrhagic necrosis. Arch Neurol 34, 332-3 (1977).
40. Goodman, J. H., Bingham, W. G., Jr. & Hunt, W. E. Ultrastructural blood-brain barrier alterations and edema formation in acute spinal cord trauma. J Neurosurg 44, 418-24 (1976).
41. Olney, J. W. & Sharpe, L. G. Brain lesions in an infant rhesus monkey treated with monsodium glutamate. Science 166, 386-8 (1969).
42. Demediuk, P., Daly, M. P. & Faden, A. I. Effect of impact trauma on neurotransmitter and nonneurotransmitter amino acids in rat spinal cord. J Neurochem 52, 1529-36 (1989).
43. Choi, D. W., Koh, J. Y. & Peters, S. Pharmacology of glutamate neurotoxicity in cortical cell culture: attenuation by NMDA antagonists. J Neurosci 8, 185-96 (1988).
44. Stys, P. K., Waxman, S. G. & Ransom, B. R. Ionic mechanisms of anoxic injury in mammalian CNS white matter: role of Na+ channels and Na(+)-Ca2+ exchanger. J Neurosci 12, 430-9 (1992).
45. Stokes, B. T., Fox, P. & Hollinden, G. Extracellular calcium activity in the injured spinal cord. Exp Neurol 80, 561-72 (1983).
46. Schlaepfer, W. W. & Bunge, R. P. Effects of calcium ion concentration on the degeneration of amputated axons in tissue culture. J Cell Biol 59, 456-70 (1973).
47. Esquerro, E., Garcia, A. G. & Sanchez-Garcia, P. The effects of the calcium ionophore, A23187, on the axoplasmic transport of dopamine beta-hydroxylase. Br J Pharmacol 70, 375-81 (1980).
48. Anderson, D. K. et al. Lipid hydrolysis and peroxidation in injured spinal cord: partial protection with methylprednisolone or vitamin E and selenium. Cent Nerv Syst Trauma 2, 257-67 (1985).
49. Banik, N. L., Matzelle, D. C., Gantt-Wilford, G., Osborne, A. & Hogan, E. L. Increased calpain content and progressive degradation of neurofilament protein in spinal cord injury. Brain Res 752, 301-6 (1997).

50. Muller, A. et al. Neisserial porin (PorB) causes rapid calcium influx in target cells and induces apoptosis by the activation of cysteine proteases. Embo J 18, 339-52 (1999).
51. Narita, M. et al. Bax interacts with the permeability transition pore to induce permeability transition and cytochrome c release in isolated mitochondria. Proc Natl Acad Sci U S A 95, 14681-6 (1998).
52. Dykens, J. A. Isolated cerebral and cerebellar mitochondria produce free radicals when exposed to elevated CA2+ and Na+: implications for neurodegeneration. J Neurochem 63, 584-91 (1994).
53. Aust, S. D., Morehouse, L. A. & Thomas, C. E. Role of metals in oxygen radical reactions. J Free Radic Biol Med 1, 3-25 (1985).
54. Yamamoto, M. et al. A possible role of lipid peroxidation in cellular damages caused by cerebral ischemia and the protective effect of alpha-tocopherol administration. Stroke 14, 977-82 (1983).
55. Malecki, A., Garrido, R., Mattson, M. P., Hennig, B. & Toborek, M. 4-Hydroxynonenal induces oxidative stress and death of cultured spinal cord neurons. J Neurochem 74, 2278-87 (2000).
56. Uchida, K. et al. Acrolein is a product of lipid peroxidation reaction. Formation of free acrolein and its conjugate with lysine residues in oxidized low density lipoproteins. J Biol Chem 273, 16058-66 (1998).
57. Popovich, P. G., Wei, P. & Stokes, B. T. Cellular inflammatory response after spinal cord injury in Sprague-Dawley and Lewis rats. J Comp Neurol 377, 443-64 (1997).
58. Dusart, I. & Schwab, M. E. Secondary cell death and the inflammatory reaction after dorsal hemisection of the rat spinal cord. Eur J Neurosci 6, 712-24 (1994).
59. Schmitt, A. B. et al. Major histocompatibility complex class II expression by activated microglia caudal to lesions of descending tracts in the human spinal cord is not associated with a T cell response. Acta Neuropathol (Berl) 100, 528-36 (2000).
60. Bethea, J. R. et al. Systemically administered interleukin-10 reduces tumor necrosis factor-alpha production and significantly improves functional recovery following traumatic spinal cord injury in rats. J Neurotrauma 16, 851-63 (1999).
61. Wada, K., Chatzipanteli, K., Busto, R. & Dietrich, W. D. Role of nitric oxide in traumatic brain injury in the rat. J Neurosurg 89, 807-18 (1998).
62. DeKosky, S. T. et al. Upregulation of nerve growth factor following cortical trauma. Exp Neurol 130, 173-7 (1994).
63. Herx, L. M., Rivest, S. & Yong, V. W. Central nervous system-initiated inflammation and neurotrophism in trauma: IL-1 beta is required for the production of ciliary neurotrophic factor. J Immunol 165, 2232-9 (2000).
64. Hauben, E. et al. Passive or active immunization with myelin basic protein promotes recovery from spinal cord contusion. J Neurosci 20, 6421-30 (2000).
65. Eng, L. F., Reier, P. J. & Houle, J. D. Astrocyte activation and fibrous gliosis: glial fibrillary acidic protein immunostaining of astrocytes following intraspinal cord grafting of fetal CNS tissue. Prog Brain Res 71, 439-55 (1987).
66. Liuzzi, F. J. & Lasek, R. J. Astrocytes block axonal regeneration in mammals by activating the physiological stop pathway. Science 237, 642-5 (1987).
67. Rudge, J. S. & Silver, J. Inhibition of neurite outgrowth on astroglial scars in vitro. J Neurosci 10, 3594-603 (1990).
68. Bush, T. G. et al. Leukocyte infiltration, neuronal degeneration, and neurite outgrowth after ablation of scar-forming, reactive astrocytes in adult transgenic mice. Neuron 23, 297-308 (1999).
69. Faulkner, J. R. et al. Reactive astrocytes protect tissue and preserve function after spinal cord injury. J Neurosci 24, 2143-55 (2004).
70. Beattie, M. S., Hermann, G. E., Rogers, R. C. & Bresnahan, J. C. Cell death in models of spinal cord injury. Prog Brain Res 137, 37-47 (2002).
71. Kao, C. C., Chang, L. W. & Bloodworth, J. M., Jr. Axonal regeneration across transected mammalian

spinal cords: an electron microscopic study of delayed microsurgical nerve grafting. Exp Neurol 54, 591-615 (1977).
72. Yong, C. et al. Apoptosis in cellular compartments of rat spinal cord after severe contusion injury. J Neurotrauma 15, 459-72 (1998).
73. Blight, A. R. Effects of silica on the outcome from experimental spinal cord injury: implication of macrophages in secondary tissue damage. Neuroscience 60, 263-73 (1994).
74. Büngner, O. V. Über die Degenerations und Regenerationsvorgange am Nerven nach Verletzungen. Beitr. Pathol. Anat. 10, 321-387 (1891).
75. Ann, E. S., Mizoguchi, A., Okajima, S. & Ide, C. Motor axon terminal regeneration as studied by protein gene product 9.5 immunohistochemistry in the rat. Arch Histol Cytol 57, 317-30 (1994).
76. Jones, L. L., Margolis, R. U. & Tuszynski, M. H. The chondroitin sulfate proteoglycans neurocan, brevican, phosphacan, and versican are differentially regulated following spinal cord injury. Exp Neurol 182, 399-411 (2003).
77. McKeon, R. J., Schreiber, R. C., Rudge, J. S. & Silver, J. Reduction of neurite outgrowth in a model of glial scarring following CNS injury is correlated with the expression of inhibitory molecules on reactive astrocytes. J Neurosci 11, 3398-411 (1991).
78. Smith-Thomas, L. C. et al. An inhibitor of neurite outgrowth produced by astrocytes. J Cell Sci 107 (Pt 6), 1687-95 (1994).
79. Davies, S. J., Goucher, D. R., Doller, C. & Silver, J. Robust regeneration of adult sensory axons in degenerating white matter of the adult rat spinal cord. J Neurosci 19, 5810-22 (1999).
80. Jones, L. L., Sajed, D. & Tuszynski, M. H. Axonal regeneration through regions of chondroitin sulfate proteoglycan deposition after spinal cord injury: a balance of permissiveness and inhibition. J Neurosci 23, 9276-88 (2003).
81. Snow, D. M., Smith, J. D., Cunningham, A. T., McFarlin, J. & Goshorn, E. C. Neurite elongation on chondroitin sulfate proteoglycans is characterized by axonal fasciculation. Exp Neurol 182, 310-21 (2003).
82. Li, Y. & Raisman, G. Sprouts from cut corticospinal axons persist in the presence of astrocytic scarring in long-term lesions of the adult rat spinal cord. Exp Neurol 134, 102-11 (1995).
83. Kwon, B. K. et al. Survival and regeneration of rubrospinal neurons 1 year after spinal cord injury. Proc Natl Acad Sci U S A 99, 3246-51 (2002).
84. Pasterkamp, R. J. et al. Expression of the gene encoding the chemorepellent semaphorin III is induced in the fibroblast component of neural scar tissue formed following injuries of adult but not neonatal CNS. Mol Cell Neurosci 13, 143-66 (1999).
85. Hagino, S. et al. Slit and glypican-1 mRNAs are coexpressed in the reactive astrocytes of the injured adult brain. Glia 42, 130-8 (2003).
86. Preston, E., Webster, J. & Small, D. Characteristics of sustained blood-brain barrier opening and tissue injury in a model for focal trauma in the rat. J Neurotrauma 18, 83-92 (2001).
87. Giulian, D., Woodward, J., Young, D. G., Krebs, J. F. & Lachman, L. B. Interleukin-1 injected into mammalian brain stimulates astrogliosis and neovascularization. J Neurosci 8, 2485-90 (1988).
88. Moon, L. D. & Fawcett, J. W. Reduction in CNS scar formation without concomitant increase in axon regeneration following treatment of adult rat brain with a combination of antibodies to TGFbeta1 and beta2. Eur J Neurosci 14, 1667-77 (2001).
89. Yong, V. W. et al. Gamma-interferon promotes proliferation of adult human astrocytes in vitro and reactive gliosis in the adult mouse brain in vivo. Proc Natl Acad Sci U S A 88, 7016-20 (1991).
90. Bundesen, L. Q., Scheel, T. A., Bregman, B. S. & Kromer, L. F. Ephrin-B2 and EphB2 regulation of astrocyte-meningeal fibroblast interactions in response to spinal cord lesions in adult rats. J Neurosci 23, 7789-800 (2003).
91. Igarashi, M., Strittmatter, S. M., Vartanian, T. & Fishman, M. C. Mediation by G proteins of signals that

cause collapse of growth cones. Science 259, 77-9 (1993).
92. Chen, M. S. et al. Nogo-A is a myelin-associated neurite outgrowth inhibitor and an antigen for monoclonal antibody IN-1. Nature 403, 434-9 (2000).
93. GrandPre, T., Nakamura, F., Vartanian, T. & Strittmatter, S. M. Identification of the Nogo inhibitor of axon regeneration as a Reticulon protein. Nature 403, 439-44 (2000).
94. Prinjha, R. et al. Inhibitor of neurite outgrowth in humans. Nature 403, 383-4 (2000).
95. Salzer, J. L., Holmes, W. P. & Colman, D. R. The amino acid sequences of the myelin-associated glycoproteins: homology to the immunoglobulin gene superfamily. J Cell Biol 104, 957-65 (1987).
96. McKerracher, L. et al. Identification of myelin-associated glycoprotein as a major myelin-derived inhibitor of neurite growth. Neuron 13, 805-11 (1994).
97. Wang, K. C. et al. Oligodendrocyte-myelin glycoprotein is a Nogo receptor ligand that inhibits neurite outgrowth. Nature 417, 941-4 (2002).
98. Liu, B. P., Fournier, A., GrandPre, T. & Strittmatter, S. M. Myelin-associated glycoprotein as a functional ligand for the Nogo-66 receptor. Science 297, 1190-3 (2002).
99. Fournier, A. E., GrandPre, T. & Strittmatter, S. M. Identification of a receptor mediating Nogo-66 inhibition of axonal regeneration. Nature 409, 341-6 (2001).
100. Oertle, T. et al. Nogo-A inhibits neurite outgrowth and cell spreading with three discrete regions. J Neurosci 23, 5393-406 (2003).
101. Wong, S. T. et al. A p75(NTR) and Nogo receptor complex mediates repulsive signaling by myelin-associated glycoprotein. Nat Neurosci 5, 1302-8 (2002).
102. Yamashita, T., Higuchi, H. & Tohyama, M. The p75 receptor transduces the signal from myelin-associated glycoprotein to Rho. J Cell Biol 157, 565-70 (2002).
103. Bregman, B. S. et al. Recovery from spinal cord injury mediated by antibodies to neurite growth inhibitors. Nature 378, 498-501 (1995).
104. Schnell, L. & Schwab, M. E. Axonal regeneration in the rat spinal cord produced by an antibody against myelin-associated neurite growth inhibitors. Nature 343, 269-72 (1990).
105. Thallmair, M. et al. Neurite growth inhibitors restrict plasticity and functional recovery following corticospinal tract lesions. Nat Neurosci 1, 124-31 (1998).
106. Kim, J. E., Li, S., GrandPre, T., Qiu, D. & Strittmatter, S. M. Axon regeneration in young adult mice lacking Nogo-A/B. Neuron 38, 187-99 (2003).
107. Simonen, M. et al. Systemic deletion of the myelin-associated outgrowth inhibitor Nogo-A improves regenerative and plastic responses after spinal cord injury. Neuron 38, 201-11 (2003).
108. Zheng, B. et al. Lack of enhanced spinal regeneration in Nogo-deficient mice. Neuron 38, 213-24 (2003).
109. Davies, S. J. et al. Regeneration of adult axons in white matter tracts of the central nervous system. Nature 390, 680-3 (1997).
110. Pettigrew, D. B. & Crutcher, K. A. White matter of the CNS supports or inhibits neurite outgrowth in vitro depending on geometry. J Neurosci 19, 8358-66 (1999).
111. Raisman, G. Myelin inhibitors: does NO mean GO? Nat Rev Neurosci 5, 157-61 (2004).
112. Buffo, A. et al. Application of neutralizing antibodies against NI-35/250 myelin-associated neurite growth inhibitory proteins to the adult rat cerebellum induces sprouting of uninjured purkinje cell axons. J Neurosci 20, 2275-86 (2000).
113. Ming, G. L. et al. cAMP-dependent growth cone guidance by netrin-1. Neuron 19, 1225-35 (1997).
114. Loew, K. I., Culbertson, M., Tessier-Lavigne, M. & Tuszynski, M. H. Characterization of the expression of netrin-1 and its receptors DCC, Unc5H1, Unc5H2 and Unc5H3 in the adult intact and lesioned rat spinal cord. Soc. Neurosci. Abstr. 498.5 (2003).
115. Loew, K. I., Bradke, F., Calvo, E., Tessier-Lavigne, M. & Tuszynski, M. H. Gene delivery to the adult spinal cord reduces axonal growth after injury. Soc. Neurosci. Abstr. (2002).

116. Schreyer, D. J. & Skene, J. H. Injury-associated induction of GAP-43 expression displays axon branch specificity in rat dorsal root ganglion neurons. J Neurobiol 24, 959-70 (1993).
117. Broude, E., McAtee, M., Kelley, M. S. & Bregman, B. S. c-Jun expression in adult rat dorsal root ganglion neurons: differential response after central or peripheral axotomy. Exp Neurol 148, 367-77 (1997).
118. Becker, T. et al. Readiness of zebrafish brain neurons to regenerate a spinal axon correlates with differential expression of specific cell recognition molecules. J Neurosci 18, 5789-803 (1998).
119. Bomze, H. M., Bulsara, K. R., Iskandar, B. J., Caroni, P. & Skene, J. H. Spinal axon regeneration evoked by replacing two growth cone proteins in adult neurons. Nat Neurosci 4, 38-43 (2001).
120. Kobayashi, N. R. et al. BDNF and NT-4/5 prevent atrophy of rat rubrospinal neurons after cervical axotomy, stimulate GAP-43 and Talpha1-tubulin mRNA expression, and promote axonal regeneration. J Neurosci 17, 9583-95 (1997).
121. Jakeman, L. B., Wei, P., Guan, Z. & Stokes, B. T. Brain-derived neurotrophic factor stimulates hindlimb stepping and sprouting of cholinergic fibers after spinal cord injury. Exp Neurol 154, 170-84 (1998).
122. Lu, P., Blesch, A. & Tuszynski, M. H. Neurotrophism without neurotropism: BDNF promotes survival but not growth of lesioned corticospinal neurons. J Comp Neurol 436, 456-70 (2001).
123. Gledhill, R. F., Harrison, B. M. & McDonald, W. I. Demyelination and remyelination after acute spinal cord compression. Exp Neurol 38, 472-87 (1973).
124. Bunge, M. B., Holets, V. R., Bates, M. L., Clarke, T. S. & Watson, B. D. Characterization of photochemically induced spinal cord injury in the rat by light and electron microscopy. Exp Neurol 127, 76-93 (1994).
125. Hammang, J. P., Archer, D. R. & Duncan, I. D. Myelination following transplantation of EGF-responsive neural stem cells into a myelin-deficient environment. Exp Neurol 147, 84-95 (1997).
126. Franklin, R. J., Gilson, J. M., Franceschini, I. A. & Barnett, S. C. Schwann cell-like myelination following transplantation of an olfactory bulb-ensheathing cell line into areas of demyelination in the adult CNS. Glia 17, 217-24 (1996).
127. Nathan, P. W. Effects on movement of surgical incisions into the human spinal cord. Brain 117 (Pt 2), 337-46 (1994).
128. Hall, E. D., Yonkers, P. A., Taylor, B. M. & Sun, F. F. Lack of effect of postinjury treatment with methylprednisolone or tirilazad mesylate on the increase in eicosanoid levels in the acutely injured cat spinal cord. J Neurotrauma 12, 245-56 (1995).
129. Teng, Y. D. & Wrathall, J. R. Local blockade of sodium channels by tetrodotoxin ameliorates tissue loss and long-term functional deficits resulting from experimental spinal cord injury. J Neurosci 17, 4359-66 (1997).
130. McTigue, D. M., Popovich, P. G., Jakeman, L. B. & Stokes, B. T. in Neural plasticity and regeneration 3-8 (Elsevier, 2000).
131. Jones, L. L., Oudega, M., Bunge, M. B. & Tuszynski, M. H. Neurotrophic factors, cellular bridges and gene therapy for spinal cord injury. J Physiol 533, 83-9 (2001).
132. Benowitz, L. I., Goldberg, D. E., Madsen, J. R., Soni, D. & Irwin, N. Inosine stimulates extensive axon collateral growth in the rat corticospinal tract after injury. Proc Natl Acad Sci U S A 96, 13486-90 (1999).
133. Steward, O. Reorganization of neuronal connections following CNS trauma: principles and experimental paradigms. J Neurotrauma 6, 99-152 (1989).
134. Raisman, G. Olfactory ensheathing cells - another miracle cure for spinal cord injury? Nat Rev Neurosci 2, 369-75 (2001).
135. Zhang, F., Ferretti, P. & Clarke, J. D. Recruitment of postmitotic neurons into the regenerating spinal cord of urodeles. Dev Dyn 226, 341-8 (2003).
136. Kuhlengel, K. R., Bunge, M. B., Bunge, R. P. & Burton, H. Implantation of cultured sensory neurons and Schwann cells into lesioned neonatal rat spinal cord. II. Implant characteristics and examination

of corticospinal tract growth. J Comp Neurol 293, 74-91 (1990).
137. Kromer, L. F. & Cornbrooks, C. J. Transplants of Schwann cell cultures promote axonal regeneration in the adult mammalian brain. Proc Natl Acad Sci U S A 82, 6330-4 (1985).
138. Graziadei, P. P. & Graziadei, G. A. Neurogenesis and neuron regeneration in the olfactory system of mammals. I. Morphological aspects of differentiation and structural organization of the olfactory sensory neurons. J Neurocytol 8, 1-18 (1979).
139. Ramon-Cueto, A., Plant, G. W., Avila, J. & Bunge, M. B. Long-distance axonal regeneration in the transected adult rat spinal cord is promoted by olfactory ensheathing glia transplants. J Neurosci 18, 3803-15 (1998).
140. Li, Y., Field, P. M. & Raisman, G. Repair of adult rat corticospinal tract by transplants of olfactory ensheathing cells. Science 277, 2000-2 (1997).
141. Reynolds, B. A. & Weiss, S. Generation of neurons and astrocytes from isolated cells of the adult mammalian central nervous system. Science 255, 1707-10 (1992).
142. Reynolds, B. A., Tetzlaff, W. & Weiss, S. A multipotent EGF-responsive striatal embryonic progenitor cell produces neurons and astrocytes. J Neurosci 12, 4565-74 (1992).
143. McDonald, J. W. et al. Transplanted embryonic stem cells survive, differentiate and promote recovery in injured rat spinal cord. Nat Med 5, 1410-2 (1999).
144. Nathan, P. W. & Smith, M. C. The rubrospinal and central tegmental tracts in man. Brain 105, 223-69 (1982).
145. Webb, A. A. & Muir, G. D. Unilateral dorsal column and rubrospinal tract injuries affect overground locomotion in the unrestrained rat. Eur J Neurosci 18, 412-22 (2003).
146. Malouin, F., Richards, C. L., Jackson, P. L., Dumas, F. & Doyon, J. Brain activations during motor imagery of locomotor-related tasks: a PET study. Hum Brain Mapp 19, 47-62 (2003).
147. Grillner, S. Neurobiological bases of rhythmic motor acts in vertebrates. Science 228, 143-9 (1985).
148. Dimitrijevic, M. R., Gerasimenko, Y. & Pinter, M. M. Evidence for a spinal central pattern generator in humans. Ann N Y Acad Sci 860, 360-76 (1998).
149. Gale, K., Kerasidis, H. & Wrathall, J. R. Spinal cord contusion in the rat: behavioral analysis of functional neurologic impairment. Exp Neurol 88, 123-34 (1985).
150. Basso, D. M., Beattie, M. S. & Bresnahan, J. C. A sensitive and reliable locomotor rating scale for open field testing in rats. J Neurotrauma 12, 1-21 (1995).
151. Metz, G. A. et al. Validation of the weight-drop contusion model in rats: a comparative study of human spinal cord injury. J Neurotrauma 17, 1-17 (2000).
152. Houle, J. D. Demonstration of the potential for chronically injured neurons to regenerate axons into intraspinal peripheral nerve grafts. Exp Neurol 113, 1-9 (1991).
153. Long, J. B., Rigamonti, D. D., Oleshansky, M. A., Wingfield, C. P. & Martinez-Arizala, A. Dynorphin A-induced rat spinal cord injury: evidence for excitatory amino acid involvement in a pharmacological model of ischemic spinal cord injury. J Pharmacol Exp Ther 269, 358-66 (1994).
154. Liu, D., Xu, G. Y., Pan, E. & McAdoo, D. J. Neurotoxicity of glutamate at the concentration released upon spinal cord injury. Neuroscience 93, 1383-9 (1999).
155. Vahlsing, H. L. & Feringa, E. R. A ventral uncrossed corticospinal tract in the rat. Exp Neurol 70, 282-7 (1980).
156. Joosten, E. A., Schuitman, R. L., Vermelis, M. E. & Dederen, P. J. Postnatal development of the ipsilateral corticospinal component in rat spinal cord: a light and electron microscopic anterograde HRP study. J Comp Neurol 326, 133-46 (1992).
157. Liang, F. Y., Moret, V., Wiesendanger, M. & Rouiller, E. M. Corticomotoneuronal connections in the rat: evidence from double-labeling of motoneurons and corticospinal axon arborizations. J Comp Neurol 311, 356-66 (1991).
158. Scheff, S. W., Rabchevsky, A. G., Fugaccia, I., Main, J. A. & Lumpp, J. E., Jr. Experimental modeling of spinal cord injury: characterization of a force-defined injury device. J Neurotrauma 20, 179-93 (2003).

Chapter 2

Adult neural progenitor cell grafts survive after acute spinal cord injury and integrate along axonal pathways

Europ. J. Neurosci., 18; 743-751 (2003)

Maurice Vroemen
Ludwig Aigner
Juergen Winkler
Norbert Weidner

ABSTRACT

The main rationale for cell-based therapies following spinal cord injury are the 1) replacement of degenerated spinal cord parenchyma by an axon growth supporting scaffold, 2) remyelination of regenerating axons and 3) local delivery of growth promoting molecules. A potential source to meet these requirements are adult neural progenitor cells, which were examined in the present study. Fibroblast growth factor 2 responsive adult spinal cord derived syngenic neural progenitor cells were either genetically modified *in vitro* to express green fluorescent protein (GFP) using retroviral vectors or prelabeled with bromodeoxyuridine (BrdU). Neural progenitor cells revealed antigenic properties of neurons and glial cells *in vitro* confirming their multipotency. This differentiation pattern was unaffected by retroviral transduction. GFP expressing or BrdU prelabeled neural progenitor cells were grafted as neurospheres directly into the acutely injured rat cervical spinal cord. Animals with lesions only served as controls. Three weeks postoperatively, grafted neural progenitor cells integrated along axonal profiles surrounding the lesion site. In contrast to observations in culture, grafted neural progenitor cells differentiated only into astro- and oligodendroglial lineages supporting the notion that the adult spinal cord provides molecular cues for glial, but not for neuronal differentiation. This study demonstrates that adult neural progenitor cells will survive after transplantation into the acutely injured spinal cord. The observed oligodendroglial and astroglial differentiation, and integration along axonal pathways represent important prerequisites for potential remyelination and support of axonal regrowth.

1. INTRODUCTION

The traumatic lesion of the mammalian spinal cord is followed by the degeneration of spinal cord specific cells such as astroglia, oligodendroglia and neurons in and around the lesion site. Ultimately a cystic lesion defect will persist, which, besides the lack of growth promoting molecules and the upregulation of growth inhibitory components [1-4], represents a key factor impeding the regeneration of injured axons. The extent of intrinsic cell renewal alone [5], even after application of mitogenic agents such as epidermal growth factor (EGF) and fibroblast growth factor 2 (FGF-2) [6, 7], is not sufficient to allow substantial recovery following spinal cord injury [8]. Therefore, exogenous cell replacement strategies have to be considered.

Ideally, cellular candidates for transplantation should be able to replace the function of astrocytes, which build the cellular scaffold of the spinal cord parenchyma and may provide guidance cues for regenerating axons, and oligodendrocytes, which myelinate axons, thus allowing proper nerve conduction. The replacement of neurons is negligible in spinal cord injury, since only neurons at the injured segmental level are lost and therefore contribute only minimally to the

functional deficits observed after spinal cord injury. The use of cellular grafts as vehicles to locally deliver growth promoting molecules is desirable. Various cell types such as fibroblasts, Schwann cells and olfactory ensheathing cells have been analyzed for their regenerative capacity after transplantation into the injured spinal cord [9-14]. Cell based therapies were able to substitute for the loss of glial cells to some degree and to mediate the application of growth promoting factors, however, structural and functional recovery was moderate at best.

Organotypic cell replacement can be achieved with neural progenitor cells (NPC). NPC from embryonic as well as adult central nervous system (CNS) tissue have the capacity for self-renewal and multipotency [15, 16]. After delayed transplantation of embryonic derived NPC into the injured rat spinal cord differentiation into glial and neuronal lineages as well as modest functional improvement have been reported [17-19]. However, ethical concerns and the limited availability restrict the large-scale use of embryonic derived NPC. To prevent rejection of allogenic embryonic cells after transplantation, suppression of the host immune system is required, which represents another major disadvantage of embryonic derived neural cell grafts. In contrast, the patients' own cells could be utilized to obtain adult NPC, thus avoiding issues regarding chronic immunosuppression and ethical concerns, as they would apply for embryonic cell sources. Transplantation of adult NPC into the intact spinal cord of adult rats revealed that grafted cells survived, migrated over considerable distances within the spinal cord and differentiated into astroglial and oligodendroglial cells [20]. Subventricular zone derived adult NPC survived after delayed transplantation (at least 7 days after the injury) into the spinal cord parenchyma surrounding the spinal cord injury site [21]. Grafted adult NPC differentiated into astroglial lineages; oligodendroglial and neuronal differentiation was not observed in the lesion condition.

The aim of the present study was to determine whether adult spinal cord derived NPC will survive transplantation directly into the acutely injured spinal cord lesion site, replace degenerated spinal cord parenchyma and promote regeneration of selectively disrupted corticospinal tract (CST) axons.

2. MATERIALS AND METHODS

2.1 Animal subjects

Adult female Fischer 344 rats weighing 160-180 g were used as donors for the isolation of NPC and for the transplantation experiments. All experiments were carried out in accordance with the European Communities Council Directive (86/609/EEC) and institutional guidelines. All efforts were made to minimize the number of animals used and their suffering.

2.2 Preparation of adult NPC

Rats were deeply anesthetized using a cocktail of ketamine (62.5 mg/kg; WDT, Garbsen, Germany), xylazine (3.175 mg/kg; WDT, Garbsen, Germany) and acepromazine (0.625 mg/kg, Sanofi-

Ceva, Düsseldorf, Germany) in 0.9% sterile saline solution and killed by decapitation. The region of the complete cervical enlargement (spinal cord level C3 through T1) was dissected out. After removal of the dura, the tissue was minced, washed in sterile Dulbecco's phosphate buffered saline/D-glucose (4.5 g/l; PAA Laboratories, Linz, Austria) and digested in a solution of papain (0.01%; Worthington Biochemicals, Lakewood, USA), neutral protease (0.1%; Roche, Mannheim, Germany), DNase I (0.01%; Worthington Biochemicals) and 12.4 mM $MgSO_4$, dissolved in Hank's balanced salt solution (HBSS; PAA Laboratories, Linz, Austria) for 30 min at 37°C. The digested tissue was centrifuged at 120 x g for 5 min at 4°C and washed three times in DMEM-HAMS F12 (Pan Biotech, Aidenbach, Germany), supplemented with 10% fetal calf serum (FCS; Pan Biotech, Aidenbach, Germany). The cells were transferred to culture dishes containing serum-free growth medium, which consists of Neurobasal medium with B27 supplement (both Gibco, Karlsruhe, Germany) and 20 ng/ml recombinant human FGF-2 (R&D System, Wiesbaden, Germany). Neurobasal medium with B27 supplement has been shown to substantially increase the proliferation rate of NPC *in vitro* [22] as compared to standard proliferation medium consisting of DMEM/F12 and N2 supplement [23, 24]. Cells were either grown as neurospheres in uncoated cell culture flasks or as adherent monolayers in culture flasks, which were coated as follows: flasks were incubated with 20 µg/cm² poly-l-ornithine (Sigma) in distilled H_2O for 2 h at 37°C, rinsed and incubated with 0.4µg/cm2 laminin (Sigma) in PBS for 2 h at 37°C. The cell culture medium was changed twice per week. In neurosphere cultures, the medium was replaced by centrifuging the medium containing neurospheres at 120 x g for 5min at 4°C, removing the supernatant and resuspending the cells in fresh growth medium. Cell cultures were passaged in 2 week intervals. Monolayer cultures were detached by incubation with 40 ml/cm² Acccutase (Innovative Cell Tech, San Diego, USA) for 5min at 37°C. Finally, the cells were centrifuged at 120 x g for 5min at 4°C and resuspended in fresh growth medium. Passaging of neurospheres was performed as follows: the medium containing the neurospheres was collected in a 15 ml centrifuge tube and centrifuged at 120 x g for 5min at 4°C. The pellet was resuspended in 1 ml of Accutase™ and incubated at 37°C for 10 min. The neurospheres were resuspended in growth medium, triturated and centrifuged at 120 x g for 5 min at 4°C. After counting an aliquot of the resulting single cell suspensions in a hemocytometer, 3000 cells/cm² were plated in fresh growth medium.

2.3 Retroviral transduction of adult NPC

Adult NPC were genetically modified to express the reporter gene green-fluorescent protein (GFP) as previously described for Schwann cells and fibroblasts [13, 25]. The coding sequence for GFP was cloned into the multiple cloning site of the Moloney leukemia virus-derived retroviral

vector pLXSN (Clontech, Heidelberg, Germany). The 293T cell line based Phoenix amphotrophic producer cells (Gary Nolan, Stanford, USA) were grown in DMEM medium supplemented with 10% FCS and transfected with the retroviral construct. After two days, the virus-containing medium was collected, filtered through a 0.45 µm syringe filter and stored at -80°C. The resulting virus contained the neomycin resistance gene under control of the SV40 promoter and the GFP transgene under control of the constitutively active Moloney murine sarcoma virus-derived 5' LTR promoter sequences.

Adult NPC taken from passage number 6 neurospheres were split 1:3 one day before transduction. The cells were incubated for 8 h on two consecutive days with retrovirus containing growth medium supplemented with 1 µg/ml Polybrene (Sigma). To select for cells, which integrated the retroviral vector, G418 (500 µg/ml; Gibco Karlsruhe, Germany) was added to the growth medium. Successful incorporation of the transgene was confirmed by detection of GFP using an inverted fluorescence microscope (Olympus IX 70).

2.4 In Vitro immunocytochemistry

To obtain monolayer cultures, neurospheres of established cultures were dissociated using Accutase (Innovative Cell Tech, San Diego, USA) and plated on poly-l-ornithine/laminin (P-Orn/Lam, Sigma) coated glass coverslips. To induce differentiation, the cells were incubated for 7 days in medium, in which FGF-2 was replaced by 1% FCS (Pan Biotech, Aidenbach, Germany).

The following antibodies were used to analyze the differentiation pattern of adult NPC *in vitro*: mouse-anti-nestin for progenitor/stem cells (Pharmingen, Heidelberg, Germany; at 1/1000), mouse-anti-GFAP for astroglia (Chemicon, Hofheim, Germany; at 1/600), mouse-anti-GalC for oligodendroglia (Chemicon, Hofheim, Germany; at 1/500) and mouse-anti-beta-III-tubulin for neurons (clone TUJ1; Babco, Richmond, USA; at 1/500).

Cells were washed three times with tris-buffered saline (TBS) after fixation with 4% paraformaldehyde in PBS, blocked with TBS containing 3% donkey serum/0,1% Triton-X (Sigma) and incubated overnight with the primary antibody in TBS + 3% donkey serum + 0.1% Triton-X at 4°C. The following day, cells were washed with TBS and incubated with rhodamine-X linked secondary donkey-anti-mouse antibodies (Jackson, Hamburg, Germany; at 1/1000) in TBS + 3% donkey serum + 0.1% Triton-X for 2h. Finally, nuclei were counterstained with Hoechst 33342 (2 µg/ml in TBS; Sigma). The coverslips were mounted onto glass slides using Prolong-Antifade (Molecular Probes, Leiden, Netherlands). For the immunocytochemical analysis, 8 bit monochrome pictures were taken at 20x magnification on a fluorescent microscope (Leica DMR) equipped with a Spot CCD camera model 2.2.1 (Diagnostic Instruments, Sterling Heights, USA). Three independently performed immunocytochemical stains were analyzed in expansion and differentiation conditions. Immunoreactive cells were determined in

Table 1: *Immunohistochemical Markers for Adult NPC Differentiation*

Neural progenitor cells	Nestin (Pharmingen)
Glial precursor cells	NG2 (B. Stallcup)
Radial glia	BLBP (N. Heintz)
Astroglia	GFAP (DAKO)
Oligodendroglia	GalC (Chemicon), APC (Oncogene)*
Neurons	Beta-III-tubulin, (Babco, Promega)

GalC was used for detection of oligodendroglial differentiation in vitro only. In vivo only cells, which were APC positive and at the same time GFAP negative, were classified as oligodendroglia.

5 random fields per immunocytochemical stain in relation to all cells present within the field (= number of Hoechst counterstained nuclei).

2.5 Preparation of adult NPC for transplantation

Adult NPC, either retrovirally transduced to express the reporter gene GFP as described above (NPC-GFP) or incubated 48h before transplantation with a 1µM solution of the proliferation marker bromodeoxyuridine (BrdU; Sigma) in the growth medium (NPC-BrdU), were transplanted. To control for the stable expression of the GFP reporter gene, a subgroup of adult GFP expressing NPC was prelabeled with BrdU (**NPC-GFP/BrdU**). The respective cells, kept as neurospheres in uncoated cell culture flasks, were cut into fragments (average size 200µm) using a McIlwain Tissue Chopper (Mickle Engineering, Gomshall, United Kingdom) [26]. To estimate the number of adult NPC, three samples (100µl each) from uncoated cell culture flasks containing the neurosphere fragments were taken and dissociated with Accutase (Innovative Cell Tech, San Diego, USA). The resulting single cell suspension was stained with Trypan Blue (Sigma) and counted using a Neubauer hemocytometer. The remaining neurosphere fragments were washed twice and resuspended in PBS to yield the final concentration of 1.6-1.8 x 10^5 cells/µl ready for transplantation.

2.6 Surgical procedures

Animals were anesthetized using a cocktail of ketamine, xylazine and acepromazine as described above. Spinal cord dorsal column transections at cervical level C3 and anterograde labeling of the CST were performed as previously described [27, 28].

After a stereotactically guided transection of the dorsal CST with a tungsten wire knife (David Kopf Instruments, Tujuna, USA) at cervical level C3, a total volume of 3 µl cell suspension containing 4.8-5.4 x 10^5 cells (n=8 **NPC-BrdU**; n=8 **NPC-GFP**; n=4 **NPC-GFP/BrdU**) was injected directly into the lesion site through a pulled glass micropipette (200µm internal diameter) using a Picospritzer II (General Valve, Fairfield, USA). Animals receiving spinal cord lesions without cell transplantation (n=6) served as controls. Supernatant from the last washing step after BrdU incubation was injected into 2 animals

(3µl per animal) to control for extracellular BrdU contamination in the cell suspension, which would produce unspecific labeling of proliferating host cells.

For anterograde tracing of the CST projections, 300 nl of a 10% solution of biotinylated dextran-amine (BDA; 10.000 MW, Molecular Probes, Leiden, Netherlands) was injected through pulled glass micropipettes (40 µm internal diameter) into each of 18 sites per hemisphere spanning the rostrocaudal extent of the rat forelimb and hindlimb sensorimotor cortex using a PicoSpritzer II [27] 1 week post lesioning/grafting.

2.7 Morphological analysis

At 3 weeks post lesioning/grafting, animals were transcardially perfused with a 0.9% saline solution followed by 4% paraformaldehyde in PBS. Sagittal 35µm cryostat sections were processed for visualization of the BDA-labeled CST and for immunohistochemistry. Every seventh section was taken for Nissl staining to determine the cystic lesion size.

Double/triple labeling immunofluorescence techniques were performed to assess cell survival, differentiation pattern and interaction of grafted adult NPC with injured CST axons. The following primary antibodies were used: rabbit-anti-BLBP (for radial glia; generous gift N. Heintz, Rockefeller University, New York, USA; at 1/1000), rabbit-anti-GFAP (for astrocytes; DAKO, Glostrup, Denmark; at 1/200), mouse-anti-APC (for oligodendrocytes, Oncogene, Darmstadt, Germany; at 1/1000), mouse-anti-beta-III-tubulin (for neurons; Promega, Mannheim, Germany; at 1/100) and rabbit-anti-NG2 (for glial restricted precursor cells; generous gift B. Stallcup, Burnham Institute, La Jolla, USA; at 1/500), all visualized using rhodamine-X linked donkey secondary antibodies (Jackson, Hamburg, Germany; at 1/1000). BrdU-prelabeled grafted cells were identified with a rat-anti-BrdU antibody (Harlan SeraLab, Loughborough, UK; at 1/500) visualized using fluorescein linked donkey secondary antibodies (Jackson, Hamburg, Germany; at 1/1000). GFP expressing grafted NPC were visualized by using a rabbit-anti-GFP antibody (Molecular Probes, Leiden, Netherlands; at 1/750). To assess the number of dividing grafted NPC double immunofluorescence labeling was performed with the proliferation marker mouse-anti-Ki-67 (Dianova, Hamburg, Germany; at 1/50).

Sections were rinsed in TBS (0.1M), incubated in TBS + 3% donkey serum + 0.1% Triton-X for 1h, then transferred into the first primary antibody and incubated overnight at 4°C on a rotating platform. For visualization of BrdU-prelabeled adult NPC the staining protocol was modified as follows: after rinsing in TBS, sections were incubated for 1h in 50% formamide/2xSSC (0.3 M NaCl, 0.03M sodium citrate) at 65ºC. Sections were rinsed in 2xSSC, incubated for 30min in 2 N HCl at 37ºC, and rinsed for 10min in 0.1 M boric acid pH 8.5. After rinsing in TBS, the protocol continued with the incubation in TBS + 3% donkey serum + 0.1% Triton-X as described above. The following day, sections were rinsed and incubated with fluo-

rescence (rhodamine-X, fluorescein, Cy5) conjugated secondary donkey antibodies (Jackson, Hamburg, Germany; at 1/1000) for 2.5 h. BDA-labeled CST axons were visualized by incubation with Cy5-conjugated streptavidin (Jackson, Hamburg, Germany; at 1/1000). After a final rinsing step in TBS, sections were mounted onto glass slides and coverslipped with ProLong Antifade Kit (Molecular Probes, Leiden, Netherlands). Immunohistochemical analysis was performed with a confocal fluorescence microscope (Leica TCS-NT). Co-localization of BrdU prelabeled NPC with the individual differentiation marker was determined by analyzing between 15-20 optical sections through the z-axis of a 35 µm thick section. Co-localization was confirmed, once the differentiation marker was spatially associated to BrdU nuclear labeling through subsequent optical sections in the z-axis. For brightfield microscopic immunohistochemical analysis of BDA-labeled CST axons, sections were incubated overnight with avidin biotinylated peroxidase complex (Vector Elite Kit, Vector Laboratories, Wertheim, Germany; at 1/1000) with TBS, followed by treatment for 5min with a 0.05% solution of 3,38-diaminobenzidine, 0.01% H_2O_2, and 0.04% nickel chloride in TBS (brown-black reaction product).

The cystic lesion size was assessed on serial sagittal Nissl stained sections in 210 µm intervals. Images containing the cystic lesion area were captured at 5x magnification on a Leica DMR microscope with a Spot CCD camera model 2.2.1 (Diagnostic Instruments, Michigan, USA). The lesion area was determined by measuring the number of pixels within cystic lesion areas using NIH Image software (version 1.62), which was converted into mm^2. Regenerative responses of CST axons were determined by looking for BDA-labeled and DAB visualized axonal profiles reaching into the cystic lesion center or ventrally around it using a LEICA DMR microscope at 40x magnification in one sagittal section per animal going through the main part of the dorsal CST.

3. RESULTS

3.1 In vitro characterization of adult NPC

The aim of the *in vitro* analysis in the present study was to validate the differentiation pattern in comparison to previous studies [20, 23], and to determine whether retroviral gene transfer may cause a shift in the differentiation pattern of FGF-2 responsive adult NPC. Cells, which were isolated from the adult rat spinal cord at cervical level and plated as monolayers on P-Orn/Lam coated glass coverslips, appear as typical uniform small cells with thin processes (Fig. 1A). Cells maintained in uncoated culture flasks form three-dimensional cell conglomerates (neurospheres) (Fig. 1B). After introducing the reporter gene GFP into NPC using a retroviral vector, which drives GFP expression by a 5' long terminal repeat promoter, transgene expression is detectable *in vitro* over at least 6 passages and a 2 months period (Fig. 1C).

In proliferation conditions using FGF-2, NPC primarily express nestin (19.9% ±

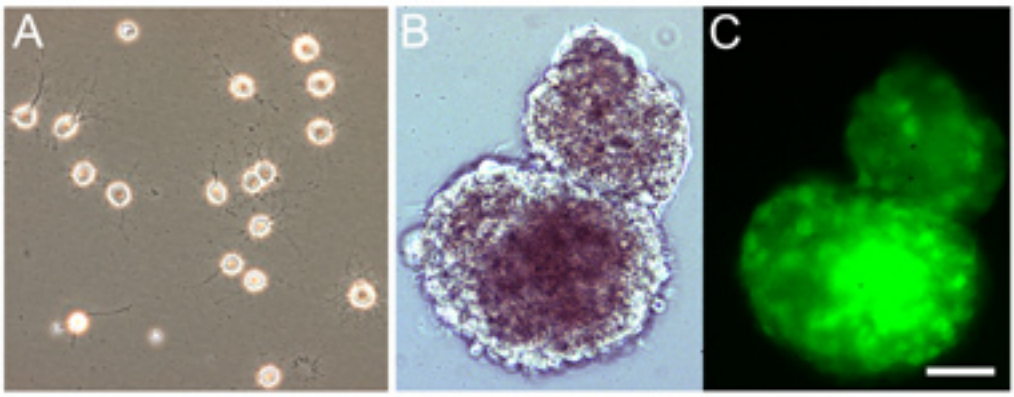

***Figure 1**: Isolation and genetic modification of adult NPC in vitro. NPC isolated from the adult cervical spinal cord were grown (A) as monolayers attached to P-Orn/Lam coated surfaces or (B) as free-floating neurospheres. Phase contrast micrograph. (C) Fluorescence microscopic analysis of the same neurosphere confirms a high transduction efficacy of adult NPC, which have been genetically modified to express GFP using a retroviral vector. Scale bar A 50µm, B, C 75µm.*

6.7) indicating the presence of undifferentiated cells, and the early neuronal marker beta-III-tubulin (18.1% ± 1.7). No cells are found with antigenic properties of astroglia (GFAP expression) or oligodendroglia (GalC expression) (Fig. 2, 3A). After incubation of NPC with 1% FCS instead of FGF-2 (differentiation condition) for one week, nestin immunoreactive cells disappear completely, whereas cells immunoreactive for the oligodendroglial marker GalC increase significantly (15.0% ± 6.5), indicating a shift from undifferentiated towards differentiated cells. The detection of early neuronal antigenicity (beta-III-tubulin) is unchanged in differentiation medium (21.2% ± 3.1). The yield of GFAP expressing cells indicating astroglial differentiation remains low (0.8% ± 0.2), even in differentiation medium (Fig. 2, 3B).

Quantitative analysis of cell differentiation after the introduction of the reporter gene GFP through a retroviral vector diluted in serum-containing supernatant reveals no significant changes compared to unmodified NPC in both, proliferation and differentiation conditions. There is a tendency for decreased neuronal antigenicity in GFP transgenic NPC (beta-III-tubulin expression 10.4% ± 3.3), which is not significantly different compared to unmodified NPC (p=0.073) (Fig. 3).

3.2 Survival, proliferation, transgene expression and differentiation of adult NPC in vivo

Adult NPC, either prelabeled with BrdU *in vitro* or genetically modified to express the reporter gene GFP, were transplanted as small neurosphere suspensions right after a cervical wire knife dorsal column transection directly into the injury site. At 3 weeks post injury/transplantation, detailed morphological analysis was performed. NPC readily survive following transplantation into the acutely injured spinal cord as

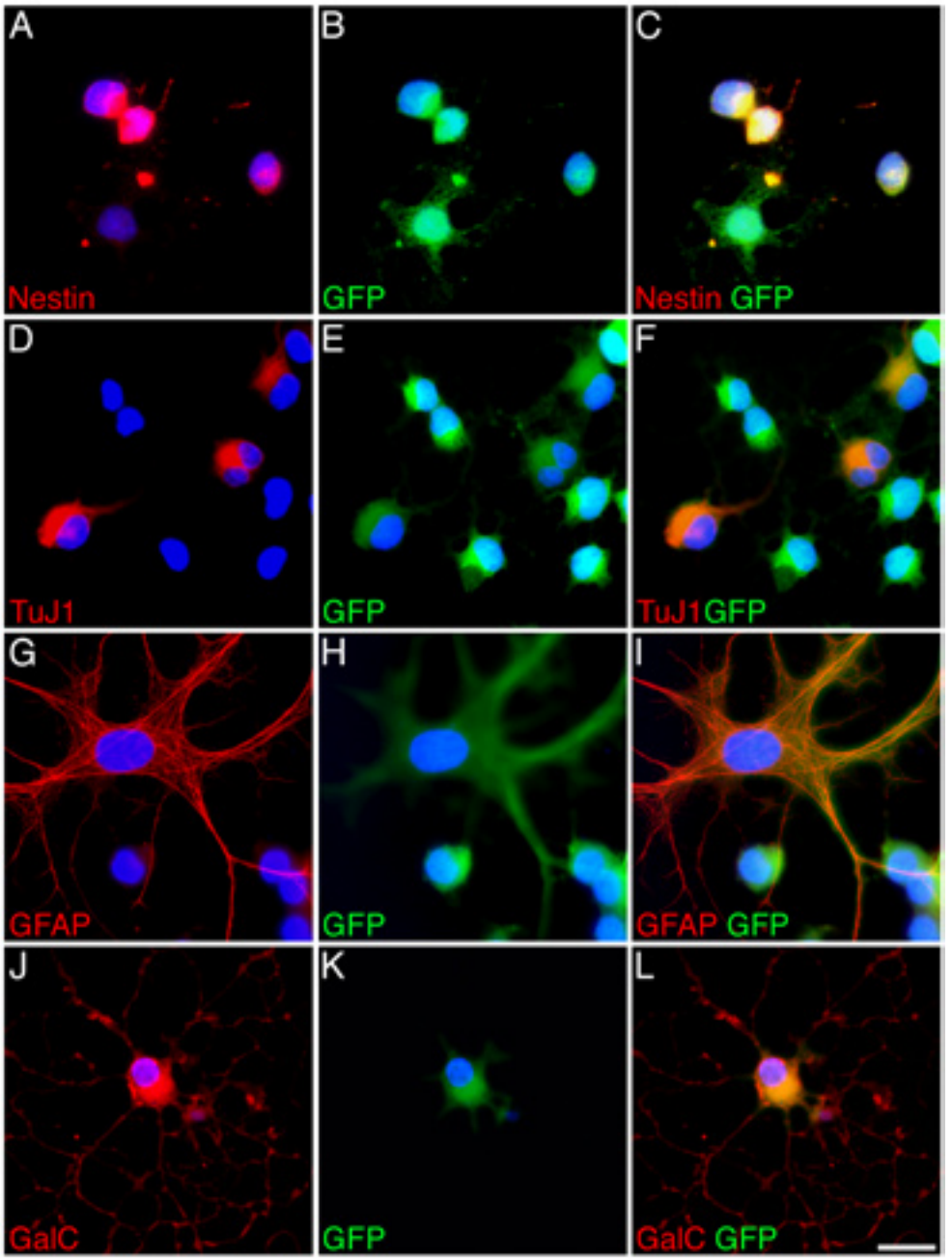

Figure 2: *Differentiation pattern of adult NPC in vitro. The typical immunocytochemical appearance of adult NPC in vitro is exemplified for nestin and beta-III-tubulin in proliferation conditions (FGF-2 added) (A-F), whereas cells expressing GFAP or GalC are shown in differentiation conditions (1% FCS added) (G-L). (A-C) Nestin for neural stem/progenitor cells, (D-F) beta-III-tubulin (clone TUJ1) for neurons, (G-I) GFAP for astroglial cells and (J-L) GalC for oligodendroglia. All differentiation markers are shown in red. Merging of the differentiation markers and GFP (shown in green) confirm the transgene expression in undifferentiated (C) and differentiated cells (F, I, L). Hoechst 33342 as nuclear counterstain (shown in blue). Scale bar A-L 20 µm.*

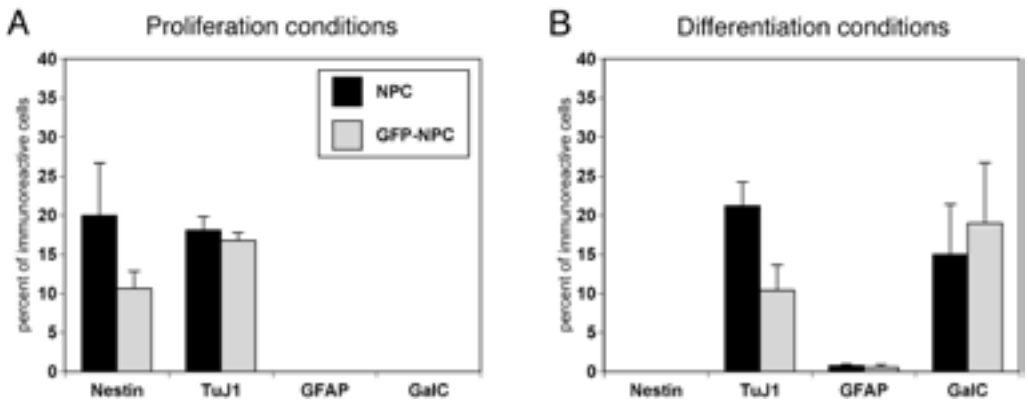

Figure 3: *Quantitative analysis of the differentiation pattern of adult NPC in vitro. (A) Adult NPC maintained in proliferation conditions with FGF-2 or (B) differentiation conditions with 1% FCS. The error bars reflect the standard error of the mean.*

indicated by the widespread detection of BrdU-prelabeled cells. NPC are found predominantly in a dense rim surrounding the cystic lesion and along the central canal (Fig. 4A). NPC detection decreases caudally and rostrally to the lesion site. Cells are found up to 3mm away from the lesion site in the rostral-caudal direction, confirming their migratory capacity. Almost no cells are found ventral to the grafting site in the dorsal column suggesting that migration in the dorso-ventral direction is restricted. BrdU contamination of the NPC containing medium can be excluded, because no BrdU immunoreactivity around the injection site is detectable in control animals receiving injections of supernatant from the last washing step after BrdU incubation into the spinal cord (data not shown). Injection of neural precursor cells, which were killed prior to transplantation by freeze-thaw cycles, did not reveal any unspecific BrdU immunoreactivity in host cells by means of BrdU washed out from dying grafted cells [29]. Another concern is the uncontrolled proliferation of transplanted NPC leading to tumor formation. However, there are no signs of swelling or change of shape of the spinal cord at the transplantation site macroscopically. The low proliferation rate of grafted NPC is confirmed on the molecular level, since very few of the BrdU prelabeled cells are found to co-localize with the proliferation marker Ki-67 3 weeks after the transplantation (Fig. 4A).

A control group of animals, which received GFP expressing and at the same time BrdU-prelabeled NPC (NPC-GFP/BrdU), allowed to assess the stable transgene expression in adult NPC *in vivo* as a prerequisite for the introduction of therapeutic transgenes in subsequent studies. After 3 weeks post transplantation, GFP expression is dramatically downregulated as indicated by the low number of GFP positive cells in contrast to the abundance of BrdU prelabeled transplanted NPC (Fig.4B). The detection of BrdU prelabeled NPC excludes the possibility that a lack

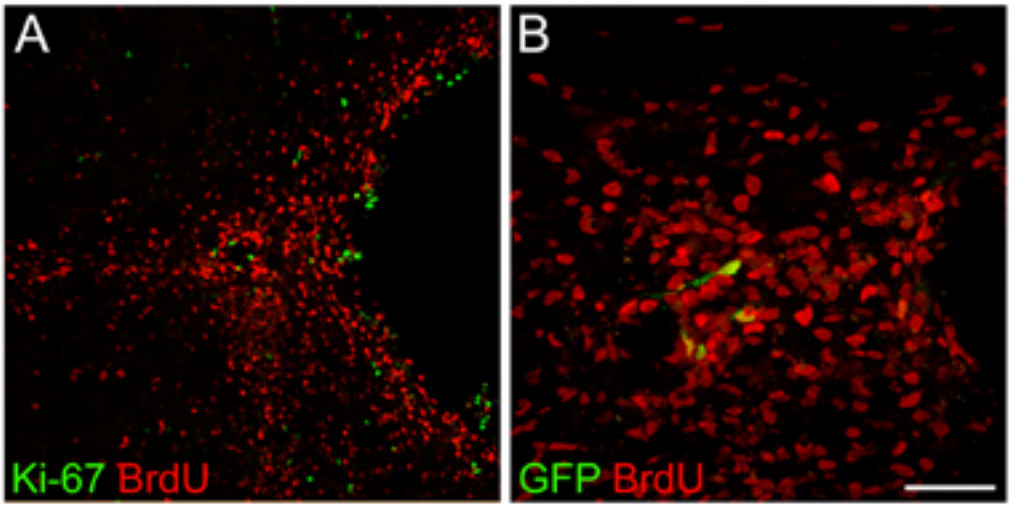

Figure 4: *Survival, proliferation and transgene expression of grafted NPC in vivo. (A) The majority of grafted BrdU prelabeled adult NPC (shown in red) is detected in a rim surrounding the spinal cord lesion site. Grafted cells can be detected in decreasing quantities rostral and caudal up to 2 mm away from the transplantation site. After 3 weeks post transplantation, almost none of the grafted NPC are co-localized with the proliferation marker Ki-67 (shown in green) indicating that the proliferation rate of NPC is rather low after mitogen withdrawal and transplantation (arrowheads highlight the central canal). (B) Almost all grafted BrdU prelabeled NPC (shown in red) lack GFP expression (shown in green) indicating silencing of the transgene in adult NPC 3 weeks after transplantation. Scale bar A 150µm, B 30µm.*

of cell survival is responsible for the poor expression of GFP *in vivo*.

Grafted NPC display antigenic properties of glial precursor cells (NG2), radial glial cells (BLBP), astroglia (GFAP) and oligodendroglia (APC) as confirmed by co-localization with BrdU prelabeled grafted NPC (Fig. 5A-L). None of the grafted NPC are identified to display antigenic properties of neurons (Fig. 5M-O), even though beta-III-tubulin expressing NPC are found frequently *in vitro*.

Most of the differentiation markers used, which are either cytoplasmatic (GFAP, BLBP, APC, beta-III-tubulin) or extracellular (NG2), become upregulated in the host spinal cord displaying a dense immunoreactivity around the injury site. Combined with the fact that BrdU represents a nuclear marker to identify grafted cells, it is impossible to discriminate in all regions unequivocally between co-localization of differentiation markers with grafted NPC versus resident spinal cord cells, which prohibits a thorough quantitative analysis. However as a general observation, the majority of grafted NPC express antigenic properties of radial glia or astroglia, fewer cells show immunoreactivity for oligodendroglial or glial precursor markers.

3.3 Replacement of the cystic lesion defect

One goal of cellular therapy following spinal cord injury is to replace the cystic lesion defect, which represents a typical

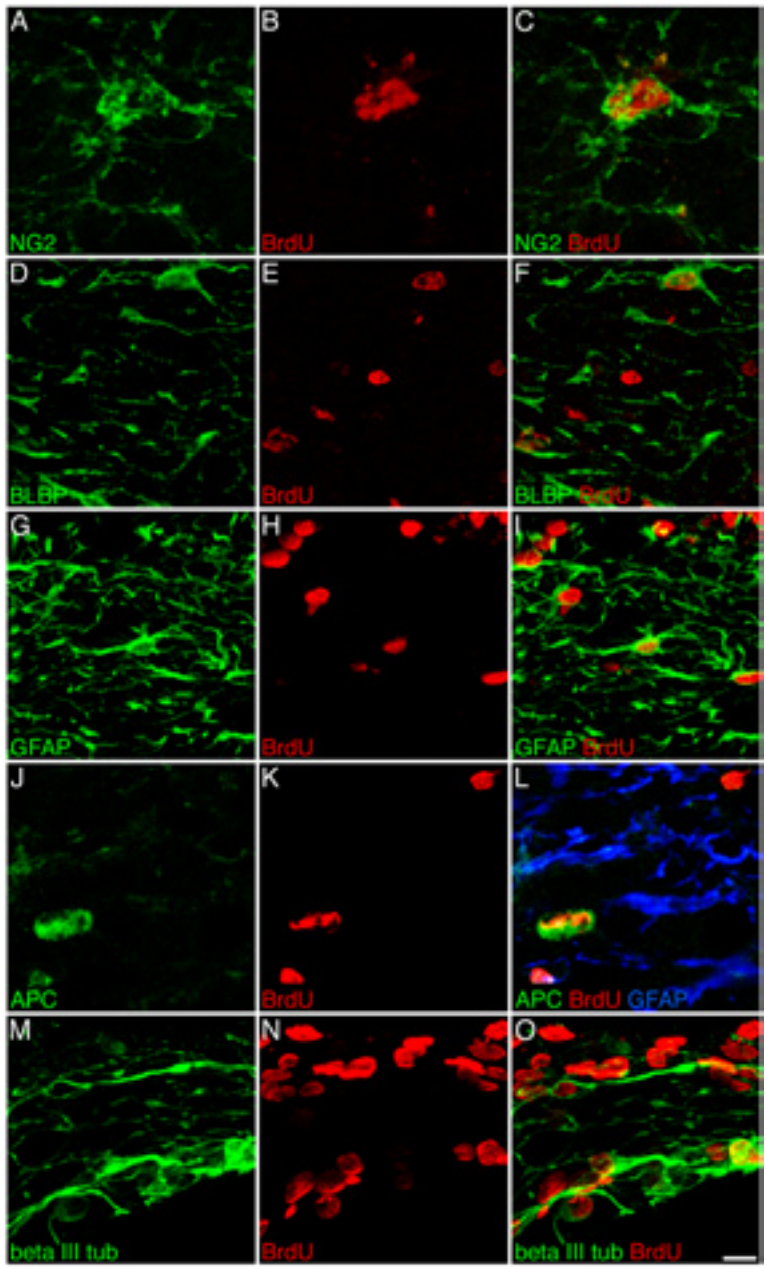

Figure 5: *NPC differentiation in vivo. The differentiation pattern of grafted NPC was assessed by determining the co-localization of individual glial/neuronal markers (shown in green) and BrdU prelabeling (shown in red). Grafted NPC are co-localized with NG2 immunoreactivity representing glial precursor cells (A-C), BLBP immunoreactivity for radial glial cells (D-F), GFAP immunoreactivity for astroglial cells (G-I) and APC immunoreactivity indicating oligodendroglial differentiation (J-L). APC immunoreactive cells do not co-express GFAP (shown in blue) confirming the oligodendroglial differentiation. Adult NPC displaying antigenic properties of neurons (beta-III-tubulin immunoreactivity) are not identifiable (M-O). Confocal fluorescence micrographs, scale bar A-C 5µm, D-O 10µm.*

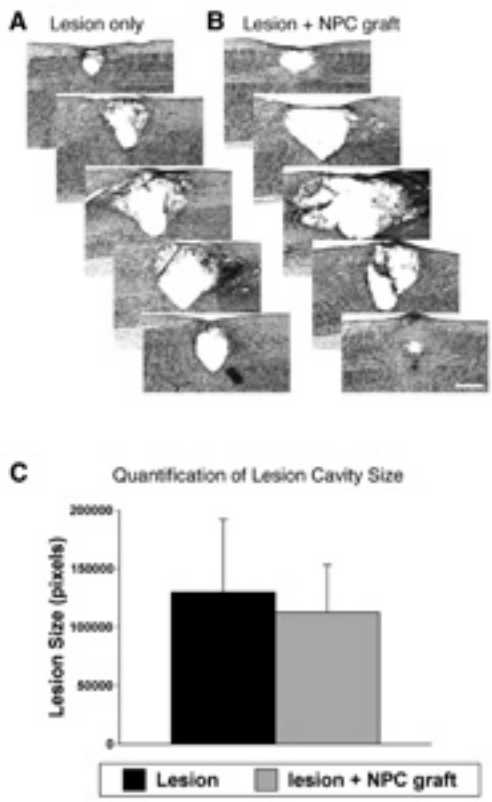

Figure 6: *Lesion size after transplantation of adult NPC. Serial sagittal Nissl stained sections through the spinal cord injury site do not reveal a decrease of the cystic lesion defect after NPC transplantation. (A) Animal with lesions only, (B) animal with a spinal cord lesion followed by NPC transplantation. (C) Quantitative analysis of the cystic lesion size in mm² (error bars represent standard error of the mean). Scale bar A, B 500µm.*

morphological sequel following CNS injury and impedes axonal regeneration. To assess whether grafts of adult NPC would at least partially reduce the lesion area, the cystic lesion compartments were quantified in serial sagittal sections of animals with lesions only versus animals with lesions followed by NPC transplantation. The typical triangular to round shape of a wire knife dorsal column transection does not differ between non-grafted and NPC grafted spinal cord injured animals (Fig. 6A, B). The quantification of the cystic lesion area in consecutive Nissl sections confirmed that, no matter whether animals receive grafts or not, the cystic lesion remains unchanged (Fig. 6C; lesion + NPC graft 0.278mm² ± 0.099; lesion only 0.281mm² ± 0.135).

3.4 Adult NPC grafts and axonal regeneration

In the present study, we performed an incomplete spinal cord injury lesioning specifically the main dorsal CST at cervical level C3. The immunohistochemical analysis of neurofilament expression as an unspecific axonal marker and the visualization of anterogradely BDA-labeled CST axons were employed to determine the spatial association of grafted NPC and injured axons. After 3 weeks of transplantation, processes from GFP expressing NPC are aligned along neurofilament expressing axons adjacent to the cystic lesion area (Fig. 7A). NPC are also identified in between BDA-labeled axonal profiles, with their GFP positive processes appearing to be in contact with CST axons (Fig. 7B). Whether axons regenerate along grafted NPC or whether grafted cells migrate towards these axons and align along them, cannot be determined. Immunohistochemical markers could not further specify the phenotype of these cells, however, morphologically they appear as either astroglia or oligodendroglia. Compared to animals with lesion only, no enhanced regrowth responses of disrupted CST axons in or around the lesion site

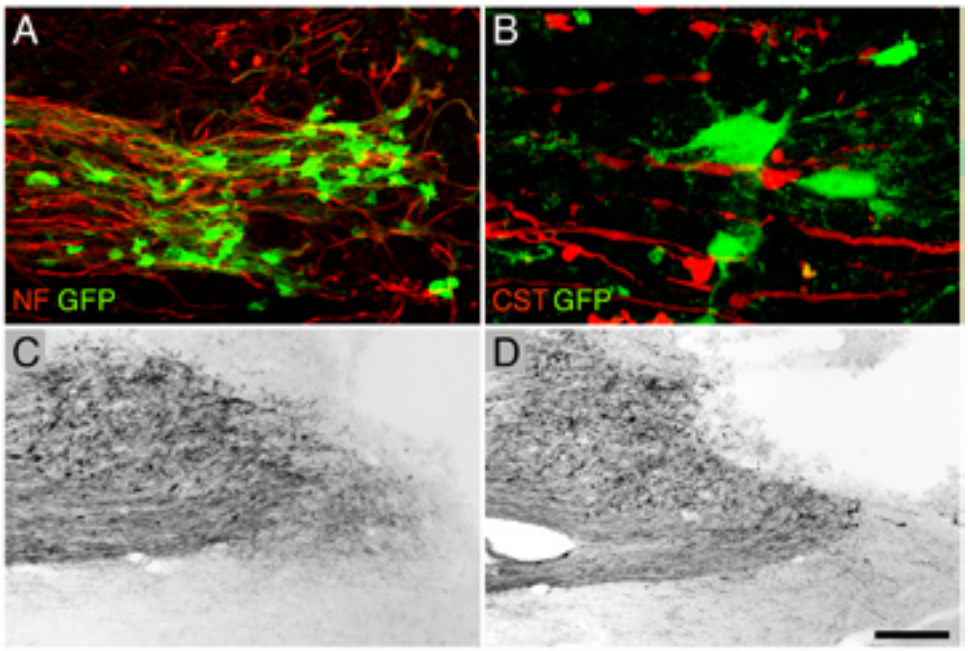

Figure 7: *Grafted NPC and axon regeneration. GFP expressing NPC (shown in green) are located in between neurofilament expressing axons (shown in red) adjacent to the lesion and appear to align along them (A). Similarly, adult NPC are identified to integrate in between BDA labeled CST axons (shown in red) immediately rostral to the lesion site (B). Compared to animals with lesions only (C), animals with lesions and NPC grafts do not reveal an increased regenerative response of interrupted CST axons (D). A,B Confocal immunofluorescence micrographs, C,D brightfield micrographs. Scale bar A 55mm, B 20mm, C and D 200µm*

are observed following NPC transplantation (Fig. 7C, D).

4. DISCUSSION

This study demonstrates that syngenic adult neural progenitors cells survive transplantation into the acutely injured spinal cord, differentiate into oligodendroglia and astroglia and integrate along injured axonal pathways surrounding the lesion defect.

Thus far, studies reported survival of adult NPC only after transplantation into the intact spinal cord [20] or after delayed transplantation into the injured spinal cord [21, 30]. Probably the most inhospitable CNS environment for any cell graft to survive in is an acutely injured area, which is characterized by the initiation of inflammatory cascades, upregulation of mediators of cell death/degeneration and secondary ischemic events [31]. Whether transplantation of NPC as small neurosphere fragments instead of single cell suspensions contributed to the observed graft survival, remains to be determined. Within neurospheres, cell cell contacts remain intact and detrimental effects by dissociation methods to generate single cell suspensions can be avoided [32]. Whether poor cell survival in the fluid-filled lesion cavity or the lack of an extracellular scaffold prevented the cyst replacement cannot be answered in the present study. Find-

ings from studies analyzing the regenerative capacity of embryonic derived neural stem cells, which completely fill out the cystic spinal cord contusion site [18], suggest that adult NPC may indeed produce insufficient extracellular matrix to maintain themselves within the lesion cyst (personal communication, J.W. McDonald).

This study provides important insights into the regenerative potential of adult NPC grafts. Very promising is the observation that adult NPC migrate and align along injured axon pathways caudal and rostral to the lesion site. This finding suggests that they are not sealed off by the surrounding host spinal cord, in contrast to other cell types used for transplantation such as fibroblasts or Schwann cells [9, 13]. Thus, adult NPC may have the capacity to build a continuum between the host and the actual graft. In the present study, there may have been axon sprouting responses around the lesion supported by grafted NPC. However, these effects would have been marginal at best, since thorough qualitative analysis of CST projections did not reveal any differences between lesioned only and NPC grafted animals. Whether adult NPC may provide a cellular scaffold for regenerating axons within the lesion center, and which glial subpopulation may serve as a cellular scaffold to guide growing axons after injury, remains to be determined.

Withdrawal of the mitogen and addition of serum resulted primarily in early neuronal (beta-III-tubulin) and oligodendroglial (GalC) differentiation *in vitro*, in contrast to very few cells expressing astroglial markers (GFAP). The already high proportion of neuronal antigenicity in proliferation conditions remains unchanged in differentiation conditions. It is difficult to validate these data by comparing them with previous studies [20, 23, 24] since differences in cell culture conditions (passage number, density of plated cells in differentiation assays, serum contents) and immunocytochemical analysis make any detailed comparison unreliable. The overall differentiation pattern replicates previous findings, however, we detect a higher proportion of neuronal antigenicity, which might be attributable to the use of Neurobasal medium with B27 supplement [22]. A systematic analysis of different media and supplements influencing the differentiation pattern of subventricular zone derived adult NPC *in vitro* revealed that replacement of B27 supplement by N2 reduces the neuronal antigenicity from 22% to 10%. In line with previous studies describing the differentiation pattern of adult NPC *in vitro* [20, 22], only around one third of NPC display glial or neuronal immunoreactivity. One has to consider that a major proportion of cells has not yet fully differentiated to express marker of mature cells such as GFAP or GalC. This notion is supported by a subsequent experiment, which demonstrates that around 50% of adult NPC *in vitro* represent glial precursor cells expressing A2B5, both in proliferation and differentiation conditions (M. Vroemen, unpublished observation). What becomes clear is that the differentiation pattern *in vitro* has only a very limited predictive value for the differentiation *in vivo*. There, NPC differen-

tiate primarily into astroglial cells, fewer into oligodendroglia, none into neurons 3 weeks after transplantation into the injured spinal cord. As demonstrated by others, molecular cues by the host spinal cord override the differentiation pattern of adult NPC before transplantation [20, 21, 33, 34]. In contrast, embryonic derived neural stem cells, predifferentiated *in vitro* or not, display antigenic properties of glial cells and neurons following transplantation into the spinal cord [17]. It is conceivable that embryonic and adult derived neural stem/progenitor cells show a differential response to instructive cues of the graft environment.

This study reports for the first time oligodendroglial differentiation after transplantation of adult NPC into the injured spinal cord. Apparently, adult spinal cord derived NPC retain the multipotency to differentiate into oligodendroglia and are able to recognize respective instructive signals by the host spinal cord. Oligodendroglial differentiation after transplantation of adult NPC has been shown previously, however, cells were grafted into the intact spinal cord [20]. The only other published study, examining the regenerative capacity of adult heterotopic subventricular zone derived NPC after delayed transplantation into the injured spinal cord, did not observe oligodendroglial differentiation [21]. Differences regarding the region of progenitor cell isolation (spinal cord versus subventricular zone), the propagating conditions *in vitro* (different culture medium or supplements), the timing of transplantation (delayed versus immediately after injury) and the analyzing methods (different antibodies for oligodendroglial differentiation) may all have accounted for the observed differences. The presence of astroglial differentiation and the lack of neuronal differentiation are in accordance with previous studies [20, 21].

The downregulation of transgene expression in transplanted NPC prohibits not only optimal tracking of grafted NPC, but in addition, approaches to introduce therapeutic genes into NPC need to be reconsidered. The phenomenon of downregulation or silencing of transgenes in undifferentiated cells introduced by retroviral vectors has been observed by others [35]. The presence of retroviral silencer elements, cytosine methylation of CpG sites and insufficient promoters are thought to contribute to transgene silencing [35, 36]. More promising approaches to successfully genetically modify adult NPC point to the use of modified promoters or different viral vectors [36-39].

Results from the present study demonstrating, that adult NPC survive transplantation into the acutely injured spinal cord, integrate into the host spinal cord in close spatial association with injured and non-injured CNS axons and differentiate into oligodendroglia and astroglia, are very promising. However, investigations have to be continued before any conclusions regarding the regenerative capacity of adult NPC in spinal cord injury can be drawn. Adult NPC need to fill out the lesion defect to assess their axon growth promoting properties. If there is a regeneration promoting effect, the ideal

cell type, which may provide a scaffold for regenerating axons, has to be identified and specified. The remyelination by grafted adult NPC differentiating into oligodendroglial cells has to be assessed. Strategies need to be developed to enrich favorable glial subpopulations *in vitro*, which maintain their differentiation pattern after transplantation. And finally, considering autologous transplantation of adult neural stem cells as a potential treatment strategy for spinal cord injured individuals, it has to be demonstrated that adult NPC can be harvested from the individual's own CNS, expanded and enriched in culture and re-implanted into the spinal cord lesion site.

5. ACKNOWLEDGMENTS

This work was supported by Institut International de Recherche en Paraplégie Geneva, on behalf of an anonymous donation, Deutsche Forschungsgemeinschaft (WE 2165), Deutsche Stiftung Querschnitt and by the ReForM-Program, University of Regensburg, School of Medicine.

We thank Ulrich Bogdahn for his continued support and critical comments. We also thank Armin Blesch for the retroviral vectors, Bill Stallcup for the NG2 antibody and Nathaniel Heintz for the BLBP antibody.

6. REFERENCES

1. Aigner, L. et al. Overexpression of the neural growth-associated protein GAP-43 induces nerve sprouting in the adult nervous system of transgenic mice. Cell 83, 269-78 (1995).
2. Blesch, A., Grill, R. J. & Tuszynski, M. H. Neurotrophin gene therapy in CNS models of trauma and degeneration. Prog Brain Res 117, 473-84 (1998).
3. Grimpe, B. & Silver, J. The extracellular matrix in axon regeneration. Prog Brain Res 137, 333-49 (2002).
4. Schwab, M. E. Repairing the injured spinal cord. Science 295, 1029-31 (2002).
5. Horner, P. J. et al. Proliferation and differentiation of progenitor cells throughout the intact adult rat spinal cord. J Neurosci 20, 2218-28 (2000).
6. Kojima, A. & Tator, C. H. Epidermal growth factor and fibroblast growth factor 2 cause proliferation of ependymal precursor cells in the adult rat spinal cord in vivo. J Neuropathol Exp Neurol 59, 687-97 (2000).
7. Martens, D. J., Seaberg, R. M. & van der Kooy, D. In vivo infusions of exogenous growth factors into the fourth ventricle of the adult mouse brain increase the proliferation of neural progenitors around the fourth ventricle and the central canal of the spinal cord. Eur J Neurosci 16, 1045-57 (2002).
8. Kojima, A. & Tator, C. H. Intrathecal administration of epidermal growth factor and fibroblast growth factor 2 promotes ependymal proliferation and functional recovery after spinal cord injury in adult rats. J Neurotrauma 19, 223-38 (2002).
9. Grill, R., Murai, K., Blesch, A., Gage, F. H. & Tuszynski, M. H. Cellular delivery of neurotrophin-3 promotes corticospinal axonal growth and partial functional recovery after spinal cord injury. J Neurosci 17, 5560-72 (1997).
10. Li, Y., Field, P. M. & Raisman, G. Repair of adult rat corticospinal tract by transplants of olfactory ensheathing cells. Science 277, 2000-2 (1997).
11. Liu, Y. et al. Transplants of fibroblasts genetically modified to express BDNF promote regeneration of

adult rat rubrospinal axons and recovery of forelimb function. J Neurosci 19, 4370-87 (1999).
12. Ramon-Cueto, A., Cordero, M. I., Santos-Benito, F. F. & Avila, J. Functional recovery of paraplegic rats and motor axon regeneration in their spinal cords by olfactory ensheathing glia. Neuron 25, 425-35 (2000).
13. Weidner, N., Blesch, A., Grill, R. J. & Tuszynski, M. H. Nerve growth factor-hypersecreting Schwann cell grafts augment and guide spinal cord axonal growth and remyelinate central nervous system axons in a phenotypically appropriate manner that correlates with expression of L1. J Comp Neurol 413, 495-506 (1999).
14. Xu, X. M., Guenard, V., Kleitman, N. & Bunge, M. B. Axonal regeneration into Schwann cell-seeded guidance channels grafted into transected adult rat spinal cord. J Comp Neurol 351, 145-60 (1995).
15. Suda, Y., Suzuki, M., Ikawa, Y. & Aizawa, S. Mouse embryonic stem cells exhibit indefinite proliferative potential. J Cell Physiol 133, 197-201 (1987).
16. Reynolds, B. A. & Weiss, S. Generation of neurons and astrocytes from isolated cells of the adult mammalian central nervous system. Science 255, 1707-10 (1992).
17. Han, S. S., Kang, D. Y., Mujtaba, T., Rao, M. S. & Fischer, I. Grafted lineage-restricted precursors differentiate exclusively into neurons in the adult spinal cord. Exp Neurol 177, 360-75 (2002).
18. McDonald, J. W. et al. Transplanted embryonic stem cells survive, differentiate and promote recovery in injured rat spinal cord. Nat Med 5, 1410-2 (1999).
19. Teng, Y. D. et al. Functional recovery following traumatic spinal cord injury mediated by a unique polymer scaffold seeded with neural stem cells. Proc Natl Acad Sci U S A 99, 3024-9 (2002).
20. Shihabuddin, L. S., Horner, P. J., Ray, J. & Gage, F. H. Adult spinal cord stem cells generate neurons after transplantation in the adult dentate gyrus. J Neurosci 20, 8727-35 (2000).
21. Cao, Q. L. et al. Pluripotent stem cells engrafted into the normal or lesioned adult rat spinal cord are restricted to a glial lineage. Exp Neurol 167, 48-58 (2001).
22. Wachs, F. P. et al. High efficacy of clonal growth and expansion of adult neural stem cells. Lab Invest 83, 949-62 (2003).
23. Shihabuddin, L. S., Ray, J. & Gage, F. H. FGF-2 is sufficient to isolate progenitors found in the adult mammalian spinal cord. Exp Neurol 148, 577-86 (1997).
24. Weiss, S. et al. Multipotent CNS stem cells are present in the adult mammalian spinal cord and ventricular neuroaxis. J Neurosci 16, 7599-609 (1996).
25. Blesch, A. et al. Leukemia inhibitory factor augments neurotrophin expression and corticospinal axon growth after adult CNS injury. J Neurosci 19, 3556-66 (1999).
26. Svendsen, C. N. et al. A new method for the rapid and long term growth of human neural precursor cells. J Neurosci Methods 85, 141-52 (1998).
27. Weidner, N., Grill, R. J. & Tuszynski, M. H. Elimination of basal lamina and the collagen “scar” after spinal cord injury fails to augment corticospinal tract regeneration. Exp Neurol 160, 40-50 (1999).
28. Weidner, N., Ner, A., Salimi, N. & Tuszynski, M. H. Spontaneous corticospinal axonal plasticity and functional recovery after adult central nervous system injury. Proc Natl Acad Sci U S A 98, 3513-8 (2001).
29. Ben-Hur, T. et al. Transplanted multipotential neural precursor cells migrate into the inflamed white matter in response to experimental autoimmune encephalomyelitis. Glia 41, 73-80 (2003).
30. Horky, L. L., Horner, P. J., Van Praag, H., Shihabuddin, L. S. & Gage, F. H. in Annual Meeting of the Society for Neuroscience (New Orleans, USA, 2000).
31. Tuszynski, M. H. & Kordower, J. CNS Regeneration (Academic Press, San Diego, 1999).
32. Svendsen, C. N. et al. Long-term survival of human central nervous system progenitor cells transplanted into a rat model of Parkinson’s disease. Exp Neurol 148, 135-46 (1997).
33. Cao, Q. L., Howard, R. M., Dennison, J. B. & Whittemore, S. R. Differentiation of engrafted neuronal-restricted precursor cells is inhibited in the traumatically injured spinal cord. Exp Neurol 177, 349-59

(2002).
34. Song, H., Stevens, C. F. & Gage, F. H. Astroglia induce neurogenesis from adult neural stem cells. Nature 417, 39-44 (2002).
35. Pannell, D. & Ellis, J. Silencing of gene expression: implications for design of retrovirus vectors. Rev Med Virol 11, 205-17 (2001).
36. Gaiano, N., Kohtz, J. D., Turnbull, D. H. & Fishell, G. A method for rapid gain-of-function studies in the mouse embryonic nervous system. Nat Neurosci 2, 812-9 (1999).
37. Englund, U. et al. The use of a recombinant lentiviral vector for ex vivo gene transfer into the rat CNS. Neuroreport 11, 3973-7 (2000).
38. Falk, A. et al. Gene delivery to adult neural stem cells. Exp Cell Res 279, 34-9 (2002).
39. Pfeifer, A., Ikawa, M., Dayn, Y. & Verma, I. M. Transgenesis by lentiviral vectors: lack of gene silencing in mammalian embryonic stem cells and preimplantation embryos. Proc Natl Acad Sci U S A 99, 2140-5 (2002).

Chapter 3

Adult neural progenitor cells provide a permissive guiding substrate for corticospinal axon growth following spinal cord injury

Europ. J. Neurosci. 20; 1695–1704 (2004)

Katharina Pfeifer
Maurice Vroemen
Armin Blesch
Norbert Weidner

ABSTRACT

Adult neural progenitor cells (NPC) are an attractive source for cell transplantation and neural tissue replacement after central nervous system (CNS) injury. Following transplantation of NPC cell suspensions into the acutely injured rat spinal cord NPC survive, however, they migrate away from the lesion site and are unable to replace the injury induced lesion cavity. In the present study we examined 1) whether NPC can be retained within the lesion site after co-transplantation with primary fibroblasts, and 2) whether NPC promote axonal regeneration following spinal cord injury. Co-cultivation of NPC with fibroblasts demonstrated that NPC adhere to fibroblasts and the extracellular matrix produced by fibroblasts. In the presence of fibroblasts, the differentiation pattern of co-cultivated NPC was shifted towards glial differentiation. Three weeks after transplantation of adult spinal cord derived NPC with primary fibroblasts as mixed cell suspensions into the acutely injured cervical spinal cord in adult rats, the lesion cavity was completely replaced. NPC survived throughout the graft and differentiated exclusively into glial cells. Quantification of neurofilament labeled axons and anterogradely labeled corticospinal axons indicated that NPC co-grafted with fibroblasts significantly enhanced axonal regeneration. Both, neurofilament labeled axons and corticospinal axons aligned longitudinally along GFAP expressing NPC derived cells, which displayed a bipolar morphology reminiscent of immature astroglia. Thus, grafted astroglial differentiated NPC promote axon regrowth following spinal cord injury by means of cellular guidance.

1. INTRODUCTION

Cell-based therapies in the injured spinal cord are intended to fill lesion cavities, which typically develop at an injury site, and to provide a cellular growth conducive substrate for re-growing axons. Various cell types such as fibroblasts, olfactory ensheathing cells, Schwann cells and neural stem/progenitor cells have been used to replace injured spinal cord parenchyma, and to elicit axonal regeneration [1-6]. Neural stem/progenitor cells represent a particularly attractive cell type for CNS transplantation, because they allow organotypic cellular replacement, and may have the capacity to establish growth promoting guidance structures, thus recapitulating cell-based axon guidance in the developing CNS. Indeed, time course studies in the early postnatal rat spinal cord demonstrate that immature astrocytes expressing vimentin and GFAP might promote the longitudinal outgrowth of corticospinal axons [7, 8]. In the injured peripheral nervous system, cellular guidance plays a key role in promoting axonal regeneration. Schwann cells build a longitudinally aligned cellular path, guide regenerating axons along their processes, and express cell adhesion molecules and growth factors in appropriate spatial and temporal sequences [9].

Adult neural progenitor cells (NPC), isolated from the subventricular zone or spinal cord, have been shown to self-renew, and to be multipotent *in vitro* and after transplantation into the CNS [10, 11]. Following transplantation of adult NPC into the intact and injured spinal cord, only astroglial and oligodendroglial differentiation is observed [12-14]. Even after transplantation into the acutely injured spinal cord lesion site, adult NPC survive. However, grafted NPC migrate completely into the surrounding host parenchyma, thus preventing the replacement of the lesion cavity [14]. Therefore, studies investigating the transplantation of NPC in the injured CNS have not been able to determine whether adult NPC promote axonal regeneration across cystic lesion defects caused by spinal cord injury.

Recently, it has been demonstrated in an ischemia model that an additional supporting scaffold such as an artificial biodegradable polymer is required to retain transplanted neural stem cells within lesion cavities developing after ischemia [15]. Fibroblasts naturally provide a cellular and acellular (extracellular matrix production) supporting scaffold in various tissues. Following transplantation into the injured spinal cord, fibroblasts replace cystic lesion defects, however, fibroblasts alone are not sufficient to provide a cellular guiding path for injured CNS axon pathways such as the corticospinal tract (CST) [16-18].

We therefore aimed to investigate if the combination of NPC and fibroblasts can retain NPC in the lesion site and augment axonal growth. Results of the present study indicate that NPC grafted together with primary fibroblasts to the injured spinal cord provide a cellular guiding substrate across the lesion cavity and enhance the growth of lesioned corticospinal axons.

2. MATERIALS AND METHODS

2.1 Animals

Adult female Fischer 344 rats (160-180 g) were used for the isolation of NPC and fibroblasts. All experiments were carried out in accordance with the European Communities Council Directive (86/609/EEC) and institutional guidelines. All efforts were made to minimize the number of animals used and their suffering. Animals had *ad libidum* access to food and water throughout the study. All surgical procedures were performed under anesthesia with a combination of ketamine (62.5 mg/kg; WDT, Garbsen, Germany), xylazine (3.175 mg/kg; WDT, Garbsen, Germany) and acepromazine (0.625 mg/kg, Sanofi-Ceva, Düsseldorf, Germany) in 0.9% sterile saline solution.

2.2 Preparation of Adult NPC and fibroblasts

Rats were deeply anesthetized as described above and killed by decapitation. The cervical enlargement (spinal cord level C3 through T1) was dissected and the dura removed. The tissue was minced, washed in sterile Dulbecco's phosphate buffered saline/D-glucose (4.5g/l; PAA Laboratories, Linz, Austria) and digested in a solution of papain (0.01%; Worthington

Biochemicals, Lakewood, USA), neutral protease (0.1%; Roche, Mannheim, Germany), DNase I (0.01%; Worthington Biochemicals) and 12.4mM $MgSO_4$, dissolved in Hank's balanced salt solution (HBSS; PAA Laboratories, Linz, Austria) for 30 min at 37°C. The tissue was centrifuged at 120 x g for 5 min at 4°C and washed three times in DMEM-HAMS F12 (Pan Biotech, Aidenbach, Germany) supplemented with 10% fetal calf serum (FCS; Pan Biotech, Aidenbach, Germany). The cells were transferred to culture dishes containing serum-free growth medium, consisting of Neurobasal medium with B27 supplement (Gibco, Karlsruhe, Germany) and 20 ng/ml recombinant human FGF-2 (R&D System, Wiesbaden, Germany). Cells were grown first as neurospheres for 2-3 passages in uncoated culture flasks. The medium was replaced by centrifuging the medium containing neurospheres at 120 x g for 5 min at 4°C, removing the supernatant and resuspending the cells in fresh growth medium. For passaging of neurospheres, the medium containing the neurospheres was collected in a 15 ml centrifuge tube and centrifuged at 120 x g for 5 min at 4°C. The pellet was resuspended in 1 ml of Accutase and incubated at 37°C for 10 min. The neurospheres were resuspended in growth medium, triturated and centrifuged at 120 x g for 5 min at 4°C. The resulting single cell suspensions were seeded at a density of 3000 cells/cm^2 in fresh growth medium. Cells were passaged every second week. For the consecutive 2-3 passages, NPC were grown as monolayers in culture flasks coated with poly-l-ornithine (20µg/cm^2; Sigma) and laminin (0.4µg/cm^2; Sigma). The cell culture medium was changed twice per week. Monolayer cultures were detached by incubation with 40 ml/cm^2 Acccutase (Innovative Cell Tech, San Diego, USA) for 5 min at 37°C. Finally, the cells were centrifuged at 120 x g for 5 min at 4°C and resuspended in fresh growth medium.

For the identification of NPC co-cultured with primary fibroblasts *in vitro* (see below), NPC were genetically modified to express the reporter gene green-fluorescent protein (GFP) using a retroviral vector as previously described [14].

Primary cultures of adult Fischer 344 fibroblasts were generated from skin biopsies and cultivated under standard culture conditions as previously described [5].

2.3 Preparation of adult NPC for transplantation

Adult NPC were incubated with 1 µM bromodeoxyuridine (BrdU; Sigma) in growth medium for 48 h just before transplantation. A sample of single cell suspensions was stained with Trypan Blue (Sigma) and counted using a Neubauer hemocytometer. The remaining single cell suspension was washed twice and resuspended in PBS to yield a final concentration of 0.8 x 10^5 cells/µl for co-transplantation of NPC and fibroblasts (NPC-FF). Fibroblasts were trypsinized and counted in a Neubauer hemocytometer. Cells were washed twice and resuspended in PBS to yield the final concentration of 0.2 x 10^5 cells/µl. Fibroblast and NPC suspensions were mixed before transplantation. For pure

fibroblast grafts (FF), fibroblasts were resuspended at a concentration of 0.4 x 10^5 cells/µl. Due to the larger cell size of fibroblasts this suspension was approximately equally dense as the mixed cell grafts.

2.4 In vitro co-cultures of adult NPC and fibroblasts

To study the adhesion behavior of adult NPC in the presence of fibroblasts, GFP expressing NPC were either kept as neurospheres in T25 flasks in proliferation medium either without (pure NPC condition) or with primary fibroblasts (NPC-FF condition). Daily for 7 days after the start of co-culturing, the adhesion behavior of NPC was monitored using an inverted phase contrast and fluorescence microscope (Olympus).

To analyze the *in vitro* differentiation of NPC, neurospheres of established NPC cultures were dissociated using Accutase (Innovative Cell Tech, San Diego, USA) and seeded on poly-l-ornithine/laminin (P-Orn/Lam, Sigma) coated cover slips either alone (NPC proliferation condition) or together with primary rat fibroblasts at a ratio of 1:2 (NPC-FF proliferation condition) for 4 days in serum-free medium (Neurobasal medium with B27 supplement and FGF-2 as described above). In parallel, cultures of NPC alone (NPC differentiation condition) were incubated in medium, consisting of Neurobasal medium, B27 supplement and 1% fetal calf serum (Pan Biotech, Aidenbach, Germany). Cells were subsequently fixed with 4% paraformaldehyde in PBS and immunolabeled using the following antibodies: mouse-anti-nestin for progenitor/stem cells (Pharmingen, Heidelberg, Germany; at 1/1000), mouse-anti-GFAP for astroglia (Chemicon, Hofheim, Germany; at 1/600), mouse-anti-A2B5 for glial precursor cells (Chemicon, Hofheim, Germany; at 1/100), mouse-anti-Gal-C for oligodendroglia (Chemicon, Hofheim, Germany; at 1/500) and mouse-anti-beta-III-tubulin for neurons (clone TUJ1; Babco, Richmond, USA; at 1/500).

Cells were washed 3 times with tris-buffered saline (TBS) after fixation, blocked with TBS containing 3% donkey serum/0.1% Triton-X (Sigma) and incubated overnight with the primary antibody in TBS + 3% donkey serum + 0.1% Triton-X at 4°C. The following day, cells were washed with TBS and incubated with rhodamine-X linked secondary donkey-anti-mouse antibodies (Jackson, Hamburg, Germany; at 1/1000) in TBS + 3% donkey serum + 0.1% Triton-X for 2h. Finally, nuclei were counterstained with Hoechst 33342 (2 µg/ml in TBS; Sigma). The coverslips were mounted onto glass slides using Prolong-Antifade (Molecular Probes, Leiden, Netherlands). For the immunocytochemical analysis, 8 bit monochrome pictures were taken at 20x magnification on a fluorescent microscope (Leica DMR) equipped with a Spot CCD camera model 2.2.1 (Diagnostic Instruments, Sterling Heights, USA). The number of specifically immunolabeled cells and the total cell number (number of Hoechst counterstained nuclei) were determined in 5 random fields for each differentiation marker to determine the percentage of cells ex-

pressing the respective differentiation marker. Three independently performed immunocytochemical stains were analyzed under expansion and differentiation conditions.

2.5 Surgical procedures

Spinal cord lesions, cell transplantation and anterograde labeling of the CST were performed as previously described [14, 19, 20]. Cells were grafted immediately post-injury to maximize the potential growth responses of corticospinal axons and to ensure that the injured tips of corticospinal axons are in close proximity to the graft site.

Briefly, the dorsal columns containing the dorsal CST were transected at cervical level C3 using a tungsten wire knife (David Kopf Instruments Tujuna, USA) leaving the surrounding dura intact. A total volume of 3 µl of a cell suspension containing either 2.4 x 10^5 NPC (prelabeled with BrdU) combined with 0.6 x 10^5 fibroblasts (**NPC-FF**; n=8) or 1.2 x 10^5 fibroblasts only (**FF**; n=8) was injected directly into the lesion site through a pulled glass micropipette (100 µm internal diameter) using a Picospritzer II (General Valve, Fairfield, USA). Animals receiving spinal cord lesions without cell transplantation (**LESION**; n=6) served as controls.

For anterograde tracing of the CST projections, 300 nl of a 10% solution of biotinylated dextran-amine (BDA; 10.000 MW, Molecular Probes, Leiden, Netherlands) was injected through pulled glass micropipettes (40 µm internal diameter) into each of 18 sites per hemisphere spanning the rostrocaudal extent of the rat forelimb and hindlimb sensorimotor cortex using a PicoSpritzer II [19] 1 week post lesioning/grafting.

2.6 Morphological analysis

At 3 weeks post lesioning/grafting, animals were transcardially perfused with a 0.9% saline solution in 0.1 M phosphate buffer followed by 4% paraformaldehyde in 0.1 M phosphate buffer. Sagittal 35 µm cryostat sections were processed for visualization of the BDA labeled CST and for immunohistochemistry. Every seventh section was mounted for Nissl staining to determine the lesion size.

Double/triple labeling immunofluorescence techniques were performed with free floating sections to assess cell survival, *in vivo* differentiation pattern, and interaction of grafted adult NPC with injured axons. The following primary antibodies were used: rabbit-anti-BLBP (for radial glia; generous gift N. Heintz, Rockefeller University, New York, USA; at 1/1000), mouse-anti-GFAP (for astrocytes; DAKO, Glostrup, Denmark; at 1/200), mouse-anti-APC (for oligodendrocytes, Oncogene, Darmstadt, Germany; at 1/1000), rabbit-anti-200 kDa neurofilament (axonal marker; Boehringer Mannheim, Germany; at 1/250). Immunolabeling was visualized using fluorescein linked donkey secondary antibodies (Jackson, Hamburg, Germany; at 1/1000). BrdU-prelabeled cells were identified with a rat-anti-BrdU antibody (Harlan SeraLab, Loughborough, UK; at 1/500) visualized using rhodamine X- linked donkey secondary antibodies (Jackson, Hamburg, Germany; at 1/1000).

Sections were rinsed in 0.1 M Tris buffered saline (TBS), incubated in TBS + 3% donkey serum + 0.1% Triton-X for 1h, then transferred into the first primary antibody and incubated overnight at 4°C on a rotating platform. For visualization of BrdU-prelabeled adult NPC the staining protocol was modified as follows: after rinsing in TBS, sections were incubated for 1h in 50% formamide/2xSSC (0.3 M NaCl, 0.03M sodium citrate) at 65ºC. Sections were rinsed in 2xSSC, incubated for 30 min in 2 N HCl at 37ºC, and rinsed for 10 min in 0.1 M boric acid pH 8.5. After rinsing in TBS, sections were incubated in TBS + 3% donkey serum + 0.1% Triton-X as described above. The following day, sections were rinsed and incubated with fluorophor (rhodamine-X, fluorescein, Cy5) conjugated secondary donkey antibodies (Jackson, Hamburg, Germany; at 1/1000) for 2.5 h. BDA labeled CST axons were visualized by incubation with Cy5-conjugated streptavidin (Jackson, Hamburg, Germany; at 1/1000). After a final rinsing step in TBS, sections were mounted onto glass slides and coverslipped with ProLong Antifade Kit (Molecular Probes, Leiden, Netherlands).

For brightfield immunohistochemical analysis of axon regeneration rabbit-anti-200-kDa neurofilament (Boehringer Mannheim, Germany; at 1/250) was used as axonal marker.

Brightfield immunohistochemical analysis was performed by incubating free-floating sections for 24 h in primary antibody solution in TBS containing 5% blocking serum and 0.25% Triton X-100; incubation for 1 h with biotinylated donkey IgG (Dianova, Germany; at 1/1000) in TBS containing 5% blocking serum; 1 h incubation with avidin biotinylated peroxidase complex (Vector Elite kit; Wertheim, Germany; at 1/1000) with TBS containing 5% blocking serum; development for 3–15 min in a 0.05% solution of 3,38-diaminobenzidine (DAB), 0.01% H_2O_2, and 0.04% nickel chloride in TBS. For brightfield microscopic immunohistochemical analysis of BDA labeled CST axons, sections were incubated overnight with avidin biotinylated peroxidase complex (Vector Elite Kit, Vector Laboratories, Wertheim, Germany; at 1/1000) with TBS, followed by treatment for 5 min with a 0.05% solution of DAB, 0.01% H_2O_2, and 0.04% nickel chloride in TBS (brown-black reaction product). Tissue sections were mounted onto gelatin-coated glass slides, air dried, dehydrated and coverslipped with Neo Mount (Merck).

Brightfield imaging was conducted on a Leica DMR microscope with a Spot CCD camera model 2.2.1 (Diagnostic Instruments, Michigan, USA). Confocal immunofluorescence microscopy was performed using a Leica TCS-NT system.

2.7 Quantification of NPC differentiation in vivo

The *in vivo* differentiation pattern of NPC was analyzed by confocal fluorescence microscopy (Leica TCS-NT). Co-localization of BrdU labeled NPC with differentiation markers was analyzed using 15-20 optical sections along the z-axis of 35 µm thick sections at 400x magnification.

Differentiation markers were considered co-localized, if they surrounded the nuclear BrdU labeling through subsequent optical sections in the z-axis. The *in vivo* differentiation pattern was quantified in one section for each differentiation marker by analyzing 2 scans within the graft at 400x magnification. The total number of BrdU positive cells within each scan was counted and correlated to the number of BrdU positive cells co-localizing with the respective differentiation marker (GFAP, BLBP, APC).

2.8 Quantification of axonal regeneration

For quantification of axon (neurofilament labeling) and CST axon profiles (BDA labeling) within the graft, every eighth section out of all sagittal sections per animal was processed for the visualization of BDA or neurofilament, respectively. Out of these sections, the section containing the center of the graft was selected for quantification of neurofilament labeling, the section covering the main portion of the dorsal CST was chosen for quantification of CST regeneration. Digital brightfield images of neurofilament-DAB or BDA-DAB visualized sections were captured using a Spot CCD camera, model 2.2.1 (Diagnostic Instruments, Michigan, USA) attached to a Leica DMR microscope at 200x magnification. For the quantification of axon profiles, neurofilament-DAB or BDA-DAB positive structures were highlighted by marking them in NIH Image 1.62 with a digital pen, while going through the z-axis of the section, to detect complete labeling of neurofilament/BDA positive axons throughout the depth of the section. The number of pixels representing the marked lines was assessed using NIH Image 1.62 software. To determine the maximum distance of CST axon regeneration into the graft (axon length), the distance between the graft host interface and the longest axon ending was measured using NIH Image 1.62. The graft host interface was determined after inserting the transmitted light condenser, which allows to discriminate between the orderly tissue architecture of the host and the randomly organized cell graft. An observer blinded to group identity rated the degree of axonal regeneration of each animal.

2.9 Statistical analysis

All data are expressed as mean ± SEM. Comparisons between NPC-FF, and FF grafted animals were made by nonparametric Mann-Whitney U tests and $P<0.05$ was considered significant.

3. RESULTS

3.1 Adhesion and differentiation pattern of adult NPC co-cultured with fibroblasts.

Previously, we have shown that the transplantation of NPC suspensions is not sufficient to replace the lesion cavity, which forms after spinal cord injury [14]. To determine if fibroblasts might be able to provide a supporting scaffold for NPC in the injured spinal cord, we first investigated the influences of primary fibroblasts on NPC adhesion and differentiation *in vitro*. Co-cultures of adult GFP expressing

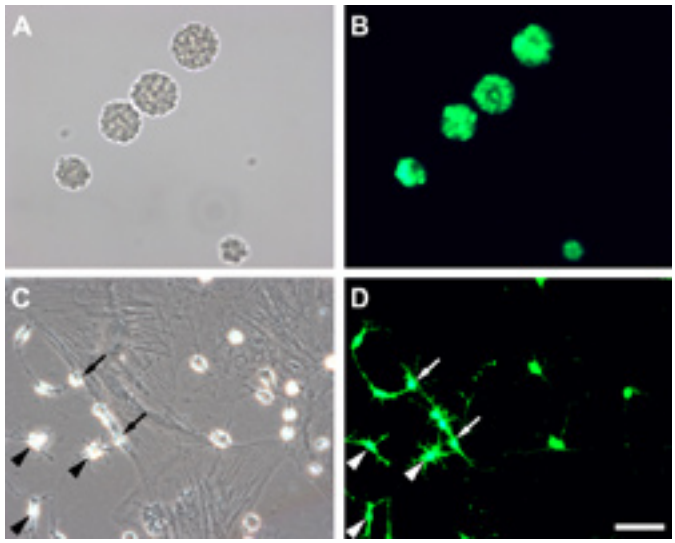

Figure 1: *Adherence of NPC co-cultured with primary fibroblasts: (A) Adult NPC spontaneously form free-floating neurospheres in uncoated culture flasks. Cells do not adhere to the plastic surface. (B) View of the same field as (A) under fluorescent illumination demonstrates GFP expression by NPC. (C) Co-cultivation of NPC with fibroblasts leads to the adherence of NPC to the plastic surface already after 24 hours either independently of surrounding fibroblasts (arrowheads) or directly attached to fibroblasts (arrows). (D) Expression of GFP (arrowheads and arrows corresponding to C) identifies the adhering cells as NPC. (A, C) phase-contrast microscopy, B, D fluorescence microscopy. Scale bar 64 µm*

NPC and skin-derived fibroblasts were prepared on uncoated standard plastic culture flasks and compared to pure NPC cultures. Consistent with previous reports, adult NPC formed free floating cell conglomerates (neurospheres), which did not attach to the surface of the plastic culture dish (Fig. 1A,B) [14]. In contrast, NPC co-cultured with primary fibroblasts adhered to the uncoated plastic surface within 24 hours (Fig. 1C,D). NPC survived in the presence of fibroblasts, were frequently in direct contact with fibroblasts and formed processes along the fibroblast surface. Although NPC/fibroblast co-cultures were maintained in serum-free FGF-2-containing proliferation medium, NPC differentiated into GFAP (31.4% ± 2.7) or Gal-C (5.9% ± 0.5) expressing glial cells with the respective astroglial and oligodendroglial morphology, and beta-III-tubulin (48.9% ± 1.7) expressing neurons (Fig. 2C-E,H). The finding that the sum of individual differentiation markers exceeds 100% is likely due to an overlap between GFAP and A2B5 in astroglial/glial precursor cells as previously described [21]. In contrast, adult NPC maintained as pure NPC cultures displayed antigenicity and morphology of stem/progenitor cells (nestin; 19.2% ± 0.9), glial precursor cells (A2B5; 41.8% ± 1.2) and early neurons (beta-III-tubulin; 22.2% ± 1.8) only (Fig. 2A,B,F). After induction of differentiation in pure NPC cultures by adding FCS instead of FGF-2 for 4 days (Fig. 2G), nestin expressing cells

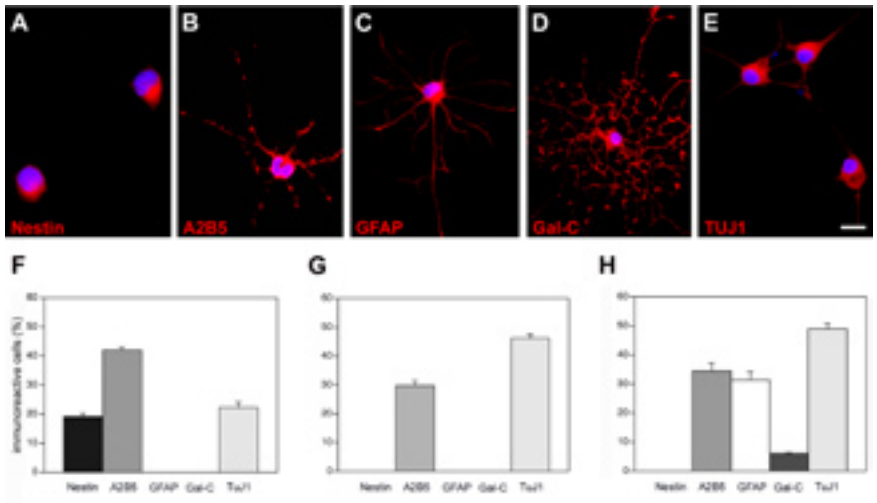

Figure 2: *Differentiation of NPC co-cultivated with fibroblasts: Morphology and immunocytochemical labeling of adult NPC in (A, B) pure NPC cultures and (C-E) NPC/FF co-culture conditions in FGF-2-containing proliferation medium. Cells display immunoreactivity for (A) the stem/progenitor marker nestin, (B) the glial precursor marker A2B5, (C) the astroglial marker GFAP, (D) the oligodendroglial marker Gal-C, and (E) the early neuronal marker beta-III-tubulin (clone TUJ1). All differentiation markers are shown in red, Hoechst 33342 nuclear counterstaining is shown in blue. (F-H) Quantification of the differentiation pattern of adult NPC in vitro 4 days after plating on P-Orn/Lam coated plates: (F) pure NPC cultures in FGF-2 containing proliferation medium, (G) pure NPC cultures in FCS containing differentiation medium and (H) FF-NPC co-cultures in FGF-2 containing proliferation medium. Scale bar A 5.7 µm, B 6.1 µm, C 8.2 µm, D 10.9 µm, E 8.2 µm.*

disappeared completely and glial precursor cells expressing A2B5 were reduced (29.5% ± 1.8). The number of beta-III-tubulin expressing cells increased to 45.9% (± 1.4). In contrast to previous studies using comparable cell culture conditions, GFAP and Gal-C expressing cells were still absent in differentiation conditions [13, 14]. However, in these studies a longer incubation period in differentiation medium (7 days versus 4 days in the present differentiation assay) was chosen. It has been suggested that the neuronal marker beta-III-tubulin is expressed in astroglial cells [22]. However, in a previous experiment we did not detect any co-localization in adult NPC *in vitro* in a double immunofluorescent analysis with beta-III-tubulin and GFAP (unpublished observation).

Taken together, fibroblasts and extracellular matrix molecules secreted by fibroblasts provided a supporting scaffold for NPC to adhere to in culture. The presence of fibroblasts shifted the differentiation pattern of FGF-2 responsive adult NPC towards glial phenotypes.

3.2 Cyst replacement, survival and cell differentiation

Pure NPC (4.8-5.4 x 10^5 cells per graft) grafted immediately after a cervical dorsal column transection [14] or delayed 1-2 weeks later (unpublished observation) were not sufficient to replace or even

reduce the cystic lesion defect. To determine whether fibroblasts are able to maintain NPC within the lesion site, NPC and fibroblasts were co-grafted as mixed cell suspension (**NPC-FF**) directly into the lesion site following an acute cervical wire knife lesion in adult rats. Animals receiving lesions without grafting (**LESION**) or pure fibroblast grafts (**FF**) served as controls. Three weeks post-lesioning, animals without transplants developed lesion cavities in the dorsal half of the spinal cord. In contrast, lesion cavities were completely replaced in all animals with NPC-FF and FF grafts (Fig. 3). Grafts integrated well into the host parenchyma. There were no signs of uncontrolled graft proliferation or tumor formation in NPC-FF and FF grafted animals. Three weeks after NPC-FF transplantation, adult NPC survived throughout the graft as indicated by the presence of BrdU labeled NPC within the graft (Fig. 4A,C-E), in contrast to the absence of BrdU immunoreactivity in FF grafts (controls) (Fig. 4B). NPC were found primarily within the graft, only few BrdU labeled NPC were identifiable in the host parenchyma adjacent to the graft (Fig. 4A). NPC were not evenly distributed in all NPC-FF co-grafts. In some animals, NPC were found in clusters in the center of the graft (Fig.4A), in others they were found predominantly along the graft-host border, but still within the graft (Fig.4C-E).

BrdU labeled NPC co-grafted with fibroblasts displayed antigenic properties of astroglial (GFAP positive; 43.5% ± 2.3), radial glial (BLBP positive; 44.2% ± 3.5)

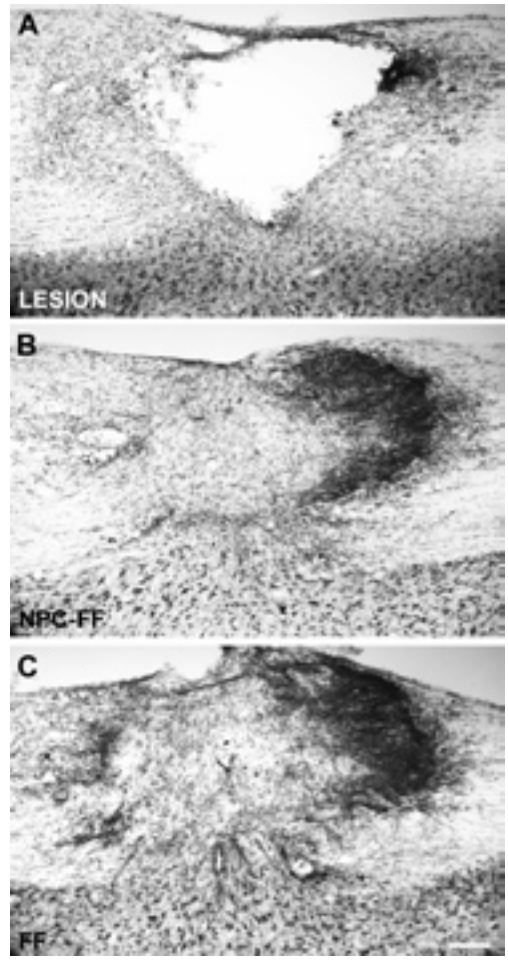

Figure 3: *Cystic lesion replacement: (A) Three weeks following a cervical wire knife dorsal column transection a typical triangular shaped cystic lesion defect develops in animals without transplantation. (B) NPC-FF co-grafts completely replace the cystic lesion cavity and integrate into the host spinal cord. (C) FF grafts also reduce the lesion defect completely. A-C sagittal Nissl stained sections; rostral left, dorsal top; scale bar A-C 196 µm.*

and oligodendroglial cells (APC positive, GFAP negative; 17.8% ± 3.1) (Fig. 5). The percentage of the individual differentiation markers adds up to more than 100% (exactly 105.5%), which is likely due to an overlap between GFAP and BLBP in astroglial cells as previously described [23].

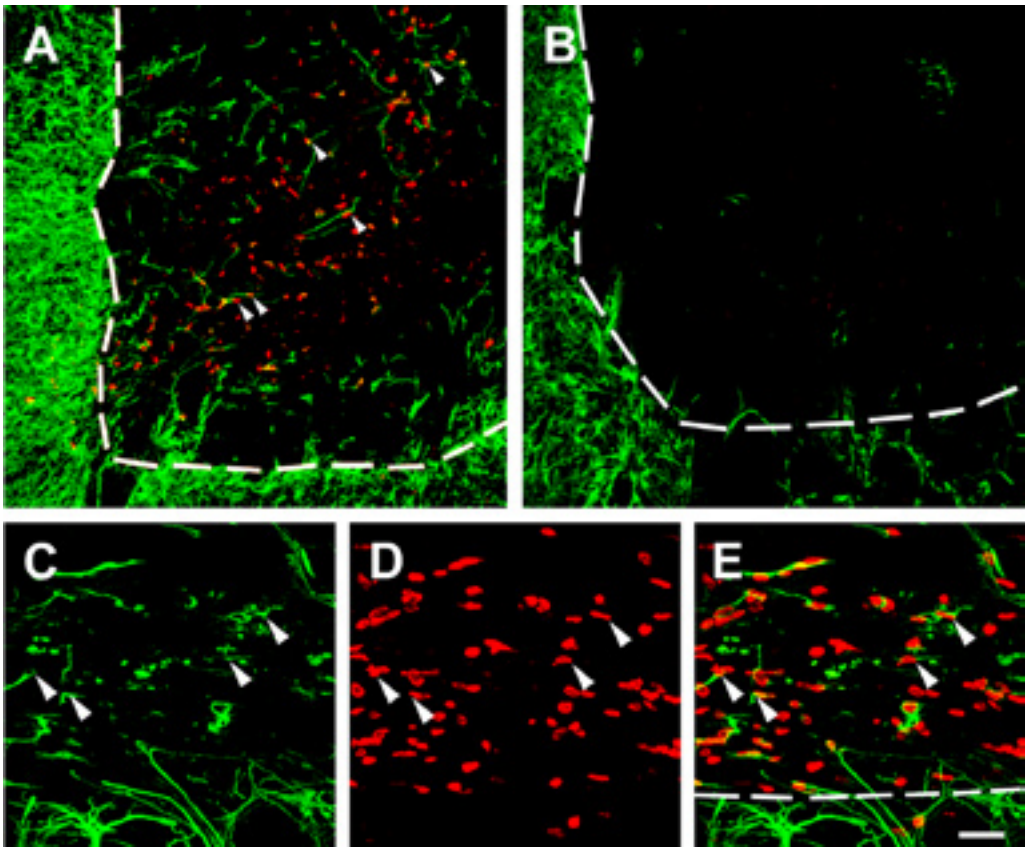

Figure 4: *NPC survival and distribution: (A) Immunohistochemical detection of BrdU prelabeled NPC (rhodamine labeled; red) throughout the graft illustrates that NPC co-grafted together with primary fibroblasts into the acutely injured spinal cord survive. A significant proportion of grafted NPC can be co-localized (arrowheads) with GFAP antigenicity (fluorescein labeled; green) indicating glial differentiation. (B) As control, BrdU is not detectable within FF grafts, GFAP expression is restricted to the surrounding host spinal cord. GFAP expressing processes reach into the fibroblast graft only for a very limited distance. (C-E) The graft-host interface is shown at higher magnification in another NPC-FF grafted animal. (C) GFAP immunolabeled cells, (D) BrdU labeled grafted NPC and (E) merged micrograph of (C) and (D). Arrowheads highlight BrdU/GFAP co-localizing grafted NPC. Orientation in all micrographs: dorsal is at the top, rostral to the left. Dashed lines delineate the graft/host transition. Confocal fluorescence micrograph; scale bar A, B 81,5 µm, C-E 49 µm.*

The majority of GFAP positive NPC displayed bipolar processes rather than multipolar/stellate processes typically found in mature or reactive astrocytes (Fig.5A-C, 6D-G). Consistent with previous studies [13, 14], none of the BrdU prelabeled cells differentiated into a neuronal phenotype as indicated by the lack of beta-III-tubulin – BrdU colocalization (data not shown).

3.3 Axonal regeneration

The maintenance of adult NPC within the lesion cavity of NPC-FF co-transplant recipients allowed us for the first time to investigate the capacity of NPC to promote axon regeneration into the graft. Axonal

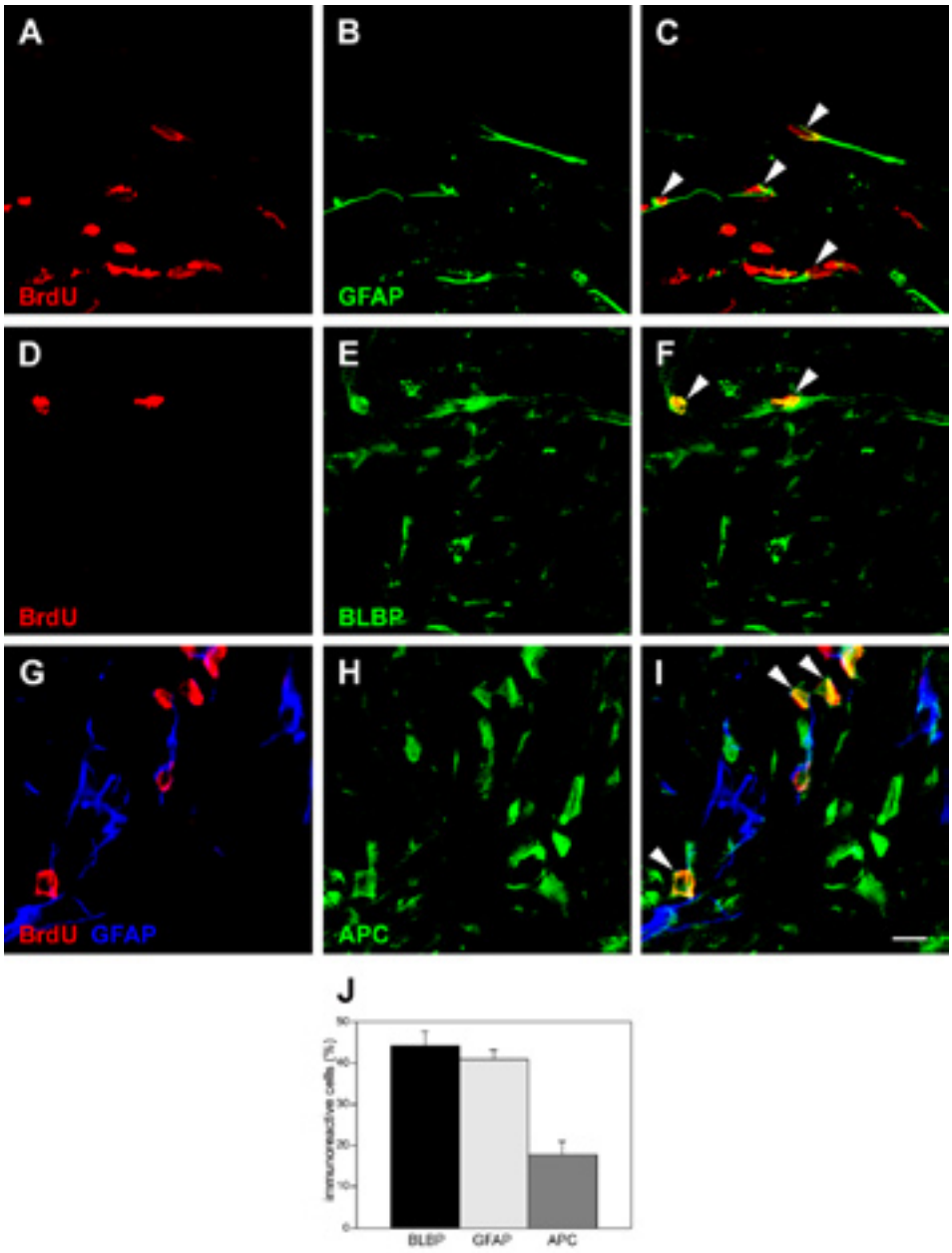

Figure 5: *Confocal analysis of NPC differentiation in NPC-FF co-grafts: (A-C) BrdU prelabeled NPC co-localize with GFAP immunoreactivity (arrowheads). GFAP expressing cells frequently display bipolar elongated processes reminiscent of immature or radial glial cells in the developing CNS. (D-F) NPC are also co-localized with BLBP (arrowheads), which is typically expressed in radial glial cells. (G-I) NPC immunoreactive for APC and at the same time negative for GFAP (Cy5 labeled; blue) indicate oligodendroglial differentiation (arrowheads). The BrdU labeled NPC, co-localized with APC in the center of the field, is also co-localized with GFAP suggesting astroglial rather oligodendroglial differentiation. (C, F, I) Merged images of the rhodamine, fluorescein and Cy5 channels. (J) Quantification of BrdU prelabeled NPC co-localized with BLBP, GFAP or APC. Scale bar A-C, 27.4 µm, D-F 24.4 µm, G-I 15.9 µm.*

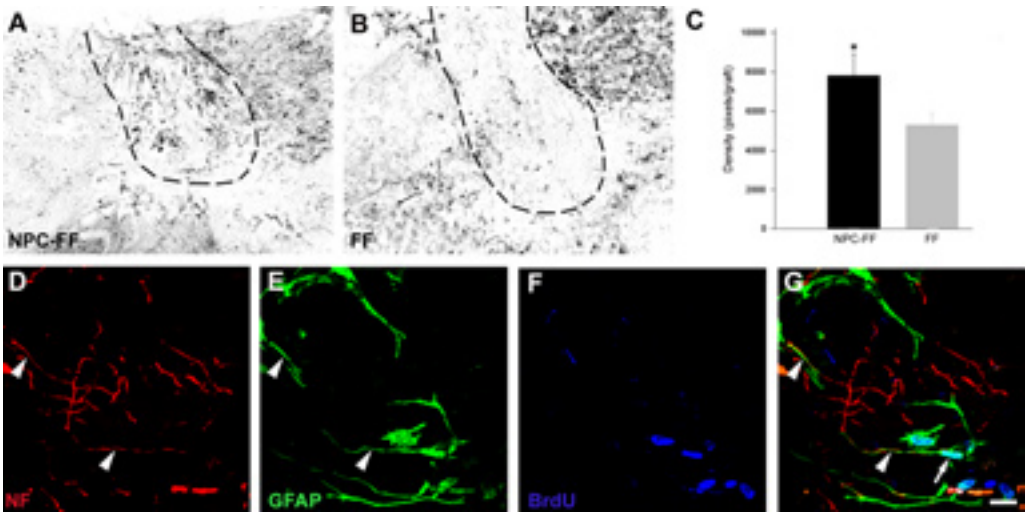

Figure 6: *Axonal growth into fibroblast (FF) and NPC/fibroblast grafts (NPC-FF): Representative micrographs of neurofilament expressing axonal profiles within (A) NPC-FF and (B) FF grafts. Dashed lines delineate the graft/host interface. (C) Quantification of neurofilament labeling reveals significantly more axonal growth into co-grafts ($p<0.05$). Error bars represent SEM. (D) Neurofilament (NF) expressing axons within the graft are longitudinally oriented along (E) GFAP labeled cells (highlighted by arrowheads in D, E and G), which are colocalized with (F) BrdU prelabeled NPC (highlighted by arrow in G). (G) Merged image of (D-G). (A, B) Immunohistochemical brightfield images, (D-G) confocal immunofluorescence images. Orientation in all images: rostral to the left, dorsal at the top. Scale bar A, B 85.7 µm, D-G 14.8 µm.*

growth into NPC-FF co-grafts was compared to FF grafts by quantifying the number of neurofilament labeled axonal profiles. Axonal growth was observed into both, FF grafts and NPC-FF co-grafts. However, the number of axonal profiles was significantly increased by 47 % into NPC-FF co-grafts (7809 ± 1120 pixels/graft) versus fibroblast grafts (5299 ± 618 pixels/graft; $p < 0.05$) (Fig. 6A-C). Neurofilament labeled axons within NPC-FF co-grafts were frequently oriented longitudinally along GFAP labeled cellular processes (Fig. 6D-G), which co-localized with BrdU labeled nuclei. GFAP expressing cells in the graft typically displayed a bipolar, immature morphology.

The cervical wire knife lesion completely disrupts the main portion of the CST descending in the dorsal columns of the spinal cord. Therefore, the presence of anterogradely BDA labeled axonal profiles traversing from the main dorsal pathway into the graft indicates regrowth of transected CST axons rather than sprouting responses of uninjured ventral corticospinal axons. In analogy to neurofilament labeled axons, significantly more CST axons regenerated into NPC-FF co-grafts (2774 pixels ± 384) in comparison to FF grafts (1027 pixels ± 356; $p<0.05$) (Fig. 7A-C). In addition, the distance of CST axon regrowth into the graft measuring the longest distance of BDA labeled CST axon endings from the graft-host interface into the graft was significantly enhanced by 69% in NPC-FF co-grafts (316 mm ± 40) versus FF grafts

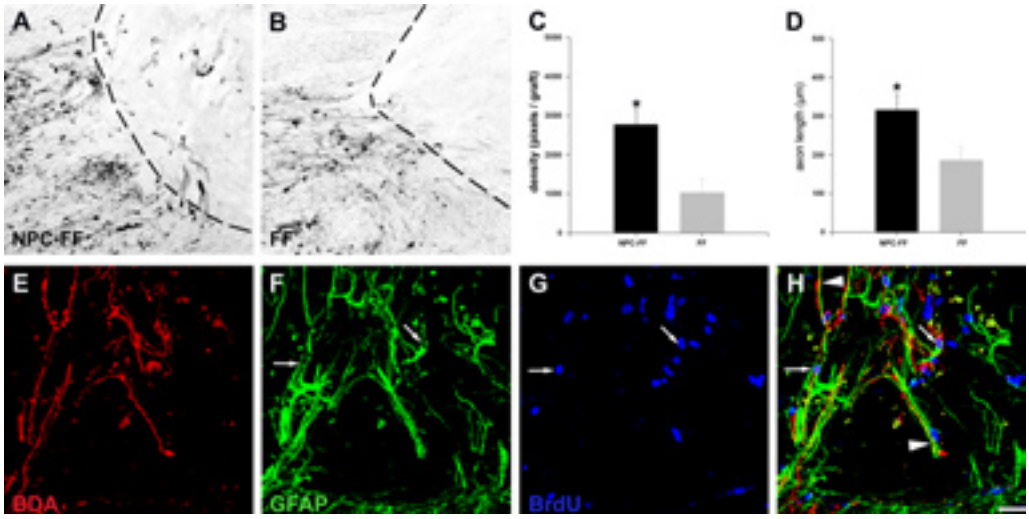

Figure 7: *Corticospinal axon regeneration: Representative micrographs of BDA labeled corticospinal axons within (A) NPC-FF and (B) FF grafts. Dashed lines delineate the graft/host transition. (C) Quantification of BDA labeling reveals significantly more axonal growth into NPC-FF grafts ($p<0.05$). (D) The distance of CST axon growth into the graft is significantly higher in NPC-FF grafts compared to FF grafts ($p<0.05$). Error bars represent SEM. (E) BDA labeled CST axons are longitudinally aligned along (F) GFAP expressing cells, which are colocalized with (G) BrdU prelabeled nuclei of grafted NPC (highlighted by arrows in F- H). (H) Merged images of (E-G). Axon endings with morphological features of growth cones (arrowheads) are oriented along GFAP positive processes, indicating that axons use GFAP expressing cells as a guiding scaffold. (A, B) Immunohistochemical brightfield micrographs, (E-H) confocal immunofluorescence micrograph. Orientation in all images: rostral to the left, dorsal at the top. Scale bar A, B 36.4 µm, E-H 25.5 µm.*

(187 mm ± 35; $p<0.05$) (Fig. 7D). Similar to neurofilament labeled axons, BDA labeled CST axons were aligned along GFAP positive processes in the graft (Fig. 7E-G). BDA labeled CST axon endings displayed morphological features of growth cones, strongly suggesting an ongoing process of axonal regrowth along cellular processes rather than grafted cells aligning their processes along axons within the grafts. GFAP positive cells showed a bipolar morphology with long processes and co-localized with BrdU labeled nuclei, identifying them as NPC derived cells (Fig. 7H). These data indicate that grafted NPC-derived GFAP expressing cells have the capacity to build a physical guiding structure for regenerating CST axons.

4. DISCUSSION

Findings of the present study indicate that grafted adult neural progenitor cell (NPC) derived glial cells enhance regeneration of CNS axons following spinal cord injury. NPC grafts facilitate axonal regeneration by providing a growth permissive guiding substrate mimicking axonal outgrowth pattern in the developing CNS.

Studies in lower vertebrates indicate that glial cells play an important role as guidance cues for axon growth and regeneration during development and after injury [24, 25]. The role of direct cellular guidance in axonal growth during development

and after injury is much less defined in the mammalian CNS. Axonal pathfinding in the corpus callosum of developing rats has been associated with cellular guidance cues provided by astroglial cells [26, 27]. Time course studies in the postnatal mammalian spinal cord demonstrate that corticospinal axons growing throughout the spinal cord between postnatal day 0 and 10 are in close spatial and temporal association with processes of vimentin and GFAP expressing glial cells [7]. *In vitro* studies have shown that astroglial cells directly guide neurite outgrowth only at a distinct immature developmental stage [28, 29]. There, growth promoting astroglial cells display a bipolar morphology with long processes [28]. This bipolar morphology can be found in grafted GFAP expressing NPC in our study indicating that these cells represent an immature glial cell type rather than mature astrocytes. Therefore, the axonal growth observed in our experiments likely recapitulates cell guided axon outgrowth during development.

Co-cultivation of NPC with fibroblasts significantly increased the percentage of cells differentiating into a glial GFAP expressing phenotype in our *in vitro* experiments. Previous *in vitro* studies also demonstrated that mesenchymal cells such as meningeal cells or corneal fibroblasts promote glial differentiation in fetal cortex derived cell cultures or postnatal cerebellar slice cultures [30, 31]. Interestingly, meningeal cells also induced a bipolar morphology in GFAP expressing cells [31] similar to the glial morphology of NPC co-grafted with fibroblasts. Whether these effects are mediated through direct cell-cell interactions or through soluble factors remains to be determined. Further evidence supporting the concept that fibroblasts might promote a more bipolar glial phenotype resembling immature astroglial cells, is provided by previous observations [14]. After transplantation of pure NPC, isolated and cultivated under the same conditions as in the present study, GFAP immunolabeled cells frequently displayed a mature, stellate appearance.

We observed an increase in axonal sprouting into NPC-FF grafts compared to control fibroblast grafts despite the presence of putative inhibitory extracellular matrix molecules such as chondroitin sulfate proteoglycans, which have been detected within and around fibroblast containing grafts following spinal cord injury [18]. It is possible that NPC influence the local expression or degradation of inhibitory extracellular matrix molecules to an extent that cannot be determined by immunohistochemistry. This notion is supported by recent findings demonstrating that immature glial cells are capable to overcome the growth-inhibitory barrier by digesting specifically the CSPG aggrecan in *in vitro* outgrowth assays [32]. Alternatively, axon growth promoting glial cells could express growth permissive signals, which outweigh inhibitory signals from various extracellular matrix molecules present within the graft [18]. In this context, it is interesting to note that growth permissive signals such as the cell adhesion molecules NCAM and L1 have been identified on growth promoting immature astroglia, however, not on mature astroglia [29].

It becomes evident from this study that any restorative strategy employing neural stem cells for transplantation without a supporting scaffold following spinal cord injury is not sufficient to replace extensive lesion defects developing in the course of a traumatic spinal cord lesion, and therefore cannot provide a bridge for axons to regenerate on. The necessity to administer a supporting scaffold together with neural stem cells has already been demonstrated following transplantation into an ischemia induced CNS lesion [15]. However, in the present study naturally occurring fibroblasts and/or extracellular matrix molecules released by fibroblasts as opposed to previously used artificially manufactured polymers were able to maintain adult NPC within the cystic lesion defect. Some extracellular matrix molecules secreted by fibroblasts such as laminin or fibronectin have been found to enhance cell motility, and thereby might accelerate the migration of adult NPC away from the graft into the surrounding host spinal cord. However, other extracellular matrix molecules such as CSPG, which are expressed in fibroblast containing grafts [18], actually inhibit NPC migration [33]. Thus, CSPG might be an important component to prevent significant migration of NPC away from the lesion site and to maintain NPC within the lesion cavity.

In terms of a putative clinical application, the question remains whether adult NPC are a cell population superior to fibroblasts alone or to fetal spinal cord tissue containing immature neural cells, which are already placed in a predefined tissue architecture before grafting. Both strategies have been shown to replace cystic lesion defects and to promote partial functional recovery following acute and chronic spinal cord injury [17, 34-40]. In particular, fibroblasts genetically modified to secrete regrowth promoting neurotrophic factors such as neurotrophin-3 (NT-3) or brain derived neurotrophic factor (BDNF) elicit regeneration of supraspinal projections into the graft, however, axons are unable to reenter the host spinal cord [35, 39]. Thus, fibroblasts represent a powerful cellular vehicle to locally deliver growth promoting molecules, however, they do not have the capacity to serve as a "bridge" reconnecting injured rostral axons with targets located distally or vice versa. Fetal spinal cord tissue has been demonstrated to elicit functional recovery, but the exact structural mechanisms remain to be determined [34, 38, 41]. Ethical concerns and the limited availability of fetal transplants further restrict their clinical applicability.

Adult NPC represent a highly promising source for regenerative cell based-strategies following spinal cord injury. However, at the time point investigated axon growth is still limited. Axons do not regenerate beyond a limited distance within the transplant and do not re-enter the caudal host spinal cord. Future studies need to investigate axonal regeneration over longer periods of time. The exact characteristics of growth promoting glial cells need to be specifically identified and these cell populations need to be enriched to augment structural and potentially functional recovery. Increasing the ratio of NPC to fibroblasts, overexpressing neurotrophic

factors such as NT-3 [17], and stimulating the neuronal cell body with cyclic nucleotides [42] might be other means to enhance the regenerative capacity of axons into and beyond NPC containing grafts. Studies in the chronically injured spinal cord are needed to determine whether NPC survival/differentiation and corticospinal growth responses are similar in chronic spinal cord injuries compared to acute injuries investigated in the present study.

5. ACKNOWLEDGMENTS

This work was supported by the Institute International de Recherche en Paraplégie Geneva, on behalf of an anonymous donation, Deutsche Forschungsgemeinschaft (WE 2165), Bavaria California Technology Center and by the ReForM-Program, University of Regensburg, School of Medicine to N.W. and the Paralysis Project to A.B.. We thank Ulrich Bogdahn for his continued support and critical comments. We also thank Nathaniel Heintz for the BLBP antibody. The laminin antibody developed by E. Engvall was obtained from the Developmental Studies Hybridoma Bank under the auspices of the NICHD and maintained by the University of Iowa, Department of Biological Sciences, Iowa City, Iowa 52242.

6. REFERENCES

1. Li, Y., Field, P. M. & Raisman, G. Repair of adult rat corticospinal tract by transplants of olfactory ensheathing cells. Science 277, 2000-2 (1997).
2. Liu, Y. et al. Transplants of fibroblasts genetically modified to express BDNF promote regeneration of adult rat rubrospinal axons and recovery of forelimb function. J Neurosci 19, 4370-87 (1999).
3. Ramon-Cueto, A., Cordero, M. I., Santos-Benito, F. F. & Avila, J. Functional recovery of paraplegic rats and motor axon regeneration in their spinal cords by olfactory ensheathing glia. Neuron 25, 425-35 (2000).
4. Teng, Y. D. et al. Functional recovery following traumatic spinal cord injury mediated by a unique polymer scaffold seeded with neural stem cells. Proc Natl Acad Sci U S A 99, 3024-9 (2002).
5. Tuszynski, M. H. et al. Fibroblasts genetically modified to produce nerve growth factor induce robust neuritic ingrowth after grafting to the spinal cord. Exp Neurol 126, 1-14 (1994).
6. Xu, X. M., Guenard, V., Kleitman, N. & Bunge, M. B. Axonal regeneration into Schwann cell-seeded guidance channels grafted into transected adult rat spinal cord. J Comp Neurol 351, 145-60 (1995).
7. Joosten, E. A. & Bar, D. P. Axon guidance of outgrowing corticospinal fibres in the rat. J Anat 194, 15-32 (1999).
8. Joosten, E. A. & Gribnau, A. A. Astrocytes and guidance of outgrowing corticospinal tract axons in the rat. An immunocytochemical study using anti-vimentin and anti-glial fibrillary acidic protein. Neuroscience 31, 439-52 (1989).
9. Griffin, J. W. & Hoffman, P. N. in Peripheral Neuropathy (eds. Dyck, P. J. & Thomas, P. K.) 361-376 (W.B. Saunders, Philadelphia, 1993).
10. Gage, F. H. et al. Survival and differentiation of adult neuronal progenitor cells transplanted to the adult brain. Proc Natl Acad Sci U S A 92, 11879-83 (1995).
11. Reynolds, B. A. & Weiss, S. Generation of neurons and astrocytes from isolated cells of the adult mammalian central nervous system. Science 255, 1707-10 (1992).
12. Cao, Q. L. et al. Pluripotent stem cells engrafted into the normal or lesioned adult rat spinal cord are

restricted to a glial lineage. Exp Neurol 167, 48-58. (2001).
13. Shihabuddin, L. S., Horner, P. J., Ray, J. & Gage, F. H. Adult spinal cord stem cells generate neurons after transplantation in the adult dentate gyrus. J Neurosci 20, 8727-35 (2000).
14. Vroemen, M., Aigner, L., Winkler, J. & Weidner, N. Adult neural progenitor cell grafts survive after acute spinal cord injury and integrate along axonal pathways. Eur J Neurosci 18, 743-751 (2003).
15. Park, K. I., Teng, Y. D. & Snyder, E. Y. The injured brain interacts reciprocally with neural stem cells supported by scaffolds to reconstitute lost tissue. Nat Biotechnol 20, 1111-7 (2002).
16. Blesch, A. et al. Leukemia inhibitory factor augments neurotrophin expression and corticospinal axon growth after adult CNS injury. J Neurosci 19, 3556-66 (1999).
17. Grill, R., Murai, K., Blesch, A., Gage, F. H. & Tuszynski, M. H. Cellular delivery of neurotrophin-3 promotes corticospinal axonal growth and partial functional recovery after spinal cord injury. J Neurosci 17, 5560-72 (1997).
18. Jones, L. L., Sajed, D. & Tuszynski, M. H. Axonal regeneration through regions of chondroitin sulfate proteoglycan deposition after spinal cord injury: a balance of permissiveness and inhibition. J Neurosci 23, 9276-88 (2003).
19. Weidner, N., Grill, R. J. & Tuszynski, M. H. Elimination of basal lamina and the collagen “scar” after spinal cord injury fails to augment corticospinal tract regeneration. Exp Neurol 160, 40-50 (1999).
20. Weidner, N., Ner, A., Salimi, N. & Tuszynski, M. H. Spontaneous corticospinal axonal plasticity and functional recovery after adult central nervous system injury. Proc Natl Acad Sci U S A 98, 3513-3518 (2001).
21. Walker, A. G., Chapman, J., Bruce, C. B. & Rumsby, M. G. Immunocytochemical characterisation of cell cultures grown from dissociated 1-2-day post-natal rat cerebral tissue. A developmental study. J Neuroimmunol 7, 1-20 (1984).
22. Katsetos, C. D. et al. Aberrant localization of the neuronal class III beta-tubulin in astrocytomas. Arch Pathol Lab Med 125, 613-24 (2001).
23. Feng, L., Hatten, M. E. & Heintz, N. Brain lipid-binding protein (BLBP): a novel signaling system in the developing mammalian CNS. Neuron 12, 895-908 (1994).
24. Hidalgo, A. & Booth, G. E. Glia dictate pioneer axon trajectories in the Drosophila embryonic CNS. Development 127, 393-402 (2000).
25. Lurie, D. I., Pijak, D. S. & Selzer, M. E. Structure of reticulospinal axon growth cones and their cellular environment during regeneration in the lamprey spinal cord. J Comp Neurol 344, 559-80 (1994).
26. Silver, J., Edwards, M. A. & Levitt, P. Immunocytochemical demonstration of early appearing astroglial structures that form boundaries and pathways along axon tracts in the fetal brain. J Comp Neurol 328, 415-36 (1993).
27. Smith, G. M., Miller, R. H. & Silver, J. Changing role of forebrain astrocytes during development, regenerative failure, and induced regeneration upon transplantation. J Comp Neurol 251, 23-43 (1986).
28. Johansson, S. & Stromberg, I. Guidance of dopaminergic neuritic growth by immature astrocytes in organotypic cultures of rat fetal ventral mesencephalon. J Comp Neurol 443, 237-49 (2002).
29. Smith, G. M., Rutishauser, U., Silver, J. & Miller, R. H. Maturation of astrocytes in vitro alters the extent and molecular basis of neurite outgrowth. Dev Biol 138, 377-90 (1990).
30. Colombo, J. A. & Napp, M. I. In vitro induction of radial-like cells by leptomeningeal and cortical astroglial conditioned media. Effect of protease inhibitors. Int J Dev Neurosci 14, 489-96 (1996).
31. Hartmann, D., Ziegenhagen, M. W. & Sievers, J. Meningeal cells stimulate neuronal migration and the formation of radial glial fascicles from the cerebellar external granular layer. Neurosci Lett 244, 129-32 (1998).
32. Miller, J. H., Tom, V. J., Doller, C. M. & Silver, J. in Soc Neurosci Abs Program No. 880.1 (New Orleans, LA, 2003).
33. Kearns, S. M., Laywell, E. D., Kukekov, V. K. & Steindler, D. A. Extracellular matrix effects on neurosphere

cell motility. Exp Neurol 182, 240-4 (2003).
34. Bregman, B. S. & Reier, P. J. Neural tissue transplants rescue axotomized rubrospinal cells from retrograde death. J Comp Neurol 244, 86-95 (1986).
35. Jin, Y., Fischer, I., Tessler, A. & Houle, J. D. Transplants of fibroblasts genetically modified to express BDNF promote axonal regeneration from supraspinal neurons following chronic spinal cord injury. Exp Neurol 177, 265-75 (2002).
36. Liu, S. et al. Embryonic stem cells differentiate into oligodendrocytes and myelinate in culture and after spinal cord transplantation. Proc Natl Acad Sci U S A 97, 6126-31 (2000).
37. Reier, P. J., Houle, J. D., Jakeman, L., Winialski, D. & Tessler, A. Transplantation of fetal spinal cord tissue into acute and chronic hemisection and contusion lesions of the adult rat spinal cord. Prog Brain Res 78, 173-9 (1988).
38. Tessler, A. et al. Embryonic spinal cord transplants enhance locomotor performance in spinalized newborn rats. Adv Neurol 72, 291-303 (1997).
39. Tuszynski, M. H. et al. NT-3 gene delivery elicits growth of chronically injured corticospinal axons and modestly improves functional deficits after chronic scar resection. Exp Neurol 181, 47-56 (2003).
40. Wirth, E. D., 3rd et al. Feasibility and safety of neural tissue transplantation in patients with syringomyelia. J Neurotrauma 18, 911-29 (2001).
41. Stokes, B. T. & Reier, P. J. Fetal grafts alter chronic behavioral outcome after contusion damage to the adult rat spinal cord. Exp Neurol 116, 1-12 (1992).
42. Qiu, J. et al. Spinal axon regeneration induced by elevation of cyclic AMP. Neuron 34, 895-903 (2002).

Chapter 4a

Purification of Schwann cells by selection of p75 low affinity nerve growth factor receptor expressing cells from adult peripheral nerve

J. Neurosci. Meth. 124; 135-143 (2003)

Maurice Vroemen
Norbert Weidner

ABSTRACT

The intrinsic capacity of Schwann cells to promote regeneration after limited peripheral nerve lesions has been successfully transferred to extensive peripheral nerve injuries and central nervous system lesions by autologous transplantation strategies. However, both the intrinsic ability of axotomized neurons to regenerate and the permissiveness of the parenchyma surrounding the acute injury site diminish over time. Therefore, the autologous transplantation mode requires a fast and effective method to isolate Schwann cells from peripheral nerve biopsies. Here, we report a method to purify p75 low affinity nerve growth factor receptor (p75LNGFr) expressing Schwann cells from peripheral nerve biopsies in adult rats using magnetic-activated cell separation (MACS). After one week of nerve degeneration in culture, nerve fragments were dissociated resulting in mixed cultures containing Schwann cells and fibroblasts. After incubation with specific anti-p75LNGFr antibodies and secondary magnetic bead conjugated antibodies followed by one cycle of MACS, 95% pure Schwann cell cultures were generated as confirmed by flow-cytometry and immunocytochemistry. In contrast to established methods, MACS separation of p75LNGFr expressing cells allows the reliable purification of Schwann cells within 9 days after biopsy employing direct selection of Schwann cells rather than fibroblast depletion assays. Therefore, this method represents an effective and fast means to generate autologous Schwann cells for clinical transplantation strategies aiming for axon repair and remyelination.

1. INTRODUCTION

After limited injury to the peripheral nervous system (PNS), endogenous Schwann cells are recruited to form a scaffold for regenerating axons to grow along, produce growth conducive extracellular matrix components, secrete neurotrophic factors and remyelinate regenerating axons in a phenotypical appropriate manner, which ultimately leads to reinnervation of the target and functional recovery [1].

By transplanting Schwann cells, these favorable properties have been successfully transferred to more severe peripheral nerve injuries and even central nervous system (CNS) lesions. After severe peripheral nerve injuries endogenous recruitment of Schwann cells is not sufficient to promote morphological and functional restoration. The availability of peripheral nerve autograft material, which represents the standard therapy in these cases, is limited. Allografts on the other hand, are subject to graft rejection [2]. Artificially produced guidance channels seeded with autologous Schwann cells could overcome these limitations. Syngenic Schwann cells seeded into guidance channels have been successfully employed to support regeneration in animal models of peripheral nerve injury [3, 4].

In the CNS, transplanted Schwann cells can regenerate and remyelinate axons, which have been completely interrupted

[5-8], or have been demyelinated by toxins or irradiation [9-12]. Furthermore, the regenerative capacity of Schwann cells can be enhanced by *ex vivo* genetic modification to overexpress neurotrophic factors [13-15].

Ideally, Schwann cells are transplanted in an autologous fashion to avoid graft immune rejection. The disadvantage is that autologous Schwann cells will not be available immediately after a nerve lesion. The generation of sufficient quantities of Schwann cells for transplantation from the patient's own peripheral nerve biopsy requires at least three to six weeks according to established protocols [16-18]. However, the regeneration supportive capacity in the PNS and CNS decreases over time due to events such as cellular degeneration, scar formation and down-regulation of growth promoting molecules [19, 20].

The separation of Schwann cells from rapidly dividing fibroblasts, which build the protecting layers (epi-, perineurium) surrounding bundles of nerve fibers, represents the major time consuming factor [21, 22]. Thus far, established methods for Schwann cell purification from peripheral nerve fragments are based on fibroblast depletion as opposed to direct selection of Schwann cells. As an initial step to separate Schwann cells from fibroblasts, nerve fragments are maintained under cell culture conditions on an adhesive substrate such as laminin for several weeks. This procedure allows fibroblasts to migrate out, while Schwann cells remain in the nerve fragment. Each consecutive transfer of these nerve fragments reduces the number of fibroblasts [17]. The number of rapidly dividing fibroblasts can be reduced by adding antimitotic drugs such as cytosine arabinoside (Ara-C) to the cell culture medium or by maintaining serum-free primary cultures [23, 24]. The yield of enriched Schwann cells can be further enhanced by predegeneration of peripheral nerves *in vivo* before biopsy [16, 25]. Besides the time required to enrich Schwann cells, these purification methods are rather unspecific [18]. More specific purification methods, such as fibroblasts depletion using specific antibodies against the cell-surface antigen Thy-1 coupled to either complement activation or immunopanning, have only been reported for neonatal peripheral nerves [26, 27].

Magnetic-activated cell separation (MACS) represents a highly effective and fast method to select individual cell populations from a mixed cell population. Cell type specific cell surface antigens are labeled with magnetic bead conjugated antibodies followed by separation on a high gradient magnetic column [28]. A suitable cell surface antigen to select Schwann cells is the p75 low affinity nerve growth factor receptor (p75LNGFr), which is widely expressed on Schwann cells *in vitro*, but not on fibroblasts [29]. A similar approach using magnetic Dynabeads to enrich p75LNGFr expressing olfactory ensheathing cells has been described recently [30]. Vice versa, the cell surface antigen Thy-1 is expressed on fibroblasts, but not on Schwann cells, and thus can be used to enrich Schwann cells by depleting Thy-1 expressing fibroblasts [31].

In the present experiment, we investigated the efficacy of MACS to purify Schwann cells from adult sciatic nerve biopsies by using either specific antibodies (1) against p75LNGFr to select Schwann cells or (2) against Thy-1 to deplete fibroblasts. Results from this study indicate that only MACS selection of p75LNGFr expressing Schwann cells represents a highly effective procedure to establish primary Schwann cell cultures for autologous transplantation strategies in the PNS and CNS.

2. MATERIALS AND METHODS

2.1 Schwann cell isolation

Sciatic nerve fragments with a length of approximately 35mm were taken bilaterally from deeply anesthetized (0.5 ml of a combination of ketamine (50 mg/kg), xylazine (2.6 mg/kg) and acepromazine (0.5 mg/kg)) adult Fischer 344 rats (average weight 160-180 g). The sciatic nerves were washed with ice-cold Hank's balanced salt solution (HBSS, PAA Laboratories, Austria) and the epineurium was stripped off with a fine forceps. Each sciatic nerve fragment weighed on average 29.6 mg ± 1.7. Nerves were cut into 1mm pieces and plated on collagen type-I (5 mg/cm^2, Pan Biotech, Germany) coated culture dishes in standard medium, which consists of Dulbecco's modified essential medium (DMEM) supplemented with 10% fetal calf serum (FCS; Pan Biotech, Germany) and Penicillin/Streptomycin (100 U of penicillin, 100 mg/ml Streptomycin; Pan Biotech, Germany). The culture dishes with the sciatic nerve pieces were kept in a cell culture incubator at 37°C in a humidified atmosphere containing 5% CO_2. After 7 days in culture, the sciatic nerve fragments were transferred into 24 well plates containing 500 µl HBSS with 3% trypsin, 1% collagenase and 1% hyaluronidase (all Sigma, Germany) per well. After two hours of incubation at 37°C, tissue fragments were dissociated by trituration through a glass Pasteur-pipette and a 20-gauge sterile needle. The suspension was centrifuged at 120 x g for 10 min at room temperature. After resuspension in standard medium, trituration through a 22-gauge hypodermic needle followed. The resulting cell suspension was cultured in standard medium for two days on poly-l-ornithin/laminin (P-Orn/Lam; both Sigma, Germany) culture flasks, which were coated as follows: flasks were incubated with 20mg/cm^2 poly-l-ornithin in distilled H_2O for 2 hours at 37°C, rinsed with distilled H_2O and incubated with 0.4 mg/cm^2 laminin in PBS for 2 hours at 37°C. After 2 days in culture, the number of viable cells total before MACS and flow-cytometry/immunocytochemistry analysis was determined by counting the Trypan blue excluding cells using a hemocytometer.

2.2 Schwann cell purification

Each purification run using MACS was conducted with nerve biopsies pooled from 3-4 rats (6-8 nerve explants). The MACS procedure was performed according to the manufacturer's instructions (Miltenyi Biotec, Germany). The flask containing the unpurified cells was washed with Dulbecco's phosphate buffered saline

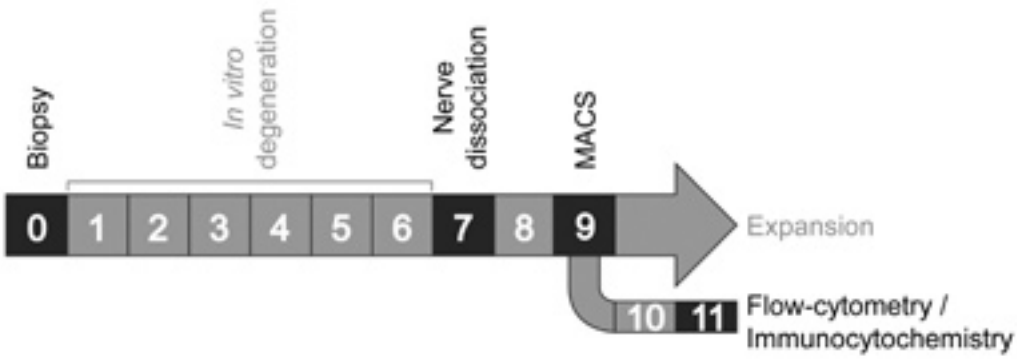

Figure 1: *Time line from peripheral nerve biopsy (day 0) through immunocytochemical/flow-cytometry analysis of MACS selected cells (day 11).*

(PBS) and incubated with 40 µl/cm^2 Accutase (Innovative Cell Tech, San Diego, USA) for 5 minutes to detach the cells. Accutase, which is a mixture of collagenases, proteases and EDTA, was used instead of trypsin to protect trypsin sensitive cell surface markers. The cells were collected in DMEM containing 10% FCS and were centrifuged at 300 x g for 5 min at 4°C, washed with PBS supplemented with 2mM EDTA (PE) and counted using a hemocytometer (= number of unpurified cells). A sample of unpurified cells (2 x.10^5) was seeded on P-Orn/Lam coated culture flask for further analysis.

For MACS Schwann cell selection, the remaining unpurified cells were incubated with 5 µl (equals 0.25 mg IgG1) of the anti-p75LNGFr monoclonal antibodies (Chemicon, Germany) in 95 µl Dulbecco's PBS, 2mM EDTA, 0.5% BSA (PEB) for 10 min at room temperature. At the end of the incubation, 5ml of PE was added and the cells were centrifuged (300 x g for 5 min at 4°C). After one wash with PE, the cells were incubated with 20 µl of the microbead-linked rat anti-mouse IgG1 (at 1:5; Miltenyi Biotec, Germany) in 80 µl PEB for 15 min at 4°C. After 2 rinsing steps with PE, a MS column (Miltenyi Biotec, Germany) was placed in the MiniMACS magnet (Miltenyi Biotec, Germany) and flushed with PEB. A maximum of 5 x 10^6 cells was resuspended in 500 µl PEB and applied onto the MS+ column. Three rinses with 500 µl PEB followed to wash out unbound cells, which represented the p75LNGFr negative fraction. After removal from the magnet, the column was flushed with 2 ml PE, which allowed the collection of the p75LNGFr positive cell fraction.

For MACS fibroblast depletion, cell suspensions were incubated with a mouse monoclonal anti-Thy-1 IgG1 (at 1:100; Harlan Sera Lab, Germany) and microbead-linked rat anti-mouse IgG1 antibodies as described. The MS column was loaded with a maximum of 5 x 10^6 labeled cells. Cells not binding to the column attached to the magnet represented the Thy-1 negative cell fraction. Flushing of the column after removal of the magnet allowed the collection of the Thy-1 positive cell fraction.

The number of viable cells in the various fractions was determined by counting the Trypan blue excluding cells using a hemocytometer. For flow-cytometry analysis 2 days later, a sample of purified cells (2 x 10^5) was plated on P-Orn/Lam coated culture flasks and standard medium was added. The remaining Schwann cells were expanded in standard medium supplemented with 2 µM forskolin (Sigma, Germany) and 0.2% bovine pituitary extract (Clonetics, Germany).

2.3 Flow-cytometry analysis of MACS selected cells

A sample of unpurified cells or cells (2 x 10^5 cells each) purified by either p75LNGFr selection or Thy-1 depletion was harvested within 48 hours after MACS using Accutase, washed with PE and immunolabeled with the anti-Thy-1 mouse antibody (at 1:100 in PEB) used for the fibroblast depletion assay. The cells were washed with PE, stained with a secondary fluorescein-conjugated donkey anti mouse IgG antibody (at 1:1000 in PEB; Jackson Immunoresearch, Germany) and washed with PE. The total number of 10,000 events was analyzed on a FACSCalibur flow-cytometer (Becton-Dickinson, Germany) directly after the staining procedure. Data were processed with the WinMDI 2.8 software (J. Trotter, USA). The percentage of fibroblasts in the various samples was determined by measuring the fraction of Thy-1 positive cells in the fluorescence intensity dotplot compared to the total amount of intact cells.

2.4 Immunocytochemistry

Cells from each sampling fraction were plated in standard medium on P-Orn/Lam coated Permanox Chamber Slides (Nunc, Germany) for 2 days. The cells were fixed with ice-cold 4% paraformaldehyde in PBS for 30 minutes, rinsed 3 times with Tris-buffered saline (TBS), blocked with TBS containing 3% donkey blocking serum (Pan Biotech, Germany) and incubated overnight with the primary antibody in TBS containing 3% blocking serum at 4°C. The following primary antibodies were used: anti-p75 low affinity NGF receptor (rabbit polyclonal; Chemicon, Germany; at 1:2000), anti-27C7 (mouse monoclonal; generous gift from K. Wewetzer, University of Hannover, Germany; at 1:200) and mouse anti-Thy-1 (mouse monoclonal; Harlan Sera Lab, Germany; at 1:2000). Cells were rinsed twice with TBS and incubated for 2 hours with the corresponding secondary fluorescein or rhodamine-X linked donkey anti-mouse/rabbit IgG antibodies (Jackson Immunoresearch, Germany; at 1:1000) in TBS containing 3% donkey blocking serum. After 5 rinses with TBS, incubation with Hoechst 33342 (2 mg/ml; Sigma) as a nuclear counterstain followed. The chambers were removed from the slides and coverslipped using Prolong Antifade (Molecular Probes, Netherlands) as mounting medium.

Phase contrast images of unfixed cell cultures were taken on an inverted Olympus IX70 phase contrast microscope (Olympus, Germany), equipped with a Color View 12 digital camera (Soft Imaging

Table 1: *Flow-cytometry analysis of Thy-1 expressing fibroblasts after MACS p75LNGFr Schwann cell selection.*

Exp. #	*unpurified fraction*	*MACS p75LNGFr positive fraction (Thy-1 expressing cells in percent (%))*	*MACS p75LNGFr negative fraction*
1	*18.56*	*4.92*	*91.37*
2	*63.36*	*5.20*	*98.40*
3	*35.58*	*1.98*	*59.25*
4	*60.33*	*10.26*	*95.04*
5	*64.58*	*5.76*	*94.61*
6	*77.72*	*1.79*	*98.06*
Mean	*53.4*	*5.0*	*89.5*
SD	*21.9*	*3.1*	*15.0*

Table 2: *Flow-cytometry analysis of Thy-1 expressing fibroblasts after MACS Thy-1 fibroblast depletion*

Exp. #	*unpurified fraction*	*MACS Thy-1 positive fraction (Thy-1 expressing cells in percent (%))*	*MACS Thy-1 negative fraction*
1	*23.10*	*88.98*	*14.63*
2	*18.56*	*85.09*	*3.08*
3	*63.36*	*93.41*	*63.86*
4	*39.63*	*91.72*	*26.80*
5	*35.58*	*77.60*	*2.65*
6	*60.33*	*95.16*	*59.48*
7	*64.58*	*80.62*	*42.27*
8	*77.72*	*88.42*	*76.76*
Mean	*47.9*	*87.6*	*36.2*
SD	*21.6*	*6.2*	*28.7*

System, Germany). Immunocytochemistry samples were analyzed using a Leica DMR fluorescence microscope (Leica, Germany). At every individual filter setting, 8 bit monochrome pictures were taken using a Spot CCD camera model 2.2.1 (Diagnostic Instruments, Michigan USA).

3. RESULTS

3.1 Schwann cell isolation

After obtaining sciatic nerve biopsies from adult rats, nerve fragments were kept in culture for 7 days before dissociation (Fig. 1). After 7 days of *in vitro* degeneration, dissociation of peripheral nerve fragments and 2 days in culture, 0.86 x 10^6 cells ± 0.09 x 10^6 (n=6) total viable cells per animal were counted, which corresponds to 1.5 x 10^4 cells per mg nerve tissue. Out of all dissociated cells less than 5% were non-viable cells. Dissociation before day 7 post biopsy resulted in a low yield of Schwann cells (data not shown). Peripheral nerve homogenates plated on

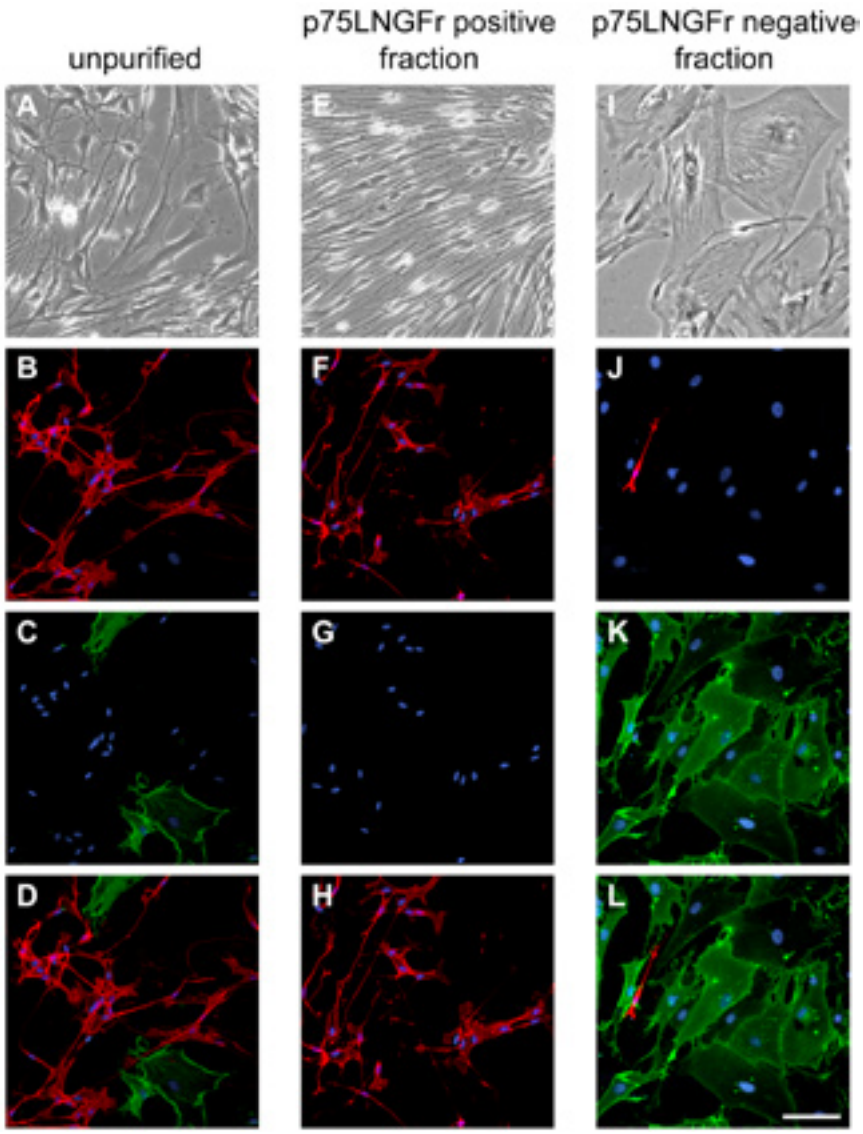

Figure 2: *Immunocytochemical analysis before and after MACS p75LNGFr Schwann cell selection from peripheral nerve biopsies. A-D show unpurified cultures right after peripheral nerve dissociation, E-H illustrate the p75LNGFr positive and I-L the p75LNGFr negative fraction (A, E, I phase-contrast micrographs; all others immunofluorescent micrographs). (A) Peripheral nerve homogenates in culture consist of bipolar Schwann cells with small cigar-shaped nuclei and flattened fibroblasts with prominent oval nuclei, which is mirrored by (B) p75LNGFr expressing Schwann cells and (C) Thy-1 expressing fibroblasts. (D) Overlay of C and D. Of note, the Hoechst 33342 nuclear counterstain is always co-localized with either Thy-1 or p75LNGFr. (E) Following MACS p75LNGFr selection, cells are found almost exclusively with the typical bipolar Schwann cell morphology in the p75LNGFr positive fraction. (F) These cells express p75LNGFr, (G) but not Thy-1. (H) Overlay of F and G. (I) In contrast, the p75LNGFr negative fraction contains cells with fibroblast morphology. This is paralleled by (J) the lack of p75LNGFr and (K) abundance of Thy-1 immunoreactivity. (L) Overlay of J and K. Thy-1 immunoreactivity (fluorescein; green), p75LNGFr immunoreactivity (rhodamine; red), Hoechst 33342 nuclear counterstain (blue). Scale bar A, E, I 75µm; B-D, F-H, J-L, 100mm.*

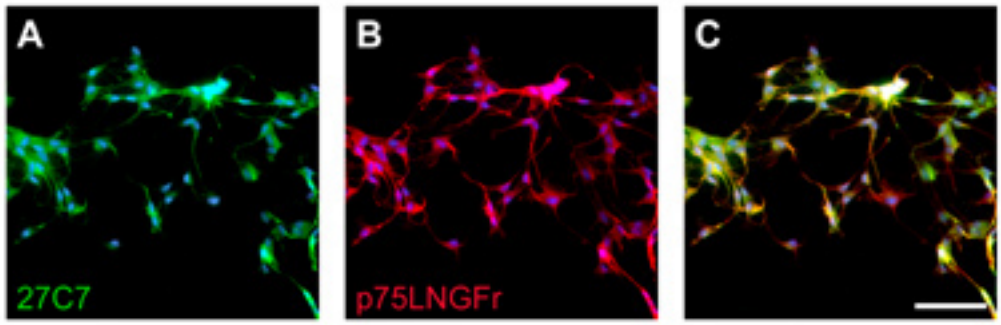

Figure 3: *p75LNGFr expressing cells are Schwann cells. (A) Immunocytochemical analysis with the Schwann cell specific antibody 27C7, which recognizes non-myelinating Schwann cells, confirms the Schwann cell phenotype of (B) p75LNGFr expressing cells. (C) Overlay of A and B. 27C7 immunoreactivity (fluorescein; green), p75LNGFr immunoreactivity (rhodamine; red), Hoechst 33342 nuclear counterstain (blue). Scale bar A-C 100mm.*

P-Orn/Lam coated culture flasks after dissociation, contained both, typical fusiforme bipolar Schwann cells with small cigar-shaped nuclei and flattened fibroblasts with prominent oval nuclei (Fig. 2A). The immunocytochemical analysis confirmed the presence of Schwann cells by p75LNGFr expression and of fibroblasts by Thy-1 expression (Fig. 2B-D). The typical phase-contrast appearance was less prominent in immunocytochemically stained cells due to paraformaldehyde fixation induced alterations of Schwann cell and fibroblast morphology. Flow-cytometry analysis of the primary cultures within 48 hours after enzymatic digestion revealed that 53.4% ± 21.9 (n=6) were Thy-1 expressing fibroblasts (Table 1; Fig. 4A).

3.2 Schwann cell purification by positive selection

Nine days after the sciatic nerve biopsy (Fig. 1), dissociated sciatic nerve fragments were purified by MACS using p75LNGFr antibodies to select Schwann cells. This procedure was repeated for 6 different nerve biopsies (Table 1). Two days later, p75LNGFr selected cells revealed the typical Schwann cell morphology on coated culture flasks (Fig 2E). Immunoreactivity for p75LNGFr and the absence of Thy-1 expression confirmed the Schwann cell identity (Fig. 2F-H). In contrast, cells obtained from the p75LNGFr negative fraction appeared as large, flattened cells with prominent nuclei resembling the typical fibroblast morphology in phase-contrast (Fig. 2I). These cells expressed Thy-1, which identifies fibroblasts, but not p75LNGFr (Fig. 2J-L). Finally, co-localization of p75LNGFr and 27C7 expression, a marker for non-myelinating Schwann cells [32], reconfirms the Schwann cell identity of p75LNGFr expressing cells (Fig. 3). Cells, neither expressing p75LNGFr or Thy-1, were not found (Fig. 2D).

Qualitative morphological data from MACS p75LNGFr selected cells were paralleled by quantitative analysis of Thy-1

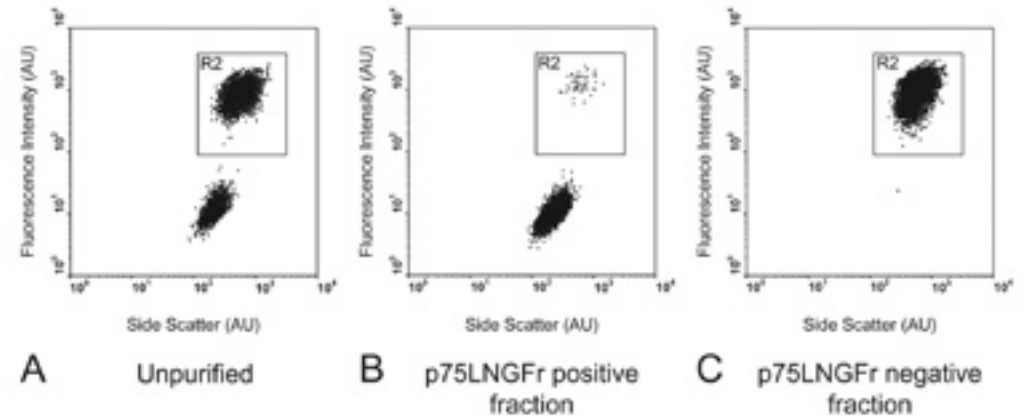

Figure 4: *Flow-cytometry analysis of MACS p75LNGFr separated cells. Dot plots were obtained by flow-cytometry analysis of Thy-1 expressing cells, showing the side scatter signal versus the fluorescence signal intensity in arbitrary units (AU). The dot plots were gated to select the viable cells from the cell population. The boxed areas labeled R2 contain the Thy-1 positive fibroblasts. (A) The unpurified peripheral nerve homogenates almost equally consist of Thy-1 positive (R2 labeled box) and Thy-1 negative cells. (B) The majority of cells of the MACS p75LNGFr positive fraction is located outside of the boxed area indicating that they do not express Thy-1 . (C) Almost all cells from the MACS p75LNGFr negative fraction express Thy-1 (inside boxed area), which identifies them as fibroblasts*

positive cells as determined by flow-cytometry two days after MACS (Table 1; Fig. 4). Cultures derived from one cycle of MACS p75LNGFr selection contained 5.0% ± 3.1 (n=6) Thy-1 positive fibroblasts, compared to 53.4% before MACS, indicating a high specificity (95.0%) for Schwann cells. As a parameter for the sensitivity of this method, cultures from the MACS p75LNGFr negative fraction contained only 10.5% Thy-1 negative cells. This fraction most likely represents Schwann cells not captured by the column. The absolute number of cells retrieved in the p75LNGFr positive fraction further confirms the high sensitivity. From 1.37 x 10^6 unpurified cells (sample from pooled cells, counted before MACS), 0.58 x 10^6 cells in the MACS p75LNGFr positive fraction were identified as Thy-1 negative by flow-cytometry, thus representing the yield of Schwann cells after one cycle of p75LNGFr MACS selection. Considering that our unpurified biopsy homogenates contain on average 46.6% Schwann cells (= 0.64 x10^6 cells; flow-cytometry Thy-1 negative unpurified cells), 91.0 % of all Schwann cells present in the peripheral nerve biopsies following dissociation can be retrieved. This means, transferred to the total numbers of cells obtainable from one single rat, that out of 0.86 x 10^6 cells 0.40 x 10^6 represent Schwann cells, from which 0.37 x 10^6 cells can be retrieved.

After adding the mitogens forskolin and bovine pituitary extract to the medium, the Schwann cells could be expanded with a cell doubling time of 5 days over at least 4 passages, without observing fibroblasts overgrowing them (data not shown).

3.3 Schwann cell purification by fibroblast depletion

Identical to the MACS p75LNGFr selection protocol, sciatic nerve fragments were dissociated 7 days after the nerve biopsy was taken and were purified by MACS Thy-1 depletion two days later. The separation procedure was repeated in 8 different experiments (Table 2). In contrast to the described MACS p75LNGFr selection assay, Schwann cell purification by MACS depletion of Thy-1 expressing fibroblasts did not prove to be effective in this experiment. The MACS column was able to bind Thy-1 expressing fibroblasts, since the Thy-1 positive fraction had a higher percentage of Thy-1 positive fibroblasts compared to unpurified cells after one cycle of MACS Thy-1 depletion as assessed by flow-cytometry (Table 2). However, the Thy-1 negative fraction still contained 36.2% ± 28.7 (n=8) Thy-1 positive cells indicating a low sensitivity to detect Thy-1 expressing fibroblasts. The specificity of MACS for Thy-1 expressing fibroblasts was only 87.6% ± 6.2 (n=8), suggesting that unlabeled cells were captured by MACS Thy-1 selection. The quantitative flow-cytometry results were confirmed by phase-contrast and immunocytochemical analysis of the MACS Thy-1 depletion assay (data not shown).

4. DISCUSSION

The results of the present study demonstrate that Schwann cells can be purified by MACS from adult peripheral nerve biopsies using the expression of the cell surface antigen p75LNGFr for selection. This method allows the fast and reliable purification of adult Schwann cells directly through positive selection rather than indirectly through depletion of fibroblasts. MACS depletion of Thy-1 expressing fibroblasts lacks the sensitivity and specificity to establish Schwann cell cultures from adult peripheral nerve biopsies.

The main advantage of MACS p75LNGFr Schwann cell selection is the fast establishment of primary Schwann cell cultures from adult peripheral nerve biopsies within 9 days after biopsy. This time factor becomes particularly relevant for autologous transplantation strategies, since the intrinsic ability of axotomized neurons to regenerate and the permissiveness of the parenchyma surrounding the acute injury site diminish over time [19, 20]. Routinely used methods to enrich Schwann cells from peripheral nerve biopsies such as the repetitive transfer of peripheral nerve fragments in culture, the treatment of cultures with cytotoxic agents to eliminate proliferating fibroblasts, and the predegeneration of peripheral nerve before biopsy, require at least three to six weeks to achieve sufficient purification of Schwann cells [16, 17]. These time requirements may already be beyond the time point, where optimal axonal regeneration can be achieved. Enriching Schwann cells by dissociation of peripheral nerve biopsies earlier than 7 days after biopsy was not possible. As confirmed by others, immediate dissociation of peripheral nerve fragments causes substantial damage to Schwann cells resulting in poor cell yields [17]. Periph-

eral nerve fragments require a minimum of time to degenerate, which will allow Schwann cells to retract their processes from the surrounding cells and to loosen junctions with extracellular matrix components within the peripheral nerve [22].

The MACS p75LNGFr selection protocol as described allows a high degree of purification without losing significant quantities of Schwann cells. Purification by MACS selection requires a balance between the specificity of Schwann cell selection and an optimal cell yield. Increasing the number of rinses before eluting the column in the positive selection assay would enhance the specificity but at the same time the overall cell yield would decrease. A more efficient means to increase the specificity without decreasing the cell yield is to purify cell homogenates repeatedly on fresh columns. In the present experiment, the degree of Schwann cell enrichment after one cycle of MACS p75LNGFr selection was sufficient for several passages of Schwann cell cultures without observing fibroblast expansion. The total cell yield of 0.86 x 10^6 cells per animal or 1.5 x 10^4 cells per mg nerve tissue obtainable with the described MACS purification protocol lies within the range of previously published data [17, 18, 33].

A concern about MACS cell selection is that microbeads still bound to the cell surface would influence viability or adherence of the purified cells. However, none of these effects were observed in the present study. The small size of the microbeads (ca. 50 nm) prevents the steric interference or mechanical stress on the cells, which occurs when cells are bound to larger magnetic particles like Dynabeads [34]. Because of the small size and the biodegradable constitution, the bound microbeads are removed by the normal membrane turnover.

In contrast, established purification methods using cytotoxic agents such as Ara-C to eliminate fibroblasts from peripheral nerve biopsies have to accept considerable side effects. Cytotoxic agents unspecifically eradicate proliferating cells and therefore proliferating Schwann cells will be eliminated as well [35]. The overall cell yield of Schwann cells will decrease and the time required to generate sufficient quantities of Schwann cells will increase. In addition, Ara-C can induce DNA damage [36] and interfere with the overall protein synthesis [37]. Thus, long-term effects on surviving Schwann cells are likely, which raises safety concerns regarding the application of purified Schwann cells for transplantation in humans.

In analogy to previous studies, which used the expression of Thy-1 as a marker to select fibroblasts either through immunopanning [27] or complement activation induced lysis [26], peripheral nerve homogenates were processed using MACS depletion of Thy-1 expressing fibroblasts. This approach did not prove to be effective, since it showed a very low sensitivity to detect fibroblasts. These data are in line with previous experiments, in which we were not able to purify Schwann cells sufficiently from adult peripheral nerve tissue using the complement activation induced lysis with Thy-1 as the selection antigen

(N.W., unpublished observation). Thus far, Thy-1 antibody labeling and subsequent complement activated lysis to deplete fibroblasts have only been applied successfully to neonatal peripheral nerve tissue [26, 27]. The difference between neonatal and adult peripheral nerve tissue can be attributed to the fact that peri- and epineurium, which represent the main fibroblast containing layers within the peripheral nerve, are just starting to develop in neonatal as compared to adult peripheral nerves. This makes fibroblast depletion methods much more efficient for neonatal nerve tissue [21].

MACS selection of p75LNGFr expressing Schwann cells from adult peripheral nerve biopsies represents a fast, effective and safe means to enrich Schwann cells in culture for clinical transplantation strategies. MACS is already an approved method for the purification of CD34 positive cells from the autologous peripheral blood for clinical applications [38]. The first clinical phase-I trail using autologous Schwann cells to remyelinate inflammatory lesions within the central nervous system caused by multiple sclerosis (personal communication, Jeffery Kocsis) emphasizes the clinical relevance of Schwann cell transplantation paradigms. Of course, MACS selection of p75LNGFr expressing Schwann cells has to be validated in the human system, before this method can be applied to clinically relevant regenerative strategies aiming for axon repair and remyelination.

5. ACKNOWLEDGMENTS

This work was supported by Institute International de Recherche en Paraplegie, Geneva, on behalf of an anonymous donation, Deutsche Stiftung Querschnitt, Deutsche Forschungsgemeinschaft and by the ReForM-Program, University of Regensburg, School of Medicine. We thank L. Aigner, H.G. Kuhn, J. Winkler, E. Marani for helpful comments and K. Wewetzer for providing the 27C7 antibody.

6. REFERENCES

1. Griffin, J. W. & Hoffman, P. N. in Peripheral Neuropathy (eds. Dyck, P. J. & Thomas, P. K.) 361-376 (W.B. Saunders, Philadelphia, 1993).
2. Berger, A. & Lassner, F. Peripheral nerve allografts: survey of present state in an experimental model of the rat. Microsurgery 15, 773-7 (1994).
3. Guenard, V., Kleitman, N., Morrissey, T. K., Bunge, R. P. & Aebischer, P. Syngeneic Schwann cells derived from adult nerves seeded in semipermeable guidance channels enhance peripheral nerve regeneration. J Neurosci 12, 3310-20. (1992).
4. Rodriguez, F. J., Verdu, E., Ceballos, D. & Navarro, X. Nerve guides seeded with autologous schwann cells improve nerve regeneration. Exp Neurol 161, 571-84. (2000).
5. Kromer, L. F. & Cornbrooks, C. J. Transplants of Schwann cell cultures promote axonal regeneration in the adult mammalian brain. Proc Natl Acad Sci U S A 82, 6330-4 (1985).
6. Paino, C. L., Fernandez-Valle, C., Bates, M. L. & Bunge, M. B. Regrowth of axons in lesioned adult rat spinal cord: promotion by implants of cultured Schwann cells. J Neurocytol 23, 433-52. (1994).
7. Li, Y. & Raisman, G. Schwann cells induce sprouting in motor and sensory axons in the adult rat spinal

cord. J Neurosci 14, 4050-63. (1994).
8. Xu, X. M., Guenard, V., Kleitman, N. & Bunge, M. B. Axonal regeneration into Schwann cell-seeded guidance channels grafted into transected adult rat spinal cord. J Comp Neurol 351, 145-60 (1995).
9. Blakemore, W. F. & Crang, A. J. The use of cultured autologous Schwann cells to remyelinate areas of persistent demyelination in the central nervous system. J Neurol Sci 70, 207-23. (1985).
10. Baron-Van Evercooren, A., Gansmuller, A., Duhamel, E., Pascal, F. & Gumpel, M. Repair of a myelin lesion by Schwann cells transplanted in the adult mouse spinal cord. J Neuroimmunol 40, 235-42. (1992).
11. Honmou, O., Felts, P. A., Waxman, S. G. & Kocsis, J. D. Restoration of normal conduction properties in demyelinated spinal cord axons in the adult rat by transplantation of exogenous Schwann cells. J Neurosci 16, 3199-208 (1996).
12. Kohama, I. et al. Transplantation of cryopreserved adult human Schwann cells enhances axonal conduction in demyelinated spinal cord. J Neurosci 21, 944-50. (2001).
13. Menei, P., Montero-Menei, C., Whittemore, S. R., Bunge, R. P. & Bunge, M. B. Schwann cells genetically modified to secrete human BDNF promote enhanced axonal regrowth across transected adult rat spinal cord. Eur J Neurosci 10, 607-21. (1998).
14. Tuszynski, M. H. et al. Grafts of genetically modified Schwann cells to the spinal cord: survival, axon growth, and myelination. Cell Transplant 7, 187-96. (1998).
15. Weidner, N., Blesch, A., Grill, R. J. & Tuszynski, M. H. Nerve growth factor-hypersecreting Schwann cell grafts augment and guide spinal cord axonal growth and remyelinate central nervous system axons in a phenotypically appropriate manner that correlates with expression of L1. J Comp Neurol 413, 495-506. (1999).
16. Verdu, E., Rodriguez, F. J., Gudino-Cabrera, G., Nieto-Sampedro, M. & Navarro, X. Expansion of adult Schwann cells from mouse predegenerated peripheral nerves. J Neurosci Methods 99, 111-7. (2000).
17. Morrissey, T. K., Kleitman, N. & Bunge, R. P. Isolation and functional characterization of Schwann cells derived from adult peripheral nerve. J Neurosci 11, 2433-42. (1991).
18. Calderon-Martinez, D., Garavito, Z., Spinel, C. & Hurtado, H. Schwann cell-enriched cultures from adult human peripheral nerve: a technique combining short enzymatic dissociation and treatment with cytosine arabinoside (Ara-C). J Neurosci Methods 114, 1-8 (2002).
19. Tuszynski, M. H. & Kordower, J. CNS Regeneration (Academic Press, San Diego, 1999).
20. Zochodne, D. W. The microenvironment of injured and regenerating peripheral nerves. Muscle Nerve Suppl 9, S33-8 (2000).
21. Bunge, M. B., Wood, P. M., Tynan, L. B., Bates, M. L. & Sanes, J. R. Perineurium originates from fibroblasts: demonstration in vitro with a retroviral marker. Science 243, 229-31. (1989).
22. Levi, A. D. Characterization of the technique involved in isolating Schwann cells from adult human peripheral nerve. J Neurosci Methods 68, 21-6. (1996).
23. Wood, P. M. Separation of functional Schwann cells and neurons from normal peripheral nerve tissue. Brain Res 115, 361-75 (1976).
24. Needham, L. K., Tennekoon, G. I. & McKhann, G. M. Selective growth of rat Schwann cells in neuron- and serum-free primary culture. J Neurosci 7, 1-9 (1987).
25. Keilhoff, G., Fansa, H., Schneider, W. & Wolf, G. In vivo predegeneration of peripheral nerves: an effective technique to obtain activated Schwann cells for nerve conduits. J Neurosci Methods 89, 17-24 (1999).
26. Brockes, J. P., Fields, K. L. & Raff, M. C. Studies on cultured rat Schwann cells. I. Establishment of purified populations from cultures of peripheral nerve. Brain Res 165, 105-18. (1979).
27. Assouline, J. G., Bosch, E. P. & Lim, R. Purification of rat Schwann cells from cultures of peripheral nerve: an immunoselective method using surfaces coated with anti-immunoglobulin antibodies. Brain Res 277, 389-92. (1983).

28. Miltenyi, S., Muller, W., Weichel, W. & Radbruch, A. High gradient magnetic cell separation with MACS. Cytometry 11, 231-8 (1990).
29. Yasuda, T., Sobue, G., Mokuno, K., Kreider, B. & Pleasure, D. Cultured rat Schwann cells express low affinity receptors for nerve growth factor. Brain Res 436, 113-9. (1987).
30. Barnett, S. C. et al. Identification of a human olfactory ensheathing cell that can effect transplant-mediated remyelination of demyelinated CNS axons. Brain 123 (Pt 8), 1581-8 (2000).
31. Fields, K. L. & Raine, C. S. Ultrastructure and immunocytochemistry of rat Schwann cells and fibroblasts in vitro. J Neuroimmunol 2, 155-66 (1982).
32. Wewetzer, K., Grothe, C., Christ, B. & Seilheimer, B. Identification and characterization of differentiation-dependent Schwann cell surface antigens by novel monoclonal antibodies: introduction of a marker common to the non-myelin-forming phenotype. Glia 19, 213-26. (1997).
33. Verdu, E. et al. Olfactory bulb ensheathing cells enhance peripheral nerve regeneration. Neuroreport 10, 1097-101. (1999).
34. Manyonda, I. T., Soltys, A. J. & Hay, F. C. A critical evaluation of the magnetic cell sorter and its use in the positive and negative selection of CD45RO+ cells. J Immunol Methods 149, 1-10. (1992).
35. Aguayo, A. J., Romine, J. S. & Bray, G. M. Experimental necrosis and arrest of proliferation of Schwann cells by cytosine arabinoside. J Neurocytol 4, 663-74. (1975).
36. Ohno, Y., Spriggs, D., Matsukage, A., Ohno, T. & Kufe, D. Effects of 1-beta-D-arabinofuranosylcytosine incorporation on elongation of specific DNA sequences by DNA polymerase beta. Cancer Res 48, 1494-8 (1988).
37. Lisak, R. P., Bealmear, B., Benjamins, J. & Skoff, A. Inflammatory cytokines inhibit upregulation of glycolipid expression by Schwann cells in vitro. Neurology 51, 1661-5 (1998).
38. Despres, D. et al. CD34+ cell enrichment for autologous peripheral blood stem cell transplantation by use of the CliniMACs device. J Hematother Stem Cell Res 9, 557-64 (2000).

Chapter 4b

Schwann cells fail to replace fibroblasts as supporting cells for adult neural progenitor cell grafts in the acutely injured spinal cord

Submitted for publication

Maurice Vroemen
Massimiliano Caioni
Ulrich Bogdahn
Norbert Weidner

ABSTRACT

Adult neural progenitor cells (NPC) co-grafted with fibroblasts replace cystic lesion defects and promote cell-contact mediated axonal regeneration in the acutely injured spinal cord. Fibroblasts are required as a platform to maintain NPC within the lesion, however, they are suspected to create an inhospitable milieu for regenerating CNS axons. Therefore, we thought to replace fibroblasts by primary Schwann cells, which might serve as a superior scaffold to maintain NPC within the lesion and might further enhance axon regrowth and remyelination following spinal cord injury. Adult rats underwent a cervical dorsal column transection immediately followed by transplantation of either NPC/Schwann cell or NPC/Schwann cell/fibroblast co-grafts. Animals receiving Schwann cell or fibroblast grafts alone, or Schwann cell/fibroblast co-grafts served as controls. At three weeks after injury/transplantation, histological analysis revealed that only fibroblast containing grafts were able to replace the cystic lesion defect. In both, co-cultures and co-grafts, Schwann cells and NPC were segregated. Almost all NPC migrated out of the graft into the adjacent host spinal cord. As a consequence, only peripheral type myelin, but no CNS type myelin, was detected within NPC/Schwann cell containing co-grafts. Corticospinal axon regeneration into Schwann cell containing co-grafts was massively diminished. Taken together, Schwann cells within NPC grafts contribute to remyelination. However, Schwann cells fail as a supporting platform to maintain NPC within the graft and Schwann cells impair CNS axon regeneration, which makes them an unfavorable candidate to support/augment NPC grafts following spinal cord injury.

1. INTRODUCTION

The development of a cystic lesion cavity represents a typical sequel of spinal cord injury preventing axonal regrowth and functional recovery. In particular, following complete spinal cord injury the introduction of a permissive substrate as replacement for the lesion cavity is required to promote axonal regeneration across the injury site and ultimately reinnervation of target neurons.

Recently, we have demonstrated that adult neural progenitor cells (NPC) not only survive and allow organotypic cell replacement after transplantation into the acutely injured spinal cord, but also replace cystic lesion defects and promote cell-contact mediated regeneration of the corticospinal tract (CST) after co-grafting with primary fibroblasts [1, 2]. Fibroblasts were required to provide a supporting scaffold to maintain adult NPC within the lesion cavity. If one considers NPC transplantation for clinical use, fibroblasts need to be replaced by a more suitable cellular or non-cellular supporting scaffold, since there are major concerns that fibroblasts and extracellular matrix molecules released by fibroblasts represent potent inhibitors of axonal regrowth in the mammalian cen-

tral nervous system (CNS) [3, 4].

Schwann cells might represent an ideal cell population to be combined with NPC instead of fibroblasts for transplantation. Schwann cells are the key factor to support spontaneous axonal regeneration following peripheral nerve injury [5]. Even after transplantation into the injured spinal cord, Schwann cells have been shown to promote axon regrowth and remyelination [6-8]. Furthermore, Schwann cells intrinsically produce favorable extracellular matrix molecules such as laminin [9], which might be suitable as a supporting scaffold for co-grafted adult NPC. Schwann cells intrinsically secrete growth promoting neurotrophic factors and, as opposed to NPC [10], Schwann cells can be easily genetically modified to overexpress therapeutic transgenes [11-13].

In the present study we thought to elucidate whether Schwann cells instead of fibroblasts might provide a more favorable cell-based supporting scaffold for co-grafted adult NPC, which would allow superior structural repair as prerequisite for substantial functional recovery. Schwann cells were co-grafted with adult NPC into acute cervical dorsal column transections in adult rats. Results demonstrate that Schwann cells alone are not sufficient to maintain co-grafted adult NPC in the lesion cavity. Only the addition of fibroblasts to Schwann cell containing grafts allows cyst replacement. However, Schwann cell containing grafts dramatically impair CNS axon regeneration.

2. MATERIALS AND METHODS

2.1 Animals

Adult female Fischer 344 rats (160-180g) were used. All experiments were carried out in accordance with the institutional guidelines for animal care. All efforts were made to minimize the number of animals used. Animals had *ad libitum* access to food and water throughout the study. All surgical procedures were performed under anesthesia with a combination of ketamine (62.5mg/kg body weight; WDT, Garbsen, Germany), xylazine (3.175mg/kg body weight; WDT) and acepromazine (0.625mg/kg body weight, Sanofi-Ceva, Düsseldorf, Germany) in 0.9% sterile saline solution.

2.2 Cell preparation

For the isolation of NPC, fibroblasts and Schwann cells, adult female Fischer 344 rats were deeply anesthetized as described above and killed by decapitation. NPC were isolated from the cervical spinal cord as described before [1]. Briefly, the cervical spinal cord (spinal cord level C3 through T1) was dissected out, minced and washed in sterile Dulbecco's phosphate buffered saline/D-glucose (PBS, 4.5g/l; PAA Laboratories, Linz, Austria). Subsequently, the tissue was digested in a solution of papain (0.01%; Worthington Biochemicals, Lakewood, USA), neutral protease (0.1%; Roche, Mannheim, Germany), DNase I (0.01%; Worthington Biochemicals) and 12.4mM $MgSO_4$, dissolved in Hank's balanced salt solution (HBSS; PAA Laboratories) for 30 min at 37°C. The

resulting cell suspension was washed and plated on culture dishes containing serum-free growth medium, consisting of Neurobasal medium with B27 supplement (Gibco) and 20 ng/ml recombinant human FGF-2 (R&D System, Wiesbaden, Germany). Cells were expanded either as neurospheres in uncoated culture flasks or as adherent monolayer in culture flasks coated with poly-l-ornithine (20µg/cm^2; Sigma) and laminin (0.4µg/cm^2; Sigma) as described before [1].

Primary fibroblasts were isolated from adult Fischer 344 rat skin biopsies and cultured in DMEM medium (Pan Biotech, Aidenbach, Germany) supplemented with 10% of FCS as described before [14].

Schwann cells were isolated from adult sciatic nerve biopsies employing magnet-activated cell separation (MACS) of p75 low affinity NGF receptor expressing Schwann cells according to established protocols [15]. The purity of Schwann cells, which was assessed by comparing the number of Hoechst stained nuclei with p75 low affinity NGF receptor expressing cells, was >99%. Purified Schwann cell cultures were expanded in DMEM medium supplemented with 10% FCS, 2 mM forskolin (Sigma) and 0.2% bovine pituitary extract (Clonetics, Oldendorf, Germany).

For the identification of co-cultured NPC *in vitro* and co-grafted Schwann cells *in vivo*, the respective cell populations were genetically modified to express the reporter gene green-fluorescent protein (GFP) using a MLV-based retroviral vector pCLE-GFP containing the internal EF-1alpha promoter [1, 10]. NPC or Schwann cells (passage 3-5) were plated in subconfluent densities and were exposed on two consecutive days with retrovirus containing growth medium supplemented with 1 µg/ml Polybrene (Sigma). G418 (500µg/ml; Gibco) was added to the growth medium for the selection of cells, which integrated the retroviral vector. Successful incorporation of the transgene was confirmed by detection of GFP using an inverted fluorescence microscope (Olympus IX 70).

2.3 Co-cultures of adult NPC and Schwann cells

For the analysis of NPC differentiation *in vitro*, GFP expressing NPC maintained as neurospheres were dissociated using Accutase (Innovative Cell Tech, San Diego, USA) and incubated in NB medium with B27 supplemented with 5% FCS for 7 days after seeding onto poly-l-ornithine/laminin (Sigma) coated cover slips (Pan Biotech). For the analysis of NPC differentiation co-cultured with Schwann cells, GFP expressing NPC were seeded onto a confluent layer of Schwann cells. Co-cultures were incubated for 7 days in NB medium with B27 supplemented with 5% FCS. Cells were fixed with 4% paraformaldehyde in PBS and immunolabeled using the following antibodies: mouse-anti-nestin for progenitor/stem cells (Pharmingen, Heidelberg, Germany; at 1/1000), mouse-anti-GFAP for astroglia (Chemicon, Hofheim, Germany; at 1/600), mouse-anti-A2B5 for glial precursor cells (Chemicon; at 1/100), mouse-anti-RIP for oligoden-

droglia (Chemicon; at 1/500), mouse-anti-beta-III-tubulin for neurons (Promega; at 1/500) and rabbit-anti-GFP for GFP expressing cells (Molecular Probes, Leiden, The Netherlands; at 1/1000). Cells were washed three times with tris-buffered saline (TBS) after fixation, blocked with TBS containing 3% donkey serum/0.1% Triton-X (Sigma) and incubated overnight with the primary antibody in TBS + 3% donkey serum + 0.1% Triton-X at 4°C. The following day, cells were washed with TBS and incubated with Alexa-568 linked secondary goat-anti-mouse (Molecular Probes; at 1/1000) and Alexa-488 linked goat-anti-rabbit secondary antibodies (Molecular Probes; at 1/1000) in TBS + 3% donkey serum + 0.1% Triton-X for 2h. Finally, nuclei were counterstained with Hoechst 33342 (2 µg/ml in TBS; Sigma). The coverslips were mounted onto glass slides using Prolong-Antifade (Molecular Probes). For the immunocytochemical analysis, 8 bit monochrome pictures were taken at 20x magnification on a fluorescent microscope (Leica DMR) equipped with a Spot CCD camera model 2.2.1 (Diagnostic Instruments, Sterling Heights, USA). The number of specifically immunolabeled cells and the total cell number (number of Hoechst counterstained nuclei) were determined in 5 random fields for each differentiation marker to determine the percentage of cells expressing the respective differentiation marker. Three independently performed immunocytochemical stains were analyzed under each condition.

2.4 Preparation of cells for transplantation

For the identification after transplantation, NPC were prelabeled with the thymidine analogue bromodeoxyuridine (BrdU; Sigma) 48h before transplantation as described [1]. Expression of the reporter gene GFP allowed to identify Schwann cell grafts *in vivo*. Immediately before transplantation, respective cells were harvested and washed three times in PBS. A sample of the resulting single cell suspensions was stained with Trypan Blue (Sigma) and counted using a Neubauer hemocytometer. NPC, Schwann cell and fibroblast suspensions were mixed and diluted in PBS to yield the appropriate cell densities in the different grafting paradigms (Table 1). Due to the larger cell size of fibroblasts in comparison to Schwann cells and NPC, the cell concentration in different grafting conditions was adapted to yield equally dense suspensions.

2.5 Surgical procedures

Spinal cord lesions, cell transplantation and anterograde labeling of the CST were performed as previously described [1, 2]. Briefly, the dorsal columns containing the dorsal CST were transected at cervical level C3 using a tungsten wire knife (David Kopf Instruments Tujuna, USA) leaving the surrounding dura intact. A total volume of 2.5 µl cell suspension (for different grafting conditions and experimental groups see Table 1) was injected directly into the lesion site through a pulled glass micropipette (100 µm internal diameter)

Table 1: *Cell concentration in different grafting conditions:*

Experimental group		Fibroblasts	Schwann cells	Neural progenitor cells
FF	(n=10)	1.5 x 10^5/µl	--	--
SC	(n=8)	--	3 x 10^5/µl	--
NPC/SC	(n=7)	--	1.25 x 10^5/µl	2.5 x 10^5/µl
SC/FF	(n=6)	1.5 x 10^4/µl	3 x 10^5/µl	--
NPC/SC/FF	(n=6)	6.3 x 10^3/µl	1.25 x 10^5/µl	2.5 x 10^5/µl

using a Picospritzer II (General Valve, Fairfield, USA). Animals receiving a dorsal column transection without cell transplantation served as control (**Lesion**; n=6). For anterograde tracing of the CST, 300 nl of a 10% solution of biotinylated dextran-amine (BDA; 10.000 MW, Molecular Probes) was injected through pulled glass micropipettes (40 µm internal diameter) into each of 18 sites per hemisphere spanning the rostrocaudal extent of the rat forelimb and hindlimb sensorimotor cortex using a PicoSpritzer II (General Valve) 1 week post lesioning/grafting.

2.6 Morphological analysis

At 3 weeks post lesioning/grafting, animals were transcardially perfused with a 0.9% saline solution in 0.1 M phosphate buffer followed by 4% paraformaldehyde in 0.1 M phosphate buffer. Sagittal 35 µm cryostat sections were processed for visualization of the BDA labeled CST and for immunohistochemistry. Every seventh section was mounted for Nissl staining to determine the lesion size. Double/triple labeling immunofluorescence techniques were performed with free floating sections to assess cell survival and *in vivo* differentiation pattern. The following primary antibodies were used: mouse-anti-GFAP for astrocytes (DAKO; at 1/200), mouse-anti-APC for oligodendrocytes (Oncogene, Darmstadt, Germany; at 1/1000), rabbit-anti-NG2 for glial precursor cells (Chemicon; at 1/200), goat-anti-doublecortin for neuronal precursor cells (Santa Cruz Laboratories, Santa Cruz, USA; at 1/500), rabbit-anti-200 kDa neurofilament as general axonal marker (Boehringer Mannheim, Germany; at 1/250), mouse-anti-P0 for peripheral myelin (generous gift from J. Archelos, University of Duesseldorf, Germany; at 1/500), mouse-anti-myelin oligodendrocyte-specific protein (MOSP) for CNS myelin (Chemicon; at 1/5000), rat-anti-BrdU for BrdU-prelabeled cells (Harlan SeraLab, Loughborough, UK; at 1/500) and rabbit-anti-GFP for GFP expressing cells (Molecular Probes; at 1/1000). Immunolabeling with primary antibodies was visualized using Alexa-488, Alexa-568 or Alexa-660 linked donkey secondary antibodies (Molecular Probes; at 1/1000). Sections were rinsed in 0.1 M Tris buffered saline (TBS), incubated in TBS + 3% donkey serum + 0.1% Triton-X for 1h, then transferred into the first primary antibody and incubated overnight at 4°C on a rotating platform. For visualization of BrdU-prelabeled adult NPC the staining protocol was modified as follows: after rinsing in TBS, sections were incubated for 1h in 50% formamide/

2xSSC (0.3 M NaCl, 0.03M sodium citrate) at 65ºC. Sections were rinsed in 2xSSC, incubated for 30 min in 2 N HCl at 37ºC, and rinsed for 10 min in 0.1 M boric acid pH 8.5. After rinsing in TBS, sections were incubated in TBS + 3% donkey serum + 0.1% Triton-X as described above. The following day, sections were rinsed and incubated with fluorophore (Alexa-488/-568/-660) conjugated secondary donkey antibodies (Molecular Probes; at 1/1000) for 2.5 h. BDA labeled CST axons were visualized by incubation with Cy5-conjugated streptavidin (Jackson; at 1/1000). After a final rinsing step in TBS, sections were mounted onto glass slides and coverslipped with ProLong Antifade Kit (Molecular Probes). Confocal immunofluorescence microscopy was performed using a Leica TCS-NT system.

2.7 Quantification of lesion size and axon regrowth

The investigator quantifying cavity size and axonal regeneration was blinded for the group identity of each analyzed section. The lesion cavity and graft sizes were quantified by surrounding respective structures with a digital pen in a 1 out of 7 series of Nissl stained sagittal sections of each animal using the NIH Image J 10.2 software. For the quantification of axon (neurofilament immunoreactive axonal profiles) and CST axon growth (BDA labeled axonal profiles) within the graft, one sagittal section per animal through the main portion of the respective graft was chosen. Digital brightfield images of neurofilament-DAB or BDA-DAB visualized sections were captured using a Spot CCD camera, model 2.2.1 (Diagnostic Instruments, Michigan, USA) attached to a Leica DMR microscope at 200x magnification. The graft–host interface was determined after inserting the transmitted light condenser, which allows to discriminate between the orderly tissue architecture of the host and the randomly organized cell graft. The number of pixels representing the labeled axons was assessed using NIH Image J software.

2.8 Statistical analysis

All data are expressed as mean ± SEM. Comparisons of NPC cultures with SC/NPC co-cultures were made by using a Student's T-test. Comparisons of cyst size and axonal regeneration were made using the Kruskal-Walis nonparametric analysis of variance, followed by Dunn's multiple comparison *post hoc* testing. For all statistical tests, $p<0.05$ was considered significant.

3. RESULTS

3.1 In vitro analysis of NPC/Schwann cell interactions.

The aim of the present study was to investigate a transplantation paradigm, where adult NPC are combined with Schwann cells representing a more growth conducive cell population as opposed to fibroblasts, which have been employed in a previous study [2]. Before transplantation, we first investigated the interaction of Schwann cells and NPC (changes in differentiation, cell adhesion) *in vitro*. NPC were co-cultured with Schwann cells un-

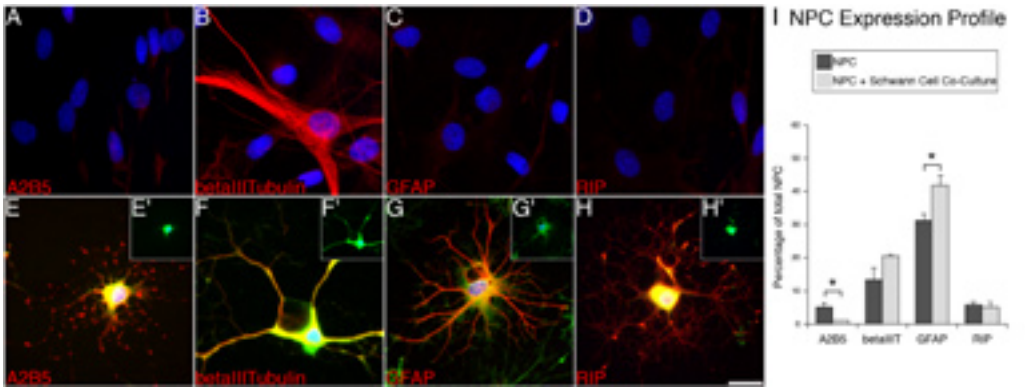

Figure 1: *Primary Schwann cells induce glial differentiation in NPC in vitro. The differentiation markers for NPC, (A, E) A2B5 for glial precursor cells, (B, F) beta-III-tubulin for neurons, (C, G) GFAP for astroglia and (D, H) RIP for oligodendroglia (all shown in red), were investigated for their cross-reactivity with primary Schwann cells (A-D). Of these markers, Schwann cells strongly expressed beta-III tubulin (B), whereas GFAP immunoreactivity was rather weak (C). Reporter gene (GFP) expressing NPC (green) are immunoreactive for A2B5, beta-III tubulin, GFAP and RIP (E-H). (I) The quantification of respective immunocytochemical stains revealed that co-culturing of NPC and Schwann cells significantly increased the proportion of GFAP expressing astroglia, while A2B5 expressing glial precursor cells were significantly reduced ($p<0.05$). A-H Hoechst 33342 as nuclear counterstain (blue). Epifluorescence micrographs. Scale bar A-H 20µm.*

der NPC differentiation conditions for 7 days as previously described [2, 10]. Unlike fibroblasts, Schwann cells do not attach to uncoated cell culture surfaces. Therefore, Schwann cells were plated on poly-l-ornithine/laminin coated glass coverslips and grown until confluent in NPC differentiation medium (NB medium supplemented with B27 and 5% FCS). Subsequently, undifferentiated NPC transduced to express the reporter gene GFP (GFP-NPC) were plated onto a Schwann cell monolayer and incubated for 7 days in NPC differentiation medium. Since Schwann cells have been described to express glial and neuronal markers relevant for NPC differentiation [16, 17], we first checked for cross-immunoreactivity of Schwann cells for the NPC differentiation markers A2B5, beta-III-tubulin, GFAP and RIP (Fig. 1A-D). Schwann cells displayed only strong immunoreactivity for beta-III-tubulin, which is commonly used to indicate early neuronal differentiation in NPC. However, beta-III-tubulin positive Schwann cells were clearly distinguishable by their prominent nucleus and compact morphology as opposed to rather small nuclei and fine processes of beta-III-tubulin immunoreactive NPC. Co-cultured NPC were immunoreactive for markers identifying glial precursor cells (A2B5 expression), astroglia (GFAP), oligodendroglia (RIP) and neurons (beta-III-tubulin) (Fig. 1E-H) in accordance with previous studies [1, 2]. The expression of these markers in NPC was quantified to detect a potential influence of co-cultured Schwann cells on the differentiation pattern of NPC (Fig.1I). The presence of Schwann cells significantly

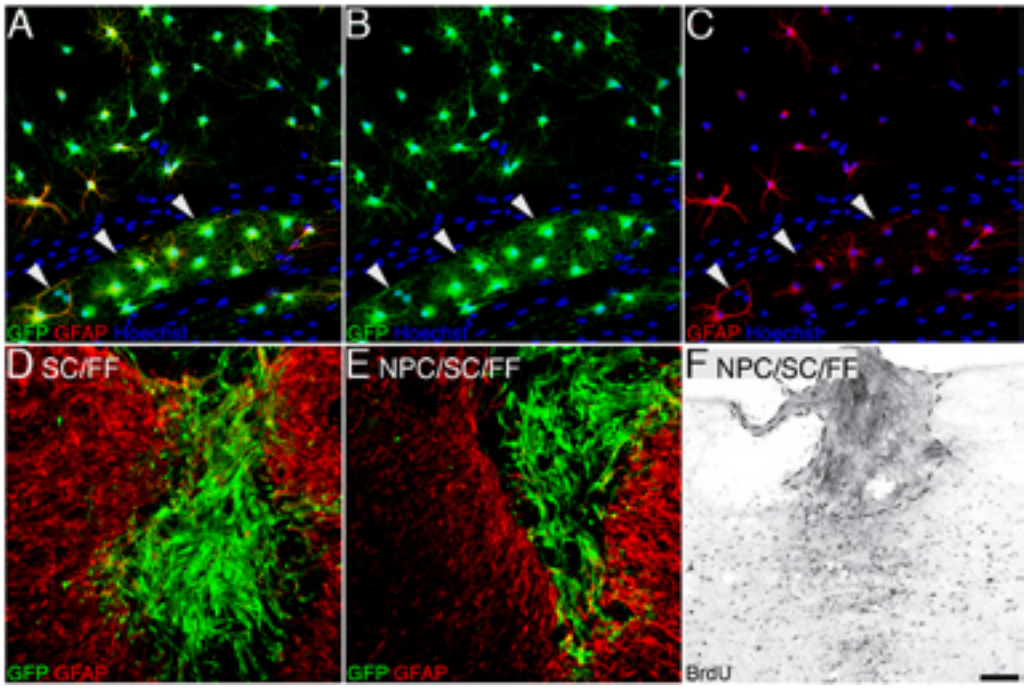

***Figure 2**: NPC and Schwann cells become segregated in vitro and in vivo. (A) After 7 days of co-culturing Schwann cells and GFP expressing NPC (green) in differentiation medium, NPC and Schwann cells (identified by GFP-negative Hoechst 33342 counterstained nuclei) appear completely segregated on the poly-l-ornithine/ laminin coated cell culture surface. GFAP positive processes (red) co-localized with GFP expressing NPC seal off the NPC from the Schwann cell area (arrowheads). Overlay GFP (green), GFAP (red) and Hoechst 33342 (blue). (B) GFP (green) and Hoechst 33342 (blue). (C) GFAP (red) and Hoechst 33342 (blue). (D) SC/FF grafts fill out the lesion defects with GFP-expressing Schwann cells (green) densely distributed throughout the graft. Doublelabeling with GFAP (red) indicates that the SC/FF graft is delineated from the adjacent host parenchyma by a astroglial border. (E) Identical situation with NPC/SC/FF grafts. GFP-expressing Schwann cells (green), GFAP (red). (F) Immunohistochemical detection of BrdU prelabeled NPC reveals that the vast majority of NPC has migrated from the NPC/SC/FF graft (dashed line) into the surrounding host spinal cord. A-C epifluorescence micrographs, D, E confocal fluorescence micrographs, F brightfield micrographs. Orientation in D-F: rostral is to the left, dorsal to the top. Scale bar A-C 50 µm, D, E 73 µm and F 87 µm.*

reduced the proportion of A2B5 positive glial precursor cells (5% ± 1.3 versus 1.1% ± 0.1), whereas the proportion of GFAP positive astroglia was increased from 31.3% (± 1.8) in the NPC differentiation condition compared to 41.8% (± 2.9) in the Schwann cell-NPC co-culture differentiation condition. Beta-III tubulin and RIP immunoreactivity was not altered by co-cultured Schwann cells.

After 7 days of co-culture, NPC, which were initially plated onto Schwann cell monolayers, were completely separated from Schwann cells (Fig. 2A-C). GFAP-positive astrocytes with a stellate morphology reminiscent of reactive astroglia appear to seal off the ‘NPC compartment’ from the ‘Schwann cell compartment’, whereas Schwann cells represented by GFP negative Hoechst stained nuclei are

arranged in compact streams in between patches of GFP positive NPC.

Taken together, Schwann cells induced a shift of adult NPC from immature to mature astroglial differentiation *in vitro*. The segregation of co-cultured NPC and Schwann cells suggests that a homogenous distribution of these cell populations after transplantation *in vivo* is unlikely.

3.2 Cyst replacement, cell survival and differentiation of grafted NPC.

The size of the cystic lesion defect in the various grafting conditions (Table 1) was quantified, to determine the capacity of Schwann cells to maintain co-grafted NPC within the cystic lesion environment. Animals with dorsal column transections at cervical level receiving either 1) fibroblasts only **(FF)**, 2) highly purified Schwann cells only (**SC**), 3) NPC and Schwann cells (**NPC/SC**), 4) fibroblasts and Schwann cells (**SC/FF**) or 5) NPC, Schwann cells and fibroblasts (**NPC/SC/FF**) were compared with lesioned only animals (**Lesion**). Without grafting, the described spinal cord lesion produces a cystic lesion cavity within the dorsal column measuring 3.68 ± 0.62 mm^2 (Fig. 3A,G). Schwann cell grafts alone (SC) or combined NPC/Schwann cell transplants (NPC/SC) allowed only a cyst reduction between 53.5 and 46.2% of its original size (Fig. 3C,D,G). Increasing the number of transplanted Schwann cells in these conditions did not further diminish the lesion defect (data not shown). Only the addition of primary fibroblasts (5% of the total number of grafted Schwann cells) dramatically improved the cyst replacement reducing the lesion size by 89.4% (SC/FF), 81.5% (NPC/SC/FF) and 88% (FF) (Fig. 3B,E,F,G).

Both regeneration promoting cell populations, Schwann cells and NPC, survived after transplantation into the acutely injured spinal cord (Fig. 2D-F). Schwann cells expressing the reporter gene GFP were restricted to the former cystic lesion area without migration into the surrounding host parenchyma in respective co-grafting conditions, whereas BrdU-prelabeled NPC were identified primarily in the spinal cord adjacent to the graft (NPC/SC/FF) with few NPC within the actual graft. Thus, cystic lesion replacement is mainly accomplished by grafted Schwann cells supported by fibroblasts. The pattern of Schwann cell/NPC distribution *in vivo* recapitulates the *in vitro* finding, where Schwann cells and NPC become segregated spontaneously within a short period of time (Fig. 2A-C). The lining of GFAP positive astroglial processes along Schwann cells streams *in vitro* is paralleled by a strongly GFAP immunoreactive astroglial rim surrounding Schwann cell containing co-grafts *in vivo* (Fig. 2D,E).

In parallel with previous observations, the co-grafted NPC mainly differentiated into GFAP positive astroglia (Fig. 4A, B), fewer GFAP negative grafted cells were also found to express APC indicating oligodendoglial differentiation (Fig. 4C). Rarely, NPC were immunoreactive for NG2, which is expressed on

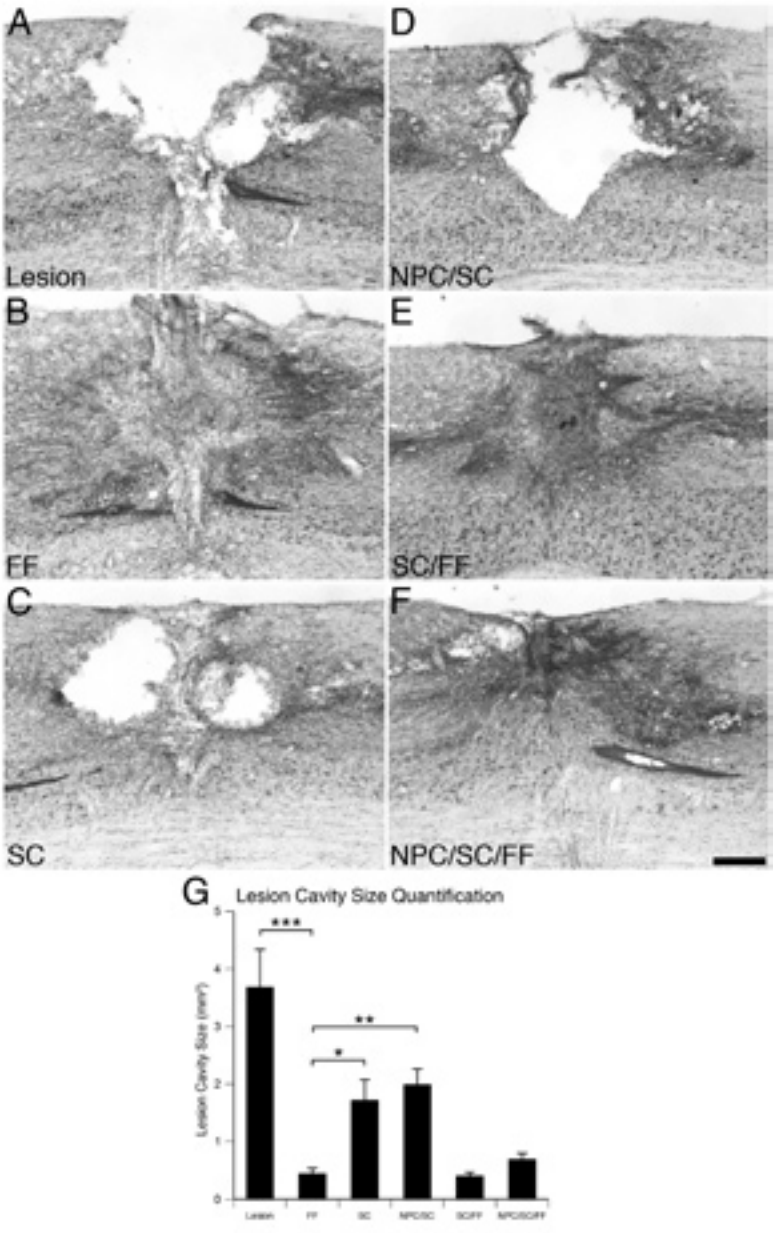

Figure 3: *Sufficient cyst replacement requires fibroblast containing grafts. (A) A cervical wire knife dorsal column transection typically results in a large cystic lesion defect without therapeutic intervention. (B) Pure fibroblasts grafts (FF) replace the lesion cyst, whereas (C) highly purified Schwann cells (SC) or (D) combined grafts of NPC and Schwann cells (NPC/SC) leave the majority of the lesion defect unchanged. As soon as 5% fibroblasts are added to (E) Schwann cell grafts (SC/FF) or (F) combined NPC and Schwann cell grafts (NPC/SC/FF) the lesion defect is almost completely replaced. (G) Quantification of the cystic lesion area in each grafting paradigm compared to animals with lesions only (Lesion). (** indicates p<0.01, *** indicates p<0.001). A-F Brightfield micrographs of sagittal Nissl-stained sections. Orientation A-F: rostral to the left, dorsal to the top. Scale bar A-F 400µm.*

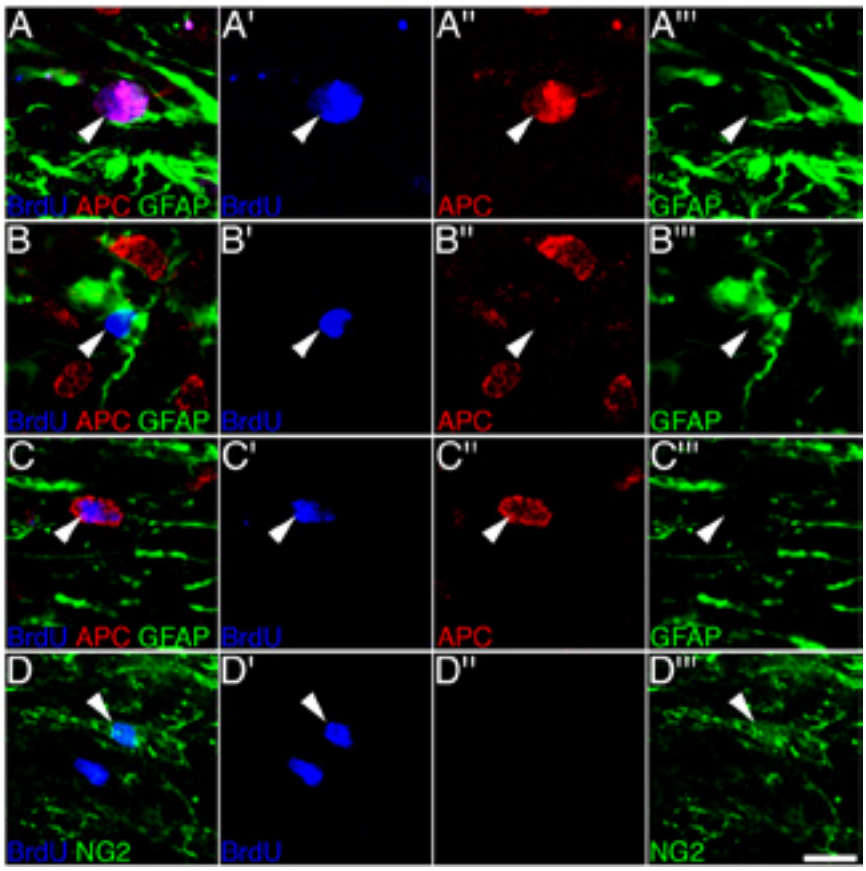

Figure 4: *NPC combined with Schwann cells differentiate into astroglia and oligodendroglia in vivo. The differentiation pattern of grafted NPC was assessed by identifying respective differentiation markers (red and green) co-localized (arrowheads) with BrdU prelabeled NPC (blue) within the adjacent spinal cord parenchyma. Grafted NPC co-localized with (A) APC and GFAP, or (B) GFAP alone indicate astroglial differentiation, whereas (C) co-localization with APC, but not with GFAP, depicts oligodendroglial differentiated NPC. (D) Few grafted NPC could be matched with NG2, a marker for glial restricted progenitor cells. Confocal fluorescence micrographs. Orientation in all micrographs rostral to the left, dorsal to the top. Scale bar A-D 10 µm.*

immature glial cells, 3 weeks after transplantation (Fig. 4D). As expected, none of the grafted NPC displayed the early neuronal differentiation marker doublecortin *in vivo* (data not shown).

3.3 Axonal response

As shown above, only fibroblast containing transplants sufficiently replaced the cystic lesion defect as a prerequisite to build a bridge for axons to regenerate on. Three weeks after lesioning and grafting the axonal response into the respective grafts was assessed quantifying 1) neurofilament immunoreactive axons and 2) specifically anterogradely BDA labeled corticospinal axons. Co-grafts containing NPC and Schwann cells (NPC/SC/FF) elicited the highest overall axonal regrowth (6366 ± 841 pixels/mm^2) com-

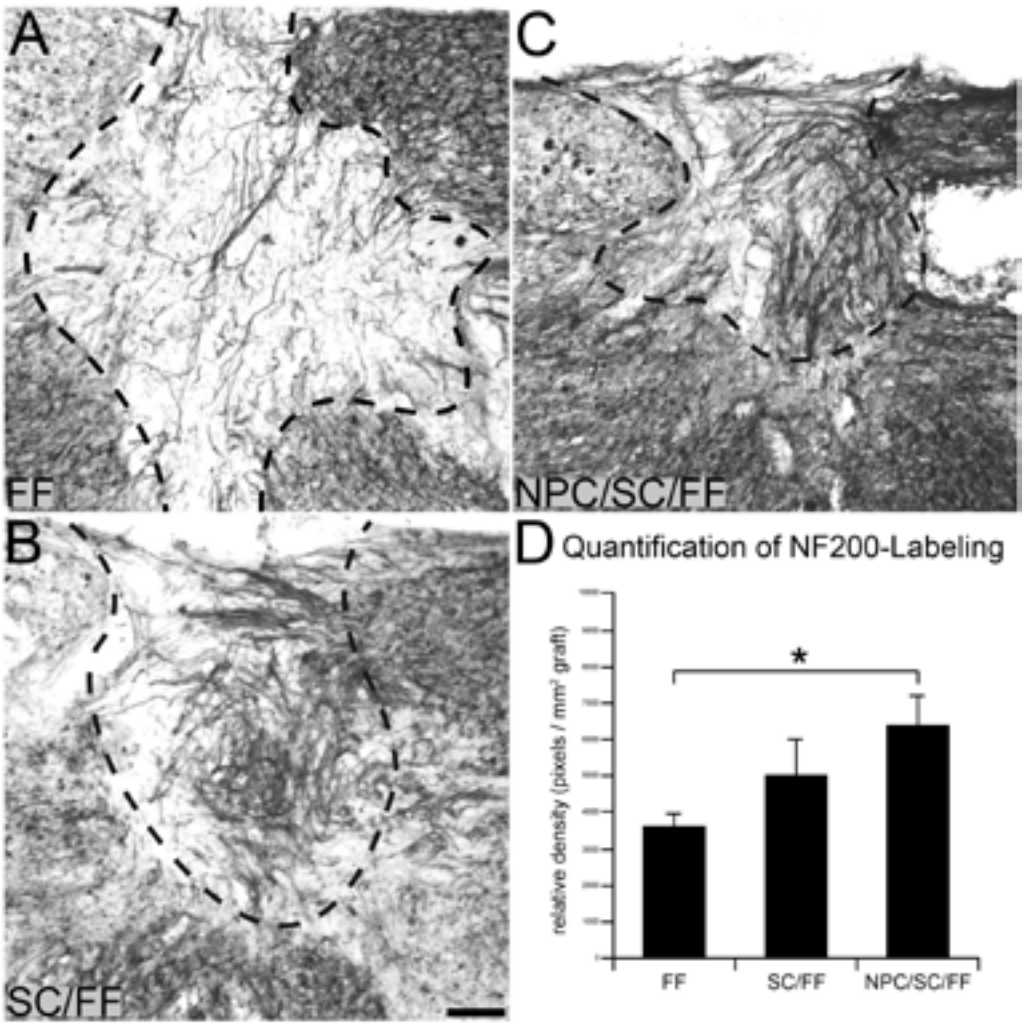

Figure 5: *Axonal growth is enhanced into Schwann cell containing grafts. Immunohistochemical analysis of 200kD neurofilament expression reveals that the density of neurofilament expressing axons within respective grafts increases from (A) FF over (B) SC/FF and (C) NPC/SC/FF grafts, which is confirmed by (D) quantification of neurofilament density (* indicates $p<0.05$). A-C dashed lines outline the graft/host border. Brightfield micrographs. Orientation in A-C: rostral to the left, dorsal to the top. Scale bar A 125 µm, B, C 100 µm.*

pared to co-grafts with Schwann cells (SC/FF; 4998 ± 1008 pixels/mm^2) and pure fibroblasts grafts (FF; 3632 ± 347 pixels/mm^2) as assessed by the density of neurofilament positive axonal profiles (Fig. 5). Analysis of neurofilament expression does not allow to distinguish between axonal regrowth from CNS derived axons versus ingrowth from peripheral nerve derived axons through the dorsal root entry zone. Therefore, corticospinal axons were specifically anterogradely labeled using BDA and quantified (Fig. 6). The degree of corticospinal axon regrowth was significantly reduced in Schwann cell containing co-grafts

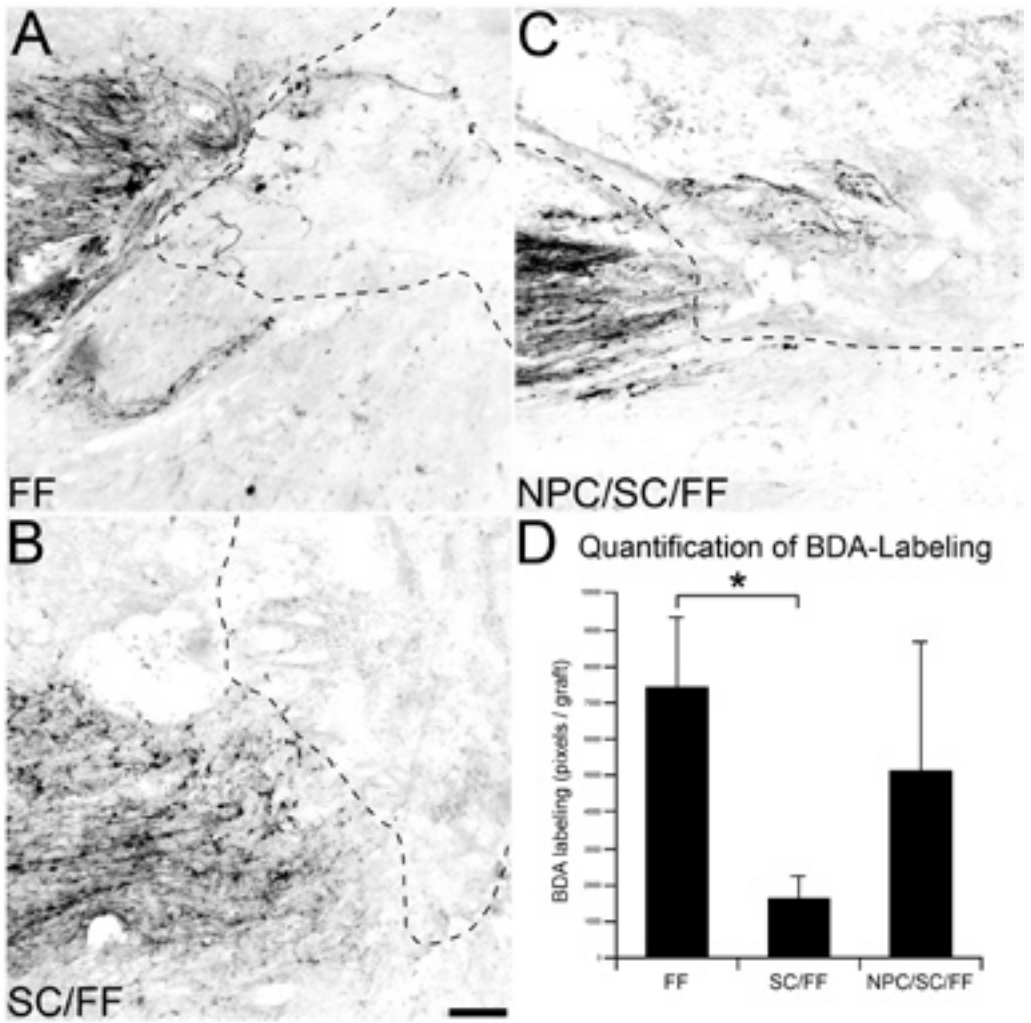

Figure 6: *Schwann cell containing grafts impair corticospinal axon regeneration. Brightfield microscopical analysis of anterogradely BDA-labeled dorsal corticospinal axons shows the regenerative response of CNS axons into (A) FF (B) SC/FF and (C) NPC/SC/FF grafts. Dashed lines outline the graft/host interface. (D) As determined by quantification of BDA labeled corticospinal axon profiles, CST regeneration is massively reduced in animals with SC/FF grafts. (*indicates p<0.01). A-C brightfield micrographs. Orientation in A-C: rostral to the left, dorsal to the top. Scale bar A-C 100 µm.*

(SC/FF; 1601 ± 628 pixels) compared to pure fibroblast grafts (FF; 6879 ± 1797) (Fig. 7A,B,D). NPC/SC/FF co-grafts did not significantly alter the degree of CST axon regeneration (Fig. 7C,D; 5105 ± 3553). Thus, as soon as Schwann cells are added to the grafting paradigm, CST regeneration is dramatically impaired. By combining Schwann cells with NPC, this impaired regeneration can be reversed, but only up to a degree of axonal regeneration observed with pure fibroblast grafts.

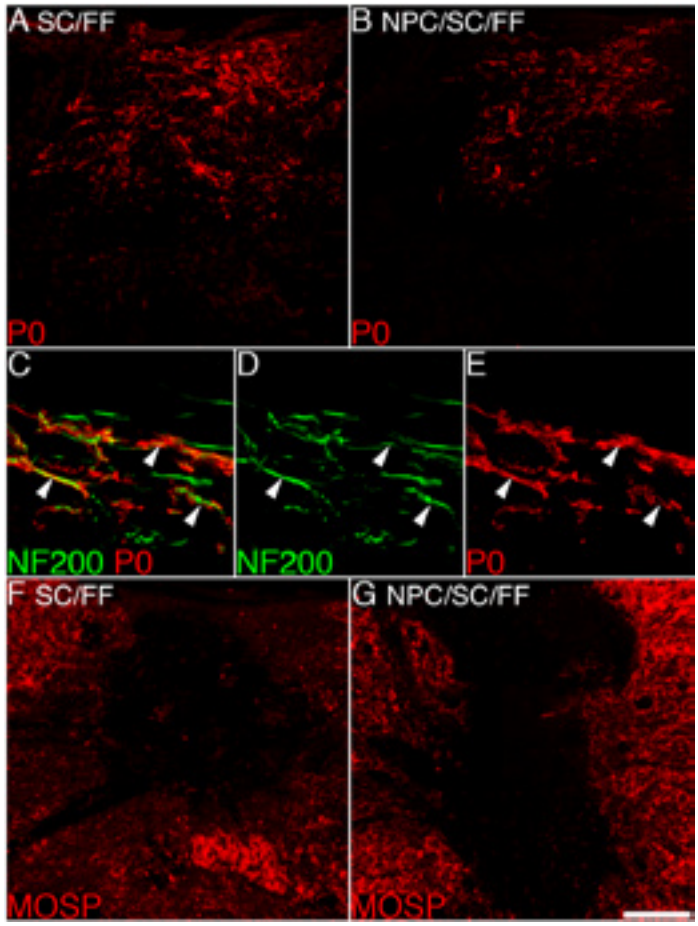

***Figure 7**: Only peripheral type myelin can be identified within co-grafts. PNS myelin indicated by P0 immunoreactivity (red) is abundant throughout Schwann cell containing grafts such as (A) SC/FF and (B) NPC/SC/FF grafts. (C) P0 (red) and neurofilament immunoreactive (green) structures within Schwann cell containing grafts display a close spatial correlation (arrowheads), which indicates remyelination of regenerating axons by grafted Schwann cells. Overlay. (D) Neurofilament. (E) P0. (F) MOSP immunoreactivity representing CNS myelin was virtually absent both in co-grafts without (SC/FF) and co-grafts with (NPC/SC/FF) NPC. Confocal fluorescence micrographs. Orientation: rostral to the left, dorsal to the top. Scale bar A, B, F, G 200 µm, C-E 18 µm.*

3.4 Schwann cell and NPC induced remyelination

Both, grafted Schwann cells and NPC have the capacity to remyelinate axons following spinal cord injury. Therefore, the expression of Schwann cell (P0) and oligodendroglia specific (myelin oligodendrocyte-specific protein; MOSP) myelin-associated molecules within the graft was analyzed. In both grafting paradigms containing Schwann cells (SC/FF and NPC/SC/FF), strong P0 immunoreactivity restricted to the graft site was detectable (Fig. 7A,B). The close spatial association of P0 labeling with neurofilament positive axons indicates that regenerating

axons within the graft become remyelinated by grafted Schwann cells (Fig. 7C-E). In contrast, virtually no immunoreactivity for CNS myelin was identifiable in any of the grafting conditions including NPC containing grafts (NPC/SC/FF) (Fig. 7F,G), which is not surprising knowing that the majority of co-grafted NPC leave the graft site (Fig. 2F). The only means to attribute (re-)myelination to grafted NPC is to co-localize BrdU prelabeled NPC with CNS myelin immunoreactivity. However, the antigen retrieval procedure required to detect BrdU is not compatible with immunohistochemical analysis of CNS myelin. Therefore, the degree of remyelination promoted by co-grafted NPC outside of the graft cannot be determined in the present study.

4. DISCUSSION

The aim of the present study was to investigate whether Schwann cells represent a more favorable cell population to be co-grafted with adult NPC instead of primary fibroblasts. Unlike fibroblasts, Schwann cells alone or in combination with NPC do not replace the cystic lesion defect developing following spinal cord injury. Schwann cells augment overall axonal regrowth, however, regeneration of corticospinal axons is impaired as soon as Schwann cells are introduced. Within the graft, remyelination by Schwann cells is observed, whereas almost all co-grafted NPC migrate into the adjacent spinal cord parenchyma, thus precluding remyelination through NPC derived oligodendroglia within the graft.

Adult NPC represent a promising cell-based strategy following spinal cord injury. However, adult NPC alone are not sufficient to replace typically developing cystic lesion defects [1]. In a recent study, we were able to demonstrate that fibroblasts and extracellular matrix produced by fibroblasts provide a scaffold for NPC to adhere to, thus maintaining co-grafted NPC within the lesion site [2]. Primary Schwann cells, which were highly purified (>99%) from adult sciatic nerves using MACS and consecutively introduced into co-grafts with NPC instead of fibroblasts, were not able to sufficiently replace cystic lesion defects in the present study. Once fibroblasts were added, even in low amounts, lesion replacement was almost complete. This finding is in line with previous studies, which report diminished injury induced cavitation with Schwann cell grafts containing a significant proportion of fibroblasts either by grafting less pure Schwann cell suspension grafts (95-98%) [8] or by grafting Schwann cells combined with 5% fibroblasts [18]. Apparently, highly purified Schwann cells alone do not produce sufficient extracellular matrix components qualitatively and quantitatively to replace cystic lesion defects or to serve as a platform for co-grafted NPC following transplantation into the injured spinal cord.

Another highly relevant aspect of any cell-based regenerative approach in the injured spinal cord is that grafted cells not only replace the lesion defect, but also integrate into the host spinal cord, thus building a continuous transition from the spinal

cord into the graft and back into the spinal cord. Schwann cells have been shown to promote substantial axonal regrowth into the graft, however, axons failed to reenter the distant spinal cord [19]. Schwann cells become sealed off by the surrounding spinal cord, which has been demonstrated by the upregulation of growth inhibitory extracellular matrix components such as chondroitin sulfate proteoglycans around Schwann cell grafts [20], preventing proper integration into the host. In parallel, we observed that CNS derived adult NPC and Schwann cells become separated *in vitro* and *in vivo*. Astroglial cells differentiated from NPC form glia limitans-like boundaries along streams of Schwann cells, which exactly recapitulates the segregation of astrocytes and Schwann cells in co-cultivation experiments [21]. As a consequence in vivo, the vast majority of NPC became segregated from the Schwann cell enriched graft milieu migrating into the adjacent host spinal cord. Accordingly, the absence of co-grafted NPC at the lesion site excludes significant NPC induced cell-contact mediated axon regeneration, which has contributed to the significant CST axon regrowth after co-grafting with fibroblasts [2]. Since considerable amounts of host-derived Schwann cells are shown to spontaneously migrate into the lesion site after the initial injury [14], the influence of Schwann cells on migration of already differentiated NPC needs to be investigated at long time periods after the injury.

In vitro, Schwann cells induced a differentiation shift from A2B5 expressing glial precursor cells towards GFAP expressing astroglia. The exact molecular differentiation factors responsible for this differentiation shift were not determined in the present study. Likely candidates are LIF and CNTF, which are known to be released by Schwann cells and to induce astroglial differentiation [22-25]. Since we did not observe a shift towards neuronal differentiation in NPC/Schwann cell co-culture conditions, it was not surprising to see that adult NPC as part of NPC/SC/FF co-grafts differentiated exclusively into glial cells. In line with previous findings [1, 2], NPC expressed markers resembling astroglial and oligodendroglial differentiation after transplantation. Thus, neither *in vitro* nor *in vivo* studies indicate that Schwann cells might express molecular cues, which instruct neuronal differentiation.

Schwann cell containing co-grafts induced a differential axon regrowth response. CST axonal regrowth into Schwann cell containing co-grafts was virtually absent replicating previous findings [8, 13], in contrast to fibroblast grafts, which elicited at least minimal CST regrowth in our lesion paradigm. This is remarkable because Schwann cells are considered to have an intrinsic axon regenerative capacity, whereas fibroblasts are perceived as axon growth inhibitory serving mainly as cellular source for growth factor production following transgene transfer. Most likely the pronounced segregation of Schwann cells by glia limitans formation and chondroitin sulfate proteoglycan upregulation [20] is responsible for the poor CST regrowth into Schwann cell containing grafts. This notion is supported by an *in vitro* study,

which demonstrated a clear segregation and glial limitians formation in astrocyte/Schwann cell versus astrocyte/fibroblast co-cultures [21]. Once NPC are added to Schwann cell grafts (NPC/SC/FF) they appear to compensate for the impaired CST regeneration in SC/FF grafts up to the level of pure fibroblasts grafts. One can speculate that NPC co-grafted with Schwann cells and fibroblasts may have promoted limited cell-contact mediated axonal regrowth across the graft-host border into the graft, which is still significantly less compared to NPC/fibroblast co-grafts examined in a previous study [2].

The neurofilament density, reflecting the overall axonal regeneration was increased into Schwann cell containing co-grafts. Due to the nature of the applied lesion (dorsal column transection), transected ascending proprioceptive axons most likely accounted for the increased neurofilament density within Schwann cell containing grafts, since dorsolateral or ventral axon tracts remain intact. Possibly, these sensory projections with their neurons located in the dorsal root ganglia, as opposed to CST axons with their neurons in the motorcortex, show a robust regenerative response in a peripheral nerve like milieu such as Schwann cell grafts, which might explain the differential axon regrowth response.

Schwann cell transplants have been described to remyelinate CNS axons in a phenotypically appropriate manner [13, 26] and to restore nerve conduction of lesioned CNS axons [27]. In the investigated grafting paradigms co-grafted Schwann cells expressed P0, which is exclusively expressed in peripheral myelin, indicating robust Schwann cell promoted remyelination in the spinal cord lesion site. No relevant expression of CNS myelin could be detected within NPC containing grafts, which is obviously due to the observed migration of NPC into the adjacent host spinal cord.

Taken together, the failure to replace cystic lesion defects and the impaired regeneration of severed CST axons into Schwann cell grafts precludes the combination with NPC for a clinically relevant cell-based regenerative approach. This does not mean that pure Schwann cell grafts may not be beneficial. Schwann cells readily remyelinate CNS axons and elicit regeneration of spinal and supraspinal axons [20]. Recent studies have demonstrated that Schwann cells are even superior to olfactory ensheathing cells and elicit partial functional recovery [8]. In respect to NPC, future studies need to investigate alternative approaches such as application of natural/synthetic matrices, to maintain NPC within the lesion defect as a prerequisite to allow cell-contact mediated axon regeneration across the injury site, proper target reinnervation and ultimately functional recovery.

5. ACKNOWLEDGMENTS

This work was supported by the Institute International de Recherche en Paraplégie Geneva, on behalf of an anonymous donation, and ReForM-Program, University of Regensburg, School of Medicine. We thank Dr. J. Archelos for the PO antibody.

6. REFERENCES

1. Vroemen, M., Aigner, L., Winkler, J. & Weidner, N. Adult neural progenitor cell grafts survive after acute spinal cord injury and integrate along axonal pathways. Eur J Neurosci 18, 743-51 (2003).
2. Pfeifer, K., Vroemen, M., Blesch, A. & Weidner, N. Adult neural progenitor cells provide a permissive guiding substrate for corticospinal axon growth following spinal cord injury. Eur J Neurosci 20, 1695-704 (2004).
3. Bundesen, L. Q., Scheel, T. A., Bregman, B. S. & Kromer, L. F. Ephrin-B2 and EphB2 regulation of astrocyte-meningeal fibroblast interactions in response to spinal cord lesions in adult rats. J Neurosci 23, 7789-800 (2003).
4. Davies, J. E., Tang, X., Denning, J. W., Archibald, S. J. & Davies, S. J. Decorin suppresses neurocan, brevican, phosphacan and NG2 expression and promotes axon growth across adult rat spinal cord injuries. Eur J Neurosci 19, 1226-42 (2004).
5. Griffin, J. W. & Hoffman, P. N. in Peripheral Neuropathy (eds. Dyck, P. J. & Thomas, P. K.) 361-376 (W.B. Saunders, Philadelphia, 1993).
6. Bunge, M. B. Transplantation of purified populations of Schwann cells into lesioned adult rat spinal cord. J Neurol 242, S36-9 (1994).
7. Imaizumi, T., Lankford, K. L. & Kocsis, J. D. Transplantation of olfactory ensheathing cells or Schwann cells restores rapid and secure conduction across the transected spinal cord. Brain Res 854, 70-8 (2000).
8. Takami, T. et al. Schwann cell but not olfactory ensheathing glia transplants improve hindlimb locomotor performance in the moderately contused adult rat thoracic spinal cord. J Neurosci 22, 6670-81 (2002).
9. Wang, G. Y., Hirai, K. & Shimada, H. The role of laminin, a component of Schwann cell basal lamina, in rat sciatic nerve regeneration within antiserum-treated nerve grafts. Brain Res 570, 116-25 (1992).
10. Vroemen, M., Weidner, N. & Blesch, A. Loss of gene expression in lentivirus- and retrovirus-transduced neural progenitor cells is correlated to migration and differentiation in the adult spinal cord. Exp Neurol In press (2005).
11. Tuszynski, M. H. et al. Grafts of genetically modified Schwann cells to the spinal cord: survival, axon growth, and myelination. Cell Transplant 7, 187-96 (1998).
12. Menei, P., Montero-Menei, C., Whittemore, S. R., Bunge, R. P. & Bunge, M. B. Schwann cells genetically modified to secrete human BDNF promote enhanced axonal regrowth across transected adult rat spinal cord. Eur J Neurosci 10, 607-21 (1998).
13. Weidner, N., Blesch, A., Grill, R. J. & Tuszynski, M. H. Nerve growth factor-hypersecreting Schwann cell grafts augment and guide spinal cord axonal growth and remyelinate central nervous system axons in a phenotypically appropriate manner that correlates with expression of L1. J Comp Neurol 413, 495-506 (1999).
14. Tuszynski, M. H. et al. Fibroblasts genetically modified to produce nerve growth factor induce robust neuritic ingrowth after grafting to the spinal cord. Exp Neurol 126, 1-14 (1994).
15. Vroemen, M. & Weidner, N. Purification of Schwann cells by selection of p75 low affinity nerve growth factor receptor expressing cells from adult peripheral nerve. J Neurosci Methods 124, 135-43 (2003).
16. Autilio-Gambetti, L., Sipple, J., Sudilovsky, O. & Gambetti, P. Intermediate filaments of Schwann cells. J Neurochem 38, 774-80 (1982).
17. Jessen, K. R., Morgan, L., Brammer, M. & Mirsky, R. Galactocerebroside is expressed by non-myelin-forming Schwann cells in situ. J Cell Biol 101, 1135-43 (1985).
18. Keyvan-Fouladi, N., Raisman, G. & Li, Y. Delayed repair of corticospinal tract lesions as an assay for the effectiveness of transplantation of Schwann cells. Glia (2005).
19. Li, Y. & Raisman, G. Schwann cells induce sprouting in motor and sensory axons in the adult rat spinal

cord. J Neurosci 14, 4050-63 (1994).
20. Plant, G. W., Bates, M. L. & Bunge, M. B. Inhibitory proteoglycan immunoreactivity is higher at the caudal than the rostral Schwann cell graft-transected spinal cord interface. Mol Cell Neurosci 17, 471-87 (2001).
21. Ghirnikar, R. S. & Eng, L. F. Astrocyte-Schwann cell interactions in culture. Glia 11, 367-77 (1994).
22. Hughes, S. M., Lillien, L. E., Raff, M. C., Rohrer, H. & Sendtner, M. Ciliary neurotrophic factor induces type-2 astrocyte differentiation in culture. Nature 335, 70-3 (1988).
23. Nakagaito, Y., Yoshida, T., Satoh, M. & Takeuchi, M. Effects of leukemia inhibitory factor on the differentiation of astrocyte progenitor cells from embryonic mouse cerebral hemispheres. Brain Res Dev Brain Res 87, 220-3 (1995).
24. Richards, L. J. et al. Leukaemia inhibitory factor or related factors promote the differentiation of neuronal and astrocytic precursors within the developing murine spinal cord. Eur J Neurosci 8, 291-9 (1996).
25. Dowsing, B. J. et al. Leukemia inhibitory factor is an autocrine survival factor for Schwann cells. J Neurochem 73, 96-104 (1999).
26. Xu, X. M., Guenard, V., Kleitman, N. & Bunge, M. B. Axonal regeneration into Schwann cell-seeded guidance channels grafted into transected adult rat spinal cord. J Comp Neurol 351, 145-60 (1995).
27. Honmou, O., Felts, P. A., Waxman, S. G. & Kocsis, J. D. Restoration of normal conduction properties in demyelinated spinal cord axons in the adult rat by transplantation of exogenous Schwann cells. J Neurosci 16, 3199-208 (1996).

Chapter 5

Loss of gene expression in lentivirus- and retrovirus- transduced neural progenitor cells is correlated to migration and differentiation in the adult spinal cord

Exp. Neurol. in press

Maurice Vroemen
Norbert Weidner
Armin Blesch

ABSTRACT

Gene transfer into multipotent neural progenitor cells (NPC) and stem cells may provide for a cell replacement therapy and allow the delivery of therapeutic proteins into the degenerating or injured nervous system. Previously, murine leukemia virus-based retroviral vectors expressing GFP from an internal EF-1alpha promoter, and lentiviral vectors expressing GFP from a hybrid CMV/ß-actin promoter have been described to be resistant to stem cell specific gene silencing. Therefore, we investigated whether these viral vectors allow stable *in vivo* gene expression in genetically modified NPC isolated from the adult rat spinal cord. *In vitro*, NPC genetically modified to express GFP using the described retroviral vector showed strong GFP expression in undifferentiated NPC. However, *in vitro* differentiation resulted in the loss of GFP expression in 50% of cells. Grafting of BrdU prelabeled NPC to the spinal cord resulted in a loss of GFP expression in 70% and 95% of surviving NPC at 7 and 28 days post grafting, respectively. The loss in gene expression was paralleled by the differentiation of NPC into a glial phenotype. Transgene downregulation although less profound was also observed in cells modified with lentiviral vectors, whereas *in vivo* lentiviral gene transfer resulted in stable transgene expression for up to 16 months. Thus, *in vivo* gene expression in genetically engineered neural progenitor cells is temporally limited and mostly restricted to undifferentiated NPC using the viral vectors tested.

1. INTRODUCTION

Gene therapy holds great potential for the treatment of several central nervous system (CNS) disorders. Delivery of therapeutic molecules by gene therapy has been shown to halt or delay the progression of neurodegenerative diseases [1-3] or to augment the regenerative capacity after CNS injury [4-9].

Different cell types including Schwann cells, fibroblasts, astrocytes and neural progenitor cells (NPC) have been used for *ex vivo* gene delivery [1, 2, 5, 10, 11]. NPC are particularly interesting due to their ability to give rise to both new neurons and glia and thus to replace lost spinal cord tissue in an organotypically appropriate manner [12, 13]. Adult NPC can be isolated from the patient's own neural tissue by minimally invasive biopsies [14, 15], propagated *in vitro* [16] and serve as autologous cell grafts in the lesioned spinal cord [17]. Cellular delivery of therapeutic genes via NPC grafts will likely require long-term transgene expression for the treatment of genetic deficiencies or chronic neurodegenerative diseases. In contrast, short-term, transient gene expression might be more desirable under certain conditions, e.g. to induce differentiation of grafted NPC into a specific phenotype that is able to enhance regeneration in the injured spinal cord [18].

To genetically modify NPC, MLV-based retroviral and lentiviral vectors have been used in several studies as these viruses allow stable integration of the transgene into the host genome [19, 20]. We and others

have previously shown that MLV-based retroviral vectors can efficiently transduce primary adult rat NPC *in vitro* [13, 21]. However, the downregulation of gene expression is a major obstacle for the persistent gene transfer into stem cells and adult NPC for long-term gene delivery [13, 21-23]. Retroviral silencing has been attributed to reduced transcriptional initiation at the promoter caused by the binding of trans-acting factors to silencer elements that are located in the viral long terminal repeats (LTRs). Furthermore, chromatin condensation caused by de novo cytosine methylation of CpG sequences located within LTRs may also contribute to transgene downregulation [22, 24]. The construction of viral vectors lacking silencer elements, the inclusion of improved positive regulatory elements [25] and the use of internal promoters have been reported to improve duration of gene expression [26]. Lentiviruses could potentially be susceptible to the same silencing mechanisms as retroviruses [27]. However, recent reports have indicated that lentiviral vectors are more resistant to stem cell specific gene silencing in various types of stem cells [28, 29]. The ability of lentiviral vectors to induce stable transgene expression in adult NPC has not been investigated to date.

In the present study we compared 3 different viral vector systems for their ability to mediate stable gene expression in NPC after engraftment into the adult spinal cord. Under these conditions NPC are known to differentiate into glial phenotypes. MLV-based retroviral vectors containing a *Xenopus* EF1a enhancer/promoter or a 5' LTR to express the reporter gene green fluorescent protein (GFP), or a lentiviral vector containing a hybrid CMV/ß-actin promoter were used to modify primary adult NPC. Two of these viral vectors have previously been described to be resistant to stem cell specific gene silencing in embryonic neural precursors [26] and mouse embryonic stem (ES) cells, respectively [28]. Our data indicate that the investigated viral vectors allow stable gene expression in undifferentiated NPC *in vitro*, whereas the vast majority of neural progenitor cells lose transgene expression after engraftment into the spinal cord. In contrast, *in vivo* lentiviral gene transfer results in long-term, stable GFP expression in the adult rat CNS.

2. MATERIALS AND METHODS

2.1 Animal subjects

Adult female Fischer 344 rats weighting 160-200 g were housed under standard laboratory conditions with 12 h light dark cycle. All experiments were carried out in accordance with institutional guidelines for animal care. Animals had *ad libitum* access to food and water throughout the study. All surgical procedures were performed under anesthesia using a cocktail of ketamine (62.5 mg/kg; WDT, Garbsen, Germany), xylazine (3.175 mg/kg; WDT, Garbsen, Germany) and acepromazine (0.625 mg/kg, Sanofi-Ceva, Düsseldorf, Germany) in 0.9% sterile saline solution.

2.2 Preparation of adult NPC

Adult NPC were isolated and cultured as described [13, 16]. Briefly, rats were deeply

anesthetized and killed by decapitation. The region of the complete cervical enlargement (spinal cord level C3 through T1) was dissected. After removal of the dura, the tissue was minced, washed in sterile Dulbecco's phosphate buffered saline/D-glucose (4.5g/l; PAA Laboratories, Linz, Austria) and digested in a solution of papain (0.01%; Worthington Biochemicals, Lakewood, USA), neutral protease (0.1%; Roche, Mannheim, Germany), DNase I (0.01%; Worthington Biochemicals) and 12.4 mM $MgSO_4$, dissolved in Hank's balanced salt solution (HBSS; PAA Laboratories, Linz, Austria) for 30 min at 37°C. The digested tissue was washed three times in DMEM-HAMS F12 (Pan Biotech, Aidenbach, Germany), supplemented with 10% fetal calf serum (FCS; Pan Biotech, Aidenbach, Germany). The cells were transferred to culture dishes containing serum-free growth medium (Neurobasal medium with B27 supplement (Gibco, Karlsruhe, Germany), 2 µg/ml heparin (Sigma) 20 ng/ml recombinant human FGF-2 (R&D System, Wiesbaden, Germany), 20 ng/ml recombinant human EGF-2 (R&D System, Wiesbaden, Germany). Until the first passage, cells were grown in uncoated cell culture flasks to form neurospheres. Neurospheres were then dissociated using Acccutase (Innovative Cell Tech, San Diego, USA) and the NPC were subsequently grown as adherent monolayer cultures on poly-l-ornithin/laminin (P-Orn/Lam) coated cell culture flasks, Cell culture medium was changed twice per week. Cell cultures were passaged after reaching confluence, approximately every other week.

2.3 Production of viral vectors

The retroviral plasmid pLXSN-GFP (Fig. 1A) is based on the plasmid pLXSN (Clontech, Heidelberg, Germany) and was constructed and used to transduce NPC as described [13]. GFP expression in this plasmid is driven by the 5'LTR, and a neomycin resistance gene driven by an internal SV 40 promoter allows for the selection of transduced cells. The retroviral plasmid pCLE-GFP (Fig. 1B) is based on the plasmid pCLE (generous gift from N. Gaiano,) [26]. This plasmid contains the human cytomegalovirus enhancer-promoter fused to the Moloney murine leukemia virus LTR at the TATA box in the 5' U3 region [30] and an *Xenopus* EF-1 alpha regulatory element as internal promoter to drive transgene expression. To allow selection of cells that stably integrated the transgene, the internal ribosome entry site and the human placental alkaline phosphatase gene of pCLE were replaced by the SV40 promoter and a neomycin resistance gene. The GFP coding sequence was cloned into the multiple cloning site resulting in the plasmid pCLE-GFP.

For retrovirus production, 293T cells were grown in Iscove's Modified Dulbecco's Medium (IMDM; Pan Biotech, Aidenbach, Germany), with 10% FCS and were transfected with the retroviral plasmid (pCLE-GFP and pLXSN-GFP, respectively) and 2 packaging plasmids coding for the vesicular stomatitis virus (VSV) envelope and the retroviral gag/pol sequences. Retrovirus-containing supernatants were collected, filtered through a 0.45 µm syringe filter and stored at -80°C.

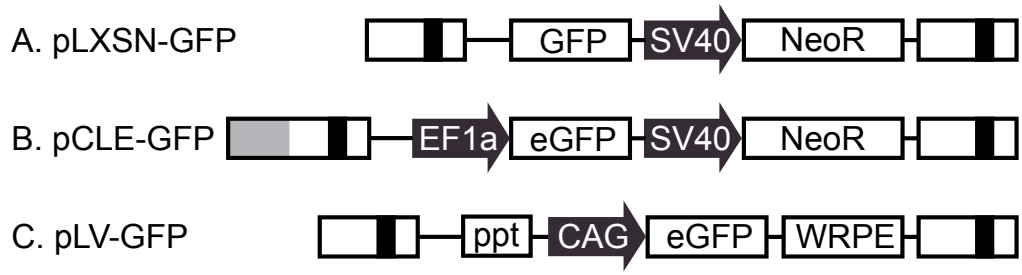

Figure 1: *Schematic representation of viral constructs. (A) In the retroviral vector pLXSN-GFP, reporter gene expression is driven by the promoter/enhancer sequences of the Moloney murine leukemia virus derived 5' LTR. (B) In contrast, the retroviral vector pCLE-GFP uses the Xenopus EF-1alpha regulatory elements (EF1a) as an internal promoter. Furthermore, pCLE-GFP contains a hybrid 5' LTR that consists of the immediate early region of the human cytomegalovirus enhancer-promoter fused to the Moloney murine leukemia virus long terminal repeat at the TATA box in the 5' U3 region. Both pLXSN-GFP and pCLE-GFP contain a neomycin resistance gene (NeoR) under control of the SV40 early promoter (SV40), which allows selection of transduced cells. (C) The lentiviral vector pLV-GFP contains the compound chicken ß-actin cytomegalovirus enhancer/promoter (CAG) followed by a ß-globin intron for GFP expression. Furthermore, pLV-GFP contains a central polypurine tract of HIV-1 (ppt), a woodchuck hepatitis virus posttranscriptional response element (WRPE) and a self-inactivating deletion in the 3'LTR.*

For lentiviral vector production, a self-inactivating lentiviral plasmid [31] derived from pRRL [32] was used. The plasmid pLV-GFP (p156sinRRLpptCAG-GFP-PRE, Fig. 1C) containing a GFP expression cassette driven by the CMV/ß-actin hybrid promoter (CAG) [33] has been described previously [28]. This plasmid also contains a woodchuck posttranscriptional response element (WPRE) to increase gene expression [31]. For lentivirus production a third generation lentivirus packaging system was utilized as previously described [34]. Viral supernatants were concentrated by ultracentrifugation. Titers of GFP expressing virus were determined by transduction of 293T cells using serial dilutions. Viral vector stocks were also assayed for p24 antigen levels using an HIV-1 p24 specific ELISA kit (DuPont). Titers of GFP expressing virus were 5 x 10^8 IU/ml (231 µg/ml p24). For *in vitro* transduction, GFP expressing lentivirus was diluted as described below.

2.4 Transduction of NPC with retroviral and lentiviral vectors

Adult NPC were genetically modified to express the reporter gene GFP as previously described [13]. Briefly, adult NPC from passage number 4 to 6 cultures were plated in sub-confluent densities (10,000 cells/cm^2) on P-Orn/Lam coated cell culture flasks. The cells were incubated for 8 hrs on two consecutive days with retrovirus containing supernatants (pCLE-GFP or pLXSN-GFP) supplemented with 1 µg/ml Polybrene (Sigma). Approximately 60% of all cells displayed GFP fluorescence 2 days following the transduction. To select for GFP expressing cells that integrated the retroviral vector, G418 (500 µg/ml active concentration; Gibco Karlsruhe, Germany) was added to the growth medium

for 6 weeks. This concentration has previously been determined to completely eliminate all untransfected NPC within 3 weeks. Successful incorporation of the transgene into all NPC was confirmed by GFP fluorescence using an inverted fluorescence microscope (Olympus IX 70). Following G418 selection, cells were cultivated in the absence of G418.

For the transduction of NPC with lentiviral vectors (pLV-GFP), low passage NPC were split 1:3 into coated T-75 flasks (5.4 x 10^6 cells/flask). On the following day GFP expressing lentiviral vectors were added and cells were cultivated for 2 days, when GFP expression was sufficient for fluorescent activated cell sorting (FACS). Flow cytometry analysis and fluorescence microscopy indicated that 80% of the cells were positive for GFP before FACS and over 99% expressed GFP after FACS. Following FACS, cells were kept in culture and passaged twice before transplantation.

2.5 Immunocytochemistry of cultured NPC

Cells of monolayer cultures were detached using Accutase (Innovative Cell Tech, San Diego, USA) and plated on P-Orn/Lam coated glass coverslips in growth medium. To induce differentiation, NPC were incubated for up to 21 days in differentiation medium (Neurobasal medium with B27 supplement and 5% FCS, Pan Biotech, Aidenbach, Germany, [13, 35].

The following antibodies were used to analyze the differentiation pattern of adult NPC *in vitro*: rabbit-anti-GFP for GFP expressing cells (Molecular Probes, Leiden, The Netherlands; at 1/1000) mouse-anti-A2B5 for glial committed progenitors (Chemicon, Hofheim, Germany; at 1/100), mouse-anti-GFAP for astroglia (Chemicon, Hofheim, Germany; at 1/600), mouse-anti-GalC for oligodendroglia (Chemicon, Hofheim, Germany; at 1/500) and mouse-anti-beta-III-tubulin for early neuronal differentiation (clone 5G8; Promega, Mannheim, Germany; at 1/500).

Cells were fixed in 4% paraformaldehyde in PBS, washed three times with tris-buffered saline (TBS), blocked with TBS containing 3% donkey serum/0.1% Triton-X (TBS++) and incubated overnight with primary antibody in TBS++ at 4°C. To label cell surface markers, Triton-X was omitted. The following day, cells were washed with TBS and incubated with fluorescein linked secondary donkey-anti-rabbit antibodies and rhodamine-X linked secondary donkey-anti-mouse antibodies (Jackson, Hamburg, Germany; at 1/1000) in TBS++ for 2h. Finally, nuclei were counterstained with Hoechst 33342 (2 µg/ml in TBS; Sigma). The coverslips were mounted onto glass slides using Prolong-Antifade (Molecular Probes, Leiden, Netherlands). For the immunocytochemical analysis, 8 bit monochrome pictures were taken at 20x magnification on a fluorescent microscope (Leica DMR) equipped with a Spot CCD camera model 2.2.1 (Diagnostic Instruments, Sterling Heights, USA).

2.6 Surgical procedures

Adult NPC virally transduced to express GFP were incubated for 48 hrs before

transplantation with a 1 µM solution of the proliferation marker bromodeoxyuridine (BrdU; Sigma) in growth medium, which results in labeling of more than 95% of all NPC. GFP expression was confirmed using an inverted fluorescence microscope (Olympus IX 70) just before harvesting the cells. An aliquot of the cells was counted in a Neubauer hemocytometer using trypan blue staining and the cells were resuspended in Dulbecco's PBS to yield a final concentration of 10^5 cells/µl.

A total of 27 animals was used in the experiments. Animals were anesthetized using a cocktail of ketamine, xylazine and acepromazine as described above and received injections of NPC transduced with the retroviral vector pCLE-GFP (n=12) or the vector pLXSN-GFP (n=3) into the cervical spinal cord. The ligament between the cervical vertebrae C3 and C4 was incised and a 2 µl cell suspension (10^5 cells/µl) was injected 1 mm deep into the spinal cord parenchyma through a stereotactically guided pulled glass micropipette (40 µm internal diameter) using a Picospritzer II (General Valve, Fairfield, USA). Animals with pCLE-GFP transduced cells were sacrificed after 2 days (n=4), 7 days (n=4) or 28 days (n=4), animals receiving pLXSN-GFP transduced NPC were sacrificed after 28 days (n=3). The lentivirus-transduced cells were grafted into the thoracic spinal cord at level T7/8 (n=3) as described above and were sacrificed after 28 days.

To control for potential unspecific labeling from unincorporated BrdU or death of BrdU prelabeled cells, a suspension of BrdU prelabeled NPC (10^5 cells/µl) was lysed by repeated freeze-thaw cycles and injected into 2 animals (2 µl per animal). Two additional animals received an injection of 2 µl PBS used to wash the cells after BrdU incubation before grafting.

For direct injection of lentiviral vectors, animals (n=5) were anesthetized as described above and received a small laminectomy at T7/8. Lentiviral vectors (2 µl) were injected 1 mm deep into the spinal cord through a pulled micropipette using a Picospritzer at a rate of 1 µl/min. Pipettes were left in place for one additional minute before withdrawal. 5 animals received lentiviral vectors containing the coding sequence for GFP and were killed at 14 days (n=3), 10 months (n=1) and 16 months (n=1).

2.7 Histological analysis

Two days, 7 days and 28 days after cell injections, and 14 days, 10 months and 16 months after lentivirus injections, animals were deeply anesthetized and transcardially perfused with 100 ml phosphate buffered saline followed by 250 ml 4% paraformaldehyde in 0.1M phosphate buffer. The brains and spinal cords were dissected, post fixed overnight and cryoprotected in 30% sucrose. Sagittal 35 µm sections were cut on a freezing microtome and processed for immunohistochemistry. Every seventh section was immediately mounted and Nissl stained to localize the injection site.

For brightfield immunohistochemical analysis of BrdU prelabeled cells, sections were rinsed in TBS (0.1M) and incubated

for 1h in 50% formamide/2xSSC (0.3 M NaCl, 0.03M sodium citrate) at 65ºC. Sections then were rinsed in 2xSSC, incubated for 30 min in 2 N HCl at 37ºC, and rinsed for 10 min in 0.1 M boric acid pH 8.5. After rinsing in TBS, sections were incubated in TBS++ for 1h, transferred into rat-anti-BrdU primary antibody (Harlan SeraLab, Loughborough, UK; at 1/500) in TBS++ and incubated overnight at 4°C on a rotating platform. On the second day, the sections were washed in TBS and incubated for 1h with a biotinylated donkey-anti-rat secondary antibody (Jackson, Hamburg, Germany; at 1/2000) in TBS++. After several rinses in TBS, the sections were incubated for 1h with avidin biotinylated peroxidase complex (Vector Elite Kit, Vector Laboratories, Wertheim, Germany; at 1/1000). Labeling was developed using a 0.05% solution of 3,3,8-diaminobenzidine, 0.01% H_2O_2, and 0.04% nickel chloride in TBS for 5 min. Sections were mounted, dehydrated and coverslipped using Neo Mount (Merck, Darmstadt, Germany). The brightfield immunohistochemical analysis was performed with a Leica DMR microscope equipped with a Spot CCD camera model 2.2.1 (Diagnostic Instruments, Michigan, USA).

Double/triple immunofluorescence labeling was performed to assess GFP expression of NPC and lentivirus transduced cells in the spinal cord, and the differentiation pattern of grafted adult NPC. The following primary antibodies were used: mouse-anti-nestin for uncommitted progenitor cells (clone 401, Pharmingen, Heidelberg, Germany; at 1/500), guinea pig-anti-NG2 for glial restricted precursor cells (; generous gift B. Stallcup, Burnham Institute, La Jolla, USA; at 1/200), mouse-anti-GFAP for astroglia (Chemicon, Hofheim, Germany; at 1/600), mouse-anti-APC that is directed against the N-terminal segment of APC for immature and mature astrocytes and oligodendrocytes [36] (Oncogene, Darmstadt, Germany; at 1/1000) and goat-anti-doublecortin for young neurons (Santa Cruz, Heidelberg, Germany; at 1/100), all visualized using Cy-5 linked donkey secondary antibodies (Jackson, Hamburg, Germany; at 1/1000). The BrdU-prelabeled grafted cells were identified with a rat-anti-BrdU antibody (Harlan SeraLab, Loughborough, UK; at 1/500) and visualized using Rhodamine-X linked donkey secondary antibodies (Jackson, Hamburg, Germany; at 1/1000). GFP expressing cells were visualized using a rabbit-anti-GFP antibody (Molecular Probes, Leiden, Netherlands; at 1/750) or a goat-anti-GFP antibody (Rockland Gilbertsville, PA; at 1/1500).

To identify BrdU prelabeled NPC sections were pretreated as described above followed by incubation with the primary antibodies in TBS++ overnight at 4°C on a rotating platform. The following day, sections were rinsed and incubated with fluorescence (rhodamine-X, fluorescein, Cy5) conjugated secondary antibodies made in donkey (Jackson, Hamburg, Germany; at 1/1000) in TBS++ for 2 h. After final rinsing steps in TBS, sections were mounted onto glass slides and coverslipped with ProLong Antifade Kit (Molecular Probes, Leiden, Netherlands). Immunohistochem-

ical analysis was performed with a confocal fluorescence microscope (Leica TCS-NT).

For the quantification of BrdU/GFP double-labeled cells, confocal micrographs containing the epicenter of the graft were taken at 40x magnification. From each animal, 3 independent image stacks were selected from different sections. Since GFP labeling in NPC was restricted to the injection site, cells were only quantified at the transplantation site. Therefore, between 15-20 optical sections through the z-axis of the 35 µm thick section were analyzed. Co-localization was confirmed once the GFP marker was spatially associated to the nuclear BrdU prelabeling through subsequent optical sections in the z-axis. BrdU positive cells and GFP/BrdU positive cells were counted from each animal to obtain a representative total count. Finally, the mean percentage of BrdU/GFP double labeled cells and the standard error of the mean (SEM) was calculated for each time point. Group comparisons were made using an analysis of variance followed by Tukey's post-hoc testing.

3. RESULTS

3.1 In vitro gene expression using the retroviral vector pCLE-GFP

Previously, we have shown that neural stem cells derived from the adult spinal cord can be transduced *in vitro* to express GFP using the retroviral vector pLXSN-GFP [13] (Fig. 1A). However, *in vivo* gene expression was lost in the majority of cells 21 days after transplantation into the adult injured spinal cord [13]. Because this loss in gene expression is likely due to the silencing of the LTR used to express the transgene, we investigated whether retroviral vectors with an internal promoter could increase the duration of gene expression. The retroviral vector pCLE-GFP derived from pCLE [26] contains a hybrid 5' LTR and an internal *Xenopus* EF1a enhancer/promoter to drive GFP expression (Fig. 1B). Adult spinal cord derived NPC were efficiently transduced and showed robust GFP expression after selection for G418 resistance. GFP expression was stable for at least 4 weeks over more than 5 passages *in vitro* after removal of G418 from the cell culture medium (Fig. 2A). To determine if differentiation of NPC results in a downregulation of transgene expression [37], NPC were cultivated in differentiation medium (NB medium, supplemented with B27 and 5% FCS; no G418) for up to 21 days [13, 35]. After 7 days of incubation in the differentiation medium, 99.2% ± 0.48 of the cells were GFP positive (Fig. 2B, 2I). Immunocytochemical staining showed that these cultures mainly contained beta III tubulin positive neuronal cells (13.4% ± 3.6, Fig. 2F, 2J) and GFAP positive astrocytes (31.3% ± 1.8, Fig. 2G, 2K). Only a small amount of GalC positive oligodendrocytes and A2B5 positive glial precursor cells could be identified (Fig. 2E, H). After 14 days of incubation in the differentiation medium, however, a considerable proportion of the pCLE-GFP transduced

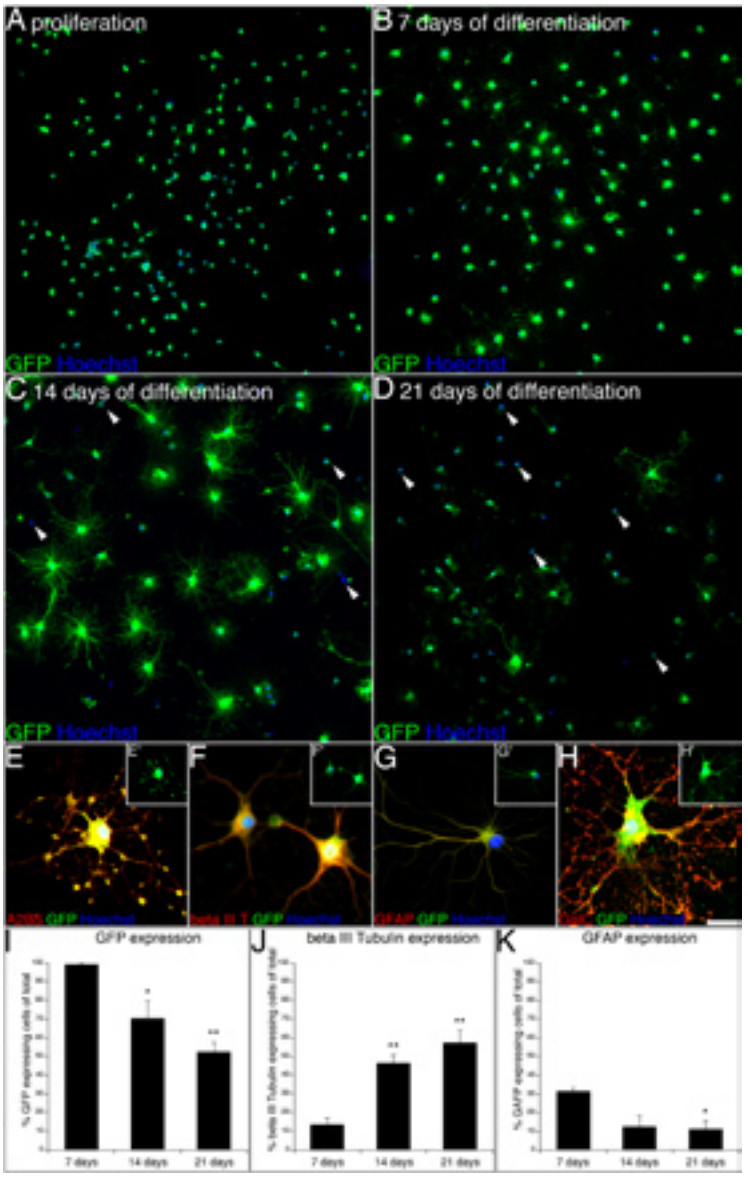

Figure 2: *In vitro analysis of NPC transduced with pCLE-GFP. (A) Under proliferation conditions and (B) after 7 days of cell culture under differentiation conditions virtually all NPC transduced with the retroviral vector pCLE-GFP expressed the reporter gene GFP (green). (C) After 14 days and (D) after 21 days of cell culture under differentiation conditions, many pCLE-GFP transduced NPC lost GFP expression (arrowheads). (E) Immunocytochemical analysis of the differentiated cells showed that A2B5 positive glial restricted progenitor cells, (F) beta III tubulin positive young neuronal cells, (G) GFAP positive astrocytes and (H) GalC positive oligodendrocytes could be found to express GFP (green) in vitro after 7 days of in vitro differentiation. All differentiation markers are shown in red. Hoechst 33342 was used as nuclear counterstain (blue). Epifluorescent micrographs, scale bar: 75 µm in (A-D), 20 µm in (E-H). (I) Bar graphs showing the proportion of GFP expressing cells, (J) beta III tubulin expressing young neurons and (K) GFAP expressing astrocytes of the total amount of cells present in the culture after 7, 14 and 21 days of in vitro differentiation (n=3, mean ± SEM, * p<0.05, ** p<0.01).*

NPC lost GFP expression, resulting in a significant reduction in GFP-labeled cells to 70.2% ± 9.4 ($p<0.05$; Fig. 2C, 2I). After 21 days of *in vitro* differentiation, the proportion of pCLE-GFP transduced NPC that still expressed GFP was further reduced to 52.4% ± 5.4 of the total amount of plated cells ($p<0.01$; Fig. 2D, 2I). The amount of beta III tubulin positive cells increased to 46.3% ± 4.5 at 14 days and to 57.2% ± 6.6 at 21 days of *in vitro* differentiation (Fig. 2J), whereas the amount of GFAP positive cells decreased to 12.4% ± 6.0 at 14 days and 11.0% ± 4.7 at 21 days (Fig. 2K). Only very few GalC positive oligodendrocytes and no A2B5 positive glial precursor cells could be identified at 14 and 21

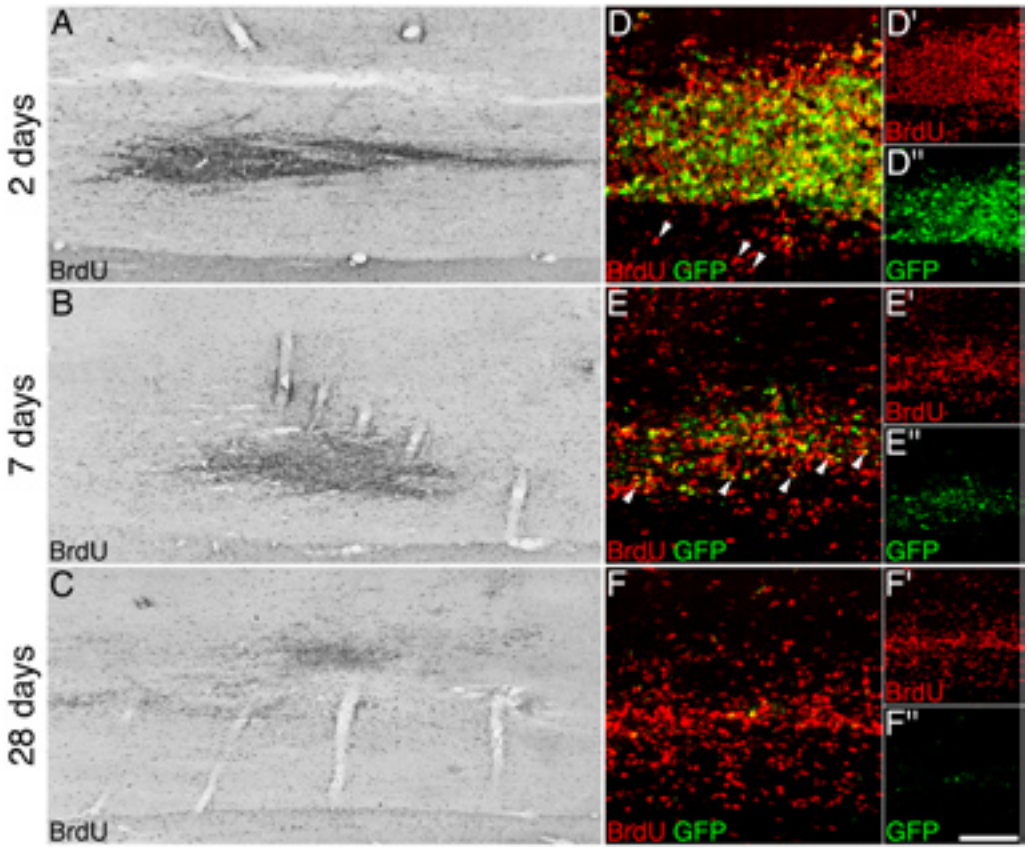

Figure 3: *Genetically modified NPC migrate in the spinal cord and lose transgene expression. (A) 2 days post-transplantation, the majority of the BrdU prelabeled NPC were concentrated in a cloud of cells at the injection site. (B) 7 days and (C) 28 days post-transplantation, many of the grafted cells migrated into the host parenchyma and were scattered in the host spinal cord. (D) Two days post-transplantation, GFP (green) could be detected in most of the BrdU prelabeled NPC (red) directly at the injection site. Cells that migrated away from the injection site had already downregulated GFP expression (arrowheads). (E) At 7 days post-grafting, the number of GFP expressing cells was further diminished, while many other cells expressed only very low levels of GFP (arrowheads, compare also D" with E"). (F) 28 days post-transplantation, GFP labeling had nearly disappeared. Scale bar: 250 µm in (A-C), 60 µm in (D), 80 µm in (E, F).*

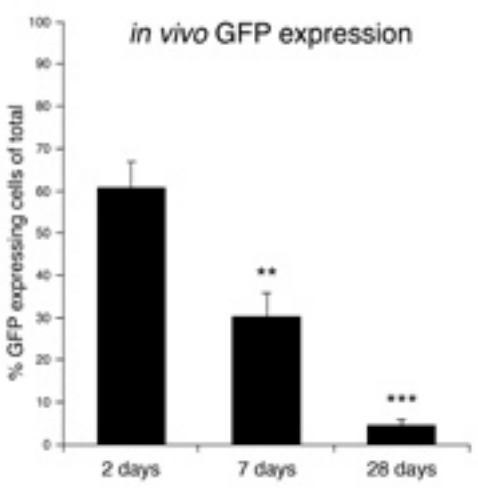

Figure 4: *Quantification of BrdU/GFP double-labeled cells in vivo. Bar graph showing the proportion of BrdU-labeled NPC that colocalize with GFP at the injection site. There is a significant reduction in the number of GFP-expressing cells over time. (n=3/time point, mean± SEM, ** p<0.01, *** p<0.001).*

days of *in vitro* differentiation. Because the proliferation of NPC ceases over the first 7 days of cultivation in differentiation medium, the observed decline in GFP expression was not due to the proliferation of non-transduced cells. Rather the percentage of GFP-labeled cells decreased over time as the proportion of cells expressing neuronal and glial differentiation markers increased.

3.2 In vivo gene expression in NPC grafted to the spinal cord

To investigate whether a similar degree and time course of transgene silencing would also occur *in vivo*, undifferentiated, pCLE-GFP-transduced NPC were labeled with BrdU and grafted to the intact spinal cord of adult rats. At 2 days, 7 days and 28 days post grafting, the spinal cord parenchyma of grafted animals contained many BrdU positive nuclei, indicating good survival of transplanted NPC (Fig. 3A-C). Two days post grafting, the majority of BrdU positive nuclei were localized in a compact cloud of cells at the transplantation site (Fig. 3A). Surrounding the graft epicenter, many BrdU positive nuclei resided in the spinal cord parenchyma at a lower density, suggesting that a fraction of the grafted cells had already migrated into the host parenchyma. At 7 days and 28 days after transplantation, the density of BrdU prelabeled nuclei at the graft epicenter decreased, and the majority of cells had migrated away from the transplantation site (Fig. 3B, C). Control animals injected with BrdU prelabeled NPC lysed by repeated freeze-thaw cycles prior to transplantation, or PBS used to wash the cells before grafting contained none or occasionally very few BrdU labeled nuclei. Thus, the BrdU positive cells in the spinal cord parenchyma of grafted animals originated from surviving, transplanted NPC.

Concomitant with the migration of NPC, expression of GFP was gradually lost (Fig. 3D-F). Two days post grafting, many BrdU/GFP double-labeled cells were detected at the graft epicenter (Fig. 3D). However, confocal analysis of BrdU positive cells residing outside the graft epicenter revealed that these cells almost completely downregulated GFP expression (Arrowheads, Fig. 3D). Quantification of BrdU/GFP double-labeled cells at the graft epicenter indicated that 60.8% ± 6.0 of the BrdU positive nuclei co-localized with the GFP reporter (Fig. 4). At 7 days

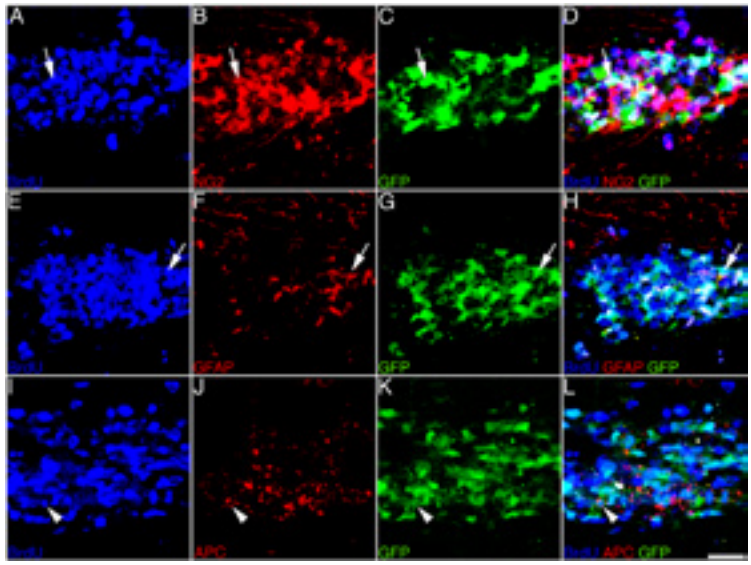

Figure 5: *GFP expression and differentiation of pCLE-GFP transduced NPC at 2 days after transplantation into the spinal cord. The differentiation pattern of grafted NPC was assessed by determining the co-localization of differentiation markers (red) with BrdU prelabeled nuclei of grafted cells (blue). (A-D) 2 days after transplantation, many grafted cells expressed the glial precursor cell marker NG2 (arrow). (E-H) Only very few grafted cells could be detected co-localizing with the astroglial marker GFAP (arrows) and (I-L) the mature glial marker APC (arrowhead). Only very few GFP expressing cells (green) could be found that co-localized with GFAP or APC (A-H, arrows). Confocal fluorescence micrographs, scale bar A-L 25 µm.*

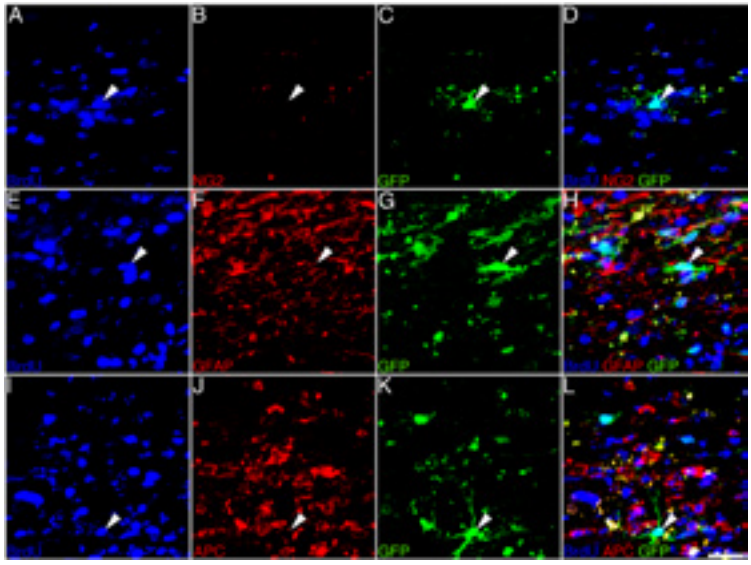

Figure 6: *GFP expression and differentiation of pCLE-GFP transduced NPC at 28 days after transplantation into the spinal cord. (A-D) At 28 days post grafting, no NG2 immunoreactivity could be detected that co-localized with the grafted NPC. However, most grafted cells differentiated into glial phenotypes, as indicated by (E-H) GFAP and (I-L) APC expression. Although many GFP labeled NPC displayed a complex morphology, almost none of these cells could be co-localized with the investigated phenotypical markers (arrowheads, D, H, L) Confocal fluorescence micrographs, scale bar A-L 25 µm.*

post grafting, the fraction of BrdU/GFP double labeled cells at the graft epicenter decreased to 30.3% ± 5.6 (Fig. 3E, Fig. 4) and many of the remaining BrdU/GFP double positive cells displayed only weak GFP expression levels (arrowheads, Fig. 3E). At 28 days post grafting, only 4.3% ± 1.5 BrdU/GFP double positive cells could be identified at the graft epicenter, indicating that the vast majority of pCLE-GFP-transduced NPC lost expression of the GFP reporter gene within 28 days after transplantation into the intact CNS (Fig. 3F, 4). Double-labeled cells were only quantified at the injection site, since cells migrating for long distances were never found to express GFP. Thus, the actual proportion of GFP/BrdU positive cells in the whole spinal cord was even lower than quantified in this study, especially at 7 and 28 days post-injection, when long distance migration of BrdU prelabeled cells could be observed.

To determine if the loss in gene expression was correlated to differentiation of NPC, colocalization studies of BrdU- and GFP-labeled cells with NG2, a marker for glial committed precursor cells [38] and the glial markers GFAP and APC were conducted. At 2 days post grafting, BrdU prelabeled pCLE-GFP-transduced NPC mainly expressed NG2 (Fig. 5A-D), few cells expressed GFAP (5E-H), and no BrdU-labeled cells co-labeled with APC (Fig. 5I-L). At 28 days post grafting, NG2 immunoreactivity had almost completely disappeared, while many of the grafted pCLE-GFP-transduced NPC differentiated into GFAP positive astrocytes (Fig. 6E-H) and APC positive glia (Fig. 6I-J). No immunoreactivity for the multipotent progenitor cell marker nestin [39] or for the early neuronal marker doublecortin [40] could be detected at any of the time-points investigated (data not shown). Strikingly, only a very small fraction of GFP/BrdU double-labeled cells could be co-localized with any of the glial or neuronal markers investigated (Arrows, Fig. 5A-D, E-H), suggesting that the vast majority of transduced NPC downregulated GFP expression upon or during differentiation. The few NPC that continued to express GFP at 28 days post transplantation displayed a highly complex morphology without detectable levels of any of the investigated differentiation markers (Arrowheads, Fig. 6D, H, L).

3.3 Lentiviral gene transfer

The studies described above indicated that the differentiation of NPC might be responsible for the discontinued gene expression in NPC transduced with MLV-based retroviral vectors. As lentiviral gene transfer into embryonic stem cells [28 41] and hematopoetic stem cells [42] has been shown to be stable after differentiation we tested the stability/duration of lentiviral gene expression in NPC. In parallel to findings with the retroviral vectors pLXSN-GFP and pCLE-GFP (see above), NPC transduced with the lentiviral vector pLV-GFP (Fig. 1C) showed stable *in vitro* GFP expression in proliferating cells (data not shown). Upon transplantation of pLV-GFP transduced NPC into the spinal cord however, gene expression declined

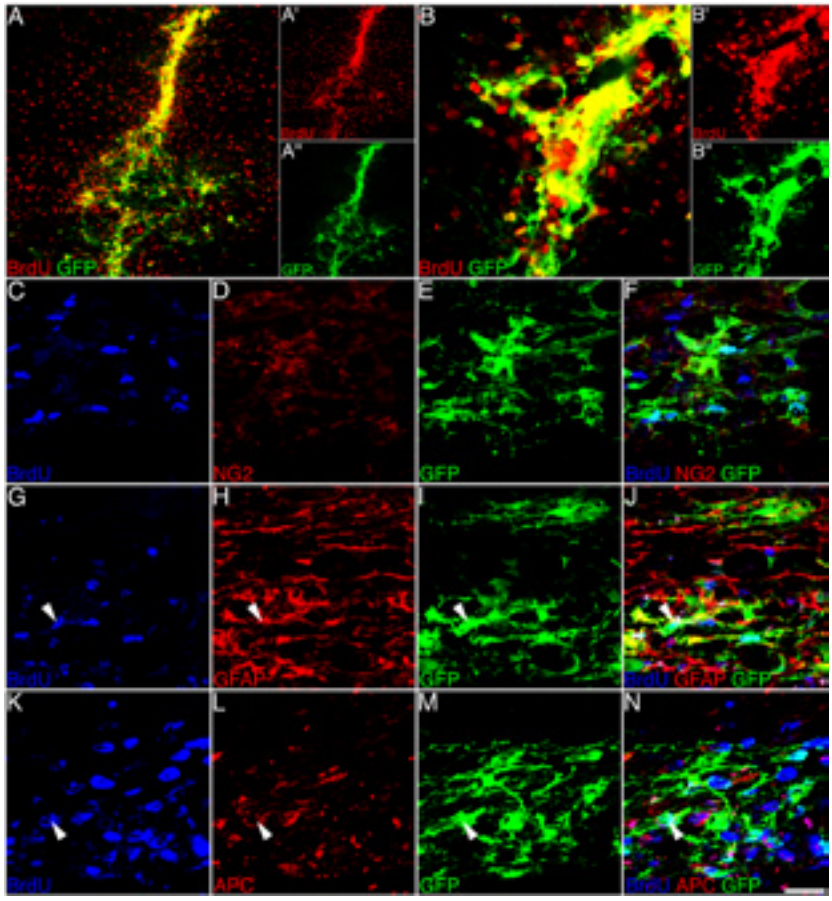

Figure 7: *GFP expression and differentiation of pLV-GFP transduced NPC at 28 days after transplantation into the spinal cord. (A, B) Although a larger proportion of lentivirus-transduced NPC continued to express GFP compared to MLV-retrovirus-transduced NPC, the majority of the grafted cells lost transgene expression 28 days after transplantation. (C-F) Similar to pCLE-GFP transduced NPC, no NG2 expressing grafted NPC could be found at 28 days post grafting, while most NPC differentiated into (G-J) GFAP expressing astroglia and (K-N) APC expressing mature glia. Only few GFP-labeled NPC could be colocalized with the investigated phenotypical marker (arrowheads, G-N). Confocal fluorescence micrographs, scale bar A 170 µm, B 32 µm, C-N 25 µm.*

to 29.2% ± 4.7 at 28 days post grafting around the injection site (Fig. 7A, B). As previously observed for pCLE-GFP transduced NPC, cells remaining close to the injection site were more likely to continue GFP expression than cells that migrated away from the transplantation site (Fig. 7A). Confocal analysis of grafted cells showed that almost no colocalization with the glial precursor cell marker NG2 could be observed at 28 days (Fig. 7C-F). Of the investigated glial differentiation markers, only a small fraction of GFP/BrdU-labeled cells colocalized with GFAP (arrowheads, Fig. 7G-J) or APC (arrowheads, Fig. 7K-N).

To determine if long-term GFP expression could be achieved in differentiated cells *in vivo*, and to exclude the possibility that im-

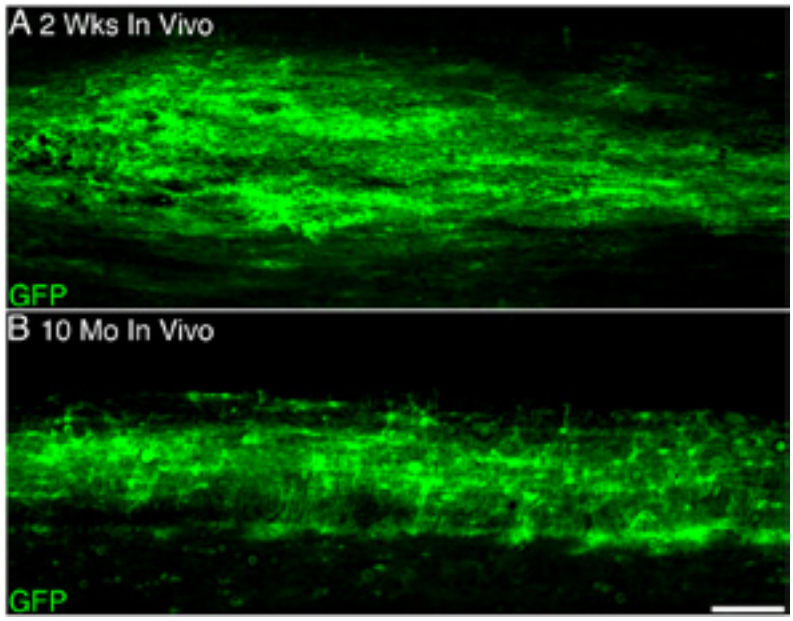

Figure 8: *GFP expression after direct injection of pLV-GFP virus into the intact rat spinal cord. (A) Direct injection of lentivirus resulted in high expression levels of transgene in the intact rat spinal cord 2 weeks post-injection. (B) No obvious changes in transgene expression level or number of expressing cells could be observed at 10 months post-injection. Epifluorescence micrographs, scale bar A, B 200 µm.*

mune responses to GFP expressing cells provided a selective survival advantage for cells that lost GFP expression, we injected the same lentiviral vectors expressing GFP into the spinal cord. Qualitative analysis of gene expression 14 days, 10 months and 16 months after virus injection indicated continued gene expression without any appreciable loss in the amount or number of GFP expressing cells (Fig. 8).

4. DISCUSSION

In the present study, we investigated transgene expression in adult rat NPC transduced to express GFP using retroviral and lentiviral vectors that have previously been described to be resistant to gene silencing in neural progenitor cells and stem cells [26, 28]. Our findings indicate that the viral vectors tested only allow for transient gene expression in adult NPC. *In vitro* differentiation of NPC and *in vivo* differentiation following transplantation to the adult spinal cord was paralleled by a rapid loss of GFP expression indicating a close relationship between NPC differentiation and transgene silencing. In contrast, direct *in vivo* injection of lentiviral vectors, resulted in stable GFP expression in both neurons and glia for up to 16 months.

The stable expression of transgenes in adult NPC represents an important prerequisite to assess and to enhance the regenerative capacity of NPC grafting to the CNS. The introduction of reporter genes such as GFP enables the visualization of grafted cells to study cell survival, integration and interaction with the host en-

vironment. Additionally, overexpression of specific genes could allow the differentiation of grafted NPC into regeneration promoting phenotypes thereby overcoming differentiation inducing cues in the microenvironment at the transplantation site [35, 43]. Finally, the intrinsic regenerative capacity of grafted NPC could be enhanced by overexpression of axonal growth and neuronal survival promoting factors [44, 45].

In vitro and *in vivo* loss of gene expression in our experiments could be due to the toxicity of GFP expression, selective survival advantages of cells that lose gene expression, elimination of grafted cells, or silencing of transgene expression previously described for many virally transduced cell types [46-48]. The first three possibilities seem highly unlikely for several reasons: 1) NPC cultivated *in vitro* under proliferation conditions continued to express GFP without any sign of toxicity or loss of gene expression; ; 2) direct injection of GFP expressing lentiviral vectors resulted in long-term stable gene expression for up to 16 months; 3) grafted cells could be identified in all animals using BrdU pre-labeling and 4) a decline in the number of GFP expressing cells was also observed *in vitro* in differentiating NPC.

Although the exact molecular basis of transgene silencing remains to be elucidated, DNA-methylation-dependent and -independent silencing mechanisms appear to play important roles [49]. Previous studies have shown that transgene silencing in stem/progenitor cells precedes methylation of newly integrated virus DNA. Whether this de novo methylation is a consequence of methylation-independent silencing or represents a redundant parallel pathway is unclear [27]. The dramatic gene silencing within 1 week post-grafting in the present experiments suggests that silencing factors other than the relatively slow acting DNA methylation play a significant role. Nevertheless, the development of viral vectors lacking CpG dinucleotides located in the LTR represents an important step in preventing methylation-dependent transgene silencing [24]. Inclusion of insulator elements, which are genomic sequences that function as expression boundaries, might also be able to reduce methylation-independent transgene silencing [25]. However, it remains to be determined whether insulators are also able to block the function of trans-acting retroviral silencers [50, 51].

Two of the viral vectors used in our studies have previously been described to be more resistant to stem cell specific transgene silencing compared to retroviral vectors expressing the transgene from the 5'LTR. The retroviral vector, pCLE-GFP, contains a hybrid 5' LTR in combination with an internal *Xenopus* EF-1alpha enhancer/promoter and has been shown to improve transgene expression after injection into the embryonic mouse CNS [26]. Our results did not indicate significant improvements in transgene expression using this viral vector. Differences between mouse and rat CNS progenitors, differences between adult and embryonic silencing mechanisms, or differences in the multiplicity of infection might have contributed to the observed lack of extended

gene expression.

The tested lentiviral vector pLV-GFP reported to be resistant to stem cell specific silencing in murine ES cells [28] only resulted in a slightly higher number of transgene expressing NPC close to the injection site. Lack of gene silencing in lentivirus-transduced ES cells has been attributed to the deletion of enhancer/promoter regions in the LTR regions of the virus construct and intrinsic resistance to long-term DNA methylation-dependent silencing of human derived lentiviral vectors in murine cells [28]. Whether this viral vector is sufficient to induce stable transgene expression in rat stem cells has not been investigated. The observed differences could therefore be due to cell-specific or species-specific differences. Recent studies in lentivirus-transduced embryonic rat NPC using an internal mouse phosphoglycerate kinase 1 promoter have observed a similar decline in gene expression [52].

Consistent with previous reports [13, 17], NPC grafted to the spinal cord differentiated rapidly into glial lineages. NG2 expressing BrdU-labeled cells however could only be detected at 2 days post-injection. Cells that continued to express GFP 7 and 28 days post-grafting typically resided close to the graft epicenter, similar to retrovirus-transduced NPC grafted to the striatum of hemiparkinsonian rats [23]. Strikingly, a lack of GFP expression in cells that migrated away from the injection site could be observed as early as 2 days post transplantation, indicating that migration of the grafted cells closely correlates with the silencing of transgene expression. Although some GFP expressing cells displayed highly complex morphologies at 4 weeks post transplantation, only relatively few GFP expressing cells could reliably be co-localized with the tested differentiation markers, confirming earlier observations [23].

In summary, the viral vectors investigated in the present experiments can only be employed to induce transient gene expression in rat NPC. Studies using viral vectors to introduce transgenes into NPC have to be carefully controlled for transgene expression levels throughout the entire experiment as only a specific subset of cells might continue to express the gene of interest. To accomplish stable transgene expression in adult rat NPC, viral vectors need to be developed that are both resistant to methylation-dependent and -independent silencing mechanisms. Viral vectors that can also persist without integration into the host cell genome, such as adeno-associated viruses, might be able to at least partially overcome stem cell specific silencing in stem/progenitor cells [53]. Whereas expression of reporter genes, survival promoting factors in chronic neurodegenerative diseases, and genes to correct genetic deficiencies are generally sought to be long-lasting, a loss of gene expression that is correlated to cell differentiation as observed in the current experiments might be ideal to express genes necessary for the phenotypical specification of stem and progenitor cells.

5. ACKNOWLEDGMENTS

This work was supported by the Institute International de Recherche en Paraplégie Geneva, on behalf of an anonymous donation, Deutsche Forschungsgemeinschaft (WE 2165), Bavaria California Technology Center, ReForM-Program, University of Regensburg, School of Medicine to N.W. and the Paralysis Project, Christopher Reeve Paralysis Foundation, NIH/NINDS (5R21NS046466) and International Spinal Research Trust to A.B. We thank Massimiliano Caioni for excellent technical assistance and Ulrich Bogdahn for his continued support and critical comments. We also thank Bill Stallcup for the NG2 antibody.

6. REFERENCES

1. Yoshimoto, Y. et al. Astrocytes retrovirally transduced with BDNF elicit behavioral improvement in a rat model of Parkinson's disease. Brain Res 691, 25-36 (1995).
2. Levivier, M., Przedborski, S., Bencsics, C. & Kang, U. J. Intrastriatal implantation of fibroblasts genetically engineered to produce brain-derived neurotrophic factor prevents degeneration of dopaminergic neurons in a rat model of Parkinson's disease. J Neurosci 15, 7810-20 (1995).
3. Tuszynski, M. H., Roberts, J., Senut, M. C., U, H. S. & Gage, F. H. Gene therapy in the adult primate brain: intraparenchymal grafts of cells genetically modified to produce nerve growth factor prevent cholinergic neuronal degeneration. Gene Ther 3, 305-14 (1996).
4. Nakahara, Y., Gage, F. H. & Tuszynski, M. H. Grafts of fibroblasts genetically modified to secrete NGF, BDNF, NT-3, or basic FGF elicit differential responses in the adult spinal cord. Cell Transplant 5, 191-204 (1996).
5. Grill, R. J., Blesch, A. & Tuszynski, M. H. Robust growth of chronically injured spinal cord axons induced by grafts of genetically modified NGF-secreting cells. Exp Neurol 148, 444-52 (1997).
6. Kobayashi, N. R. et al. BDNF and NT-4/5 prevent atrophy of rat rubrospinal neurons after cervical axotomy, stimulate GAP-43 and Talpha1-tubulin mRNA expression, and promote axonal regeneration. J Neurosci 17, 9583-95 (1997).
7. Liu, Y. et al. Transplants of fibroblasts genetically modified to express BDNF promote regeneration of adult rat rubrospinal axons and recovery of forelimb function. J Neurosci 19, 4370-87 (1999).
8. Blesch, A. & Tuszynski, M. H. Cellular GDNF delivery promotes growth of motor and dorsal column sensory axons after partial and complete spinal cord transections and induces remyelination. J Comp Neurol 467, 403-17 (2003).
9. Tuszynski, M. H. et al. NT-3 gene delivery elicits growth of chronically injured corticospinal axons and modestly improves functional deficits after chronic scar resection. Exp Neurol 181, 47-56 (2003).
10. Weidner, N., Blesch, A., Grill, R. J. & Tuszynski, M. H. Nerve growth factor-hypersecreting Schwann cell grafts augment and guide spinal cord axonal growth and remyelinate central nervous system axons in a phenotypically appropriate manner that correlates with expression of L1. J Comp Neurol 413, 495-506 (1999).
11. Falk, A. et al. Gene delivery to adult neural stem cells. Exp Cell Res 279, 34-9 (2002).
12. Horner, P. J. & Gage, F. H. Regenerating the damaged central nervous system. Nature 407, 963-70 (2000).
13. Vroemen, M., Aigner, L., Winkler, J. & Weidner, N. Adult neural progenitor cell grafts survive after acute spinal cord injury and integrate along axonal pathways. Eur J Neurosci 18, 743-51 (2003).
14. Pfeifer, K., Vroemen, M., Caioni, M. & Weidner, N. Feasibility of autologous adult neural progenitor cell

transplantation into the chronically injured rat spinal cord. Soc Neurosci Abs (2003).
15. Sanai, N. et al. Unique astrocyte ribbon in adult human brain contains neural stem cells but lacks chain migration. Nature 427, 740-4 (2004).
16. Wachs, F. P. et al. High efficacy of clonal growth and expansion of adult neural stem cells. Lab Invest 83, 949-62 (2003).
17. Pfeifer, K., Vroemen, M., Blesch, A. & Weidner, N. Adult neural progenitor cells provide a permissive guiding substrate for corticospinal axon growth following spinal cord injury. Eur J Neurosci 20, 1695-704 (2004).
18. Hofstetter, C. P. et al. Allodynia limits the usefulness of intraspinal neural stem cell grafts; directed differentiation improves outcome. Nat Neurosci 8, 346-53 (2005).
19. Steffen, D. & Weinberg, R. A. The integrated genome of murine leukemia virus. Cell 15, 1003-10 (1978).
20. Naldini, L. et al. In vivo gene delivery and stable transduction of nondividing cells by a lentiviral vector. Science 272, 263-7 (1996).
21. Tanigaki, K. et al. Notch1 and Notch3 instructively restrict bFGF-responsive multipotent neural progenitor cells to an astroglial fate. Neuron 29, 45-55 (2001).
22. Jahner, D. et al. De novo methylation and expression of retroviral genomes during mouse embryogenesis. Nature 298, 623-8 (1982).
23. Dziewczapolski, G., Lie, D. C., Ray, J., Gage, F. H. & Shults, C. W. Survival and differentiation of adult rat-derived neural progenitor cells transplanted to the striatum of hemiparkinsonian rats. Exp Neurol 183, 653-64 (2003).
24. Swindle, C. S., Kim, H. G. & Klug, C. A. Mutation of CpGs in the murine stem cell virus retroviral vector long terminal repeat represses silencing in embryonic stem cells. J Biol Chem 279, 34-41 (2004).
25. Pannell, D. & Ellis, J. Silencing of gene expression: implications for design of retrovirus vectors. Rev Med Virol 11, 205-17 (2001).
26. Gaiano, N., Kohtz, J. D., Turnbull, D. H. & Fishell, G. A method for rapid gain-of-function studies in the mouse embryonic nervous system. Nat Neurosci 2, 812-9 (1999).
27. Pannell, D. et al. Retrovirus vector silencing is de novo methylase independent and marked by a repressive histone code. Embo J 19, 5884-94 (2000).
28. Pfeifer, A., Ikawa, M., Dayn, Y. & Verma, I. M. Transgenesis by lentiviral vectors: lack of gene silencing in mammalian embryonic stem cells and preimplantation embryos. Proc Natl Acad Sci U S A 99, 2140-5 (2002).
29. Lois, C., Hong, E. J., Pease, S., Brown, E. J. & Baltimore, D. Germline transmission and tissue-specific expression of transgenes delivered by lentiviral vectors. Science 295, 868-72 (2002).
30. Naviaux, R. K., Costanzi, E., Haas, M. & Verma, I. M. The pCL vector system: rapid production of helper-free, high-titer, recombinant retroviruses. J Virol 70, 5701-5 (1996).
31. Zufferey, R. et al. Self-inactivating lentivirus vector for safe and efficient in vivo gene delivery. J Virol 72, 9873-80. (1998).
32. Follenzi, A., Ailles, L. E., Bakovic, S., Geuna, M. & Naldini, L. Gene transfer by lentiviral vectors is limited by nuclear translocation and rescued by HIV-1 pol sequences. Nature Genetics 25, 217-22 (2000).
33. Niwa, H., Yamamura, K. & Miyazaki, J. Efficient selection for high-expression transfectants with a novel eukaryotic vector. Gene 108, 193-9. (1991).
34. Dull, T. et al. A third-generation lentivirus vector with a conditional packaging system. J Virol 72, 8463-71. (1998).
35. Shihabuddin, L. S., Horner, P. J., Ray, J. & Gage, F. H. Adult spinal cord stem cells generate neurons after transplantation in the adult dentate gyrus. J Neurosci 20, 8727-35 (2000).
36. Horner, P. J. et al. Proliferation and differentiation of progenitor cells throughout the intact adult rat

spinal cord. J Neurosci 20, 2218-28 (2000).
37. Lindemann, C. et al. Down-regulation of retroviral transgene expression during differentiation of progenitor-derived dendritic cells. Exp Hematol 30, 150-7 (2002).
38. Nishiyama, A. NG2 cells in the brain: a novel glial cell population. Hum Cell 14, 77-82 (2001).
39. Reynolds, B. A., Tetzlaff, W. & Weiss, S. A multipotent EGF-responsive striatal embryonic progenitor cell produces neurons and astrocytes. J Neurosci 12, 4565-74 (1992).
40. Brown, J. P. et al. Transient expression of doublecortin during adult neurogenesis. J Comp Neurol 467, 1-10 (2003).
41. Gropp, M. et al. Stable genetic modification of human embryonic stem cells by lentiviral vectors. Mol Ther 7, 281-7 (2003).
42. Biffi, A. et al. Correction of metachromatic leukodystrophy in the mouse model by transplantation of genetically modified hematopoietic stem cells. J Clin Invest 113, 1118-29 (2004).
43. Han, S. S., Kang, D. Y., Mujtaba, T., Rao, M. S. & Fischer, I. Grafted lineage-restricted precursors differentiate exclusively into neurons in the adult spinal cord. Exp Neurol 177, 360-75 (2002).
44. Lu, P., Jones, L. L., Snyder, E. Y. & Tuszynski, M. H. Neural stem cells constitutively secrete neurotrophic factors and promote extensive host axonal growth after spinal cord injury. Exp Neurol 181, 115-29 (2003).
45. Himes, B. T. et al. Transplants of cells genetically modified to express neurotrophin-3 rescue axotomized Clarke's nucleus neurons after spinal cord hemisection in adult rats. J Neurosci Res 65, 549-64 (2001).
46. Palmer, T. D., Rosman, G. J., Osborne, W. R. & Miller, A. D. Genetically modified skin fibroblasts persist long after transplantation but gradually inactivate introduced genes. Proc Natl Acad Sci U S A 88, 1330-4 (1991).
47. Challita, P. M. & Kohn, D. B. Lack of expression from a retroviral vector after transduction of murine hematopoietic stem cells is associated with methylation in vivo. Proc Natl Acad Sci U S A 91, 2567-71 (1994).
48. Gram, G. J., Nielsen, S. D. & Hansen, J. E. Spontaneous silencing of humanized green fluorescent protein (hGFP) gene expression from a retroviral vector by DNA methylation. J Hematother 7, 333-41 (1998).
49. Cherry, S. R., Biniszkiewicz, D., van Parijs, L., Baltimore, D. & Jaenisch, R. Retroviral expression in embryonic stem cells and hematopoietic stem cells. Mol Cell Biol 20, 7419-26 (2000).
50. Modin, C., Pedersen, F. S. & Duch, M. Lack of shielding of primer binding site silencer-mediated repression of an internal promoter in a retrovirus vector by the putative insulators scs, BEAD-1, and HS4. J Virol 74, 11697-707 (2000).
51. Hino, S., Fan, J., Taguwa, S., Akasaka, K. & Matsuoka, M. Sea urchin insulator protects lentiviral vector from silencing by maintaining active chromatin structure. Gene Ther 11, 819-28 (2004).
52. Ostenfeld, T. et al. Neurospheres modified to produce glial cell line-derived neurotrophic factor increase the survival of transplanted dopamine neurons. J Neurosci Res 69, 955-65 (2002).
53. Wu, P., Ye, Y. & Svendsen, C. N. Transduction of human neural progenitor cells using recombinant adeno-associated viral vectors. Gene Ther 9, 245-55 (2002).

Chapter 6

In vivo high resolution MRI of neuropathological changes in the injured rat spinal cord

Am. J. Neuroradiol. in press

Thomas Weber[#]
Maurice Vroemen[#]
Volker Behr
Thomas Neuberger
Peter Jakob
Axel Haase
Gerhard Schuierer
Ulrich Bogdahn
Cornelius Faber
Norbert Weidner
[#] These authors contributed equally to this work.

ABSTRACT

Magnetic resonance imaging (MRI) is the most comprehensive means to assess structural changes in injured central nervous system (CNS) tissue in humans non-invasively over time. The few published *in vivo* MRI studies of spinal cord injury in rodent models using field strengths up to 7 T suffer from low spatial resolution, flow, and motion artifacts. The aim of this study was to assess the capacity of a 17.6 T imaging system to detect pathological changes occurring in a rat spinal cord contusion injury model *ex vivo* and *in vivo*. Therefore seven adult female Fischer 344 rats received a contusion injury at thoracic level Th 10, which caused a severe and reproducible lesion of the injured spinal cord parenchyma. From 2 to 58 days post-injury, high-resolution MRI was performed *ex vivo* (n=2) or *in vivo* in anesthetized rats (n=5 spinal cord injured + 1 intact control animal) using 2D multi-slice spin and gradient echo imaging sequences, respectively, combined with electrocardiogram triggering and respiratory gating. The acquired images provided excellent resolution and gray/white matter differentiation without significant artifacts. Signal changes, which were detected with *ex vivo* and *in vivo* MRI following spinal cord injury, could be correlated with histologically defined structural changes such as edema, fibroglial scar and hemorrhage. These results demonstrate that MRI at 17.6 T allows high-resolution structural analysis of spinal cord pathology after injury.

1. INTRODUCTION

Magnetic resonance imaging (MRI) represents a powerful means to non-invasively visualize pathomorphological changes in humans following spinal cord injury [1, 2]. MRI findings correlate with histopathological sequela observed after spinal cord injury such as edema, hemorrhage and secondary degenerative changes such as cyst formation. Moreover, MRI allows to predict the severity of neurological deficits after spinal cord injury [3]. On an experimental level, regenerative strategies have been validated in animal models of spinal cord injury, which promote functional and structural recovery. In particular, cell based transplantation strategies hold great promise in regenerating the injured spinal cord [4-10]. Ultrastructural restoration in animals is primarily assessed by post mortem microscopical analysis of spinal cord parenchyma. In order to be able to monitor regenerative strategies in clinical applications, non-invasive imaging techniques are mandatory. Only animal studies allow the direct correlation of in vivo MRI data with histological post mortem data as a prerequisite for proper interpretation of MRI findings in human studies after therapeutic interventions. Anatomical structures that must be resolved in mice or rats are five to ten times smaller than in humans. This implies that volume elements in imaging data are smaller by a factor of roughly 100 to 1000. MRI studies of the spinal cord of rodent models, wide-

ly used to assess the efficacy of regenerative strategies following spinal cord injury, require a sufficiently high signal-to-noise ratio (SNR) in order to resolve small-scale structures with satisfactory contrast. Furthermore, respiratory motion and blood flow may induce image artifacts. Structural changes occurring after spinal cord injury such as edema, cystic defects, atrophy and hemorrhage have been detected in several MRI based in vivo studies. [11-18] [19]. However, partial volume effects resulting from a lower spatial resolution in these studies reduced the reliability to exactly allocate and interpret signal changes seen with MRI. Furthermore, studies demonstrating an acceptable spatial resolution employed implantable coils, which as opposed to surface coils require an additional invasive procedure. In the present study, we investigated, whether high field MRI at 17.6 T would allow superior spatial resolution and thus improved detection of structural changes in the adult rat spinal cord following a defined contusion injury ex vivo and in vivo.

2. MATERIALS AND METHODS

2.1 Animals

The spinal cord injury and imaging experiments were conducted using young adult female Fisher 344 rats (n=8) weighing 160-180g. *Ex vivo* MRI was performed in 2 spinal cord injured animals, *in vivo* MRI in 5 spinal cord injured (Table 1) and 1 uninjured rat. All experiments were carried out in accordance with the European Communities Council Directive (86/609/EEC) and institutional guidelines for animal care. All efforts were made to minimize the number of animals used, as wells as their suffering.

2.2 Surgical procedures

For the surgical procedure animals underwent anesthesia made up of a mixture of ketamine (62.5mg/kg body weight; WDT, Garbsen, Germany), xylazine (3.175mg/kg body weight; WDT, Garbsen, Germany) and acepromazine (0.625mg/kg body weight, Sanofi-Ceva, Düsseldorf, Germany) in 0.9% sterile saline solution. Rats received spinal cord contusion injuries using the Infinite Horizon (IH) spinal cord injury device (Precision Systems & Instrumentation, Lexington, USA) as previously described [20]. A laminectomy was performed at thoracic level Th 10 to expose the dorsal portion of the spinal cord. The animals were suspended by attaching Adson forceps to the rostral Th 9 and caudal Th 11 vertebral bodies. Particular care was taken to align the exposed spinal cord perpendicular to the axis of the Impactor. The 2.5 mm stainless steel impounder tip was lowered to approximately 3–4 mm above the surface of the exposed spinal cord. The contusion injury was finally induced by applying an impact force of 2 Newton (equals 200 kilodyne) to the exposed spinal cord at a velocity of 130 mm/sec. Overlying muscle layers were sutured and the skin was closed. Postoperatively, animals were kept warm, placed on beds of sawdust and given manual bladder evacuation twice per day for a period of up to 10 days as necessary and received intramuscular injections of 10

mg Cotrimoxazol (Ratiopharm, Ulm, Germany) once daily for a period of 10 days. Animals regained automatic neurogenic bladder function after 5 to 10 days.

2.3 MR scanner

All MR imaging experiments were conducted on a vertical Bruker 750 wide bore magnet system (Bruker Biospin, Rheinstetten, Germany) at 17.6 T with a bore size of 89 mm.

2.4 In vivo MR imaging

Anesthesia was induced by inhalation of 4% isoflurane and maintained with 2% isoflurane in carbogen (95% oxygen and 5% carbon dioxide). Body temperature was maintained by heating the gradient cooling unit to 37 ± 2°C.

A total of 5 rats underwent in vivo MRI between 2 and 58 days after thoracic spinal cord contusions were applied (Table 1). An uninjured rat with an intact spinal cord served as control. An animal gradient system with 57 mm inner diameter and 0.2 T/m was used. Due to space restrictions within the gradient system, imaging of the rat spinal cord in wide bore magnets was not possible with commercially available hardware. Therefore, a probehead and surface coil were custom-built to provide maximum space for adult rats as described [21]. The surface coil was designed as a transmit-receive coil in a half-cylindrical carrier mounted on an optimized probebase. The probebase included balancing units (baluns), which are important at higher frequencies due to the increased sensitivity of the electrical setup to imbalances.

To avoid artifacts caused by blood flow and respiratory motion a triggering unit (RAPID Biomedical, Wuerzburg, Germany) for combined electrocardiogram (ECG) triggering and respiratory gating was used.

A multi-slice 2D spoiled gradient echo sequence was used with a TE around 4 ms, depending on the exact spatial resolution used, and a TR around 200 ms depending on the heart rate. Up to 9 slices were acquired per scan. Using surface coils, gradient echo sequences are advantageous for transmission, as they are far less sensitive to radio frequency (RF) inhomogenities. Two interleaved multi-slice data sets were acquired to cover a full 3D volume. The spatial resolution was at least 78 x 78 µm in-plane with a slice thickness of 370 µm in axial slices and 156 x 98 µm in-plane with a slice thickness of 370 µm in sagittal slices. Each series took between 15 and 20 minutes.

2.5 Ex vivo MR imaging

For ex vivo MRI, one animal was perfused at 2 weeks and another animal at 4 weeks after the contusion injury with 150 ml cold 0.1 M phosphate buffered saline (PBS) followed by 400 ml 4% paraformaldehyde in PBS. Spinal cords were removed and post-fixed overnight in 4% paraformaldehyde in PBS and then left for 1 day in PBS containing 30% sucrose at 4°C. This fixation procedure is required for the histological evaluation following ex vivo MRI. For the actual imaging process, spinal cord specimens were transferred into 5 mm wide

Table 1: *Time table of in vivo MRI scans for each individual animal.*

animal #	1. MRI scan (days post-injury)	2. MRI scan (days post-injury)	3. MRI scan (days post-injury)	Histology
1	18	25	39	no[1]
2	18	25	39[3]	no[1]
3	6	38	58	no[1]
4	2	38	--	yes[2]
5	2	13[4]	58[5]	yes[2]

[1] animals died during or shortly after last MRI scanning procedure.

[2] animals sacrified one day after the last MRI scan.

[3] illustrated in Fig. 5

[4] illustrated in Fig. 4A-C

[5] illustrated in Fig. 4D-F

NMR tubes (Wilmad, Buena, NJ, USA) filled with PBS containing 30% sucrose. Air bubbles were removed from the tube using a vacuum pump and leaving each sample at a pressure of approximately 50 mbar for around 10 minutes.

A gradient system with 1 T/m and an inner diameter of 40 mm was used with a commercial 5 mm linear birdcage resonator as transmit- and receive coil. The sample was kept at 20±1°C during imaging experiments.

Positioning of the sample was performed using a 3D low-resolution gradient echo sequence. A 2D multi-slice spin echo with an echo time (TE) of 7.5 ms, a repetition time (TR) of 2 s, 24 signal averages (NA), and a total scan time 3.5h was used. With a field of view (FOV) of 6 x 6 mm and an acquisition matrix of 256 x 256, the spatial resolution was 23 x 23 µm in-plane with a slice thickness of 300 µm. A total of 30 slices was acquired in axial direction and 14 slices in sagittal direction.

2.6 Histology

Animals were transcardially perfused with a 0.9% saline solution followed by 4% paraformaldehyde in PBS 2 days after the final in vivo MRI. The spinal cords were removed, postfixed overnight in 4% paraformaldehyde in PBS and left for one day in PBS containing 30% sucrose. Sagittal 35 µm thick sections of the thoracic spinal cord containing the injured area were cut with a cryostat. Every seventh section was mounted immediately on glass slides for Nissl staining. In the remaining sections, Prussian blue staining and light level immunohistochemistry was performed for a more detailed morphological analysis of the contused spinal cord tissue. Prussian blue staining, which was employed to detect hemosiderin deposits, was performed as follows: sections mounted on gelatin coated slides were immersed in a solution of 4% potassium ferrocyanide and 4% HCl for 15 min. After several rinses sections were counterstained with Vector Nuclear Fast Red solution (Linaris, Wertheim, Germany) for 5 min and dehydrated before coverslip-

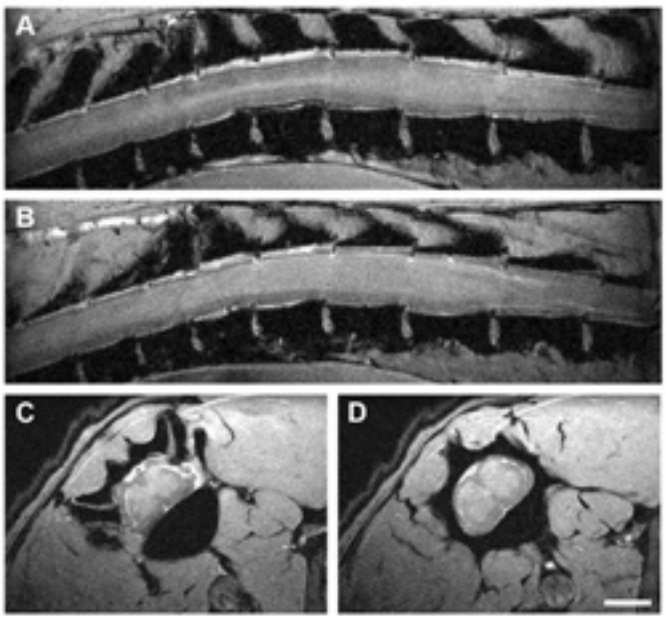

Figure 1: *In vivo MRI of intact spinal cord at 17.6 T.* A,B *show sagittal scans through the thoracic spinal cord. Acquisition parameters: slice thickness 239 µm, FOV 40 x 30 mm, in plane resolution 156 x 117 µm, TR approx. 200 ms (depending on heart rate), TE 4.4 ms.* C,D *display axial scans through the thoracic spinal cord. Acquisition parameters: slice thickness 500 µm, FOV 17.7 x 35.5 mm, in plane resolution 69x69 µm, TR and TE as above. Scale bar 2 mm (A) A more lateral sagittal scan depicts primarily white matter (lower signal) with some longitudinally oriented more hyperintense structure, reflecting the gray matter of the lateral ventral horn. Cerebrospinal fluid appears hyperintense, vertebral bodies are hypointense. (B) Most of the spinal cord parenchyma displayed here represents gray matter (hyperintense) surrounded by white matter tracts (hypointense) in a paramedian sagittal scan through the spinal cord. (C) An axial scan through the thoracic spinal cord allows the clear distinction between the typical butterfly appearance of the spinal cord gray matter and the surrounding hypointense white matter. Also of note, spinal roots can be clearly identified at this level. (D) A subsequent scan more caudally shows the spinal cord in cross-section away from the spinal root entry zone.*

ping with Neo Mount (Merck, Darmstadt, Germany). For immunohistochemistry, the following primary antibodies were used: mouse-anti-GFAP (for astrogliosis; DAKO, Glostrup, Denmark; at 1/2000), goat-anti-collagen type III (for the fibrous scar; Southern Biotechnology, Birmingham, USA, at 1/100) and mouse anti-rat monocytes/macrophages (clone ED1; Chemicon, Hofheim, Germany, at 1/1000). The sections were blocked in TBS + 3% donkey serum + 0.1% Triton-X, and incubated with the primary antibody in TBS + 3% donkey serum + 0.1% Triton-X overnight at 4°C on a rotating platform. The following day, sections were incubated with the secondary antibody (biotinylated donkey IgG, Jackson, Hamburg, Germany; at 1/1000) in TBS containing 3% donkey serum + 0.1% Triton-X. Sections were incubated with avidin-biotinylated-peroxidase complex (Vector Elite kit; Linaris, Wertheim, Germany) followed by development for 3–15 min in a 0.05% solution of 3,3'-diaminobenzi-

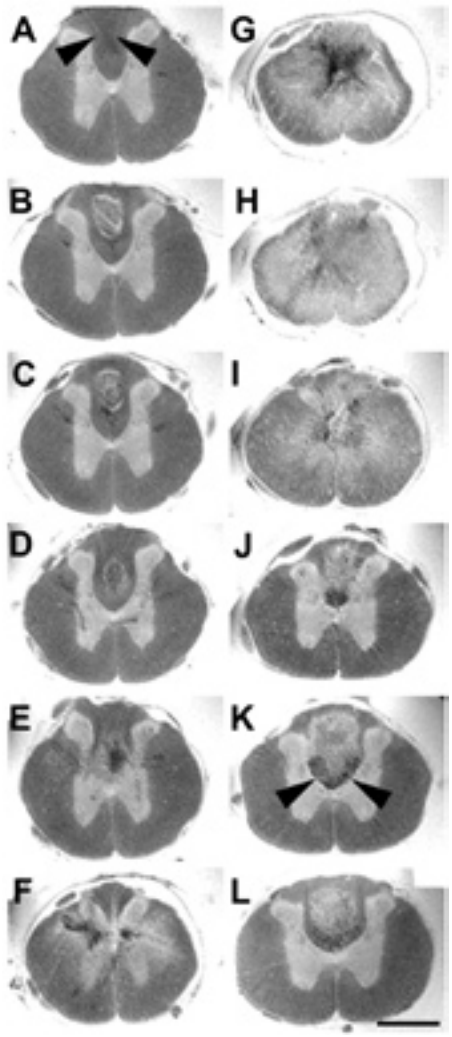

Figure 2: *Axial ex vivo MRI scans of contused rat spinal cord. Axial slices of ex vivo MRI show microscopy grade visualization of morphological changes in the injured rat spinal cord 4 weeks after contusion injury at midthoracic level. Acquisition parameters: 2D multi-slice spin echo, slice thickness 300 µm, FOV 6x6 mm, in plane resolution 23 x 23 µm, TE 7.5 ms, TR 2 s. Scale bar 1 mm.* A-L *show consecutive sections in the rostral-caudal direction. In rats the dorsal columns contain not only ascending proprioceptive projections, which are located in the dorsal half of the dorsal column. The crossed corticospinal tract projects in the ventral half of the dorsal columns, unlike humans, where the majority of corticospinal axons are located in the lateral columns. (A-F) In sections rostral to the contusion site, the spinal cord morphology is still maintained with a clear differentiation of white and gray matter. Note the loss of signal in the dorsal part of the dorsal columns (arrowheads) identical with ascending proprioceptive projections. (G-I) At the lesion center, the spinal cord diameter is reduced, and gray and white matter can no longer be separated. Hypointensities located in the center (G) reflect hemosiderin deposits. (J-L) Caudal to the lesion, the gray-white matter contrast is preserved. Both in rostral and caudal scans (B-D,J-L) hyperintense signals are found in the dorsal columns consistent with cystic defects (see also Fig. 3). Hypointensities in axial scans rostral to the lesion correspond to ascending sensory projections, whereas in caudal scans they represent the area of the corticospinal tract (J-L; arrowheads).*

dine (DAB), 0.01% H_2O_2 and 0.04% nickel chloride in TBS yielding a brown-black reaction product. Sections were mounted onto gelatin-coated glass slides, air-dried, dehydrated and coverslipped with Neo Mount (Merck, Darmstadt, Germany). The histological analysis was performed using a Leica DMR microscope equipped with a Spot CCD camera model 2.2.1 (Diagnostic Instruments, Michigan, USA).

3. RESULTS

3.1 In vivo MRI of intact spinal cord

Gradient echo MRI with ECG triggering and respiratory gating yielded high resolution images of intact thoracic rat spinal cord in vivo without significant motion artifacts (Fig. 1). The typical butterfly-shaped gray matter could be clearly distinguished from the less intense surrounding white matter axonal tracts. The cerebrospinal fluid surrounding the spinal cord appeared as a small hyperintense rim adjacent to the

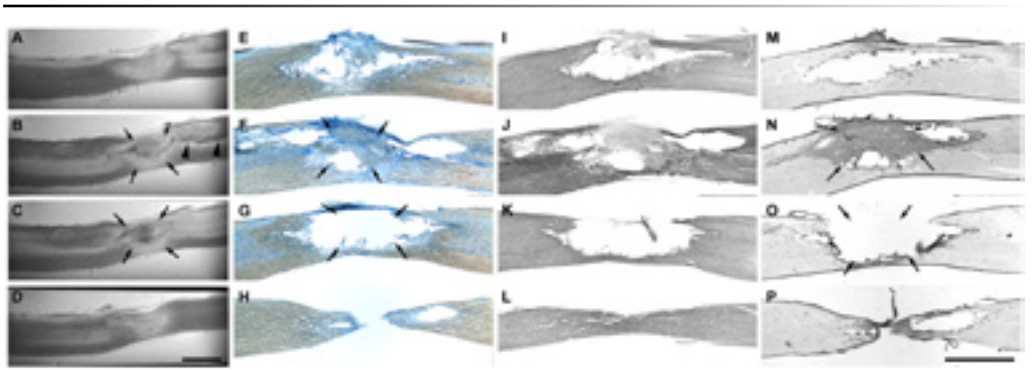

Figure 3: *Sagittal ex vivo MRI scans of contused rat spinal cord and corresponding histology. Midthoracic contusion injury 4 weeks post lesioning, same specimen as Fig. 2. Acquisition parameters: 2D multi-slice spin echo, slice thickness 208 µm, FOV 20x6 mm, in plane resolution 23 x 78 µm, TE 7.5 ms, TR 2 s. Scale bar 2 mm.* A-D *Ex vivo MRI scans from lateral to medial.* E-H *Corresponding Nissl stained sections.* I-L *Corresponding GFAP immunostained sections.* M-P *Corresponding collagen type III immunostained sections. Homogenous hyperintensities at the injury center (A) correspond to cystic lesion defects in histological sections (E,I,M). In other sections. mixed hypo-/hyperintensities in the lesion center (B,C; arrows) are associated either with cystic lesion defects, hemosiderin deposits or fibrotic scar formation (F,N,G,O; arrows). A hypointensity following the path of the dorsal corticospinal tract caudal to the lesion - corresponding to hypointensities in the dorsal columns in axial MR scans (see Fig.2) - is highlighted by arrowheads (B).*

spinal cord due to its longer T_2 and T_2^* relaxation times. With the applied sequence vertebral bodies appeared completely dark, while vertebral disks were bright.

3.2 Ex vivo MRI of contused spinal cord

Spin echo images of excised spinal cord 4 weeks after a thoracic contusion injury revealed a signal pattern away from the injury epicenter in axial slices (Fig. 2), which was almost identical to in vivo gradient echo images in unlesioned animals (Fig. 1 C,D). Gray matter was hyperintense compared to white matter. The central canal could be clearly identified. The gray/white matter differentiation completely vanished at the contusion center (Fig. 2 G,H). The homogenous hyperintense signal, which was pronounced in the spinal cord center and diminished towards the surface of the cord in all directions, was only interrupted by areas of signal loss in the center of the cord, which were confined mostly to the gray matter (Fig.2 G). Trauma induced hemorrhage and consecutive hemosiderin deposits are the likely pathologic correlates for this signal free area, which have been described to occur frequently within the spinal cord gray matter after injury [17]. Hypointensities within the lesion center (in particular in sagittal MR scans) - not as pronounced as the described hemosiderin associated changes - corresponded to immunoreactivity for collagen type III, but not GFAP, in sagittal histological sections (Fig. 3 B,J,N), thus representing components of the fibrous rather than the gliotic scar. The overall diameter of the cord was reduced, in particular the dorsolateral columns were symmetrically diminished in volume (Fig. 2 G,H), reflecting substantial irreversible

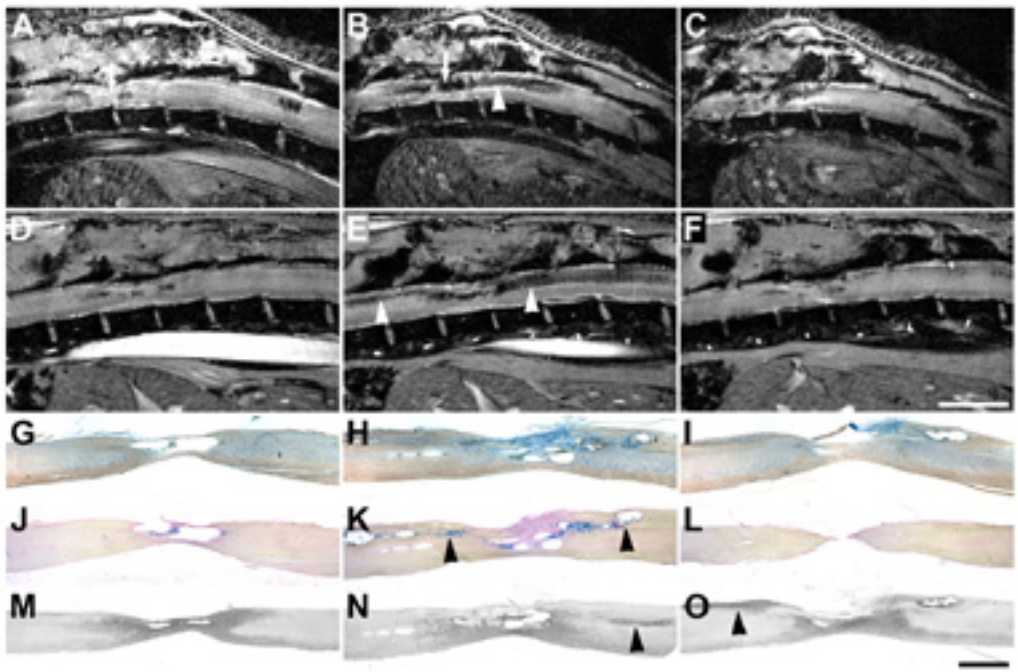

Figure 4: *Sagittal in vivo MRI scans of contused rat spinal cord and corresponding histology. In vivo MRI in adult rats at 2 and 8 weeks after thoracic contusion injury displays signal changes, which parallel the ex vivo MRI data. Acquisition parameters: 2D multi-slice gradient echo,* A-C *slice thickness 311 µm, FOV 30 x 30 mm, in plane resolution 117 x 117 µm, TE 4.4 ms, TR approx. 200 ms (depending on heart rate).* D-F *slice thickness 300 µm, FOV 40 x 25 mm, in plane resolution 156 x 98 µm, TE 3.7 ms, TR 200 ms (depending on heart rate). Scale bar A-F 5 mm, G-O 1 mm. Consecutive sagittal MR scans are shown at 2 weeks (A-C) and 8 weeks (D-F) post injury with corresponding histological Nissl (G-I) and Prussian Blue (J-L) stained sections, and sections processed for ED1 immunohistochemistry (macrophages, monocytes) (M-O), all from the same animal. Arrows in* A,B *highlight the site of the impact. Hypointensities along ascending and descending axon projections in the dorsal columns (B,E) correlate with hemosiderin deposits (K) rather than macrophage/ monocyte infiltration (O) (respective areas are highlighted by arrowheads). These changes increase from 2 weeks (C) until 8 weeks (G) post injury. The clear reduction in cord diameter over time (B versus E; C versus F) corresponds to the atrophy seen in histological sections (G-O).*

atrophy as soon as 4 weeks after injury. In some Nissl stained sections (Fig. 3 G) all types of organized tissue were absent, suggesting a developing fluid-filled cavity. However, corresponding MRI scans did not display a homogenous hyperintensity (Fig. 3 C), which would be the MR equivalent of a cystic lesion defect. Instead, only a small hyperintense band - the correlate of the true cystic lesion defect - surrounded a hypointense core. Thus, it is likely that this hypointense area contained non-organized material (inflammatory cells and cell debris mixed with hemosiderin deposits), which is regularly lost during the process of histological analysis.

Remote from the lesion center, some neuroanatomically restricted signal changes could be observed (Fig. 2 A,J-L; Fig. 3 B). Caudal to the lesion center, hypointensities strictly confined either to the former main dorsal corticospinal tract caudal to

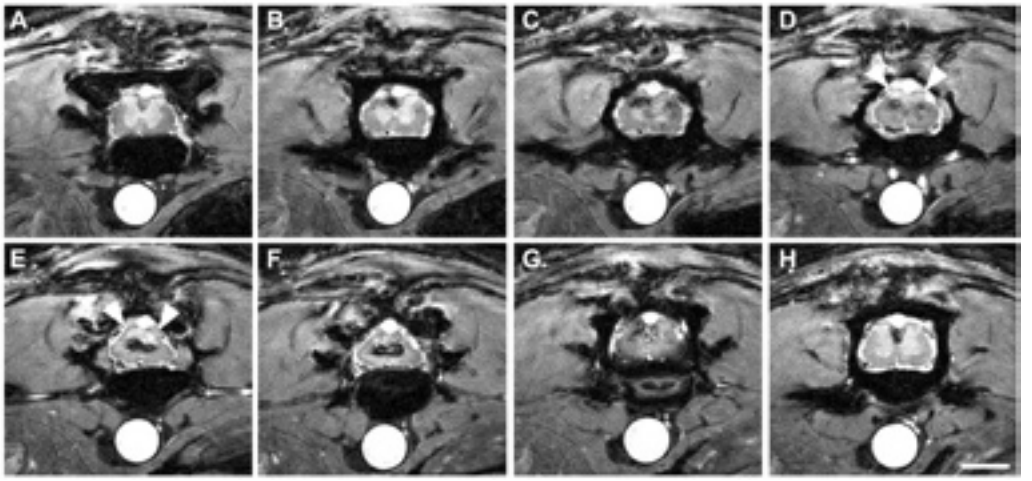

Figure 5: *Axial in vivo MRI scans of contused rat spinal cord. In vivo MR axial scans in adult rats 6 weeks post injury. Acquisition parameters: 2D multi-slice gradient echo, slice thickness 370 µm, FOV 20 x 20 mm, in plane resolution 78 x 78 µm, TE 4.2 ms, TR approximately 200 ms (depending on heart rate). Scale bar 2 mm. Scans rostral to the contusion (A-C), at the lesion center (D-G) and caudal to the lesion (H). The clear differentiation between white and gray matter disappears over subsequent sections. At the lesion center, hypointensities are surrounded by hyperintensities, which are less pronounced towards the cord surface (E,F). The dorsal aspect of the spinal cord at the lesion site appears more homogenously hyperintensive, most likely representing cystic changes (D,E; arrowhead). Signs of atrophy are present in the dorsolateral spinal cord (E,F)*

the lesion or to the ascending proprioceptive pathways (gracile fascicle) rostral to the lesion were identified. Hyperintense regions within the dorsal columns rostrally and caudally (Fig. 2 B-D,J-L; 3 A,B) can be attributed to cystic necrotic zones, which were identified in the corresponding sagittal histological sections (Fig.3 F). There was no difference in overall signal changes compared to the spinal cord sample, which was taken 2 weeks after the contusion injury (data not shown).

3.3 In vivo MRI of contused spinal cord

Five animals with spinal cord contusions at thoracic level applied by the IH Impactor and one intact animal were analyzed with MRI at 2, 6 and 8 weeks postoperatively. Only 2 out of 5 injured animals survived the MR imaging procedure and were thus obtainable for histological evaluation. The majority of signal changes observed in ex vivo spin echo images in the contused spinal cord were almost identical to in vivo gradient echo images of the contused spinal cord. The cord diameter was reduced at the lesion center; in particular, the dorsolateral aspects were atrophic (Fig. 4 A-F; 5 E,F), which was confirmed by identical findings in corresponding Nissl stained histological sections. Towards the lesion epicenter, the gray/white matter differentiation completely vanished (Fig. 5 D-G). The signal pattern of the gray matter in the intact spinal cord (Fig. 1 C,D) was replaced by hypointense areas in the center of the cord surrounded by a hyperintense rim dorsally

Table 2: *A comparison of the different spatial resolution in previous rat spinal cord injury in vivo MRI studies. If one study used different resolutions, the highest resolution is quoted.*

Voxel volume (nl)	In-plane-Resolution (µm)	Slice thickness (µm)	Field strength (T)	Coil type	Reference
2.25	78x78	370	17.6 T	surface coil	present study
12.2	78x156	1000	1.9 T	implanted	[11]
304	780x780	500	1.5 T	surface coil	[12]
17.3	76x76	3000	4.7 T	surface coil	[13]
76	195x195	2000	2.1 T	surface coil	[14]
	not provided	2800	2 T	surface coil	[15]
80	200x200	2000	4.7 T	birdcage coil	[16]
12.7	130x98	1000	2 T	implanted	[17]
8.1	78x104	1000	7 T	implanted	[18]

and ventrally (Fig. 5 D-G). As described in ex vivo MRI (Fig. 2 F,G), the hypointensities at the lesion center represent hemosiderin deposits, which are remnants of the hemorrhage caused by the trauma corresponding to dark areas in Nissl and Prussian Blue stained sections (Fig. 4 K,N). In addition, hypointensities were found confined to the dorsal columns rostral and caudal to the lesion, both in sagittal and axial scans (Fig. 4 B,E; 5 H), which are also paralleled by ex vivo MRI findings. These hypointensities could be correlated with hemosiderin deposits as depicted by Prussian Blue staining of corresponding spinal cord sections (Fig. 4 K). There was no correlation with areas of macrophage/monocyte infiltration (Fig. 4M-O), which are - besides location adjacent to the injury center - commonly identified in white matter tracts remote from the lesion site highlighting areas of ongoing wallerian degeneration (N. Weidner, unpublished observation).

In Nissl stained histological sections (Fig. 4 H), small cigar shaped cystic areas decreasing in size rostrally were identified, which represent areas of beginning post-traumatic syrinx formation. In in vivo MRI, a corresponding signal was not clearly identifiable (Fig.4 B,E). Most likely, the chosen sagittal imaging planes did not include the location of the central canal.

4. DISCUSSION

This study was undertaken to evaluate the capabilities of high field (17.6 T) MRI to identify morphological changes occurring after experimental spinal cord contusion injury in adult rats. Findings from this study will serve as a basis for future preclinical experiments employing high field MRI to monitor cell-based regenerative strategies in the injured spinal cord, which might become a relevant therapy for spinal cord injured human subjects.

Thus far, only a few publications are available describing findings of morphological changes obtained by MR imaging in vivo in spinal cord injured rats [11-19]. Of these, only two MRI studies investigated spinal cord contusion injuries [16, 18], which are considered to closely mimic pathomor-

phological changes occurring after spinal cord injury in human subjects. In all previous studies, only a very limited resolution was achieved at field strengths ranging from 1.5 up to 7 T. Lower field strengths limit the achievable spatial resolution due to SNR restrictions. Therefore, in-plane resolution and slice thickness have to be reduced. The best resolution was achieved with implanted coils [11, 17, 18], which improve the SNR compared to surface coils, but require an additional surgical procedure. Despite the use of a surface coil, we were able to achieve a spatial resolution at 17.6 T, which is four times higher than the best previously reported resolution with an implanted coil (Table 2). White and gray matter differentiation [13, 16, 17], the delineation of cyst formation and hemorrhage from surrounding intact spinal cord parenchyma have been reported [13, 17]. However, none of these studies was able to spatially allocate respective signal changes as precise as in the present study. The ability to visualize signal changes at a high spatial resolution will become particularly relevant for future MRI studies employed to track the survival and migration of a small number of paramagnetically labeled transplanted cells in the injured spinal cord in small animals [22].

Both ex vivo and in vivo MRI of injured rat spinal cords consistently depicted hypointensities in the dorsal columns rostral and caudal to the contusion injury at thoracic level. The comparison with corresponding histological sections revealed that these hypointense areas represent hemosiderin deposits due to trauma induced hemorrhage rather than wallerian degeneration, which has also been described to induce hypointensities following spinal cord injury [23]. Both, neuropathological and the neuroradiological studies frequently report structural changes representing hemorrhage following spinal trauma [17, 24, 25]. However, respective changes are observed in the gray matter accentuated in and adjacent to the lesion center. To our knowledge, extensive white matter MRI signal changes representing hemosiderin deposits as observed in the present study have not been described yet. Field strength dependent changes in terms of relaxation rates and the higher spatial resolution seem to have increased the contrast in regions of iron deposition [26], thus allowing visualization of relatively discrete hemosiderin deposits within the spinal cord. Whether the signal changes observed in this animal model of spinal cord injury reflect pathological sequels of this disease condition in humans remains to be determined. In case, hemosiderin deposits reflecting a former hemorrhage are more widespread than previously thought, free radicals accumulating after an intraspinal hemorrhage might further contribute to the poor intrinsic regenerative capacity of the injured mammalian spinal cord [27].

Ex vivo and in vivo MRI results show a mismatch of MR images and corresponding histological sections (Nissl stains) in regard to the extent of cystic defects. In histological sections, we frequently observe a rather large cystic lesion defect upon microscopic analysis, which overestimates the true size of cystic changes. During the preparation of histological sections from

contused spinal cord tissue, non-organized material such as cell debris, macrophages mixed with remnants of previous hemorrhages filling the cyst in part is lost. In contrast, MR signal changes in corresponding areas are much more diverse, displaying not only hyperintensities reflecting cystic degeneration as suggested by histology, but in addition hypointensities representing hemosiderin and cell debris. Thus, in vivo visualization by MRI provides invaluable additional information, which cannot be obtained from histological examination. For example, it is extremely important to differentiate between these alterations in cell transplantation approaches. Transplanting cells in a milieu rich in inflammatory cells and hemosiderin will decrease the survival rate of transplanted cells, thus jeopardizing the transplantation success [28]. Analyzing these changes over time using MRI will help to establish the optimal timing and location for transplantation after injury.

A significant limitation for small animal imaging at 17.6 T at this point is the reported poor survival rate of rats induced by the scanning procedure. Even though a custom-built probe head was used to overcome spatial restrictions [21], the tight fitting of experimental animals can sometimes lead to insufficient air circulation resulting in a rise of the isoflurane concentration around the animal. Furthermore the gradient cooling unit was maintained at 37°C ± 2°C throughout the imaging protocol to keep the animal at body temperature. Since only the temperature of the gradient cooling unit, but not the actual body temperature of the animals, was monitored, it is conceivable that the temperature of the animal was beyond physiological levels, thus contributing to the observed mortality. The present study was conducted to investigate the capabilities of high field MRI to monitor structural changes occurring after spinal cord injury in rats. Results demonstrate that MR imaging at 17.6 T using a surface coil provides extremely high-resolution visualization of structural changes occurring in the rat spinal cord following a contusion injury ex vivo and in vivo, which is superior to the best known spatial resolution even with implantable coils. The achieved spatial resolution allows to exactly localize morphological changes such as cyst formation and hemosiderin deposition, which are sometimes not even seen with histological analysis of spinal cord injured animals over time. In principle, in vivo high resolution MRI should allow repeated structural analysis in individual animals, which would also help to significantly reduce the number of animals required for preclinical investigations. However, the problem of poor animal survival during MR imaging needs to be solved.

5. ACKOWLEDGEMENTS

This study was supported by Deutsche Forschungsgemeinschaft (Ha 1232/13). We would like to thank S. Aussenhofer and M. Caioni for expert technical assistance. We also would like to thank V. Herold and E. Rommel for helpful discussions throughout the course of this study and N. Seiberlich for helpful comments on the manuscript.

6. REFERENCES

1. Manelfe, C. Imaging of the spine and spinal cord. Curr Opin Radiol 3, 5-15 (1991).
2. Hadley, D. M. & Teasdale, G. M. Magnetic resonance imaging of the brain and spine. J Neurol 235, 193-206 (1988).
3. Flanders, A. E., Spettell, C. M., Tartaglino, L. M., Friedman, D. P. & Herbison, G. J. Forecasting motor recovery after cervical spinal cord injury: value of MR imaging. Radiology 201, 649-55 (1996).
4. Grill, R., Murai, K., Blesch, A., Gage, F. H. & Tuszynski, M. H. Cellular delivery of neurotrophin-3 promotes corticospinal axonal growth and partial functional recovery after spinal cord injury. J Neurosci 17, 5560-72 (1997).
5. Xu, X. M., Guenard, V., Kleitman, N. & Bunge, M. B. Axonal regeneration into Schwann cell-seeded guidance channels grafted into transected adult rat spinal cord. J Comp Neurol 351, 145-60 (1995).
6. Li, Y., Field, P. M. & Raisman, G. Repair of adult rat corticospinal tract by transplants of olfactory ensheathing cells. Science 277, 2000-2 (1997).
7. Liu, Y. et al. Transplants of fibroblasts genetically modified to express BDNF promote regeneration of adult rat rubrospinal axons and recovery of forelimb function. J Neurosci 19, 4370-87 (1999).
8. Ramon-Cueto, A., Cordero, M. I., Santos-Benito, F. F. & Avila, J. Functional recovery of paraplegic rats and motor axon regeneration in their spinal cords by olfactory ensheathing glia. Neuron 25, 425-35 (2000).
9. Teng, Y. D. et al. Functional recovery following traumatic spinal cord injury mediated by a unique polymer scaffold seeded with neural stem cells. Proc Natl Acad Sci U S A 99, 3024-9 (2002).
10. Pfeifer, K., Vroemen, M., Blesch, A. & Weidner, N. Adult neural progenitor cells provide a permissive guiding substrate for corticospinal axon growth following spinal cord injury. Eur J Neurosci 20, 1695-704 (2004).
11. Ford, J. C. et al. A method for in vivo high resolution MRI of rat spinal cord injury. Magn Reson Med 31, 218-23 (1994).
12. Guizar-Sahagun, G. et al. Magnetic resonance imaging of the normal and chronically injured adult rat spinal cord in vivo. Neuroradiology 36, 448-52 (1994).
13. Fraidakis, M., Klason, T., Cheng, H., Olson, L. & Spenger, C. High-resolution MRI of intact and transected rat spinal cord. Exp Neurol 153, 299-312 (1998).
14. Fukuoka, M., Matsui, N., Otsuka, T., Murakami, M. & Seo, Y. Magnetic resonance imaging of experimental subacute spinal cord compression. Spine 23, 1540-9 (1998).
15. Ohta, K., Fujimura, Y., Nakamura, M., Watanabe, M. & Yato, Y. Experimental study on MRI evaluation of the course of cervical spinal cord injury. Spinal Cord 37, 580-4 (1999).
16. Metz, G. A. et al. Validation of the weight-drop contusion model in rats: a comparative study of human spinal cord injury. J Neurotrauma 17, 1-17 (2000).
17. Bilgen, M., Abbe, R., Liu, S. J. & Narayana, P. A. Spatial and temporal evolution of hemorrhage in the hyperacute phase of experimental spinal cord injury: in vivo magnetic resonance imaging. Magn Reson Med 43, 594-600 (2000).
18. Narayana, P. A., Grill, R. J., Chacko, T. & Vang, R. Endogenous recovery of injured spinal cord: longitudinal in vivo magnetic resonance imaging. J Neurosci Res 78, 749-59 (2004).
19. Franconi, F., Lemaire, L., Marescaux, L., Jallet, P. & Le Jeune, J. J. In vivo quantitative microimaging of rat spinal cord at 7T. Magn Reson Med 44, 893-8 (2000).
20. Scheff, S. W., Rabchevsky, A. G., Fugaccia, I., Main, J. A. & Lumpp, J. E., Jr. Experimental modeling of spinal cord injury: characterization of a force-defined injury device. J Neurotrauma 20, 179-93 (2003).
21. Behr, V. C. et al. High-resolution MR imaging of the rat spinal cord in vivo in a wide-bore magnet at 17.6 Tesla. Magma (2004).
22. Stroh, A. et al. In vivo detection limits of magnetically labeled embryonic stem cells in the rat brain

using high-field (17.6 T) magnetic resonance imaging. Neuroimage 24, 635-45 (2005).
23. Kuhn, M. J., Johnson, K. A. & Davis, K. R. Wallerian degeneration: evaluation with MR imaging. Radiology 168, 199-202 (1988).
24. Tator, C. H. & Koyanagi, I. Vascular mechanisms in the pathophysiology of human spinal cord injury. J Neurosurg 86, 483-92 (1997).
25. Holtz, A., Nystrom, B., Gerdin, B. & Olsson, Y. Neuropathological changes and neurological function after spinal cord compression in the rat. J Neurotrauma 7, 155-67 (1990).
26. Schenck, J. F. & Zimmerman, E. A. High-field magnetic resonance imaging of brain iron: birth of a biomarker? NMR Biomed 17, 433-45 (2004).
27. Petzold, A. et al. Axonal pathology in subarachnoid and intracerebral hemorrhage. J Neurotrauma 22, 407-14 (2005).
28. Okano, H. et al. Transplantation of neural stem cells into the spinal cord after injury. Semin Cell Dev Biol 14, 191-8 (2003).

Chapter 7

Conclusions and general discussion

In this thesis, the possibilities and limitations of cell-based therapies after spinal cord injury are explored. Particularly, the potential of adult derived neural progenitor cell (NPC) grafts to function as a permissive Substrate for axonal regeneration was investigated. Therefore, NPC were isolated from the adult rat spinal cord, propagated and were grafted to animals that received an acute spinal cord injury. Furthermore, techniques that are essential for the application of cell-based therapy were developed, including the preparation of graft material, *ex vivo gene therapy* and the development of non-invasive *in vivo* imaging techniques.

1. GRAFT PROPERTIES ESSENTIAL FOR REGENERATION OF THE INJURED SPINAL CORD

The main rationale for the use of NPC grafts in the injured spinal cord is the ability of NPC to replace lost spinal cord cells with cells that originally are present within the central nervous system (CNS). Since the adult CNS milieu however does not allow substantial regeneration, a simple substitution of CNS cells at the tissue defect that typically develops due to the injury most likely is not sufficient. The objective therefore is to mimic the axonal outgrowth pattern of the developing CNS, by transplanting NPC grafts [1, 2]. In order to reach this goal, grafted NPC first must be able to: 1) replace the lesion cyst that typically develops after the wire knife spinal cord injury, 2) offer trophic support and correct guidance cues to the regenerating axons in analogy to Schwann cell function in the injured peripheral nervous system and 3) replace lost spinal cord cells by differentiating into mature CNS cells that become functionally integrated into the spinal cord cytoarchitecture.

1.1 Lesion cyst replacement

The replacement of the lesion defect that develops after spinal cord injury (SCI) represents an important prerequisite to allow substantial axonal regeneration in the injured spinal cord. Since the used wire knife model of SCI induces a single cystic lesion cavity without inducing massive infiltration of peripheral cells, this model is very well suited to study the capacity of various cell grafts to restore lost spinal cord tissue. Although NPC survive transplantation into the acutely lesioned spinal cord, grafts of NPC alone are not able to replace the lesion defect since the NPC migrate away from the graft site (*Chapter 2*). Until so far, only the co-transplantation of NPC with fibroblasts allowed lesion cavity repair in combination with the successful delivery of NPC at the lesion site (*Chapter 3*). Experiments in which Schwann cells replaced the fibroblasts showed that although lesion cyst could be restored, the co-grafted NPC migrated into the spared spinal cord parenchyma, away from the Schwann cells that resided at the graft site (*Chapter 4b*).

1.2 Trophic- and guidance support for axonal regeneration by NPC

In the NPC-fibroblast co-grafted animals, regenerative sprouting of lesioned axons was induced when compared to

animals that received grafts of fibroblasts alone. Moreover, corticospinal tract (CST) regeneration was significantly induced by 170% in NPC-fibroblast co-grafted animals when compared to animals that received grafts of fibroblasts only (*Chapter 3*). The ability of NPC to induce regenerative sprouting of lesioned CST axons without the need of additional application of neurotrophic factors represents a unique property of NPC. This has only been unambiguously shown before with the grafts of olfactory ensheating cells [3, 4]. It has been reported that neural stem cells derived from the neonatal mouse cerebellum secrete by themselves various neurotrophic factors including nerve growth factor, brain-derived neurotrophic factor, and glial cell line-derived neurotrophic factor [5]. Whether the unmodified adult derived NPC that are used in the presented studies also secrete neurotrophic factors has not been investigated so far.

Regenerative sprouting of lesioned CST axons within the graft area of animals that were co-grafted with NPC and fibroblasts was observed along glial fibrillary acidic protein (GFAP) expressing grafted NPC (*Chapter 3*). These GFAP expressing cells are notably distinctive to the reactive astroglia that normally can be identified at the lesion site. First, both in the intact and the injured adult spinal cord, astrocytes mainly display a typical stellate morphology. The GFAP expressing cells that favor regenerative sprouting of lesioned axons however mostly appear as cells that possess a more elongated shape. Furthermore, a large proportion of the GFAP expressing grafted cells can be co-labeled with antibodies against brain lipid-binding protein (BLBP). BLBP is a marker for radial glial cells and immature astrocytes or astrocyte precursors [6]. We therefore postulate that the grafted NPC that differentiate into astroglila maintain an immature phenotype while serving as a scaffold for sprouting axons. This hypothesis is further validated by the fact that adult astrocytes are shown to be inhibitory to axonal regeneration [7, 8] It remains unclear whether all differentiating NPC are able to function as a permissive Substrate for CNS axon regeneration. Grafts consisting of homogenous populations of NPC derived cells could allow the identification of specific NPC phenotypes that augment axonal regeneration. Therefore further experiments need to be conducted that allow manipulation of NPC fate.

It remains unclear whether the co-grafted fibroblasts alter NPC function to stimulate outgrowth, or whether the fibroblasts are solely needed to retain the co-grafted NPC at the lesion site. In the peripheral nerve injuries, fibroblasts have been described to induce the production of extracellular matrix (ECM) and basal lamina components by Schwann cells [9]. Furthermore, the co-culture experiments of GFP expressing NPC with fibroblasts at least suggest that the morphology of the differentiating GFP expressing NPC is changed towards a more bipolar shape, a morphological phenotype that can be spatially associated with regenerating axons *in vivo* (*Chapter 3*).

The invasion of fibroblasts from the me-

ninges has been associated in the literature with astroglial scarring, a detrimental event for axonal regeneration [10]. Nevertheless, the presence of fibroblasts in co-grafts does not appear to prevent axonal regeneration in these experiments. Co-cultured fibroblasts do not induce the formation of a glia limitans like structure *in vitro*, which is in contrast to Schwann cells (*Chapter 3, 4b*). Therefore, the effect of the presence of fibroblasts within the lesioned area on axonal regeneration needs to be further investigated e.g. by grafting a NPC filled artificial matrix. If such a NPC-loaded matrix allows substantially more regenerative sprouting than the matrix only, the notion that undifferentiated NPC per se are capable of inducing regenerative sprouting of lesioned CNS axons would be further strengthened [11].

The direction of the observed regenerative sprouting of axons into the graft occurs randomized, which reduces the likelihood of axons to completely bridge the graft and reenter the spinal cord parenchyma distal to the lesion site and reinnervate target structures. Moreover, since the cytoarchitecture of the spinal cord axon projections is highly organized, oriented sprouting of lesioned axons is essential if the native organization of the spinal cord axon projections have to be reinstalled. Therefore, it is most likely that introducing directive cues are an important aspect in order to allow sprouting axons to align to their correct targets. Different methods have been proposed to induce a more oriented axonal sprouting, including the induction of a chemoattractive neurotrophic factor gradient or by transplanting an anisotropic matrix that consists of oriented pores that bridges the lesion site [12, 13]. Especially the use of an oriented anisotropic guidance matrix is of great interest, since it eventually also could replace the co-grafted fibroblast as a Substrate to retain the grafted NPC at the lesion site.

1.3 Appropriate replacement of lost spinal cord cells

In order to study fate and function of the used NPC upon transplantation, grafted cells need to be identified *in vivo* using a method that allows the reliable co-localization with phenotypical markers. Throughout this thesis, NPC are prelabeled using the thymidine analogue Bromodeoxyuridine (BrdU). BrdU is incorporated in the DNA of proliferating cells prior to transplantation, which later can be visualized using immunocytochemical methods [14]. Although BrdU prelabeling represents a reliable method for the identification of grafted cells, it is a far from ideal technique since the label is restricted to the cell nucleus. Therefore, to reliably co-localize the BrdU label with phenotypical markers that mostly are located in the cytoplasm can be problematic (*Chapter 2*). Furthermore, BrdU immunohistochemistry is preceded by an antigen retrieval protocol that is not compatible with immunohistochemical myelin stainings, which complicates the identification of grafted NPC that adapted to an oligodenroglial phenotype (*Chapter 4b*). A possible solution for this problem is the labeling of the grafted cells with a genetic marker. Therefore, it was tested

whether NPC could be genetically modified to express the cytoplasmatic marker green fluorescent protein (GFP) using various retro- and lentiviral vectors. Although undifferentiated NPC strongly expressed GFP, transgene expression was rapidly lost after transplantation of the GFP expressing NPC into the spinal cord (*Chapter 5*). The development of improved vectors that are able to induce stable transgene expression in adult derived NPC therefore is of great importance, in order to allow reliable cytoplasmatic labeling of grafted cells.

The grafted BrdU positive NPC were found to differentiate into glia only (*Chapter 2, 3, 4b*). At 3 weeks post transplantation, the grafted NPC mainly expressed the astroglial markers GFAP. Furthermore, the grafted NPC differentiate into glial cells that flawlessly integrate into the host tissue (*Chapter 2, 3, 4b*). The grafted NPC thus were able to build a reticulum that continues into the host parenchyma, without being sealed of by a rim of reactive astrocytes, which often can be observed when other cell types are grafted into the injured spinal cord [15, 16]. Whether substituted astroglial cells become functionally integrated as well has not been investigated yet.

The grafted NPC did not uniformly differentiate into GFAP expressing cells. NPC that adapted to oligodendroglial lineages could be detected at the lesion site as well (*Chapter 2, 3, 4b*). The introduction of new oligodendrocytes at the lesion site by NPC has several implications. First, it has been described in detail earlier that oligodendroglia and oligodendrocyte precursor cells can be associated with extracellular matrix molecules that are inhibitory to axonal sprouting [17, 18]. In the described fibroblast-NPC co-graft experiment, the negative effect of the present oligodendroglia on corticospinal axonal sprouting appears to be outweighed by the factors that instead induce axonal regeneration (*Chapter 3*). The newly formed oligodendrocytes further could have the potential to remyelinate both demyelinated spared axons and regenerating axons. Although it has been shown that grafted glial progenitor cells possess the capacity to remyelinate axons in the adult spinal cord [19], additional investigations are needed to analyze whether indeed remyelination occurs in the applied SCI model. Nevertheless, it is most likely that remyelination is a critical aspect of future therapies that aim to induce functional regeneration in the injured spinal cord [20, 21].

The phenotype in which the grafted NPC differentiate is primarily determined by cues in the micro-environment at the site of transplantation [22, 23], which not necessarily reflects the differentiation pattern desired and required for optimal axonal regeneration and functional recovery [11]. The over-expression of individual genes, which drive neural stem cells into specific phenotypes, has been demonstrated to generate homogenously differentiated cell populations [24, 25]. Neural stem cells modified in this way for transplantation might be able to override the differentiation inducing signals of the host environment at the injury site of grafted cells into specifi-

cally growth promoting phenotypes. It is most likely that only a transient expression of fate determining genes is preferred to induce the differentiation of NPC into a specific phenotype [11]. Therefore, the viral vectors that are described in this thesis may very well serve as a tool to reach this goal (*Chapter 5*).

Although at least a proportion of the used NPC have the capacity to differentiate into neuronal phenotypes (*Chapter 2, 3, 4b*), the micro-environment at the non-neurogenic regions of the adult CNS restricts the differentiation of the grafted NPC to glial lineages [22]. This however, does not impair the usefulness of the employed NPC since it was investigated whether NPC grafts are able to support regenerative sprouting of disrupted axons by providing a growth-permissive Substrate. Alternatively, functional recovery in the injured SC could be induced when NPC-derived neuronal cells function as a signaling relais that bridges the lesion site. This means that lesioned axons must project on the grafted neuronal cells that on their turn must innervate either spared spinal cord projections or the original target regions. Particularly embryonic stem cells have gained much attention to reach this goal since these cells appear to possess the potential to differentiate into neurons when grafted in the adult spinal cord [26]. Alternatively, fetal CNS tissue derived neurons also are shown to functionally integrate into the injured spinal cord cytoarchitecture [27]. The engraftment of neuronal cells by inducing neuronal differentiation of adult derived NPC in the adult spinal cord could serve as an interesting alternative to fetal derived graft material. Previous research however showed that neuronal differentiation of adult derived NPC that ere grafted to the injured spinal cord is extremely difficult to achieve [11].

2. ARE NPC GRAFTS ABLE TO INDUCE FUNCTIONAL RECOVERY AFTER SCI?

The promising results showing contact-mediated regenerative sprouting of corticospinal axons raise the question whether it is able to induce functional regeneration by grafting adult derived NPC in the injured spinal cord. Since the used dorsal wire-knife lesion of the CST at the cervical level only represents an incomplete lesion that does not lead to permanent functional deficits [28], the clinical relevance of the potential of grafted NPC to function as a scaffold for regenerating CNS axons needs to be tested in a SCI animal model that possesses a relevant functional correlate to the structural injury. Thoracic contusion models that are combined with various locomotor tests represents the most clinical relevant SCI animal model and is very well established in the literature [29-31]. The reduced reproducibility of the injury however has great implications for the application of cell-based therapy in contusion injuries. Especially in more chronic injuries, the size and the exact location of the rather diffuse injury site varies from subject to subject. It is evident that the exact placement of the cell graft is essential for the functional outcome. Non-invasive *in vivo* imaging of the lesion site

could serve as important tool to reach this goal, moreover since high field magnetic resonance imaging (MRI) was shown to allow the non-invasive, high-resolution visualization of pathomorphological changes such as hemorrhage, tissue degeneration and cyst formation in the rat spinal cord following contusion injury (*Chapter 6*). Unlike after transsection- or aspiration injuries of the spinal cord, contusion injuries only induce the development of a limited lesion cavity defect at the lesion epicenter (*Chapter 6*). The tissue defect at the lesion epicenter of contusion injuries therefore more likely represents a mixture of tissue debris, infiltrated immune cells and unorganized tissue. Since the lesion defect needs to be replaced by a graft in order to allow axonal regeneration over the lesion site, it is very well possible that a simple injection of large amounts of cells at lesion site induces an additional injury to the remaining spinal cord tissue that surrounds the lesion site and that is likely to contain spared axons.

3. ISOLATION OF AUTOLOGOUS NPC FOR SPINAL CORD REPAIR

The NPC that are used throughout this thesis are isolated from the adult spinal cord. Even though the grafted cells are typed as progenitor cells, at least a proportion of the used NPC possess stem cell characteristics including multipotency and self-renewal [22]. Although it remains unclear whether the NPC that are isolated from the adult spinal cord represent the same cell type as the NPC that are isolated from the subventricular zone (SVZ) or the hippocampus, both cell populations share most of their stem cell properties [32]. It should be noted the actual neural stem cell that is present in the SVZ and hippocampus of the adult brain expresses GFAP *in vivo* and possesses the properties belonging to astroglial cells [33, 34]. It is however very unlikely that the GFAP expressing cells that are shown to support regenerative axonal sprouting in this thesis represent undifferentiated neural stem cells, The expression of GFAP by the grafted NPC is only induced after transplantation, together with an immediate decline of cell proliferation of the grafted cells and the upregulation of other mature glial markers (*Chapter 2, 3, 4b*). Previous studies that investigated neural stem cell activity in the adult spinal cord did not describe the presence of GFAP expressing neural stem cells [22, 35].

Crucial for the applicability of a cell based therapy using progenitor / stem cells is the availability of sufficient amounts of cell material. In this respect, adult derived NPC have a decisive advantage over embryonic- and fetal derived progenitor cells. Even when the ethical concerns that are associated with the use of embryonic- and fetal derived progenitor cells are not considered, the limited availability of these cells most likely will result in logistic problems. Moreover, the use of adult derived NPC allows the advantageous autologous transplantation mode in which the receiving patient functions as his own tissue donor, preventing the occurrence of side effects that are associated with graft rejection or immune suppression. In a previous

study, we were able to show that in the rat, sufficient amounts of adult derived autologous NPC can be isolated using the minimal invasive brain biopsy technique, without inducing unacceptable additional damage. These NPC furthermore are able to induce axonal regeneration in the injured spinal cord of the donor animal [36].

The purification of specific sub-populations of glial progenitor cells from the heterogenous progenitor cell population represents a promising method to further enhance the capacity of NPC grafts to induce regeneration in the lesioned spinal cord. The Schwann cell purification method that employs magnetic-activated cell separation (MACS) as described in this thesis (*Chapter 4a*) can be adapted to enable the separation of specific NPC subpopulations for grafting purposes [37, 38].

4. COMBINING NPC GRAFTS WITH ADDITIONAL TROPHIC SUPPORT

An additional promising means to further enhance the sprouting response of lesioned axons is the local overexpression of neurotrophins such as neurotrophic factor-3 (NT-3), brain-derived neurotrophic factor (BDNF), glial cell line-derived neurotrophic Factor (GDNF) or nerve growth factor (NGF), which previously has been shown to enhance regenerative sprouting of CST axons [16, 39-42]. A very attractive method to reach this goal would be to induce over-expression of NT-3 by grafting transduced NPC in an *ex vivo* gene therapy approach. The stable over-expression of transgenes in NPC however is very problematic due to gene silencing (*Chapter 5*). Of all vectors tested, only transient gene expression could be achieved that was rapidly downregulated upon transplantation of the transduced cells into the spinal cord. The local delivery of trophic factors in the CNS alternatively can be induced by direct injection of lentiviral vectors in the CNS parenchyma, which is sufficient to allow transgene expression for up to 16 months (*Chapter 5*).

In none of the observed cases, the regenerative sprouting of the CST was able to completely bridge the lesion site and sprout into the distal portion spinal cord parenchyma. Therefore, the observed regenerative sprouting must be further enhanced before a functional correlate of the observed regenerative sprouting is likely to evolve. Unlike the sprouting of lesioned axons from the spinal cord tissue into the graft, the reentering of sprouting axons from the graft into the distal spinal cord tissue is extremely difficult to achieve, which most likely is related to the development of the glial scar that surrounds the cellular graft (*Chapter 4b*). When the lesioned axons sprout into a graft that is more permissive for axonal regeneration than the surrounding spinal cord tissue, the sprouting axons are not very likely to reenter the distal spinal cord tissue [43]. This problem can only be solved partially by the local overexpression trophic factors at the graft site, since this creates an “oasis of trophic factors” inside the inhospitable spinal cord milieu [43, 44]. A possible solution could be the creation of a neurotrophic gradient over the lesion site. By using in-

jections of a lentiviral vector, a NT-3 gradient could be established, which promoted axonal regeneration beyond the lesion site and into the distal spinal cord tissue. [45]

5. FINAL CONCLUSIONS AND OUTLOOK

Syngenic adult derived neural progenitor cells are able to survive transplantation in the acutely lesioned spinal cord and differentiate into glial phenotypes. When co-grafted with fibroblasts, GFAP expressing grafted NPC are able to replace the lesion defect and are able to induce contact mediated axon guidance and regenerative sprouting, which is in analogy with the peripheral nervous system in which Schwann cells function as a guiding substrate. NPC that are co-grafted with highly purified Schwann cells however migrate away from the lesion site, which is paralleled with a reduced axonal outgrowth. A close investigation of NPC that are transduced to express ectopic genes by using different viral vectors revealed that *in vivo* gene expression in genetically engineered neural progenitor cells is temporally limited and mostly restricted to undifferentiated NPC.

Additional experiments in small animal models of SCI will have to be conducted in order to further evaluate the capacity of autologous NPC grafts to induce functional axonal outgrowth of the injured spinal cord before even considering the application in human patients. Moreover, it remains unclear in which extent promising results that are obtained using animal models of SCI are transferable to the human situation. It first must be unambiguously shown that neural progenitor cell mediated regenerative sprouting is able to induce target reinnervation and regain of function without inducing adverse side effects such as allodynia, chronic pain and muscle spasms. Furthermore, the risks that are associated with the isolation, propagation and transplantation of neural progenitor cells in human subjects remain to be established. The promising results that are partially described in this thesis nevertheless justify further research efforts in order to reveal the full potential of adult derived NPC. The combination of MRI imaging to monitor structural regeneration and longitudinal behavioral studies of spinal cord injured rats would greatly facilitate the verifications of the observed structural regeneration in functional relevant small animal models of SCI. This allows direct correlation of structure with function. Furthermore, the ability to visualize pre-labeled cells, at high resolution *in situ,* represents an important prerequisite for preclinical studies with the objective to develop an effective and safe therapy that is able to at least partially relieve the devastating consequences of spinal cord injury.

6. REFERENCES

1. Smith, G. M., Miller, R. H. & Silver, J. Changing role of forebrain astrocytes during development, regenerative failure, and induced regeneration upon transplantation. J Comp Neurol 251, 23-43 (1986).
2. Smith, G. M. & Silver, J. Transplantation of immature and mature astrocytes and their effect on scar formation in the lesioned central nervous system. Prog Brain Res 78, 353-61 (1988).
3. Li, Y., Field, P. M. & Raisman, G. Repair of adult rat corticospinal tract by transplants of olfactory ensheathing cells. Science 277, 2000-2 (1997).
4. Nash, H. H., Borke, R. C. & Anders, J. J. Ensheathing cells and methylprednisolone promote axonal regeneration and functional recovery in the lesioned adult rat spinal cord. J Neurosci 22, 7111-20 (2002).
5. Lu, P., Jones, L. L., Snyder, E. Y. & Tuszynski, M. H. Neural stem cells constitutively secrete neurotrophic factors and promote extensive host axonal growth after spinal cord injury. Exp Neurol 181, 115-29 (2003).
6. Hartfuss, E., Galli, R., Heins, N. & Gotz, M. Characterization of CNS precursor subtypes and radial glia. Dev Biol 229, 15-30 (2001).
7. Rudge, J. S. & Silver, J. Inhibition of neurite outgrowth on astroglial scars in vitro. J Neurosci 10, 3594-603 (1990).
8. Richardson, P. M., McGuinness, U. M. & Aguayo, A. J. Axons from CNS neurons regenerate into PNS grafts. Nature 284, 264-5 (1980).
9. Obremski, V. J., Wood, P. M. & Bunge, M. B. Fibroblasts promote Schwann cell basal lamina deposition and elongation in the absence of neurons in culture. Dev Biol 160, 119-34 (1993).
10. Bundesen, L. Q., Scheel, T. A., Bregman, B. S. & Kromer, L. F. Ephrin-B2 and EphB2 regulation of astrocyte-meningeal fibroblast interactions in response to spinal cord lesions in adult rats. J Neurosci 23, 7789-800 (2003).
11. Hofstetter, C. P. et al. Allodynia limits the usefulness of intraspinal neural stem cell grafts; directed differentiation improves outcome. Nat Neurosci 8, 346-53 (2005).
12. Geller, H. M. & Fawcett, J. W. Building a bridge: engineering spinal cord repair. Exp Neurol 174, 125-36 (2002).
13. Stokols, S. & Tuszynski, M. H. The fabrication and characterization of linearly oriented nerve guidance scaffolds for spinal cord injury. Biomaterials 25, 5839-46 (2004).
14. Brown, D. B. & Stanfield, B. B. The use of bromodeoxyuridine-immunohistochemistry to identify transplanted fetal brain tissue. J Neural Transplant 1, 135-9 (1989).
15. Weidner, N., Blesch, A., Grill, R. J. & Tuszynski, M. H. Nerve growth factor-hypersecreting Schwann cell grafts augment and guide spinal cord axonal growth and remyelinate central nervous system axons in a phenotypically appropriate manner that correlates with expression of L1. J Comp Neurol 413, 495-506 (1999).
16. Grill, R., Murai, K., Blesch, A., Gage, F. H. & Tuszynski, M. H. Cellular delivery of neurotrophin-3 promotes corticospinal axonal growth and partial functional recovery after spinal cord injury. J Neurosci 17, 5560-72 (1997).
17. Caroni, P., Savio, T. & Schwab, M. E. Central nervous system regeneration: oligodendrocytes and myelin as non-permissive substrates for neurite growth. Prog Brain Res 78, 363-70 (1988).
18. Jones, L. L., Yamaguchi, Y., Stallcup, W. B. & Tuszynski, M. H. NG2 is a major chondroitin sulfate proteoglycan produced after spinal cord injury and is expressed by macrophages and oligodendrocyte progenitors. J Neurosci 22, 2792-803 (2002).
19. Groves, A. K. et al. Repair of demyelinated lesions by transplantation of purified O-2A progenitor cells. Nature 362, 453-5 (1993).

20. Horner, P. J. & Gage, F. H. Regeneration in the adult and aging brain. Arch Neurol 59, 1717-20 (2002).
21. Keirstead, H. S. et al. Human Embryonic Stem Cell-Derived Oligodendrocyte Progenitor Cell Transplants Remyelinate and Restore Locomotion after Spinal Cord Injury. J. Neurosci. 25, 4694-4705 (2005).
22. Shihabuddin, L. S., Horner, P. J., Ray, J. & Gage, F. H. Adult spinal cord stem cells generate neurons after transplantation in the adult dentate gyrus. J Neurosci 20, 8727-35 (2000).
23. Han, S. S., Kang, D. Y., Mujtaba, T., Rao, M. S. & Fischer, I. Grafted lineage-restricted precursors differentiate exclusively into neurons in the adult spinal cord. Exp Neurol 177, 360-75 (2002).
24. Gaiano, N., Nye, J. S. & Fishell, G. Radial glial identity is promoted by Notch1 signaling in the murine forebrain. Neuron 26, 395-404 (2000).
25. Tanabe, Y., William, C. & Jessell, T. M. Specification of motor neuron identity by the MNR2 homeodomain protein. Cell 95, 67-80 (1998).
26. McDonald, J. W. et al. Transplanted embryonic stem cells survive, differentiate and promote recovery in injured rat spinal cord. Nat Med 5, 1410-2 (1999).
27. Palmer, M. R. et al. Functional innervation of spinal cord tissue by fetal neocortical grafts in oculo: an electrophysiological study. Exp Brain Res 87, 96-107 (1991).
28. Weidner, N., Ner, A., Salimi, N. & Tuszynski, M. H. Spontaneous corticospinal axonal plasticity and functional recovery after adult central nervous system injury. Proc Natl Acad Sci U S A 98, 3513-8 (2001).
29. Basso, D. M., Beattie, M. S. & Bresnahan, J. C. A sensitive and reliable locomotor rating scale for open field testing in rats. J Neurotrauma 12, 1-21 (1995).
30. Basso, D. M., Beattie, M. S. & Bresnahan, J. C. Graded histological and locomotor outcomes after spinal cord contusion using the NYU weight-drop device versus transection. Exp Neurol 139, 244-56 (1996).
31. Basso, D. M. et al. MASCIS evaluation of open field locomotor scores: effects of experience and teamwork on reliability. Multicenter Animal Spinal Cord Injury Study. J Neurotrauma 13, 343-59 (1996).
32. Wachs, F. P. et al. High efficacy of clonal growth and expansion of adult neural stem cells. Lab Invest 83, 949-62 (2003).
33. Doetsch, F., Caille, I., Lim, D. A., Garcia-Verdugo, J. M. & Alvarez-Buylla, A. Subventricular zone astrocytes are neural stem cells in the adult mammalian brain. Cell 97, 703-16 (1999).
34. Seri, B., Garcia-Verdugo, J. M., McEwen, B. S. & Alvarez-Buylla, A. Astrocytes give rise to new neurons in the adult mammalian hippocampus. J Neurosci 21, 7153-60 (2001).
35. Horner, P. J. et al. Proliferation and differentiation of progenitor cells throughout the intact adult rat spinal cord. J Neurosci 20, 2218-28 (2000).
36. Pfeifer, K., Vroemen, M., Caioni, M. & Weidner, N. Feasibility of autologous adult neural progenitor cell transplantation into the chronically injured rat spinal cord. Soc Neurosci Abs (2003).
37. Wright, A. P., Fitzgerald, J. J. & Colello, R. J. Rapid purification of glial cells using immunomagnetic separation. J Neurosci Methods 74, 37-44 (1997).
38. Nunes, M. C. et al. Identification and isolation of multipotential neural progenitor cells from the subcortical white matter of the adult human brain. Nat Med 9, 439-47 (2003).
39. Yan, Q., Elliott, J. & Snider, W. D. Brain-derived neurotrophic factor rescues spinal motor neurons from axotomy-induced cell death. Nature 360, 753-5 (1992).
40. Tuszynski, M. H. et al. Fibroblasts genetically modified to produce nerve growth factor induce robust neuritic ingrowth after grafting to the spinal cord. Exp Neurol 126, 1-14 (1994).
41. Nakahara, Y., Gage, F. H. & Tuszynski, M. H. Grafts of fibroblasts genetically modified to secrete NGF, BDNF, NT-3, or basic FGF elicit differential responses in the adult spinal cord. Cell Transplant 5, 191-204 (1996).
42. Houweling, D. A., Lankhorst, A. J., Gispen, W. H., Bar, P. R. & Joosten, E. A. Collagen containing

neurotrophin-3 (NT-3) attracts regrowing injured corticospinal axons in the adult rat spinal cord and promotes partial functional recovery. Exp Neurol 153, 49-59 (1998).

43. Tuszynski, M. H. & Kordower, J. CNS Regeneration (Academic Press, San Diego, 1999).
44. Menei, P., Montero-Menei, C., Whittemore, S. R., Bunge, R. P. & Bunge, M. B. Schwann cells genetically modified to secrete human BDNF promote enhanced axonal regrowth across transected adult rat spinal cord. European Journal of Neuroscience 10, 607-21 (1998).
45. Taylor, L., Tuszynski, M. H. & Blesch, A. NT-3 gradients generated by lentiviral gene delivery promote axonal bridging into and beyond sites of spinal cord injury. Soc. Neurosci. Abstr. 877.19 (2004).

Nederlandse samenvatting

Het ruggenmerg bevat een groot gedeelte van alle verbindingen tussen de hersenen en de rest van het lichaam, samengepakt op een kleine ruimte. Een letsel aan het ruggenmerg heeft daarom vaak zwaarwegende gevolgen, omdat een relatief kleine beschadiging een groot gedeelte van de verbindingen kan verbreken. Het daaruit resulterende functieverlies is meestal onomkeerbaar omdat het centrale zenuwstelsel (CZS) van hogere werveldieren, en dus ook van de mens, een zeer beperkte capaciteit heeft om reeds ontstane schade te herstellen. Ondanks de grote vorderingen die de medische wetenschap de laatste 50 jaar heeft gemaakt is er nog steeds geen effectieve therapie beschikbaar die regeneratie in het CZS mogelijk maakt. Dit gebrek aan perspectief in combinatie met het feit dat de meeste dwarslaesie patiënten jonge volwassenen zijn zorgt ervoor dat een ruggenmergletsel een zware belasting vormt voor zowel het slachtoffer als ook voor de maatschappij in het algemeen.

Er zijn meerdere oorzaken aan te wijzen die voor het gebrek aan zelfherstellend vermogen van het beschadigde ruggenmerg verantwoordelijk zijn. Het is daarbij van belang om aan te merken dat het niet in de eerste plaats de beschadigde axonen zijn die geen nieuwe verbindingen kunnen aangaan, maar dat vooral de algemene omstandigheden zoals die in het CZS voorkomen een eventueel herstel van de verbindingen tegenwerken. Een therapie die gebaseerd is op het transplanteren van adulte neurale progenitor cellen (NPC) is een veelbelovende methode om herstel na ruggenmergletsel mogelijk te maken. NPC zijn ongespecialiseerde cellen die veel op stamcellen lijken en die uit het CZS-weefsel van volwassen individuen gewonnen kunnen worden. Het is dus in principe mogelijk dat de dwarslaesiepatiënt zelf als donor fungeert. Onder de juiste omstandigheden kunnen geïsoleerde NPC gekweekt en vermeerderd worden. Daarnaast zijn nakomelingen van NPC in staat om uit te groeien tot de drie belangrijkste celtypes van het CZS: neuronen, astrocyten en oligodendrocyten. NPC zijn daarom in staat om de cellen die door een beschadiging van het ruggenmerg verloren zijn gegaan organotypisch te vervangen. Aangezien er onder normale omstandigheden geen spontane regeneratie in het CZS mogelijk is, is het simpelweg vervangen van CZS-cellen waarschijnlijk niet voldoende. Doel van het transplanteren van NPC is daarom het opnieuw creëren van de omstandigheden zoals die tijdens de aanleg van de axonale verbindingen tijdens de ontwikkeling voorhanden zijn.

In de studies die in dit proefschrift beschreven zijn wordt deze hypothese getest door NPC te transplanteren in het beschadigde ruggenmerg van de rat. Hiervoor wordt er gebruik gemaakt van een proefdiermodel voor traumatisch ruggenmergletsel waarbij het belangrijkste deel van de piramidebaan wordt doorgesneden. De piramidebaan is

de directe verbinding tussen de motorcortex in de hersenen en het ruggenmerg. Direct aansluitend worden er in de ruimte die ontstaat door het letsel de te bestuderen cellen getransplanteerd. De piramidale axonen worden ten slotte een week na het ruggenmergletsel gemarkeerd waardoor een eventueel herstel van de piramidale axonen zeer specifiek aan te tonen is.

Een belangrijke voorwaarde voor het mogelijk maken van axonaal herstel na ruggenmergletsel is het vervangen van de cyste die op de plaats van het ruggenmergletsel ontstaat. Een transplantaat bestaande uit enkel NPC blijkt echter niet in staat te zijn om de cyste te vervangen aangezien de getransplanteerde cellen van de plaats van transplantatie weg migreren zonder dat het beschadigde weefsel wordt gerepareerd (*Hoofdstuk 2*). Door de NPC echter gezamenlijk met andere cellen te transplanteren is het mogelijk om het weefseldefect door het transplantaat te vervangen. Het zijn vooral fibroblasten die het mogelijk maken om voldoende NPC in de cyste te transplanteren (*Hoofdstuk 3*). Worden de NPC gezamenlijk met Schwann cellen getransplanteerd is het weliswaar mogelijk om de cyste door Schwann cellen te vervangen, de NPC in het transplantaat worden echter door de Schwann cellen afgestoten en migreren in het ruggenmergweefsel (*Hoofdstuk 4b*).

Getransplanteerde NPC stoppen met delen en differentiëren in meer ontwikkelde neurale celtypes (*Hoofdstuk 2*). Opvallend daarbij is dat de getransplanteerde cellen nauwelijks meer te onderscheiden zijn van de reeds aanwezige neurale cellen. Dit wijst erop dat de getransplanteerde cellen in staat zijn om naadloos in het bestaande weefsel te integreren. Om de functie van deze cellen te kunnen vaststellen is het van groot belang dat de getransplanteerde cellen betrouwbaar geïdentificeerd kunnen worden. In dit proefschrift zijn daarvoor 2 verschillende methodes gebruikt. Enerzijds zijn de getransplanteerde NPC gemarkeerd met de thymidine analoog Bromodeoxyuridine (BrdU). Het BrdU wordt in het DNA van de te transplanteren NPC ingebouwd en kan door middel van immunohistochemische kleuringreacties zichtbaar gemaakt worden. Anderzijds is geprobeerd om de te transplanteren cellen genetisch te markeren door middel van virale transductie. De NPC worden hiervoor genetisch gemanipuleerd waardoor deze het groen fluorescerende eiwit GFP produceren. GFP producerende NPC kunnen na transplantatie door middel van fluorescentie microscopie zichtbaar gemaakt worden. In een gedetailleerde studie die deel uitmaakt van dit proefschrift blijkt echter dat alle virale vectoren die getest werden enkel en alleen in staat zijn om ongedifferentieerde NPC te markeren. Na differentiatie van de NPC onder celkweek omstandigheden of na transplantatie van de cellen in het ruggenmerg, blijkt dat de meeste NPC stoppen met het produceren van GFP en dus hun markering verliezen (*Hoofdstuk 5*). Dit betekend dus ook dat het toedienen van herstel bevorderende groeifactoren door middel van het

transplanteren van genetisch gemanipuleerde NPC niet goed mogelijk is.

De getransplanteerde cellen blijken enkel in gliacellen te differentiëren, waarbij de meeste cellen het eiwit GFAP exprimeerden hetgeen typisch is voor astrocyten. Daarbij valt op dat de meeste van deze GFAP exprimerende cellen een afwijkend langgerekt uiterlijk hebben, en het eiwit BLBP bevatten, hetgeen erop wijst dat deze astrocyten nog onrijp zijn (*Hoofdstuk 2, 3, 4b*). Verder neemt een kleiner deel van de getransplanteerde cellen de vorm aan van oligodendrocyten. Dit zijn gliacellen die de myelineschede rond de axonen kunnen vormen. Of de getransplanteerde NPC daadwerkelijk in staat zijn om nieuwe myelineschedes te vormen kan echter niet worden aangetoond, omdat een kleuring die de myelineschede zichtbaar maakt niet te combineren is met de gebruikte BrdU markering (*Hoofdstuk 2, 3, 4b*). Een mogelijke oplossing voor dit probleem is het ontwikkelen van verbeterde methodes om de getransplanteerde NPC met bijvoorbeeld GFP te markeren.

Naast het vervangen van cellen die door de beschadiging van het ruggenmerg verloren zijn gegaan moeten de getransplanteerde NPC in staat zijn om het herstel van beschadigde axonen te ondersteunen. Als voorwaarde hiervoor moeten de getransplanteerde NPC daadwerkelijk op de juiste plaats in het traumatische weefseldefect blijven zitten. Zoals beschreven in dit proefschrift lukt dit het beste in dieren die getransplanteerd worden met een mengsel van NPC en fibroblasten. In deze groep blijkt dan ook de meeste regeneratie van beschadigde axonen plaats te vinden. Bovendien blijken bij deze dieren piramidale axonen in het transplantaat te groeien (*Hoofdstuk 3*). Dit is opvallend want juist piramidale axonen staan erom bekend dat deze zich uiterst moeilijk kunnen herstellen. Typerend hierbij is dat herstellende axonen contact opnemen met getransplanteerde NPC die zich hebben ontwikkeld tot onrijpe astrocyten (*Hoofdstuk 3*). Worden de NPC gezamenlijk met Schwann cellen getransplanteerd vindt er weliswaar in geringe mate axonaal herstel plaats, een herstel van piramidale axonen blijft echter nagenoeg uit. (*Hoofdstuk 4b*).

Er kan dus geconcludeerd worden dat door middel van het transplanteren van NPC na ruggenmergletsel verloren CZS cellen vervangen kunnen worden. Verder zijn de getransplanteerde NPC in staat om regenererende axonen te geleiden, hetgeen vergelijkbaar is met de functie van onrijpe gliacellen die gedurende de ontwikkeling de aanleg van axonale verbindingen ondersteunen. Deze veelbelovende resultaten roepen de vraag op of door het transplanteren van NPC ook functioneel herstel geïnduceerd kan worden. Door middel van de beschreven studies kan dit echter niet aangetoond worden omdat het gebruikte proefdiermodel geen blijvende uitval van functies veroorzaakt. Er zijn dus vervolgstudies nodig waarbij gebruik gemaakt wordt van een functi-

oneel relevant diermodel waarin de mate van herstel gemeten kan worden in gedragsstudies. Het is daarbij van groot belang dat het functioneel herstel gerelateerd kan worden aan de structurele reorganisatie die daarbij optreedt. De *in vivo* imaging door middel van magneet resonantie tomografie (MRT) zoals die beschreven is in *hoofdstuk 6* kan daarbij in vergaande mate van dienst zijn.

Abbreviations

APC	adenomatous polyposis coli
Ara-C	cytosine arabinoside
ATP	adenosine 5'triphosphate
BBB	blood-brain barrier
BDA	biotinylated dextran amine
BDNF	brain derived neurotrophic factor
BLBP	brain lipid binding protein
BrdU	bromodeoxyuridine
BSA	bovine serum albumine
cAMP	cyclic-adenosine 5'-monophosphate
cGMP	cyclic-guanosine 5'-monophosphate
CMV	Cytomegalovirus
CNS	central nervous system
CPG	central pattern generator
CSPG	chondroitin sulphate proteoglycan
CST	corticospinal tract
DAB	3,38-diaminobenzidine
DCX	doublecortin
DMEM	Dulbecco's modified essential medium
DNA	deoxyribonucleic acid
ECG	electrocardiogram
ECM	extracellular matrix
EDTA	Ethylenediaminetetraacetic acid
EGF	epidermal growth factor
FACS	fluorescence-activated cell sorting
FCS	fetal calf serum
FF	fibroblasts
FGF-2	fibroblast growth factor-2
FOV	field of view
Gal-C	galactocerebroside
GAP-43	growth-associated protein-43
GDNF	glial-derived neurotrophic factor
GFP	green fluorescent protein
HBSS	Hank's balanced salt solution
LTR	long terminal repeat
MACS	magnet-activated cell separation
MAG	myelin-associated glycoprotein
MLV	murine leukemia virus
MRI	magnet resonance imaging
MW	molecular weight
NB medium	Neurobasal medium
N-CAM	neuronal cell adhesion molecule
NF200	Neurofilament 200 kD fragment
NGF	nerve growth factor
Ng-R	Nogo receptor
NPC	neural progenitor cells

NSC	neural stem cell
NT-3	neurotrophic factor-3
NT-4/5	neurotrophic factor-4/5
OEC	olfactory ensheathing cells
OMGP	oligodendrocyte myelin glycoprotein
p75-LNGR	p75 low affinity NGF receptor
PBS	phosphate-buffered saline
PFA	paraformaldehyde
PNS	peripheral nervous system
P-Orn/Lam	poly-L-Ornithin/laminin
RAG	regeneration-associated genes
RF	radiofrequency
SC	Schwann cells
SC	spinal cord
SCI	spinal cord injury
SD	standard deviation
SEM	standard error of the mean
SNR	signal-to-noise ratio
SVZ	subventricular zone
TBS	Tris-buffered saline
TE	echo time
TGF-ß	transforming growth factor-ß
TR	repetition time
TX-100	Triton X-100

Curriculum vitae

De auteur van dit proefschrift werd geboren op 14 november 1973 te Heerlen en groeide op in het Limburgse Ulestraten. Na het behalen van het VWO diploma in het jaar 1993 aan het Stella Maris College te Meerssen, begon hij in hetzelfde jaar de studie Biologie aan de Universiteit Leiden. Tijdens zijn studie koos hij voor de medische afstudeerrichting en volgde hij een stage met het thema “In vivo effects of E2F-1 and E2F-2 deficiency on proliferation in the adult mouse brain” bij de Klinik und Poliklinik für Neurologie der Universität Regensburg, Duitsland. Vervolgens volgde hij een stage met het thema “Effects of pharmacological protein kinase C inhibitors on MTLn3 rat mammary tumor cells” aan de afdeling toxicologie van het Leiden Amsterdam Center for Drug Research te Leiden. Na het behalen van het doctoraal diploma in 1999, keerde hij in 2000 terug naar de Klinik und Poliklinik für Neurologie der Universität Regensburg en verrichte aldaar het onderzoek dat beschreven is in dit proefschrift. Momenteel is hij werkzaam als post-doc aan een gezamenlijk project van Klinik und Poliklinik für Neurologie der Universität Regensburg, de Urologische Klinik und Poliklinik van het Klinikum rechts der Isar der technischen Universität München, Duitsland en de firma Innovacell te Innsbruck, Oostenrijk met als thema “Generation of autologeous Schwann cell coated nerve conduits for cavernosal nerve reconstruction after radical prostatectomy”.

The author of this thesis was born on November 14 1973 in Heerlen, the Netherlands and grew up in Ulestraten. After obtaining his secondary school diploma in the year 1993 at the Stella Maris college in Meerssen, the Netherlands, he started to study biology in the same year at Leiden University. During his study, he decided to specialize in Medical Biology and conducted an internship at the Klinik und Poliklinik für Neurologie der Universität Regensburg, Germany investigating the in vivo effects of E2F-1 and E2F-2 deficiency on proliferation in the adult mouse brain and at Leiden Amsterdam Center for Drug Research, Leiden, investigating Effects of pharmacological protein kinase C inhibitors on MTLn3 rat mammary tumor cells. After obtaining his Masters degree, he returned to the Klinik und Poliklinik für Neurologie der Universität Regensburg to conduct the research that is described in this thesis. At the moment, he is working as a post-doc researcher on a cooperative project between the Klinik und Poliklinik für Neurologie der Universität Regensburg, the Urologische Klinik und Poliklinik of the Klinikum rechts der Isar der technischen Universität München, Germany and the company Innovacell from Innsbruck, Austria establishing the generation of autologeous Schwann cell coated nerve conduits for cavernosal nerve reconstruction after radical prostatectomy.

Publications

Cooper-Kuhn C.M, **Vroemen M.**, Brown J., Ye H., Thompson M.A., Winkler J., Kuhn H.G. (2002) Impaired Adult Neurogenesis in Mice Lacking the Transcription Factor E2F1. Mol. & Cell. Neuroscience 21(2): 312-323

Vroemen M., Winkler J., Weidner N. (2003) Purification of Schwann cells by selection of p75 low affinity nerve growth factor receptor expressing cells from adult peripheral nerve. J. Neurosci. Methods. 124(2): 135-143

Wachs F.-P., Couillard-Despres S., Engelhardt M., Wilhelm D., Ploetz S., **Vroemen M.**, Kaesbauer J., Uyanik G., Klucken J., Karl C., Tebbing J., Svendsen C.N., Weidner N., Kuhn H.-G., Winkler J., Aigner L. (2003) High efficacy of clonal growth and expansion of adult neural stem cells. Lab. Invest. 83(7): 949-962.

Vroemen M., Winkler J., Weidner N. (2003) Adult Neural Progenitor Cell Grafts Survive after Acute Spinal Cord Injury and Integrate Along Axonal Pathways. Europ. J. Neurosci.18(4): 743-751

May F., Weidner N., Matiasek K., Caspers C., Mrva T., **Vroemen M.**, Lehmer A., Swaibold H., Gänsbacher B., Hartung R. (2004) Schwann Cells Seeded Guidance Tubes Restore Erectile Function After Ablation of Cavernosal Nerves in Rats J. Urol. 172(1): 374-377

Pfeifer K., **Vroemen, M.**, Blesch A., Weidner N. (2004) Adult Neural Progenitor Cells Provide a Permissive Guiding Substrate for Corticospinal Axon Growth Following Spinal Cord Injury. Europ. J. Neurosci. 20(7): 1695-1704

Behr V.C., Weber T., Neuberger T., **Vroemen M.**, Weidner N., Bogdahn U., Haase A., Jakob P.M., Faber C. (2004) High resolution MR imaging of the rat spinal cord in vivo in a wide bore magnet at 17.6 Tesla. MAGMA 17(3-6): 353-358.

Couillard-Despres SD., Winner B., Schaubeck S., Aigner R., **Vroemen M.**, Weidner N., Winkler J., Kuhn H.G., Aigner L. (2005) Doublecortin: A Marker to Quantify Neurogenesis in the Adult Brain. Europ. J. Neurosci.21(1): 1-14

Vroemen M., Weidner N., Blesch A. (2005) Transient Gene Expression in Lentivirus and Retrovirus-Transduced Neural Progenitor Cells Grafted to the Adult Rat Spinal Cord. Exp. Neurol. 195(1): 127-139

May F., **Vroemen M.**, Matiasek K., Henke J., Brill T., Lehmer A., Apprich M., Erhardt W., Schoeler S., Paul R., Blesch A., Hartung R., Gansbacher B., Weidner N. (2005) Nerve replacement strategies for cavernous nerves. Eur Urol. 48(3): 372-378.

Weber T., **Vroemen M.**, Behr V., Neuberger T., Haase A., Schuierer G., Bogdahn U., Faber C., Weidner N: 17.6T MRI Allows High Resolution Visualization of Neuropathological Sequels in the Injured Rat Spinal Cord In Vivo. In press in Am. J. Neuroradiol.

May F., Matiasek K., **Vroemen M.**, Caspers C., Mrva T., Arndt C., Henke J., Lehmer A., Gais P., Brill T., Blesch A., Erhardt W., Hartung R., Gänsbacher B., Weidner N. GDNF-Transduced Schwann Cell Grafts Enhance Regeneration of Erectile Nerves Submitted for publication

Vroemen M., Caioni M., Weidner N., Adult Neural Progenitor Cells Co-Grafted with Schwann Cells fail to induce Corticospinal Axon Growth Following Spinal Cord Injury. Submitted for publication

Acknowledgments

Meinem Dank gilt zuerst an der gesamte Neurologie in Regensburg. Hier habe ich schon seit 1998 mein wissenschaftliches Zuhause gefunden, es war eine besonders fruchtbare Zeit! Ins besondere möchte ich mich bei Massimiliano Caioni, Prof. Dr. Ullrich Bogdahn, Georg Kuhn, Ludwig Aigner und sämtliche Arbeitskollegen bedanken. Ferner möchte ich mich ausdrücklich bei meinem hervorragenden Arbeitsgruppenleiter bedanken, der mir das Meiste beigebracht hat, was man braucht um als Doktorand erfolgreich bestehen zu können.

Außerdem möchte ich meinen Dank bei Bernd Meurers bekunden, der mich an Jürgen Winkler und die Regensburger Truppe vorgestellt hat und deshalb letztendlich zu „verantworten“ hat dass ich in der Regensburger Neurologie gelandet bin.

Merci beaucoup a Sébastien. Vous êtes un ami extraordinaire en privât et un grand collègue dans le labo.

Furthermore, I would like to thank the entire Tuszynski lab and specifically Armin Blesch for allowing me to have a look at their „kitchen“.

Zonder doctoraal geen promotie. Ik mag het daarom niet nalaten om de Singelaers te bedanken voor een uitermate geslaagde „Leidsche tijd“.

Bove alles wil ich mich bie mien pap en mam bedanke. Zonder hun neet aafloatende sjteun en vertrouwe zou ich noats zoa wiet gekomme zin. Dat gild veur zoawaal de gooie es auch de minder gooie tieje. Mien interesse in alles wat er zoa om os heen lèft en bewègt hub ich veural aan uch te danke! Verder wil ich mich auch bie Vera en Monique bedanke veur de gooie geschprekke en dat ze ten alle tieje bereid zin um mien monologen aan te heure. Chrit, bedaank dats diech miech met ut drukke vaan mein proefschrift hubs wille hèllepe. Verder gilt mien dank aan alle badjes en aanverwanten, ondanks dat ich noe al miér es tién joar in ut boeteland woon zurgt geer in belangrieke mate erveur dat de band met ut thoesland behouwe blieft.

Es letste wil ich mich bie Astrid bedanke omdat ze ut zoa goot met deze “verschtreuede professor” oethulst. Dich maakst do woa ich woon thoes.